

Synthesis and Characterization of Genotoxic and Process Impurities of Active Pharmaceutical Ingredients (APIs)

A Thesis Submitted

IN PARTIAL FULFILLMENT OF THE REQUIREMENTS

FOR THE DEGREE OF

DOCTOR OF PHILOSOPHY

IN

FORENSIC SCIENCE

By

MAYURI KUMARI

18SBAS3010005

SCHOOL OF BIO-MEDICAL SCIENCES

Supervisor

Prof. Divya Tripathy
School of Basic Sciences

Co-Supervisor

Prof. Anjali Gupta
School of Basic Sciences

Co-Supervisor

Dr. Vikas Bansal
Head (R&D)
Agnitio Pharma (Noida)



GALGOTIAS UNIVERSITY
UTTAR PRADESH

April 2024

APPROVAL SHEET

This thesis/dissertation/report entitled **SYNTHESIS AND CHARACTERISATION OF GENOTOXIC AND PROCESS IMPURITIES OF ACTIVE PHARMACEUTICAL INGREDIENTS (APIs)** by **MAYURI KUMARI** is approved for the degree of **DOCTOR OF PHILOSOPHY IN FORENSIC SCIENCE.**

Examiners

Supervisor (s)

Chairman

Date:_____

Place:_____

CANDIDATE'S DECLARATION

I hereby certify that the work which is being presented in the thesis, entitled “**Synthesis and Characterization of Genotoxic and Process Impurities of Active Pharmaceutical Ingredients (APIs)**”, in fulfilment of the requirements for the award of the degree of Doctor of Philosophy in Forensic Science, School of Bio-Medical Sciences, Galgotias University, Greater Noida is an authentic record of my own work carried out during a period from 2019 to 2023 under the supervision of Prof. (Dr) Divya Tripathy, Prof. (Dr) Anjali Gupta and Dr Vikas Bansal.

The matter embodied in this thesis has not been submitted by me for the award of any other degree of this or any other University/Institute.

(Mayuri Kumari)

This is to certify that the above statement made by the candidate is correct to the best of our knowledge.

Dr. Divya Tripathy
Supervisor
School of Basic Science

Dr. Anjali Gupta
Co-Supervisor
School of Basic Science

Dr. Vikas Bansal
Head (R&D)
Agnitio Pharma (Noida)

The Ph.D. Viva-Voice examination of _____ Research Scholar,
has been held on ____.

Sign. of Supervisor

Sign. of Co-Supervisor

Sign. of Co_Supervisor

Sign. of External Examiner

ABSTRACT

Active Pharmaceutical Ingredients (APIs) are biologically active substances responsible for medication's therapeutic efficacy and safety. They are the backbone of the pharmaceutical industry, and their assurance and effectiveness are critical to the health and well-being of the public. As such, strict quality control standards and regulatory guidelines are in place to validate the assurance and effectiveness of APIs. Developing new and innovative APIs is a critical research domain in the therapeutic industry, as it can revolutionize the treatment of a wide range of diseases and health conditions. The discovery of new APIs requires significant investment in research and development, and the process can take many years due to the rigorous testing necessary to ensure their safety and efficacy. Impurities formed during the bulk manufacturing of drugs present in APIs can significantly affect drug formulations' assurance, excellence, and effectiveness. The formation pathways of impurities play a vital role in understanding their properties and designing appropriate measures to control them. Impurities can arise due to various factors, including the raw materials used in producing, storing, and transporting the final product. So, it is essential to detect the primary origin of impurities and control their formation to ensure the assurance of the final product. This research focuses on two APIs, Rufinamide and Lidocaine, subject to strict regulatory guidelines. Impurities in these APIs are known to be a significant concern, and their synthesis and characterization are essential to understanding their properties and effects.

Rufinamide is a type of medication that belongs to the antiepileptic drug class and is primarily used to treat seizures that are linked with Lennox-Gastaut syndrome. This neurological disorder is characterized by multiple types of seizures that start in early childhood and are usually difficult to manage with conventional treatments. Rufinamide stabilizes the brain's electrical activity and reduces the frequency and intensity of seizures. A total of 9 impurities of Rufinamide were synthesized using a green and cost-effective 1,3-dipolar cycloaddition approach with benzyl bromide derivatives methodology, optimizing reaction conditions, solvents, and catalysts to enhance efficiency and yield. This

study also investigated the hydrolysis process to convert a cycloadduct product to Rufinamide under different conditions, emphasizing the critical role of specific solvents and catalyst concentrations for successful hydrolysis. The research provides a sustainable route for Rufinamide production. The maximum yield of most of the products was obtained between 90 and 97% by the stoichiometry of the reactions.

Lidocaine, being an amino amide, is a well-known drug that is utilized for several numbing purposes. Through systemic intravenous injection, lidocaine becomes more extensive in many situations of acute and chronic pain, such as visceral pain, labor pains, postoperative pain, neuropathic pain, postherpetic neuralgia, hyperalgesia, visceral pain, and centralized pains. A total of 13 impurities of Lidocaine were synthesized through a cost-effective green methodology with high yields, utilizing palladium over carbon as a reducing agent and less hazardous inorganic salts to create an eco-friendly and safer process. The synthesized compounds exhibit potential biomedical applications, including inducing cancer cell death or protective autophagy. The maximum yield of most of the products was obtained between 90 and 97% by the stoichiometry of the reactions.

The research also discusses the synthesis of impurities in Rufinamide and Lidocaine, highlighting their academic and industrial relevance across various scientific disciplines. Efficient synthetic protocols for these impurities open new avenues for innovation and drug discovery in the pharmaceutical industry. The optimization process for synthesizing Rufinamide without isolating it as a single intermediate has significantly reduced cycle time, saving time and cost while maintaining high product quality. Monitoring lidocaine levels is crucial to prevent toxicity, with healthcare professionals needing to understand its toxicity and effective management strategies, especially in high-risk scenarios involving intravenous lidocaine infusions.

These impurities were formed through various pathways, including oxidation, dealkylation, and nitration. It found that the impurities could be controlled by optimizing the synthesis process and using appropriate storage conditions. For example, these are formed due to oxidation, which could be controlled by using antioxidants during synthesis

and storing the final product in a dark and cool environment. The synthesized impurities and their formation pathways are identified and characterized using NMR and MS spectroscopy. The results contribute to the ongoing efforts to improve pharmaceutical quality control and regulatory compliance, ultimately benefiting public health and ensuring the effectiveness of these critical medications. It is essential to understand the formation pathways of impurities and design appropriate measures to control them. Advanced analytical techniques in this study have provided valuable information that will help pharmaceutical companies improve product integrity.

Lastly, APIs are critical to the pharmaceutical industry, and their safety and effectiveness are paramount to the health and well-being of the public. Impurities in API can reduce the integrity, assurance, and effectiveness of the drug. So, excipient and product quality rely on understanding impurities formation pathways. The application of state-of-the-art analytical procedures in this research has presented essential information that pharmaceutical companies' success depends on to guarantee the integrity and success of their products. At large, the public is the beneficiary, and the effectiveness of medications is not compromised. Considering the impurities pivots, they acquire greater relevance in polymer chemistry, biological chemistry, and materials science, characterized by unique features. The implication of azole and amide-type groups into polymers could substantiate the advent of materials with predesigned and distinctive qualities. Along with azole as the basic building block, such compounds can serve multiple purposes as molecular probes for investigating biomolecular connections and biological processes in this subject. The fact that they can be used to study a particular biomolecule's structural and functional features comes from the ability to interact with biomolecules and proteins directly. For example, introducing these contaminations can cause the user to interact with biomolecules and proteins directly from materials with higher conductivity, mechanical strength, and thermal stability. In addition, a fusion of these impurities contributes to the resistance of polymers to such factors as heating, moisture, and UV rays from the sun inside the material.

DEDICATED

TO

MY FAMILY

ACKNOWLEDGEMENTS

I would like to express my appreciation to everyone from Agnitio Pharma, Noida, and Galgotias University who have made this research possible:

First and foremost, I wish to express my wholehearted thanks and gratitude to our Honourable Chancellor and His Excellency **Mr Suneel Galgotia**, CEO **Mr. Dhruv Galgotia**, and Director Operations **Ms. Aaradhana Galgotia**, Galgotias University for extending their support in completing this research.

I wish to express my sincere thanks to Honourable Vice Chancellor **Dr. K Mallikharjuna Babu**, Pro Vice-Chancellor **Dr. Avadhesh Kumar**, Registrar, Controller of **Examinations**, and Deans Galgotias University for their guidance and support.

I would like to express my gratitude to my supervisor, **Prof. (Dr.) Divya Tripathy**, and Co-supervisor, **Prof. (Dr.) Anjali Gupta**, and **Dr. Vikas Bansal (Head, R & D)**, **Agnitio Pharma**, for providing me with invaluable guidance and support throughout the research process. Their insightful comments and suggestions have been instrumental in shaping the direction of this research.

I would like to express my gratitude to **Professor Ranjana Pattnaik (Dean, School of Biomedical Science)** and **Prof (Dr.) Rajeev Kumar (Program Chair Research), Department of Forensic Science**, for their valuable contributions to knowledge. I also want to express my gratitude to **Associate Professor (Dr.) Vinny Sharma** for her continuous encouragement and suggestions. Additionally, I would like to extend my thanks to all staff and faculty members of the Department of Forensic Science as a whole. I truly learned a lot from each one of you. I am also grateful to the staff and faculty of the School of Biomedical Science for their support and provision of resources throughout this research. Lastly, I must acknowledge the indispensable opportunities and resources provided by the Research and Development department at Agnitio Pharma, Noida, which were instrumental in the successful completion of this research.

I am thankful to my father, **Mr. Shyam Babu**, my loving mother, **Mrs. Mamta Kumari**, and my dear brother, **Mr. Himanshu Raj**; they have supported me in every way; without their blessing and financial support, I would not have been able to complete this accomplishment.

I would like to show my special regards to my close friends **Kirti Sharma, Das Anamika**, and **Mukul Kumar** for their continuous encouragement, suggestions, and help. Their consistent patience and understanding have been a constant source of motivation and inspiration for me.

I sincerely appreciate all those who have contributed to this research. Without their support, this thesis would not have been completed.

Thank you.

TABLE OF CONTENTS

APPROVAL SHEET	ii
CANDIDATE’S DECLARATION	iii
ABSTRACT	iv
DEDICATION	vii
ACKNOWLEDGEMENTS	viii
LIST OF FIGURES	xiv
LIST OF TABLES	xxi
LIST OF PUBLICATIONS	xxii
LIST OF ABBREVIATIONS AND SYMBOLS	xxiii
CHAPTER 1: ACTIVE PHARMACEUTICAL INGREDIENTS (APIS)	1
1.1 INTRODUCTION	1
1.2 CLASSIFICATION OF APIS	2
1.3 CHRONOLOGY OF APIS	7
1.4 QUALITY ASSURANCE FOR API	9
1.5 DRUG IMPURITIES	10
1.5.1 Regulatory Rules on impurities in APIs	11
1.5.2 Terminologies Used in the drug impurities	12
1.5.3 ICH Limits for Impurities	15
1.5.4 Sources of Impurities	16
1.5.4.1 Crystallization-related impurities	16
1.5.4.2 Stereochemistry-related impurities	16
1.5.4.3 Residual solvents	17
1.5.4.4. Synthetic by-products and intermediates	19
1.5.4.5. Formulation-related impurities	19
1.5.4.6 Impurities arising during storage	22

1.6. GENOTOXIC IMPURITIES (GIs)	23
1.6.1 TAXONOMY OF GIs	23
1.7. ANALYTICAL METHOD DEVELOPMENT FOR IMPURITY DETECTION	25
1.7.1 Method of Reference Standards	26
1.7.2. Spectroscopical Methods	27
1.7.3. Methods of Separation	28
1.7.4. Isolation Methods	29
1.8. CHARACTERIZATION OF IMPURITY	32
1.8.1 Characterization Techniques	32
1.8.2 Hyphenated Techniques	33
1.9 SIGNIFICANCE OF SYNTHESIS OF	
DRUG IMPURITIES	36
1.9.1 Forensic Significance of Drug Impurities	36
CHAPTER 2: LITERATURE REVIEW	38
OBJECTIVES	72
CHAPTER 3: SYNTHESIS AND CHARACTERISATION OF ANTI-EPILEPTIC	
DRUGS (RUFINAMIDE) IMPURITIES	73
3.1 INTRODUCTION TO RUFINAMIDE	73
3.1.1 Chemistry	74
3.1.2 Pharmacology	74
3.1.2.1 Activity in experimental models of seizures and epilepsy	74
3.1.2.2 Mechanism of action	75

3.1.3 Pharmacokinetics	76
3.1.3.1 Bioavailability and Absorption	76
3.1.3.2 Distribution	77
3.1.3.3 Elimination and Metabolism	78
3.1.4 Pharmacokinetics in Special Populations	78
3.1.4.1 Impaired Renal Function	79
3.2 EXPERIMENTAL PART	80
3.2.1 Materials/Chemicals	80
3.2.2 Methods	81
3.3 Result and Discussion	89
3.4 Characterisation of Impurities	97
3.5 Spectral Analysis of Impurities	98
CHAPTER 4: SYNTHESIS AND CHARACTERISATION OF ANAESTHETIC DRUGS (LIDOCAINE) IMPURITIES	110
4.1 INTRODUCTION TO LIDOCAINE	110
4.1.1 Indications	110
4.1.2 Mechanism of Action	111
4.1.3 Administration	112
4.1.4 Side Effects	112
4.1.5 Contraindications	113
4.1.6 Monitoring	113
4.1.7 Toxicity	114

4.2 Enhancing Healthcare Team Outcomes	114
4.3 EXPERIMENTAL PART	115
4.3.1 Materials/ Chemicals	115
4.3.2 Methods	119
4.3.3 Characterization of Impurities	128
4.4 Results and Discussion	129
CONCLUSION	156
REFERENCES	159

LIST OF FIGURES

Figure No.	Name	Page No.
Figure 1.1	The flow map of the synthesis of APIs	8
Figure 1.2	Physical characteristics of API	10
Figure 1.3	Different authorities rules of impurities	11
Figure 1.4	Formation of Diacetylated Paracetamol as by-products	13
Figure 1.5	Impurities categorized by USP	14
Figure 1.6	Types of impurities as per ICH	15
Figure 1.7	Example of stereochemistry-related impurity	17
Figure 1.8	Classification of Residual Solvent	18
Figure 1.9	Examples of residual solvents	18
Figure 1.10	Formation of Indoline derivative	19
Figure 1.11	Salicylic acid impurity	22
Figure 1.12	Examples of GIs	25
Figure 2.1	Chemical Reagents found in drug	38
Figure 2.2	Impurities of ropinirole hydrochloride	39
Figure 2.3	Synthesis of Olanzapine	40
Figure 2.4	Impurities of Raloxifene hydrochloride	41
Figure 2.5	Impurities of Retigabine	42
Figure 2.6	Chemical Structure of Impurity	43
Figure 2.7	Impurities of Flupirtine maleate	44

Figure 2.8	Chemical Structure of Impurity	45
Figure 2.9	Synthesis of Zidovudine	45
Figure 2.10	Chemical Structure of API	46
Figure 2.11	Chemical Structure of Impurity	46
Figure 2.12	Chemical Structure of Co-crystal	47
Figure 2.13	Chemical structure of API	48
Figure 2.14	Chemical structure of 7-tetradecenal and Octadecenoic acid	48
Figure 2.15	Impurities found in Amphetamine Type Stimulants	49
Figure 2.16	Impurities found in Vortioxetine	50
Figure 2.17	Chemical structure of API	50
Figure 2.18	Chemical structure of MDMA	50
Figure 2.19	Chemical Structure of Levothyroxine Impurities	51
Figure 2.20	Impurities of Eletriptan	52
Figure 2.21	Impurities of Ticaglor	53
Figure 2.22	Impurity of Vildagliptin	54
Figure 2.23	Chemical Structure of Levothyroxine	54
Figure 2.24	Impurities of isoproterenol hydrochloride	55
Figure 2.25	Impurities of clobazam	56
Figure 2.26	Impurities of Sertalone	57
Figure 2.27	The conversion of MMS into DMS and sulfuric acid	58
Figure 2.28	Impurities of Carisoprodol	59

Figure 2.29	Chemical Structure of Olanzapine Impurities	60
Figure 2.30	Chemical Structure of Ornidazole	60
Figure 2.31	Chemical Structure of Eplerenone	61
Figure 2.32	Impurities of Dalfampridine	62
Figure 2.33	Impurities of Ritonavir Hydrochloride	62
Figure 2.34	Impurities of Rabeprazole	63
Figure 2.35	Chemical Structure of Sartan Drugs	64
Figure 2.36	Impurities of Sildenafil Citrate	65
Figure 2.37	Chemical Structure of API	65
Figure 2.38	Impurities of Salbutamol Sulphate	66
Figure 2.39	Chemical Structure of API	66
Figure 2.40	Chemical Structure of Impurities	67
Figure 2.41	Chemical Structure of Nitrosamine	68
Figure 2.42	Chemical Structure of API	68
Figure 2.43	Chemical Structure of API	69
Figure 2.44	Chemical Structure of Mirabegron	69
Figure 2.45	Chemical Structure of API	70
Figure 2.46	Chemical Structure of teriflunomide and moclobemide	70
Figure 2.47	Impurities of Ezetomibe	71
Figure 3.1	Chemical Structure of Rufinamide	74
Figure 3.2	Mechanism of action of Rufinamide	76

Figure 3.3	Synthesis of 3a–3c	82
Figure 3.4	Synthesis of 3d	84
Figure 3.5	Synthesis of 4a–4c	85
Figure 3.6	Synthesis of 4d	86
Figure 3.7	Synthesis of 5a and 5b	87
Figure 3.8	Synthesis of 5c	88
Figure 3.9	Retrosynthesis scheme of Rufinamide Impurities	89
Figure 3.10	Impurity of Rufinamide Acid derivatives	94
Figure 3.11	Synthesis of 4c	95
Figure 3.12	Synthesis of Rufinamide Impurities	96
Figure 3.13	NMR Spectra (3c)	101
Figure 3.14	Mass Report (3c)	101
Figure 3.15	NMR Spectrum (3d)	102
Figure 3.16	Mass Report (3d)	102
Figure 3.17	NMR Spectrum (4a)	103
Figure 3.18	Mass Report (4a)	103
Figure 3.19	NMR Spectrum (4b)	104
Figure 3.20	Mass Report (4b)	104
Figure 3.21	NMR Spectrum (4c)	105
Figure 3.22	Mass Report (4c)	105
Figure 3.23	NMR Spectrum (4d)	106
Figure 3.24	Mass Report (4d)	106

Figure 3.25	NMR Spectrum (5a)	107
Figure 3.26	Mass Report (5a)	107
Figure 3.27	NMR Spectrum (5b)	108
Figure 3.28	Mass Report (5b)	108
Figure 3.29	NMR Spectrum (5c)	109
Figure 3.30	Mass Report (5c)	109
Figure 4.1	Chemical structure of Lidocaine	110
Figure 4.2	Mechanism of action of lidocaine	111
Figure 4.3	Synthesized Lidocaine impurities	118
Figure 4.4	Synthesis of Chloro-substituted Lidocaine Impurities	120
Figure 4.5	Synthesis of Diethylamino-substituted lidocaine impurities	121
Figure 4.6	Synthesis of Dimethylphenyl-substituted lidocaine impurities	122
Figure 4.7	Synthesis of Ethylamino-substituted lidocaine impurities	123
Figure 4.8	Synthesis of intermediate	124
Figure 4.9	Synthesis of isopropyl-substituted lidocaine impurities	124
Figure 4.10	Synthesis of Ethyl methylamino-substituted lidocaine impurities	125
Figure 4.11	Synthesis of Dimethyl phenylamino-substituted lidocaine impurities	126
Figure 4.12	Synthesis of Propienamide-substituted lidocaine impurities	127

Figure 4.13	Synthesis of piperazine-substituted lidocaine impurities	127
Figure 4.14	NMR Spectra (3a)	130
Figure 4.15	Mass Report (3a)	130
Figure 4.16	NMR Spectra (3b)	131
Figure 4.17	Mass Report (3b)	132
Figure 4.18	NMR Spectra (3c)	133
Figure 4.19	Mass Report (3c)	133
Figure 4.20	NMR Spectra (4a)	135
Figure 4.21	Mass Report (4a)	135
Figure 4.22	NMR Spectra (4b)	136
Figure 4.23	Mass Report (4b)	137
Figure 4.24	NMR Spectra (4c)	138
Figure 4.25	Mass Report (4c)	138
Figure 4.26	NMR Spectra (5)	140
Figure 4.27	Mass Report (5)	140
Figure 4.28	NMR Spectra (6b)	142
Figure 4.29	Mass Report (6b)	142
Figure 4.30	NMR Spectra (7b)	144
Figure 4.31	Mass Report (7b)	144
Figure 4.32	NMR Spectra (8)	146
Figure 4.33	Mass Report (8)	146

Figure 4.34	NMR Spectra (9)	148
Figure 4.35	Mass Report (9)	148
Figure 4.36	NMR Spectra (10)	150
Figure 4.37	Mass Report (10)	150
Figure 4.38	NMR spectra (11)	152
Figure 4.39	Mass Report (11)	152

LIST OF TABLES

Table No.	Name	Page No.
Table 1.1	Classification of APIs	3-5
Table 1.2	Types of APIs according to their source and origin	6,7
Table 1.3	Types of impurities in drug substances	24
Table 1.4	Process Description of the Development	26
Table 1.5	Goals of Impurity Investigations	36
Table 3.1	List of Organic solvents used for the synthesis of Rufinamide process impurities	80
Table 3.2	List of chemicals used for the synthesis of Rufinamide process impurities	81
Table 3.3	Reaction Conversion in Different Solvents	91
Table 3.4	Optimization of Volume of water	92
Table 3.5	Reaction Conversion at different temperatures	93
Table 3.6	Mass and HNMR spectra of impurities	98-100
Table 4.1	List of Organic solvents used for the synthesis of Lidocaine process impurities	116
Table 4.2	List of chemicals used for the synthesis of Lidocaine process impurities	117
Table 4.3	Maximum yield of lidocaine impurities	153-155

LIST OF PUBLICATIONS

S. NO	TITLE	STATUS	YEAR	INDEX	JOURNAL
1	Analytical Methods and their significance in pharmaceutical process impurities: A review	Published	2024	Scopus/ Web of Science	Macromolecular Symposia
2	Synthesis of Anti-Epileptic Drug: Rufinamide and Its Process-Related Impurities	In Press	2024	Scopus	Russian Journal of Organic Chemistry
3	Cost Effective Synthesis and Spectral Characterization of Lidocaine Analogs	Submitted	2024	Scopus	Chemical and Pharmaceutical Bulletin
4	Microwave Synthesis, Characterization and Properties Evaluation of Gemini Imidazoline Surfactants based on dibromopropane	Published	2022	Scopus	Surface Review and Letters
5	Method of Preparing Adsorbent For Removal of Dye From Water	Published	2021	Indian Patent	Official Journal of The Patent Office
6	Protein Based Surfactants (Book Chapter)	Published	2021	Scopus	Surfactants based on Renewable Raw Materials
7	The Landscape on the metal analysis in green vegetables: A review	Published	2020	Scopus	Journal of Natural Remedies

LIST OF ABBREVIATIONS AND SYMBOLS

APIs	Active pharmaceutical ingredients
OTC	over-the-counter
DNA	Deoxyribose Nucleic Acid
GTIs	Genotoxic Impurities
ICH	International Conference on Harmonization
IP	Indian Pharmacopoeia
USP	United States Pharmacopeia
BP	British Pharmacopoeia
MS	Mass spectrometry
HPLC	High-Performance Liquid Chromatography
NMR	Nuclear Magnetic Resonance
FTICR-MS	Fourier Transform Ion Cyclotron Resonance Mass Spectrometry
FTIR	Fourier Transform Infrared
GC-FID	Gas Chromatography-Flame Ionisation Detection
HPLC-FLD	High-Performance Liquid Chromatography with Fluorescence Detection
NCE	New chemical entity
GC-MS	Gas Chromatography-Mass Spectrometry
MDMA	Methylenedioxymethamphetamine
NaO ₂	Sodium Oxide
SiO ₂	Silicon Oxide
CaO	Calcium Oxide
MgO	Magnesium Oxide
Na	Sodium
DEHP	Diethylhexylphthalate
PVC	Polyvinyl Chloride
EMA	European Medicines Agency

FDA	Food and Drug Administration
SAR	Structure-Activity Relationships
TTC	Threshold of Toxicological Concern
LSS	Linear solvent strength
UV	Ultraviolet
IR	Infrared
CE	Capillary electrophoresis
GC	Gas Chromatography
SFC	Supercritical Fluid Chromatography
TLC	Thin-layer Chromatography
HPLC	High-Performance Liquid Chromatography
HPTLC	High-Performance Thin Layer Chromatography
SCF	Supercritical fluid
ESI	Electrospray ionization
LRMS	Low-resolution Mass Spectral
LC-MS	Liquid Chromatography-Mass Spectrometry
LC-GC	Liquid chromatography-gas chromatography
HPLC-MS	High-performance liquid chromatography-mass spectrometry
RP-HPLC	Reverse Phase-High-performance liquid chromatography
RP-LC	Reverse Phase-Liquid Chromatography
CZE-MS	Capillary zone electrophoresis-mass spectrometry
ESI-MS	Electrospray Ionization-mass spectrometry-mass spectrometry
APCI-MS	Atmospheric pressure chemical ionization-mass spectrometry
APPI-MS	Atmospheric pressure photoionization-mass spectrometry
TSI-MS	Thermospray ionization-mass spectrometry
DMS	Dimethyl sulphate
MMS	Monomethyl sulphate
TSE	Twin-screw extrusion

LGS	Lennox-Gastaut syndrome
VGSCs	Voltage-gated sodium channels
NIH	National Institute of Health
MES	Maximal electroshock
PTZ	Pentylentetrazole
NMDA	N-methyl-d-aspartate
LRMS	Low-resolution mass spectral analysis
TOF	Time of Flight
DMSO	Dimethyl sulfoxide
DCM	Dichloromethane
ACN	Acrylonitrile
MeOH	Methanol
SOCl ₂	Thionyl Chloride
RM	Reaction Mixture
H ₂ O	Water
H ₂ SO ₄	Sulfuric Acid
NaOH	Sodium Hydroxide
NaHCO ₃	Sodium Bicarbonate
KOH	Potassium Hydroxide
K ₂ CO ₃	Potassium Carbonate
KI	Potassium Iodide
HCL	Hydrochloric Acid
KMnO ₄	Potassium Permanganate
CH ₃ CN	Acetonitrile
MNNG	Methylnitronitrosoguanidine
PDA	Powder Diffraction Analysis
TNX	Tenoxicam
ED	Effective Dose

VD	Volume of Distribution
GP	Glycoprotein
CC	Cardiac Collapse
CNS	Central Nervous System
RT	Room Temperature
DM	Demineralization
SM	Starting Material
a.k.a	As known as
Ruf	Rufinamide
XRDA	X-ray Diffraction Analysis
SIF	Simulated Intestinal Fluid
TRIS	Transient Radicular Irritation Syndrome
Mg/kg	Milligram/kilogram
COOH	Carboxylic Acid
OH	Methoxy
NH ₄ HCO ₂	Ammonium Carbamate
H ₄ N ₂ S	Diazathiane
GABA	Gamma-aminobutyric Acid
5A2Cl	5-amino-2-chloropyridine
TIC	Ticaglor

CHAPTER 1: ACTIVE PHARMACEUTICAL INGREDIENTS (APIs)

1.1 INTRODUCTION

A drug is utilized to diagnose, treat, alleviate, and prevent illnesses in humans and animals. It consists of two components. APIs serve as the components produced by pharmaceutical companies, playing a role in making the desired effects of the medication. APIs have a range of applications. It can be found in various products, for instance, OTC and prescription medicines. The global market for APIs is projected to expand due to the growing demand for new and innovative treatments due to changing disease patterns, ageing populations in some areas, and the emergence of novel medications and technologies. These factors all impact the development process for new drugs. The healthcare sector is witnessing a significant transformation due to the growing influence of emerging economies. These countries have unique healthcare requirements, driving investments in drug research & development and attracting multinational companies to set up operations across different regions. The API market is expected to grow by 5.90% due to several factors. First, the production of APIs has been increasing, which is expected to continue. Second, the number of people suffering from chronic diseases like cancer and cardiovascular conditions is rising, which is driving up demand for APIs. Third, government regulations supporting API manufacturing and geopolitical factors influence the market's growth [1–5].

APIs are essential organic molecules used in the production of final pharmaceutical products. Their primary function is to deliver the intended therapeutic effect to diagnose, cure, mitigate, treat, or prevent diseases. Simply put, APIs are the active components in medicines that make them effective. They play a pivotal role in developing modern medicine by restoring, correcting, or modifying human physiological functions. In contrast, the second component of a drug, known as the excipient, serves as the filler or binder material to create the drug or tablet. This excipient is an inactive substance added to a

medication to impact its physical qualities, like stability and solubility. It has a vital role in the drug's formulation, not its therapeutic effect. If, for instance, a drug is in liquid form, its excipient could be a liquid like carbohydrates, stearate, or antioxidants. The excipient ensures the drug's stability, safety, and effectiveness, working hand in hand with API to create a well-formulated drug [6–12].

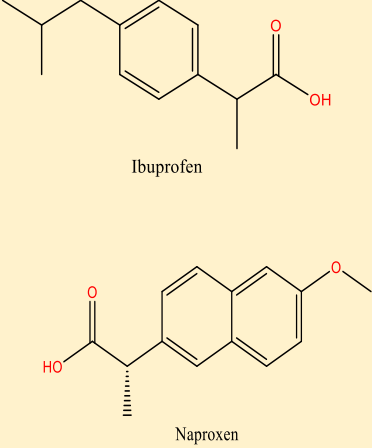
APIs can be obtained from natural sources like plants or in a laboratory. These are usually formulated into tablets or capsules before being marketed. APIs are manufactured through many processes, such as:

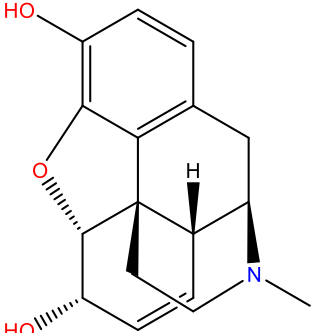
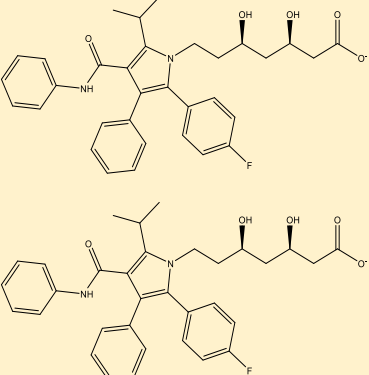
- ✚ Chemical synthesis combines different chemical compounds to create new molecules.
- ✚ Fermentation processes use microorganisms to produce the desired API.
- ✚ Recombinant DNA technology involves modifying DNA to produce proteins with therapeutic properties.
- ✚ Isolation and recovery from natural sources involve extracting APIs from plants, animals, or minerals.
- ✚ Combining these processes may sometimes manufacture APIs [13–16].

1.2 CLASSIFICATION OF APIs

There are four primary categories of APIs, which are categorized based on their structure and medical applications as mentioned in **(Table 1.1)** [17–23] and types of APIs according to their source and origin as mentioned in **(Table 1.2)**:

Table 1.1: Classification of APIs

<i>Types of APIs</i>	Definition	Uses and Examples	Structure
<i>Synthetic API</i>	<p>Synthetic API is manufactured through chemical synthesis, combining specific chemical ingredients in a replicable ordered process. They have well-defined chemical structures; hence, batches are identical. They can be further processed into different dosage forms and administered through various routes (tablets, syrup, capsules, injections, etc.)</p>	<p>Ibuprofen and naproxen treat pain and inflammation caused by musculoskeletal disorders and arthritis.</p>	 <p>The image shows two chemical structures. The top structure is Ibuprofen, which consists of a benzene ring with a 4-(4-isobutylphenyl)butanoic acid side chain. The bottom structure is Naproxen, which consists of a naphthalene ring system with a 6-methoxy group and a 2-(6-oxoheptanoic acid) side chain. The carboxylic acid groups in both structures are highlighted in red.</p>

<p><i>Natural API</i></p>	<p>Natural API is manufactured in a living system, e.g., a microorganism, animal, or plant cell. These APIs are extremely large, complex molecules or mixtures of molecules, making them hard to characterize. Generally, they are made in genetically engineered cell cultures, and batch-to-batch variation is an inherent characteristic of biology.</p>	<p>Morphine, codeine, and quinine are manufactured to reduce the risk of addiction and respiratory depression.</p>	 <p>Morphine</p>
<p><i>Non-Potent API</i></p>	<p>Non-potent APIs are compounds that do not produce a biological response at an extremely low dose.</p>	<p>They are used to treat various diseases in humans and animals. E.g., Atorvastatin</p>	 <p>Atorvastatin</p>

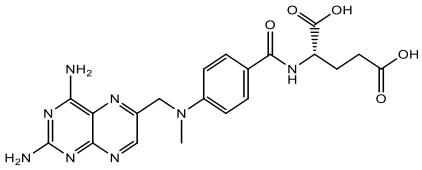
<p><i>Highly Potent APIs</i></p>	<p>Highly Potent APIs are compounds that exert a biological activity that can potentially cause cancer, mutations, developmental effects, or reproductive toxicity at low doses.</p>	<p>They are traditionally used for the treatment of cancer.</p> <p>Ibrutinib, Etoposide, Carfentanil, and Methotrexate</p>	 <p>The image shows the chemical structure of Ibrutinib, a BTK inhibitor. It features a quinazoline ring system with amino groups at the 2 and 8 positions. A methyl group is attached to the nitrogen at the 4-position. This is linked via a methylene group to a para-substituted benzene ring. The benzene ring is further substituted with a propionic acid chain (CH2-CH2-COOH) and a hydroxamic acid group (-NHOH) at the 1-position.</p>
----------------------------------	--	--	---

Table 1.2: Types of APIs according to their source and origin [24,25]

Active Type	Source	Examples
Conventional small-organic molecules	Synthetic organic chemistry	Paracetamol, Ibuprofen, Imatinib
Conventional small-organic molecules	Natural products	Paclitaxel, Aminoglycoside antibiotics, Opiates & Ciclosporin
Conventional small-organic molecules	Semisynthetic compounds (derived from nature and modified in the laboratory)	Penicillin (Ampicillin) and simvastatin
Peptides & proteins	Synthetic	Vasopressin & Somatostatin
Peptides & proteins	Extracted from natural sources (human, animal, or microbial)	Insulin, Growth hormone & Human γ -globulin
Peptides & proteins	Recombinant DNA technology	Insulin, Erythropoietin, TNF-alpha
Antibodies	Animal antisera & human immunoglobulins	Snake & Spider venoms & HNIG
Antibodies	Monoclonal antibodies	Rituximab, Trastuzumab, etc.
Enzymes	Recombinant DNA technology	Dornase, Galactosidase

Vaccines	Whole organisms (live or attenuated)	Smallpox, TB, tetanus, etc., vaccines
Vaccines	Antigen-based vaccines produced by recombinant DNA technology	Several
DNA and mRNA products	Recombinant DNA technology	Patisiran
Cells	Human donors and engineered cells	Various stem cell therapies
Tissues	Human-animal donors engineered tissues	Various
Organs	Human donors	Transplant surgery

1.3 CHRONOLOGY OF APIs

The medicinal industry has a rich history of developing industrial processes to manufacture new medications. As far back as the 19th century, companies began developing efficient processes to produce these drugs. The increasing complexity of medications has led to a need for more sophisticated manufacturing strategies, particularly in outsourcing. In the 21st century, there has been a renewed focus on chemical process safety and the environmental impacts of drug synthesis. These issues are of paramount importance to process chemists and engineers alike, as they must find ways to develop safe and environmentally friendly processes. The main application of organic synthesis in the process development industry is designing and developing synthetic routes for active pharmaceuticals. In addition, the research and development process is an essential part of

the generic medicinal industry, which plays a necessary role in delivering a safe, efficient, robust, and environmentally friendly synthesis of medicines to treat human diseases. Furthermore, the global demand for cost-effective drugs is rising, which is expected to continue. Therefore, the medicinal industry continuously seeks innovative methods to enhance operations and create advanced technologies to address this increasing need [26–29]. The synthesis of API shown in **Figure 1.1**.

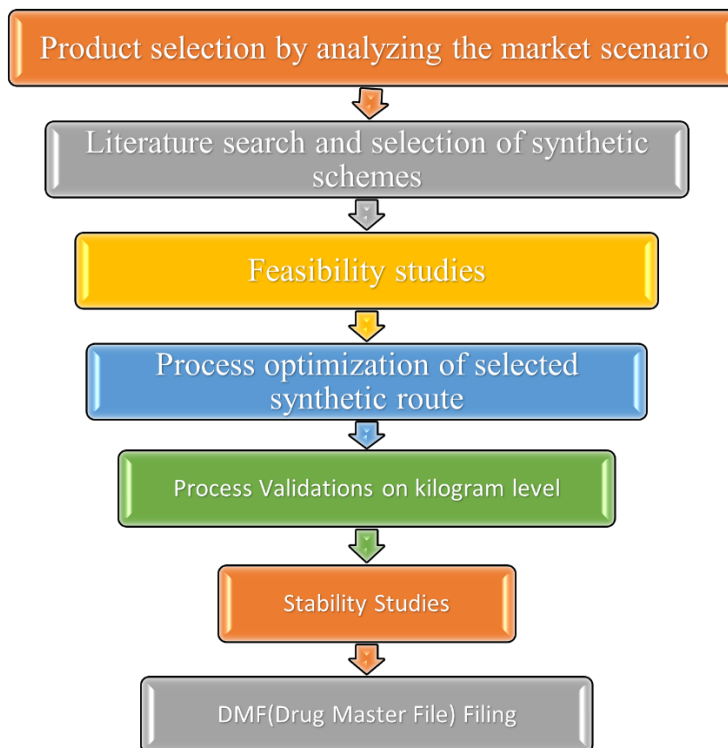


Figure 1.1: The flow map of the synthesis of APIs [30]

The points that need to be followed to manufacture the APIs in a safe and eco-friendly manner are [31,32]:

1. To develop the production process, it is essential to use safe chemicals for the environment and human health.
2. Reduce the number of solvents used to minimize their environmental impact.
3. Ensure that all raw materials are fully utilized in the production process to achieve material balance.

4. experiments should be conducted at room temperature to reduce energy usage during production.
5. Use renewable raw materials, reagents, solvents, and feedstock instead of non-renewable ones.
6. Avoid or minimize protective groups to reduce waste generation.
7. Plan for catalytic reactions instead of stoichiometric reactions to increase efficiency and reduce waste.

1.4 QUALITY ASSURANCE FOR APIs

Bringing innovative drugs to the market has become progressively expensive, exceeding a billion dollars. The high cost is due to a lengthy, challenging, and costly drug development process, which involves complex modalities and a high degree of uncertainty. The cost of developing drugs is high due to the necessity for increased knowledge about the disease's mechanism, process understanding, and the pressure from regulatory authorities to produce safe, effective, and high-quality drugs. As a result, the industry is changing its approach to focus on quality from the foundational level, leading scientists to spend more time on early-phase drug development activities [33, 34].

A drug product's success or failure depends on the API's physical and chemical properties and how it interacts with the excipient in its container closure system. The API's physical characteristics, such as particle size, polymorphism, and solubility, can affect its stability, efficacy, and delivery, as discussed in **Figure 1.2**.

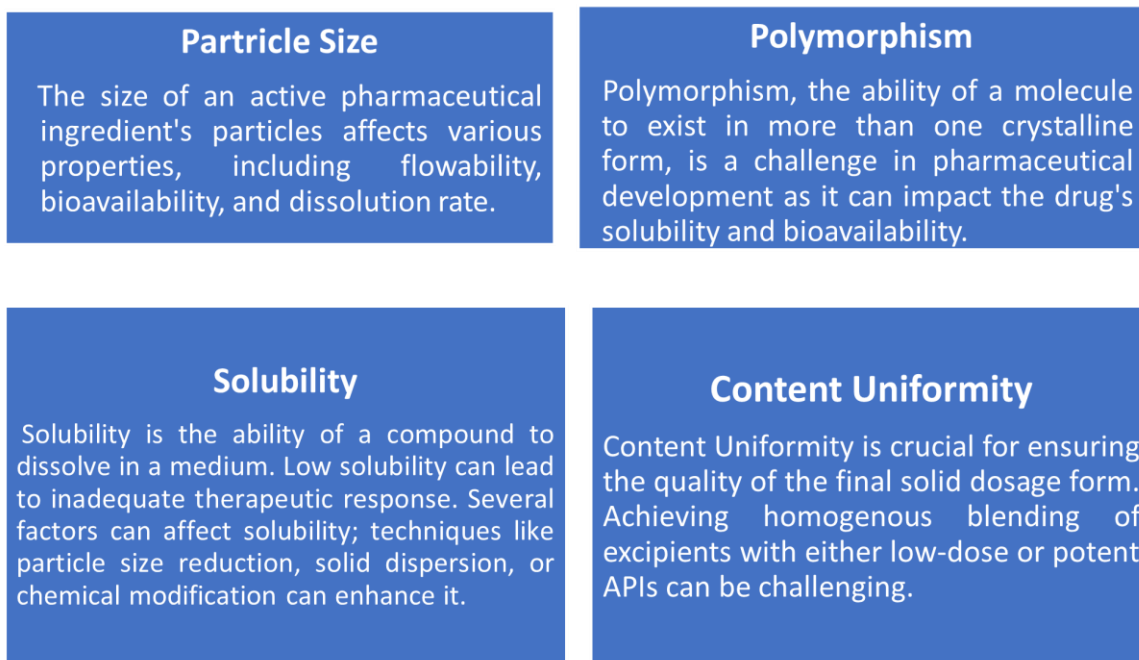


Figure 1.2: Physical characteristics of API [35–37]

In addition to the parameters mentioned above, the impurity found in the drug is additional and one of the most important parameters that decide the activity of any drug. This may be formed during manufacturing as well as in the final drug.

1.5 DRUG IMPURITIES

An impurity of the drug can be understood as a substance present in the reactants, excipients, and leading products but not in the central and active component. These impurities may form during the drug manufacturing process that can result from parallel chemical reactions along with the main route or can be generated within the product due to external conditions like degradation or weather conditions [International Conference on Harmonization (ICH) Q6A: Specifications]. Even minute quantities of impurities impact the effectiveness and assurance of therapeutic products. It is crucial to conduct impurity profiling to regulate the type and amount of such impurities. The "impurity profile" characterization includes specified and unspecified impurities of a group of typical batches

of an API produced under a fully organized production cycle. These impurities have become a concern for regulatory authorities (Pharmacopoeias). Various Pharmacopoeias, such as the IP, USP, and BP, are gradually establishing limits on the acceptable quantities of impurities in APIs or their processing. ICH of Technical Requirements for Registration of Pharmaceuticals for Human Use has issued rules for validating methods to analyze microbiological impurities, by-products, and residual solvents in new drugs. These rules can help ensure the accuracy of the analysis and maintain safety in developing new pharmaceutical products [38–40].

1.5.1 Regulatory rules on impurities in APIs

It is essential to monitor impurities in drug products for ethical, economic, competitive, safety, and efficacy reasons. The definition of monitoring and controlling impurities can vary from person to person or even for the same person at different times, especially in the therapeutic industry. It is essential to establish a unified terminology to ensure a mutual understanding of inquiries related to impurities. [41–43].

The varied governing rules of different authorities regarding impurities are as follows in **Figure 1.3**:

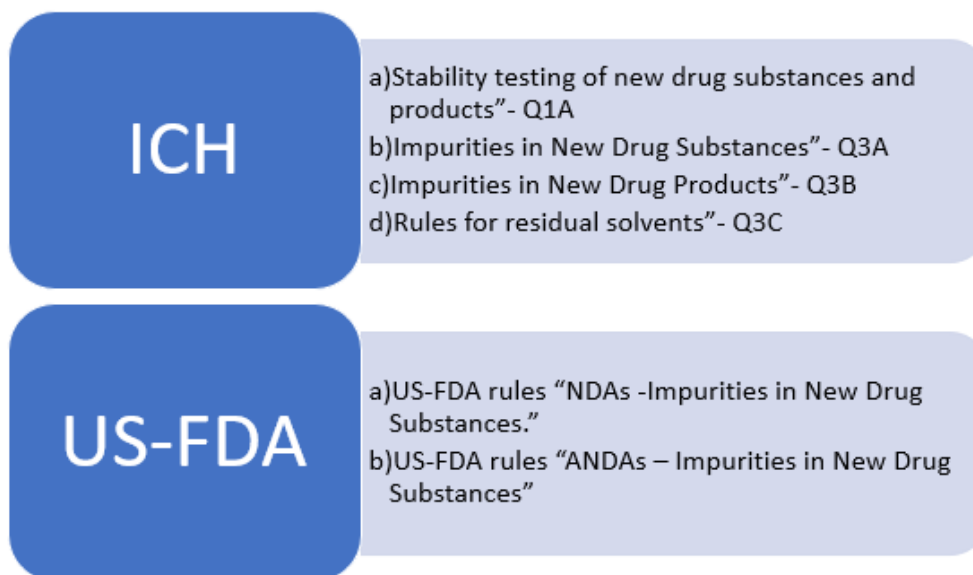


Figure 1.3: Different authorities rules of impurities

Such governing bodies have also published rules for identifying and isolating degradation products and PRIs using NMR, HPLC, MS, Tandem MS, and FTICR-MS for pharmaceutical substances [44].

1.5.2 Terminologies Used in the Drug Impurities

The ICH has classified impurities and given them different names as follows: [45–47]:

a) Common names

- ❖ **By-products:** The compounds formed because of a chemical reaction but are not the intended intermediates. They are essentially unintended or undesired products of a reaction. They can arise for various reasons, such as unwanted side reactions, overreaction, incomplete reactions, demonization, rearrangement, or undesired interactions between intermediates, starting materials, catalysts, or chemical reagents. These impurities can be formed in various amounts, from trace to significant quantities. They can have various properties, such as toxicity, flammability, or reactivity, and pose health, safety, and nature risks. Therefore, it is essential to understand the mechanisms and factors that influence the formation of by-products in chemical reactions and to minimize their production by optimizing reaction conditions, selecting appropriate reaction pathways, and designing efficient and selective catalysts.
- ❖ **Intermediates:** These are chemical compounds formed because of a series of chemical reactions that occur during the synthesis of a desired material. They are neither the final product nor the starting material; instead, they are formed at some point in the synthetic route. These compounds play an essential role in the synthesis process by serving as building blocks or intermediaries that undergo further reactions to yield the final product. Moreover, they are often isolated and purified to be used as starting materials for subsequent chemical reactions, or they may be recycled back into the synthesis process to increase overall yield and reduce waste.

❖ **Penultimate intermediates:** In synthesizing a desired compound, the specific compounds are the second to last step in the synthesis chain before the final product is produced. These intermediates are critical to the overall synthesis process, as they significantly control the quality and quantity of the final desired compound. Observing and preventing the formation of penultimate intermediates is crucial to confirm the synthesis process and the desired outcome.

For example, some manufacturers use aminophenol as a starting material or intermediate in producing paracetamol bulk, but it requires a limited test. Obtaining only a final compound with a 100% yield is exceptional in synthesis chemistry and the possibility of having by-products. The bulk paracetamol may result in the formation of diacetylated paracetamol as a by-product shown in **Figure 1.4**.

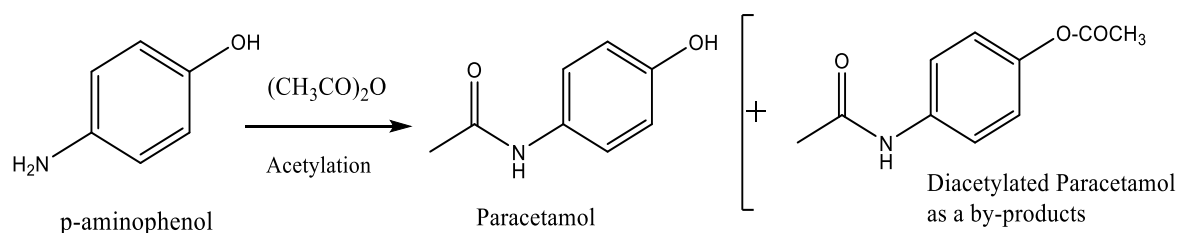


Figure 1.4: Formation of Diacetylated Paracetamol as by-products

❖ **Interaction products:** During synthesizing drugs, specific chemical reactions may occur unexpectedly, forming byproducts that were not intentionally produced or desired. These byproducts can result from various factors, such as the choice of reagents, reaction conditions, and the stability of the intermediates involved in the synthesis. These unintended products can sometimes have undesirable effects on the product's quality, purity, and value, so they are closely observed and controlled during the drug development process.

- ❖ **Related products:** The substances that share chemical similarities with drug substances and may exhibit some biological activity. These products are often synthesized for research purposes and may be used to develop new drugs or study the effects of specific chemical structures on biological systems. However, it is essential to note that these compounds are not intended for consumption and should be handled cautiously by trained professionals in a laboratory setting.
- ❖ **Transformation products:** These products can be known or unknown products that may form due to the transformation of reactants, intermediate, or even products that can occur in a reaction. These products include those produced during a reaction due to the transformation of reactants, intermediates, or products.
- ❖ **Degradation products:** These products are formed by decomposing active ingredients or other materials by external factors like heat and moisture. During bulk drug manufacturing, the end product may degrade and become impurities. Cephalosporin degradation is an eminent example of degradation products, which depend on the presence of a β -lactam ring and an α -amino group in the C⁶/C⁷ side chain.

b) The USP categorizes impurities into three groups shown in **Figure 1.5**.

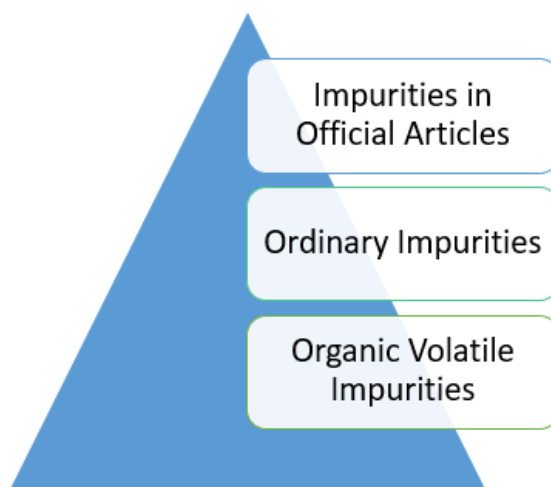


Figure 1.5: Impurities categorized by USP

- c) As stated by ICH, impurities found in drugs manufactured chemically can be classified into three types as shown in **Figure 1.6**:

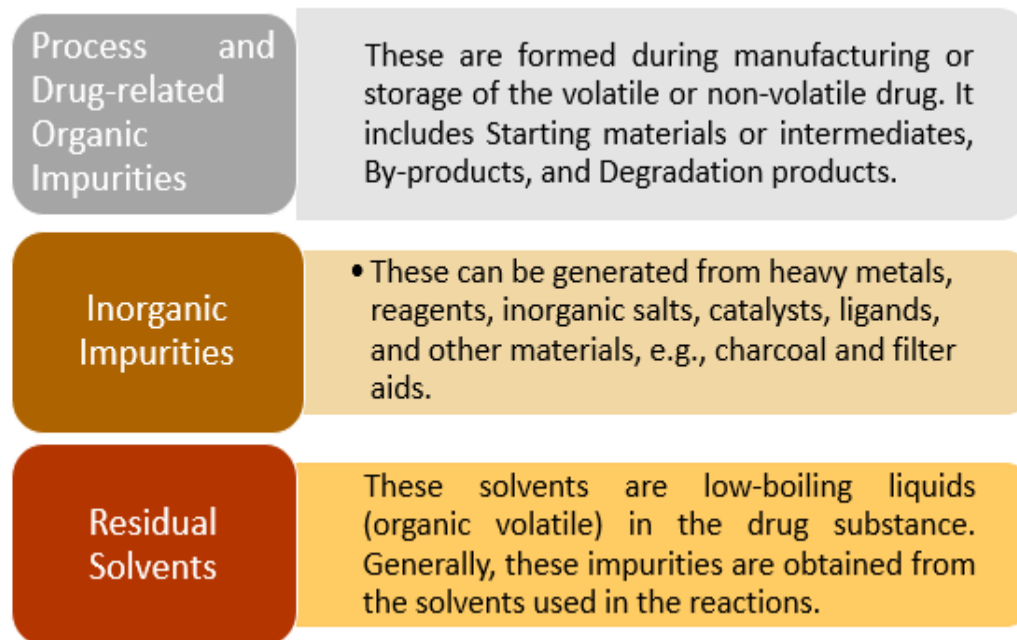


Figure 1.6: Types of impurities as per ICH

Proper care during every step of the multi-step synthesis process is necessary to avoid impurities in APIs.

1.5.3 ICH Limits for Impurities

The rules recommended by ICH for identifying impurities in innovative compounds only when likely to be remarkably toxic or potent, as their levels below 0.1% are not considered necessary. As stated by ICH, if the daily dosage exceeds 2g, the maximum qualification threshold to be considered is 0.05%, or 1mg/day intake, whichever is lower. If the daily dosage is below 2g, the maximum qualification threshold is 0.1% [48,49].

The drug substance specifications must include limitations for every individual impurity that has been identified, as well as any unidentified impurities that are present at or above 0.1%. Additionally, there should be a restriction for any unspecific impurities, with a

maximum limit of 0.1%. Lastly, the specifications should also include the total amount of impurities.

1.5.4 Sources of Impurities

There are numerous sources from which impurities can originate, which are explained as follows:

1.5.4.1 Crystallization-related impurities

Regulatory authorities mandate the medicinal industry to pay close attention to polymorphism and solvatomorphism. Polymorphism and solvatomorphism can be understood as the properties of the compound during crystallization and post-crystallization [50].

1.5.4.2 Stereochemistry-related impurities

Searching for compounds with the same chemical structures but unlike 3-D orientations is essential, as these can be considered impurities in the APIs. Chirality is a common characteristic of several drugs available in the market, which are often provided as a combination of enantiomers rather than individual ones. However, improved chemical entities with better pharmacological profiles are certain single enantiomeric forms of chiral drugs. Some drugs that exist as single isomers are naturally produced and possess a high level of enantioselectivity, eliminating the possibility of enantiomeric impurities. For example, the pharmacokinetic profiles of the R-isomeric form of ofloxacin and the S-isomeric form of levofloxacin are similar, suggesting that single isomers do not have any advantages. Currently, marketed single-isomer drugs include lavalbuterol, and esomeprazole [51]. Example are shown in **Figure 1.7**.

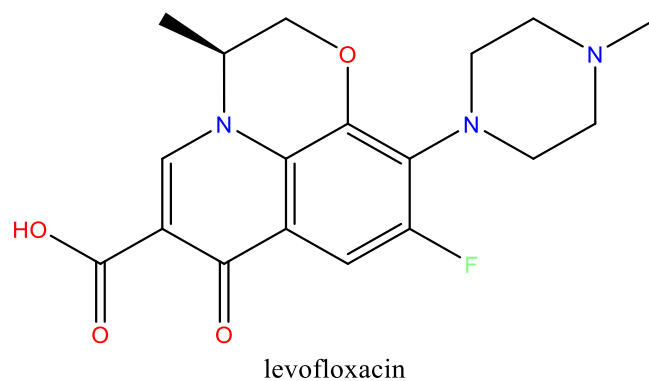


Figure 1.7: Example of stereochemistry-related impurity

1.5.4.3 Residual solvents

Low-boiling solvents that can cause toxicity are called residual solvents. They usually arise from the solvents that produce bulk drugs during the reaction. Three categories of residual solvents are categorized based on the level of risk they pose to human health. These classifications are determined to ensure safety. **Figure 1.8** describes these classes and examples are shown in **Figure 1.9** [52].

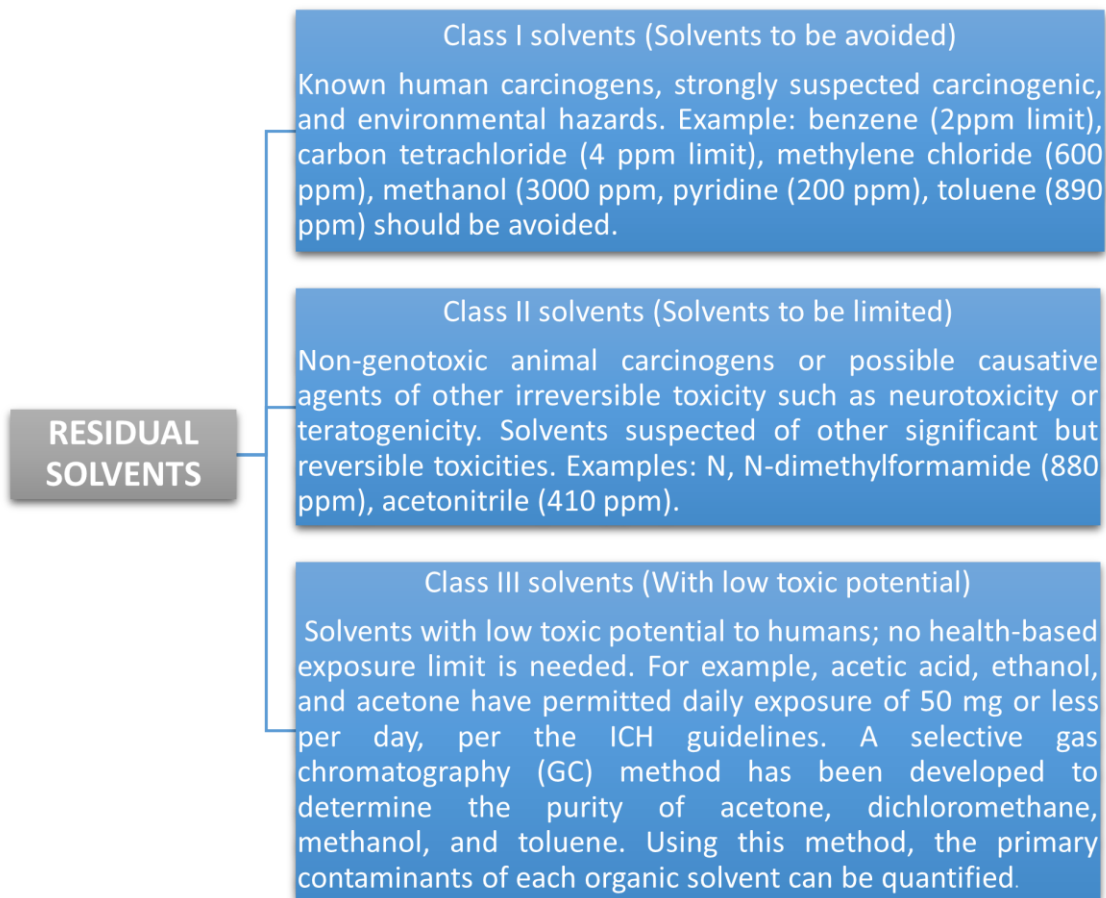


Figure 1.8: Classification of Residual Solvent

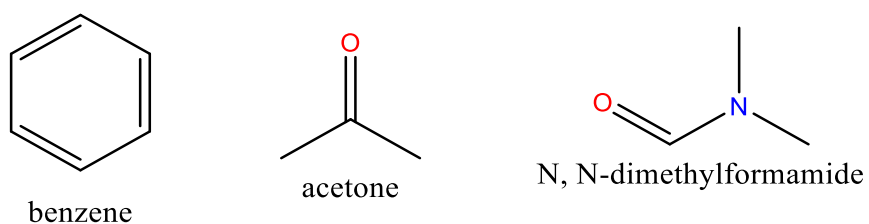


Figure 1.9: Examples of residual solvents

1.5.4.4. Synthetic by-products and intermediates

By-products, raw materials, and intermediates in the synthetic process can be the sources of impurities in therapeutic compounds or NCE. The reductive amination route in MDMA samples and impurity profiling of frenzy tablets by GC-MS are examples of how impurities can originate from intermediates [53].

1.5.4.5. Formulation-related impurities

During the formulation process, a drug substance may undergo various conditions that can affect its degradation or lead to unwanted reactions. Degradation is widespread in solutions and suspensions due to hydrolysis or solvolysis [54]. Hydrolysis and catalysis can occur due to impurities in the water used for formulation, and other solvents may also result in similar reactions. The formation of formulated related impurities can occur through different mechanisms:

a) Method-related impurity

Method-related impurity is a substance that appears during the production of a drug. It occurs because of the specific methods or conditions used during manufacturing. For instance, when diclofenac sodium is terminally sterilized using an autoclave, 1-(2, 6-dichlorophenyl), indolin-2-one is created when the intramolecular cyclic reaction of diclofenac sodium ensues, which forms NaOH and indolinone analog shown in **Figure 1.10**. This formation depends on the formulation's initial pH [55].

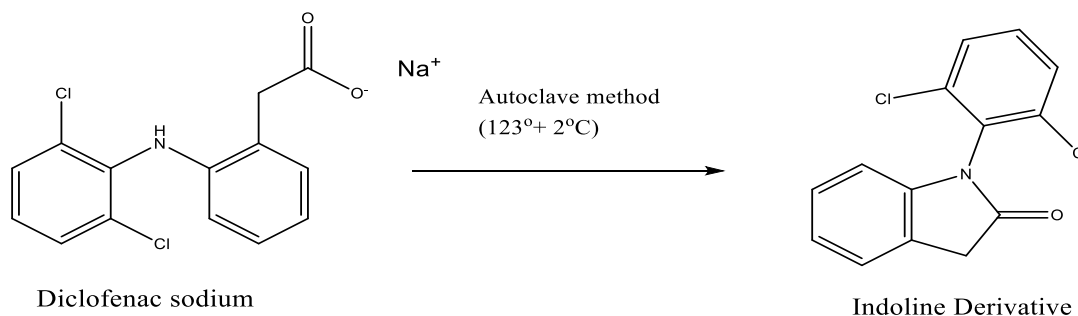


Figure 1.10: Formation of Indoline derivative

b) Environmental related [56]

Environmental factors can make things unstable. Here are some factors that can reduce stability:

- Extreme temperatures like tropical climates can negatively affect some active APIs. One instance is vitamins used as drug compounds, susceptible to heat. This often results in a reduction in their potency, particularly in liquid formulations where degradation can occur.
- Light (UV light): Some studies indicate that methyl ergometrine and ergometrine injection are unstable under hot climates, including light and heat. As a result, numerous field samples have shown a low level of active ingredients. Even a customized injection of ergometrine (0.2 mg/mL) showed nearly total degradation when exposed to direct sunlight for 42 hours.
- Humidity: Humidity adversely affects the formulation of solid dosage and bulk powder forms of hygroscopic products. Classic examples of such products include aspirin and ranitidine.

c) Dosage forms related impurities

Pre-formulation studies, including stability testing, are conducted by pharmaceutical companies before their products are marketed. In some cases, drug stability may be affected by factors related to the dosage form, resulting in product recalls. Liquid dosage forms are generally vulnerable to microbial contamination and degradation. Factors such as water content, pH levels of the suspension, compatibility of anions and cations, and interactions between ingredients and the primary container are critical. Bacteria, fungi, and yeast may cause microbiological growth in a warm and humid environment, rendering oral liquid products unfit for human consumption. Inappropriate use of certain preservatives during preparation or the semi-permeable nature of primary containers may lead to microbial

contamination during the shelf life and subsequent usage of multi-dose products [57].

Different dosage form-related impurities are [58]:

- **Mutual interaction amongst ingredients:** Most vitamins are susceptible to degradation, especially in liquid dosage forms, which presents a challenge in their formulation for aging populations. Although the degradation of specific vitamins, such as thiamine, cyanocobalamin, pantothenic acid, and folic acid, does not result in toxic impurities, the active ingredient's potency falls below the required standards. A vitamin B-complex injection comprising four vitamins, such as thiamine, nicotinamide, and riboflavin, causes thiamine to degrade to a deficient level within 1 year. The pH range of marketed vit B-complex injections is between 2.8 and 4.0. The mutual interaction between the components in a custom-made formulation of vit B-complex injection in DM water and a typically formulated medium that included disodium edetate and hydroxytoluol was also found, and akin degradation was noted.
- **Functional group-related typical degradation:** This degradation refers to the chemical decomposition process in a molecule due to the chemical properties of specific functional groups. This type of degradation can alter the intensive properties of the molecule, making it less effective or even harmful. Understanding the varied functional groups present in a molecule can aid in anticipating and averting its decay. For instance, drugs that possess a -OH group linked with an aromatic ring, like morphine and catecholamines, are predisposed to oxidative degradation. Similarly, heterocyclic aromatic rings, aldehydes, vitamin A, nitroso, and nitrite derivatives, particularly flavors, are also vulnerable to degradation. The oxidative and hydrolytic degradation pathway of mazipredone was studied in 0.1 mol L⁻¹ HCL and NaOH at 800 °C. Photolytic cleavage is observed in medicinal products exposed to light during manufacturing as

solid/solution, packaging, or stored in hospitals or medical shops for consumer use. Salicylic acid impurity shown in **Figure 1.11**.

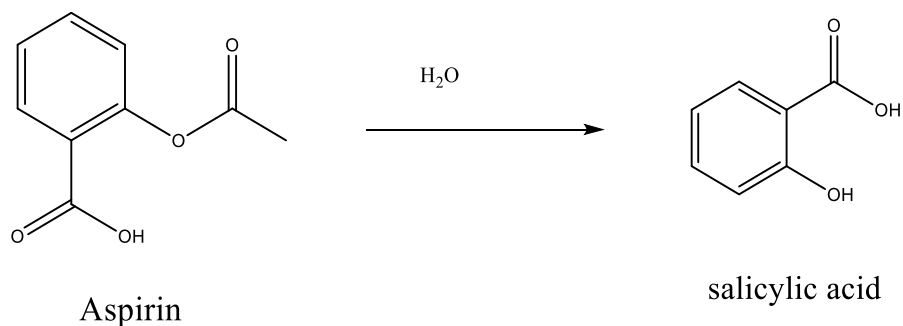


Figure 1.11: Salicylic acid impurity

1.5.4.6 Impurities arising during storage

Drug products may accumulate impurities during shipping or storage, making it crucial to conduct stability studies to assess and guarantee their safety. As previously mentioned, drug impurities can originate from either the drug or excipients themselves, or they can infiltrate the system through contact with the wrapping material during the in-process stage. The reactive species for most drugs are composed of.

- a) Water- Certain drugs can be affected by water through hydrolysis or by altering the performance of the dose.
- b) Small electrophiles- Derivatives of carboxylic acid and aldehydes are examples of small electrophiles.
- c) Peroxides- Peroxides can cause oxidation of certain drugs.
- d) Metals- The oxidation of drugs and their degradation can be catalyzed by metals.
- e) Leachable or Extractables- Materials such as glass, rubber stoppers, and plastic packaging can produce leachable or extractable substances. Glass can produce metal oxides such as NaO₂, MgO, SiO₂, and CaO. Synthetic materials like polystyrene can produce styrene, while PVC can produce DEHP as a plasticizer, dioctyl tin isooctylmercaptoacetate as a stabilizer, and zinc stearate as a stabilizer in PVC and polypropylene [59, 60].

1.6. GENOTOXIC IMPURITIES (GIs)

Chemical substances known as genotoxic impurities can cause damage to DNA, which includes mutagenicity. These impurities have the potential to cause harm to various cellular components, such as spindle division, and enzymes like topoisomerases, which are responsible for modifying genetic material. Genotoxic impurities can affect germinal cells (mutations passed from affected individuals to their offspring) and somatic cells (mutations transferred within the same generation of cells), potentially leading to mutations and cancer. These impurities can be present in pharmaceutical products or their manufacturing processes. Genotoxic pharmaceutical impurities pose a significant risk to human health; thus, controlling and limiting exposure to these impurities is crucial. It is essential to control and limit exposure to genotoxic impurities to ensure the assurance and value of the drugs. Governing authorities such as EMA, ICH, and FDA have set limits for the acceptable levels of GIs in pharmaceuticals to minimize the threat of adverse health effects [61–63].

1.6.1 TAXONOMY OF GIs

The taxonomy of genotoxic impurities is determined through a risk assessment process. This involves analyzing actual and potential impurities by literature searches and conducting databases for bacterial mutagenicity and carcinogenicity data. Based on this analysis, the impurities are classified into one of three categories: Class 1, 2, or 5. If there is no available data for classification, an assessment of Structure-Activity Relationships (SAR) is performed. This assessment focuses on bacterial mutagenicity predictions and could result in the impurity being classified into Class 3, 4, or 5. Each class has its specific definition [64,65].

- **Class 1:** These have been linked to mutations and cancer and, as such, pose a significant danger that must be addressed by altering the production process. If it is not feasible to eliminate these contaminants, the alternative option is to restrict them within the "Threshold of Toxicological Concern (TTC)."

- **Class 2:** It is well-established with mutagenic properties, but its potential to cause carcinogens is still unknown. Therefore, it is essential to control these impurities using the TTC approach.
- **Class 3:** These have different structures from those of the drug substances, and their genotoxicity is uncertain. Based on the functional groups present in their molecule, these impurities may be categorized as genotoxic. This toxicity is assessed by studying their structure-activity relationship (SAR). Rather than evaluating their toxicity, these impurities are recognized through chemistry and expertise-driven systems that establish correlations between structure and activity (SAR).
- **Class 4:** These impurities have structures like drug substances' structures. In addition, they feature a moiety/function that shares a potentially alarming trait with the main structure and is not genotoxic.
- **Class 5:** No definite structures are associated with these impurities; research suggests they do not have genotoxic effects. As per the ICH guidelines, these compounds should be regulated like other impurities. Types of impurities in drug substances mentioned in **Table 1.3**. Examples of GIs as shown in **Figure 1.12**.

Table 1.3: Types of impurities in drug substances [66]

Category	Compounds
Starting material	Hydrazine, Nitroso, and acrylonitrile compounds
Intermediate	Benzaldehyde, Nitro compounds
By-product	Sulphonate esters, phosgene
Reagent	Formaldehyde, epoxides, esters of phosphate, sulphonates
Solvent	Benzene, 1,2-dichloroethane
Catalyst	Toxic heavy metals, metal phosphates
Degradation product	N-oxides, aldehydes

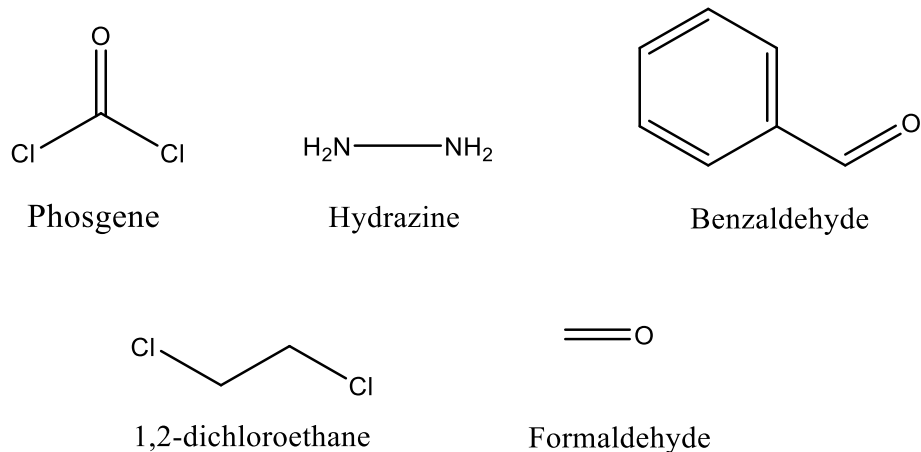


Figure 1.12: Examples of GIs

1.7. ANALYTICAL METHOD FOR IMPURITY DETECTION

To ensure successful new drug development, it is crucial to generate accurate and trustworthy analytical data throughout the different stages of development [67-69].

- a) It is vital to select the sample set carefully to develop analytical methods.
- b) The linear solvent-strength model tests Chromatographic conditions and Phases in the gradient elution process.
- c) The method should be optimized to adjust limitations related to ruggedness and sturdiness.

Brief discussions of the above three methods are described in **Table 1.4**.

Table 1.4: The Process for impurity detection

Step 1: Key Predictive Sample Set	Step 2: Screening	Step 3: Optimization
Identification of Key Predictive Sample Set	Linear solvent strength model	Gradient methods
-Degradation samples	-Two gradients per condition	-LSS Model
-Process Related Impurities	Compound specific screening	-pH
Mother Liquors	-LSS predictions	-Slope
-Excipients	-Refined optimization	Isocratic methods
-Flavors	-Documentation	-LSS Model pH
-Preservatives		-Ion strength
-Fractions		Temperature
Impurity Isolation		-Factorial when LSS model fails
-Documentation		

The following methods are primarily used to identify impurities.

1.7.1 Method of Reference Standards

The primary goal of this method is to clarify the qualification and governance of ref standards for developing and controlling innovative drugs. Ref standards are essential for evaluating the performance of processes and products and ensuring patients' medicines' safety. These standards are required for main ingredients in dosage, excipients, degradation products, process intermediates, and starting materials [70].

1.7.2. Spectroscopical Methods

The Raman UV, Mass, NMR, and IR spectroscopical methods are usually used to characterize impurities [5].

- ✚ **UV- Spectroscopy:** Ultraviolet (UV) spectroscopy is a physical fashion of optic spectroscopy that uses light in visible, ultraviolet, and near-infrared ranges. The Beer-Lambert law states that the absorbance of a result is directly commensurable to the attention of the absorbing species in the result and the path length. Therefore,

for a fixed path length, UV/ VIS spectroscopy can be used to determine the attention of the absorber. It is necessary to know how fleetly the absorbance changes with attention UV spectrophotometric styles have also been reported for measuring levofloxacin exercising other detergents like 0.1 M hydrochloric acid, 100 methanol, or acetonitrile [71].

- ✚ **IR-spectroscopy:** Infrared spectroscopy examines the electromagnetic spectrum's infrared region. It identifies substances and analyses sample compositions using various methods, with absorption spectroscopy being the most popular. Infrared spectrophotometers are commonly used in laboratory equipment for this purpose. The infrared spectrum is segmented into three distinct regions: near-infrared, mid-infrared, and far-infrared. The far-infrared segment, situated near the microwave range and characterized by low energy, is helpful in rotational spectroscopy. In contrast, the mid-infrared range, spanning wavelengths from 4000-400 cm^{-1} , is commonly employed in investigating fundamental vibrations and associated rotational-vibrational structures [72].
- ✚ **Mass Spectroscopy:** Mass spectrometers are utilized in industry and academia for everyday tasks and original research. The principal mass spectrometric applications are briefly summarized below: Biotechnology, Pharmaceuticals, clinical, and geological [73].
- ✚ **Raman spectroscopy:** This advanced spectroscopic technique delves deep into a system's rotational, vibrational, and low-frequency modes. It relies on monochromatic light's inelastic or Raman scattering, typically from a laser, within the visible, near-infrared, or near-ultraviolet spectrum. As the laser light interacts with photons or other excitations in the system, it causes an energy shift in the laser photons upwards or downwards. This energy shift yields valuable insights into the phonon modes active within the system [74].

1.7.3. Methods of Separation

Capillary electrophoresis, supercritical fluid chromatography, gas chromatography, TLC, HPLC, and HPTLC are commonly employed to separate impurities and degradation products.

- ✚ **Capillary Electrophoresis (CE):** It is a separation technique based on the difference in charge-to-size ratios in an electric field through a conductive medium. The larger the ratio, the faster an ion migrates in the electric field. Ions are primary candidates for separation.[27]. Capillary electrophoresis is a valuable impurity profiling technique. The determination of impurities can be a challenging task as they may have complex structures and bear resemblance to the core drug substance. However, the peak efficiency of CE sets it apart from other separation techniques. CE can also be employed in various modes, further enhancing its separation capability [75].
- ✚ **Gas Chromatography (GC):** GC is a widely used method in analytical chemistry for separating and analyzing vaporizable compounds. It is commonly used to test the purity of substances, separate components in a mixture, and even identify specific compounds in some cases. GC is also helpful in preparative chromatography for isolating and characterizing volatile components if a non-destructive detector is used. Today, GC is often paired with mass spectrometry (GC/MS) to describe impurities accurately [76].
- ✚ **Supercritical Fluid Chromatography (SFC):** SFC is used in pharmaceuticals to separate chiral drugs on an analytic and preparatory scale. The process involves selecting dissimilar stationary phases and using retention factors to measure them. Using principal component analysis and k-values, a set of 6 distinct stationary phases can be selected. The retention mechanisms of compound mixtures are evaluated in these phases [77].

- ✚ **Thin-layer Chromatography:** TLC is an affordable and straightforward method used to assess the purity of a substance or track the advancement of a chemical process. It entails placing a small sample on a TLC plate coated with a thin silica gel or alumina layer. The plate is then immersed in a solvent chamber that moves up the plate through capillary action, separating the analytes at varying speeds. TLC has numerous uses, including identifying plant components, monitoring organic reactions, and analyzing ceramides and fatty acids [78].
- ✚ **High-Performance Thin Layer Chromatography:** HPTLC is also based on the principle of separation, which depends on the relative affinity of compounds towards stationary and mobile phases. The compound, under the influence of the mobile phase (driven by capillary action), travels over the surface of the stationary phase. During this movement, the compounds with higher affinity to the stationary phase travel slowly while the others travel faster. Thus, the mixture's components are separated [79].
- ✚ **High-Performance Liquid Chromatography:** HPLC is a widely used separation technique that utilizes a liquid mobile phase and high pressure to separate components of a mixture. It is used to identify various substances, including amino acids, proteins, and pharmaceuticals. A method was developed and validated using HPLC to determine methionine, which produced few impurities. The process is also effective for measuring the purity of DL-methionine and D-methionine [80].

1.7.4. Isolation Methods

Isolating impurities is often necessary, but instrumental methods can prevent direct characterization. Typically, liquid-liquid impurities are separated through chromatographic or non-chromatographic techniques before characterization. The term "chromatographic reactor" is a chemical reactor that uses chromatography to separate and purify chemical compounds. In a chromatographic reactor, a stationary phase is used to isolate the different components of a mixture based on their chemical properties. In this study, we examined

the hydrolysis kinetics of fosaprepitant dimeglumine, the prodrug of Aprepitant (Emend™), using an HPLC chromatographic reactor approach [44]. Examples include loratidine, amikacin, and celecoxib [45, 46].

The methods used to isolate impurities are:

1. Solid-phase extraction methods: This is a highly valuable technique for sample preparation. It offers several advantages over liquid extraction, such as avoiding problems like incomplete phase separation, less-than-quantitative recoveries, and the need for expensive and fragile specialty glassware. Additionally, it reduces the amount of organic solvents that need to be discarded and saves laboratory time. SPE is a rapid and straightforward method for automated quantitative extractions. It is beneficial for preparing liquid samples and extracting semi-volatile and non-volatile analytes. Additionally, it can be utilized with solids that have already been pre-extracted into solvents. Selecting the most appropriate product for each application and sample type is crucial to achieving precise and reliable outcomes. Various sizes, chemistries, and adsorbents are available for SPE products, making informed selection necessary [82].

2. Liquid-liquid extraction methods: Solvent extraction and partitioning, a.k.a liquid-liquid extraction, is a crucial method used in laboratories to separate compounds based on how soluble they are in two different liquids that cannot be mixed (water and an organic solvent). This technique involves a separating funnel to transfer a substance from one phase to another. It is commonly performed as part of the workup process following a chemical reaction. [83].

3. Accelerated solvent extraction methods: This technique is unique and widely used for extracting chemically active constituents from solid matrices. It involves using a solvent to penetrate the matrix to remove the desired chemical constituent. This technique has many applications in the pharmaceutical industry, particularly in eliminating natural chemical constituents from herbal plants. Its usefulness is not limited to natural constituents, as it has also been employed in impurity profiling of drug substances, screening microorganisms, analyzing dietary supplements, detecting insecticide residue,

examining environmental samples, and identifying organic contaminants. This technique offers numerous advantages compared to traditional methods such as maceration, purification, turbo-extraction, and sonication [84].

4. Supercritical Fluid Extraction: When a substance is exposed to temperatures and pressures above its critical point, it transforms into a supercritical fluid (SCF). It possesses fluid and gas characteristics, such as gas-like mass transmission and solvating power. This unique combination offers distinct advantages over other methods. Supercritical fluid is widely used for extracting natural components from plant materials and remains effective in impurity profiling [85].

5. Column Chromatography: Column chromatography, a method for purifying chemicals and separating individual compounds from mixtures, is widely used in various applications ranging from mg to kg. The column, a typical chromatography apparatus, is a glass tube with a diameter ranging from 50mm to 1m and a height varying from 50cm to 1m. It has a stopcock at the base. It can be prepared using both dry and wet techniques. The stationary phase selectively retains each component, allowing separation as they move through the column at different speeds with the eluent. The eluent is gathered in portions throughout the process. Each of these portions is then examined dissolved compounds using either analytical chromatography, fluorescence./UV. [86].

6. Flash Chromatography: Various methods, such as extraction, distillation, and re-crystallization, are used for purifying organic compounds. However, modern organic research mainly employs 'flash' chromatography, which differs from traditional columns. In the column, a sample is introduced from the top packed with silica gel, followed by a solvent/mixture of solvents. The solvent passes through the column by gravity, and the different components get separated at varying rates. The separated components are collected as they exit from the bottom. The rate of solvent flow in column chromatography is relatively low. On the other hand, flash chromatography utilizes air pressure to speed up the solvent flow, reducing the time required for sample purification. [87].

7. Thin Layer Chromatography (TLC): This is a reliable and unique method that can test the identity and purity of any compound. It offers a shorter development time, easy visualization of separated compounds, quicker and cheaper separation procedures, and requires a minor sample size with reduced solvent consumption. Additionally, it can detect all contamination within a more comprehensive polarity range. Mass spectrometry (MS) determination is utilized to clarify the structure of unknown impurities. TLC)/ HPTLC and other planar chromatography find many pharmaceutical applications in drug analysis [88].

8. Gas Chromatography (GC): GC can be advantageous for isolating and characterizing components that are either already volatile or made volatile using derivatization techniques. Additionally, a non-destructive detector is recommended for this process. Nowadays, (GC-MS) to identify impurities [89]

9. High-Performance Liquid Chromatography: This sophisticated separation method delivers exceptional sensitivity, selectivity, and resolution. Its rapid and efficient performance makes it ideal for testing drug substance purity and separating impurities. In particular, the reverse phase HPLC method is widely employed to identify impurities in biological materials. The HPLC method can also produce high-quality UV spectra with a UV detector. Sample preparation is straightforward, and the system is designed to minimize errors [91].

10. Supercritical fluid chromatography (SFC): This is normal phase chromatography commonly used to analyze and purify molecules with low-to-moderate molecular weights that are thermally unstable. Additionally, it is effective in separating chiral compounds. SFC operates on the same principles as HPLC, but it requires the entire chromatographic flow path to be pressurized, as it employs CO₂ as the mobile phase [92].

1.8. CHARACTERIZATION OF IMPURITY

1.8.1 Characterization Techniques

Different highly sophisticated techniques are used for characterizing impurities in various matrices, which are as follows.

- a) **Nuclear Magnetic Resonance (NMR):** This is highly effective for defining pharmaceutical molecules' bonding structure and stereochemistry. Its ability to do so has made it an invaluable asset in structural elucidation. Additionally, NMR-based diffusion coefficient measurements have been shown to accurately differentiate between monomeric and dimeric compounds, as confirmed by a standard mixture of authentic materials containing both types [93].

- b) **Mass Spectrometry:** In recent years, advancements in the interfaces connecting separation techniques with mass spectrometers have significantly impacted the pharmaceutical development process. These improvements have enabled better monitoring, quantification, and characterization of drug-related substances in APIs during production. If one method fails to provide necessary selectivity, alternative chromatographic techniques like HPLC-TLC/CE and HPLC-MS/NMR may be considered for development purposes only, not routine QC tools. [94].

1.8.2 Hyphenated Techniques:

In analytical science, a new method known as the hyphenated technique has emerged. This approach involves combining two or more techniques through an interface. As impurity standards may be challenging, the hyphenated technique is crucial in accurately characterizing unknown impurities. Coupling MS with another chromatography method leads to a higher signal-to-noise relation, decreasing noise, and increasing analyte selectivity through increased couplings [95].

Different hyphenated techniques are described below:

- i. **LC-MS/NMR:** Pharmaceutical labs commonly use a directly coupled LC-MS/NMR technique. This technique combines HPLC with MS and NMR, allowing for a definitive correlation between NMR spectra and trace-level analytes. The eluent from the HPLC column is split into two parts: a smaller portion for MS (ESI), which offers higher sensitivity than the NMR, and the remaining portion is directed to it. Combining these two data types yields complete structural elucidation of the

drug and other data on its structural configuration, NMR silent heteroatoms (N, Cl, O) in unknown impurities and functional groups [96].

- ii. Liquid chromatography-gas chromatography (LC-GC):** This powerful technique merges the comprehensive separation capabilities of LC with the high proficiency of GC. It is beneficial when working with pure samples requiring high sensitivity and selectivity. It can handle large sample volumes and is commonly used in offline mode. However, there are some downsides to operating this mode, including time-consuming analysis, exhaustive operation, and decreased reproducibility [97].
- iii. High-performance liquid chromatography-mass spectrometry (HPLC-MS):** Combining LC and MS has many compensations, resulting in widespread use in pharmaceutical research. This technique offers high selectivity, dynamic range, ruggedness, and sensitivity, making it an excellent choice for various applications. Tandem LC-MS, or LC-MS/MS, is particularly useful for quantitative analysis and structure elucidation of unknown impurities. The LC-MS interface is also minimally prone to solvent and flow rate interference. HPLC/UV/MS/MS is widely regarded as the most comprehensive technique for providing all the necessary information for the structural explication of impurities [98].
- iv. Gas chromatography-mass spectrometry (GC-MS):** This chemical analysis and structure determination tool is valuable. Its precise compound separation and detection capabilities make it a go-to method in the pharmaceutical industry for identifying impurities, determining the composition of chemicals, and establishing compound structure. In cases where complicated samples require identifying unknown chemicals, solid-phase micro-extraction and MS-MS can be employed. GC-MS is known for its ability to accurately determine chemical molecular weight and structure, making it a cost-effective and widely recognized technique. Mass fragmentography is frequently employed to detect residual solvents [99].

- v. **Capillary zone electrophoresis-mass spectrometry (CZE-MS):** One of the primary benefits of pairing CZE-MS is the exceptional separation power of CE coupled with the structural information provided by mass spectra. Achieving a high degree of perpendicularity between the methods during impurity separation can yield a better resolution of separated impurities [60-65]. A range of profiling techniques is available through coupling CE with various MS ionization systems, including APPI-MS, APCI-MS, TSI-MS, and ESI-MS. ESI-MS and TSI-MS are well-suited for detecting ionic compounds, while APCI-MS and APPI-MS are not [66-72]. This can be particularly helpful in distinguishing between ionic and non-ionic impurities of unknown origin [100].

The analysis of product degradation-related and process impurities aims to detect impurities produced during manufacturing and those that occur under specific storage conditions. An outline of the impurity investigation objective is presented in **Table 1.5**

Table 1.5: Goals of Impurity Investigations [101]

Process-related impurities	Degradation-related impurities
Identify significant impurities	Identify potential degradation products through stress testing and actual degradation products through stability studies.
Determine the origin of impurities and the method for elimination or reduction.	Understand degradation pathways and methods to minimize degradation.
Establish a control system for impurities involving: 1) Processing/manufacturing conditions 2) Suitable analytical methods/specifications,	Establish a control system for impurities involving: 1) Processing/manufacturing conditions 2) Suitable analytical methods/specifications 3) Long-term storage conditions, including packaging 4) Formulation

1.9 SIGNIFICANCE OF SYNTHESIS OF DRUG IMPURITIES

ICH has issued rules for impurities in innovative drugs and residual solvents. Regulatory authorities and pharmaceutical companies both require impurity and API reference standards. Impurity profiling begins with detecting impurities through chromatographic techniques. Spectral analyses are utilized for impurity characterization. In cases where impurities are not easily obtainable or are difficult to isolate using chromatographic methods, impurity synthesis is a critical step for API or drug substances. The comprehensive use of organic chemistry studies supports the synthetic approach to impurity synthesis. Once impurities are identified through chromatographic and spectral analysis, the organic chemist proposes various routes to synthesize the impurity. The synthesized impurity is then characterized through spectral analysis, making the synthesis of impurities a vital component of API or drug substance impurity profiling [102].

1.9.1 Forensic Significance of Drug Impurities

The synthesis of drug impurities can have significant forensic implications in several ways:

- a) **Counterfeit Drugs:** Analyzing drug impurities is crucial in detecting counterfeit drugs. Counterfeit drugs can pose a substantial threat to public health as they may contain harmful or ineffective ingredients. Various factors, such as the manufacturing or the packing conditions of the drug, can cause drug impurities. These impurities can differ from those found in genuine drugs, and their analysis can help identify counterfeit drugs. Furthermore, impurities in drugs can also be used to trace a drug sample's origin and detect drug diversion. Different manufacturers may produce impurities with unique signatures, allowing for the identification of the source of the drug. This can help prevent drug diversion, which is when a drug is illegally sold or distributed outside of its intended use. Drug diversion can be detected by analyzing impurities, and the supply chain can be traced back to its source.

- b) Drug Tampering:** Detecting drug tampering is a crucial task that involves analyzing the impurities present in the drugs. This process helps identify foreign substances or contaminants that may have been introduced intentionally or unintentionally during manufacturing. By examining these impurities, manufacturers and regulatory authorities can identify any unexpected substances that may threaten the drug's safety and effectiveness. This enables them to take appropriate measures to ensure the drug is safe and effective.
- c) Quality Control:** Impurities present in drugs can be an effective tool for evaluating and monitoring the stability and quality of drug formulations over a period. This information is precious for quality control and can help pharmaceutical companies ensure their drugs are safe, effective, and meet regulatory standards. By analyzing the impurities present in drugs, scientists and researchers can gain insights into the chemical composition and properties of the drug, which can help them identify any potential issues or concerns with the drug's stability or efficacy. This can ultimately lead to improvements in manufacturing and the development of more effective patient drugs.
- d) Criminal Investigations:** During criminal investigations, one of the critical aspects is to determine the authenticity of drug samples and link them to their respective manufacturers or sources. In this regard, impurities in the drug sample can serve as crucial evidence to either support or refute its authenticity. Forensic experts can determine the sample's origin and whether it matches the claimed source by analyzing the impurities in the drug sample. This information can then be used in court as evidence to prove or disprove the allegations against the accused party.

CHAPTER 2: LITERATURE REVIEW

Many researchers have synthesized the impurities of active pharmaceutical ingredients. Besides this, numerous researchers have discussed the different methods for producing impurities and their characterization. A brief review of the literature related to the synthesis and manufacture of impurities and their impurities is given here from 1994 to the date:

Frischia and colleagues (1994) conducted a study to inspect the potential of specific chemical reagents in synthesizing beta-lactam, quinolone, antiviral, and general drug categories to cause genetic damage. The study revealed that alkylating agents such as chloromethanol acetate, bromomethanol acetate, carbon disulfide, and various dimethylanilines shown in **(Figure 2.1)** exhibited genotoxic activity in beta-lactam synthesis. However, no genotoxic activity was observed in the Ames test when evaluating chemical reagents for quinolone and antiviral synthesis. Additionally, the study found that 2,5-dibromopentyl acetate and halogenated methanol acetates induced gene mutation, which was expected due to their chemically alerting structure [103].

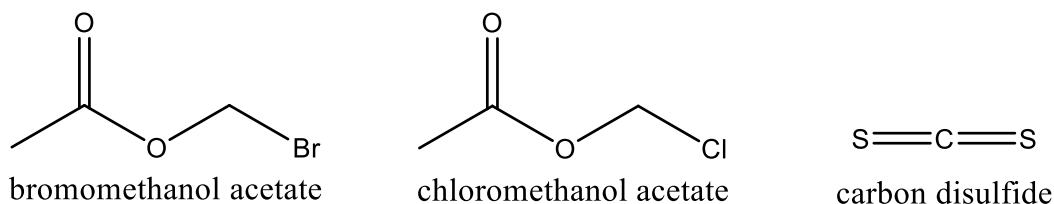
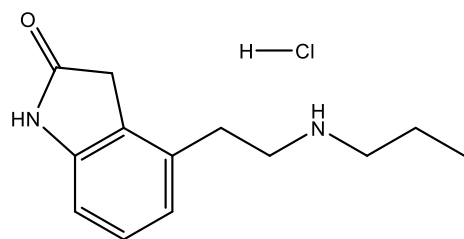
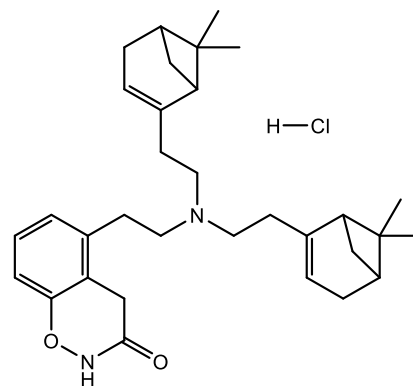


Figure 2.1: Chemical Reagents found in drug

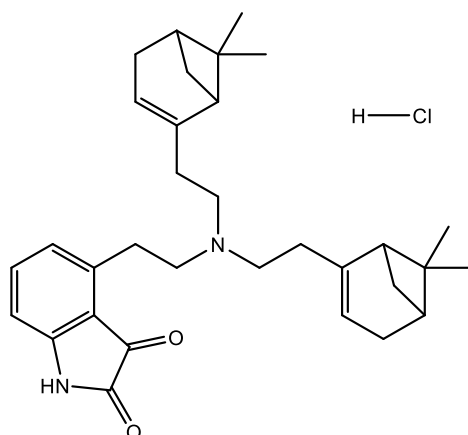
A study by **Sahasrabuddhe and co-researchers (2007)** discussed synthesizing, detecting, and isolating three impurities in the Ropinirole HCL drug substance. These impurities were found to be at approximately 0.06-0.15%. These impurities were carried out using RP-HPLC and their structure. These impurities shown in **(Figure 2.2)** were characterized based on IR, NMR, and MS [104].



4-[2-(propylamino) ethyl]-1,3-dihydro-2H-indol-2-one hydrochloride



5-[2-(dinopylamino) ethyl]-1,4-dihydro-3h-benzoxazin-3-one hydrochloride



4-[2-(dinopylamino) ethyl]-1H-indol-2,3-dione hydrochloride

Figure 2.2: Impurities of ropinirole hydrochloride

Thatipalli and coworkers (2008) discussed the formation, synthesis, and characterization of olanzapine impurities shown in **(Figure 2.3)**. The HPLC analysis of six impurities exhibited peaks ranging from 0.05 to 0.15 % and was identified at m/z 341, 230, 361, 511, 326, and 329. These olanzapine impurities were characterized by Mass, NMR, and IR [105].

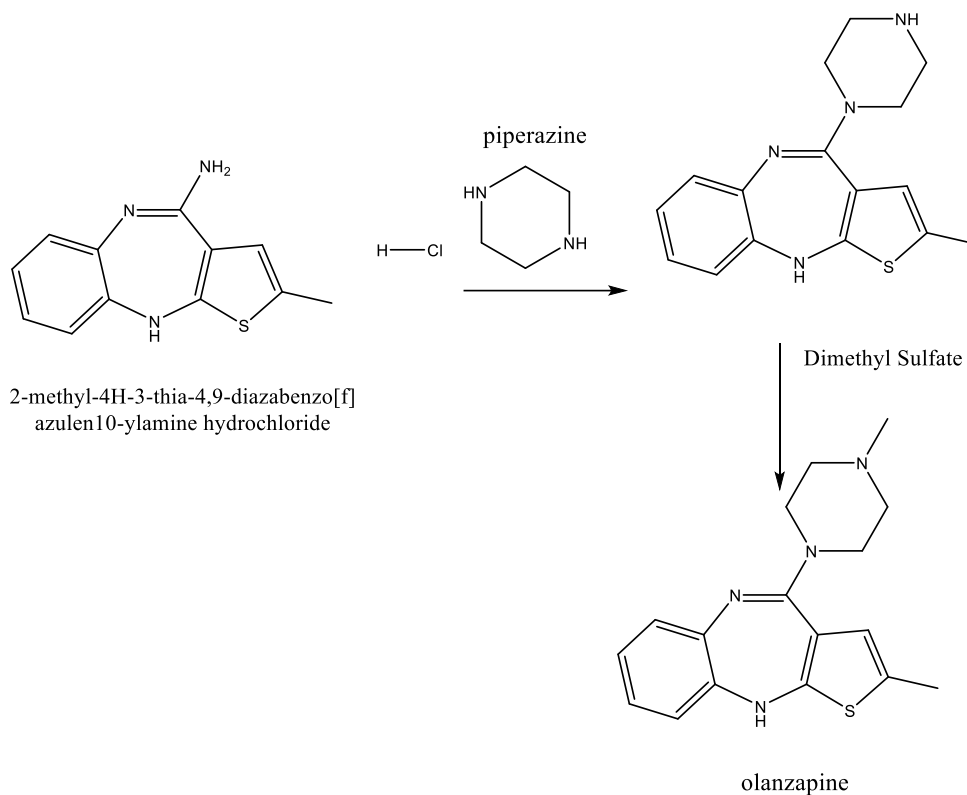


Figure 2.3: Synthesis of Olanzapine

Buchi and colleagues (2012) conducted a study on producing Raloxifene hydrochloride. During the study, eight impurities were detected, with four of them being newly discovered. A gradient HPLC method was used to identify these impurities. The percentages of impurities range between 0.05% and 0.1%. Additionally, MS identified massive numbers of impurities. A comprehensive investigation was then carried out to categorize them. They were also treated to co-injection in HPLC, and their characteristics matched the impurities in the sample. These are identified as Raloxifene Dimer, N-Oxide, EP impurities A, B, HABT, PEBE, HHBA, and 7-MARLF shown in **(Figure 2.4)** [106].

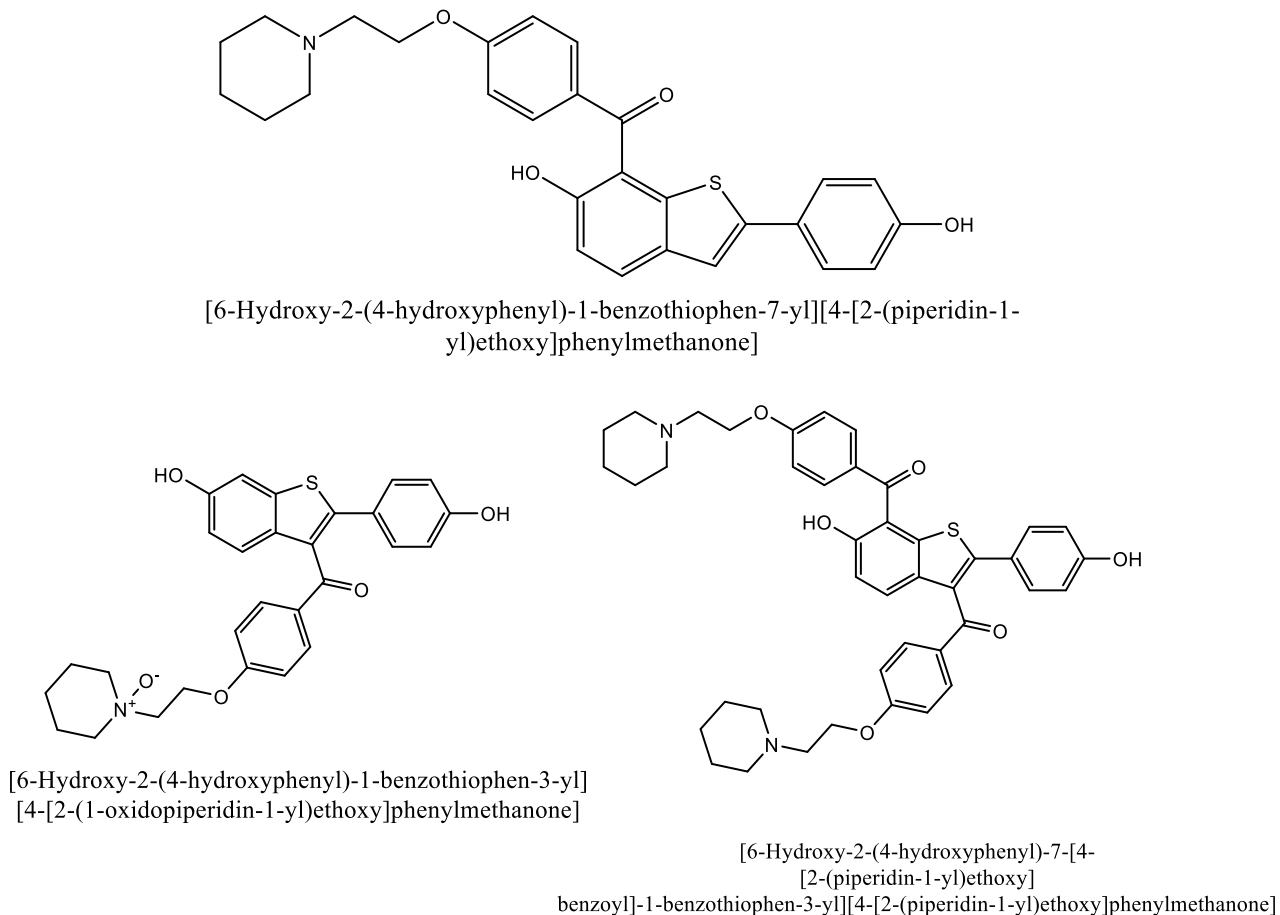


Figure 2.4: Impurities of Raloxifene hydrochloride

Wang and his co-researchers (2012) conducted an HPLC analysis of retigabine and discovered 4 unknown impurities that were identified using mass spectrometry and other methods. The impurities were confirmed and remembered through the synthesis process. They also discussed possible mechanisms for forming these impurities shown in **(Figure 2.5)** [107].

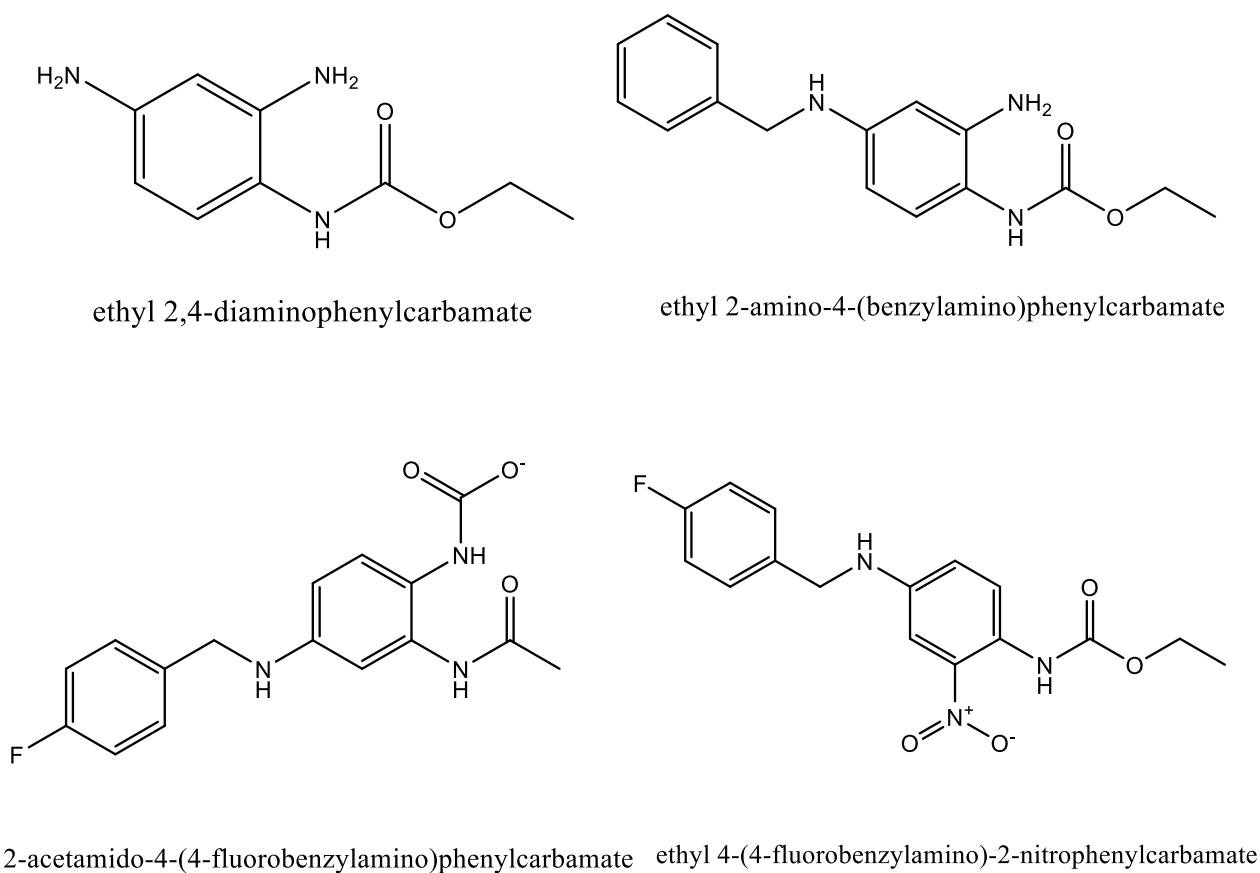


Figure 2.5: Impurities of Retigabine

Schulz and colleagues (2013) investigated commercially available proguanil tablets to determine the primary degradation product shown in **(Figure 2.6)**, which is genotoxic. The investigation utilized GC-FID and HPLC-FLD systems. Proposed plans were created to arrange further disintegrated components of proguanil using the outcomes obtained from HPLC-MS. The database was analyzed to commence a primary toxicological assessment of the proposed chemical frameworks. In the end, it was verified that the recently identified arrangements were not present in the preserved proguanil tablets [108].

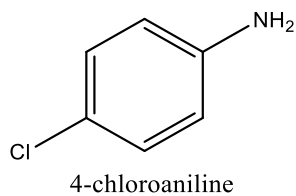
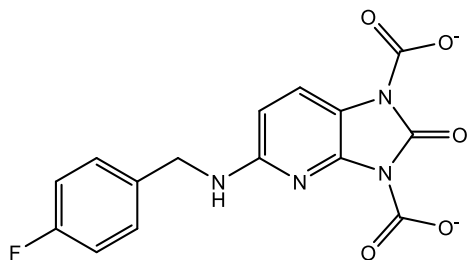
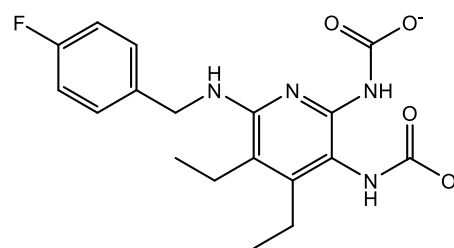


Figure 2.6: Chemical Structure of Impurity

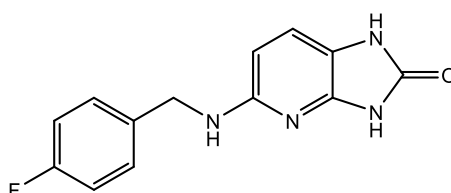
In their study, **Zhang and colleagues (2014)** examined two unidentified impurities in laboratory batches of flupirtine maleate, a nonsteroidal anti-inflammatory and non-opioid analgesic. The researchers successfully identified these impurities by conducting a thorough spectral analysis and leveraging their understanding of the synthetic process of flupirtine maleate. Furthermore, they isolated, identified, structured, and elucidated these impurities shown in **(Figure 2.7)**. Additionally, the study involved the preparation and structure elucidation of another impurity [109].



5-((4-fluorobenzyl)amino)-2-oxo-1H-imidazo[4,5-b]
pyridine-1,3(2H)-dicarboxylate



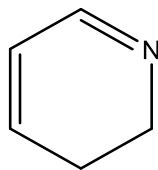
diethyl(6-((4-fluorobenzyl)amino)
pyridine-2,3-diyl)dicarbamate



5-((4-fluorobenzyl)amino)-1H-imidazo[4,5-b]pyridin-2(3H)-one

Figure 2.7: Impurities of Flupirtine maleate

Turhan and colleagues (2014) conducted a study to evaluate the antigenotoxic and genotoxic properties of four recently developed dihydropyridine shown in **(Figure 2.8)** analogs in *Escherichia coli* WP2 and *Salmonella* bacterial reversion assay systems. The genotoxic effects of the test compounds were assessed using bacterial mutant tester strains, *Salmonella typhimurium* TA1537 with a frameshift mutation and *E. coli* WP2uvrA with a point mutation. According to the findings, none of the compounds exhibited important genotoxic activity. However, all test compounds, except compound 4, demonstrated important antigenotoxic activity against mutations induced by MNNG and 9-AA. Finally, none of the compounds exhibited mutagenic potential on the bacterial strains, and some showed antigenotoxic effects in contrast to 9-AA- and MNNG-induced mutagenesis [110].



dihydropyridine

Figure 2.8: Chemical Structure of Impurity

Vadgaonkar and co-researchers (2014) worked to identify, quantify, isolate, and characterize impurities associated with Zidovudine bulk shown in (**Figure 2.9**) and its production. Governing authorities have stringent conditions regarding purity requirements and identifying impurities in APIs. The occurrence of impurities in a drug compound can influence the quality and safety of the product. The study used UV, HPLC, Mass, IR, and NMR techniques to characterize the impurity. An isocratic RP-HPLC method was developed, improved, and authenticated as per ICH rules [111].

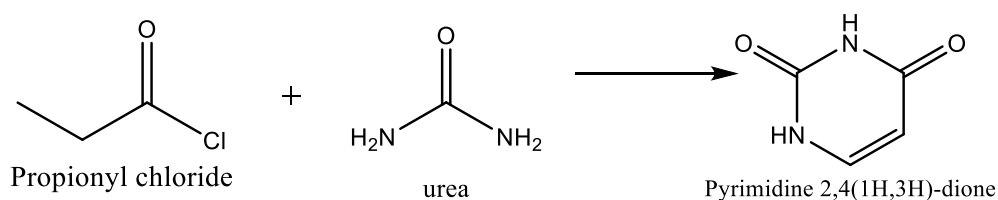
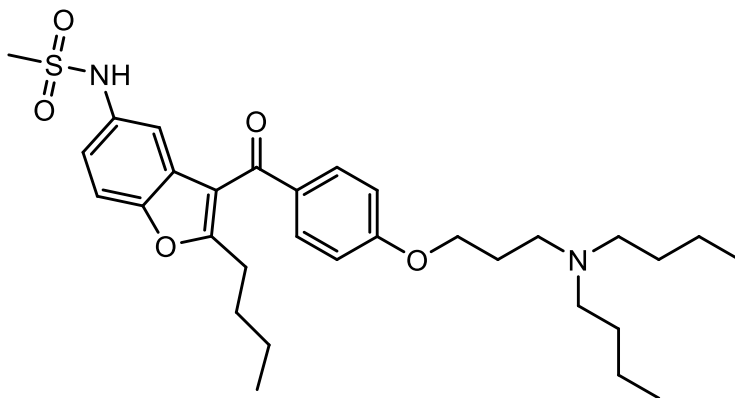


Figure 2.9: Synthesis of Zidovudine

Rudovica and coworkers (2014) worked on the quality control of drug compounds, which significantly controls inorganic chemicals in APIs. Various governing rules have defined concentration limits for metal deposits in compounds. They focused on the handling approach of laboratory-prepared milieu calibration values for quantifying elemental contaminants in APIs using LA-ICP-MS [112].

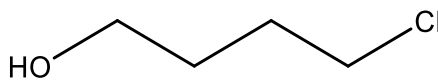
Mahendra and coworkers (2014) studied an impurity profile of an antiarrhythmic drug called Dronedarone shown in **(Figure 2.10)**, and 6 potential PRIs were detected. HPLC and HPLC-MS were used to perceive these PRIs. The structures of these impurities were characterized and discussed in detail based on the synthesis and spectral data [113].



Dronedarone

Figure 2.10: Chemical Structure of API

Harigaya and co-researchers (2014) worked on an innovative approach for detecting GTIs in APIs using LC- ICP-MS. The process was validated and demonstrated one-dimensionality within a 0.5 to 50 ppm range, with a high R(2) value of 0.9994. The detection and quantitation limits were established at 0.2 and 0.5 ppm, respectively, surpassing relevant guidelines. The accurateness was verified within a 1-50 ppm concentration range, exhibiting results between 95.1% and 114.7%. The method's efficacy was confirmed by analyzing six batches of an API, with all results remaining below the established threshold of 1 ppm [114]. Impurity shown in **(Figure 2.11)**.



4-chloro-1-butanol

Figure 2.11: Chemical Structure of Impurity

Halim and co-workers (2014) developed co-crystals of uracil and 5-fluorouracil with urea shown in **(Figure 2.12)** to improve therapeutic development solubility, bioactivity, and stability. The co-crystals were formed through molecular recognition, resulting in 2-D networks created by determined H-bonding patterns from specific moiety groups. The study investigated co-crystal binding energy analysis, characterization, structural investigations, and examination of CDOCKER interactions [115].

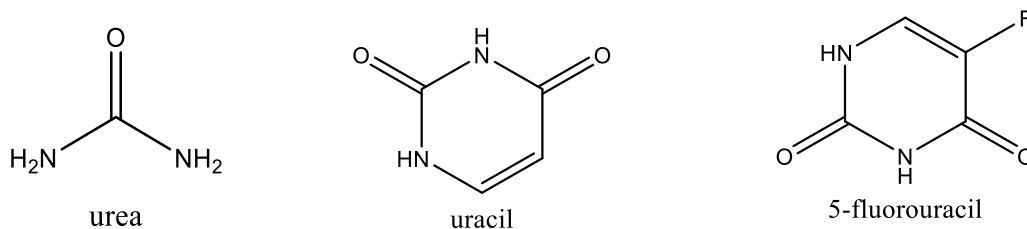


Figure 2.12: Chemical Structure of Co-crystal

Evrykleia and co-researchers (2014) explored a comprehensive approach to characterizing Duloxetine hydrochloride shown in **(Figure 2.13)** and ensuring its purity in the structure. The techniques utilized to identify Duloxetine HCl and its impurities were MS, high-resolution MS, H-NMR, C-NMR, and IR. Additionally, the polymorph of Duloxetine HCL API is characterized through X-ray PDA. Differential scanning calorimetry and hot stage polarizing optic genotoxic activity microscopy contribute to understanding its thermal behavior. An RP-HPLC with a PDA detector is developed to ensure stability and selectivity. This method allowed for determining the purity of Duloxetine HCL API. Chromatography used a Symmetry C18 column (250*4.6mm, 5 μ m), employing a gradient elution of two mobile phases [116].

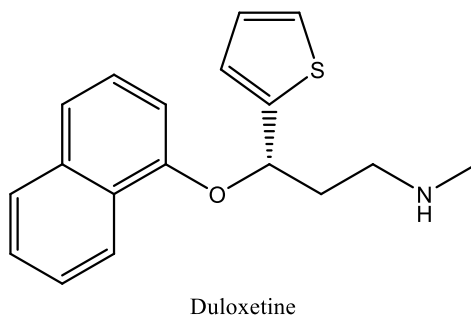


Figure 2.13: Chemical structure of API

Godhwani and co-authors (2015) examined the ethanol leaf extract from *Jasminum sambac Linn* in their study. They conducted phytochemical screening, as well as FT-IR and GC-MS studies, to analyze the extract. The researchers discovered various compounds, including tannins, alkaloids, carbohydrates, carboic acid, glycosides, steroids, and terpenoids. Through GC-MS analysis, they specifically identified compounds like 7-tetradecenal and octadecenoic acid shown in (**Figure 2.14**). The FT-IR analysis confirmed the presence of alcohols, amides, phenols, alkanes, aldehydes, carboxylic acids, alkenes, primary amines, ketones, aromatic esters, aliphatic amine, and alkyl halides compounds in the leaf extract. These findings provide valuable information about the chemical constituents present in *Jasminum sambac* and their potential pharmacological activities [117].

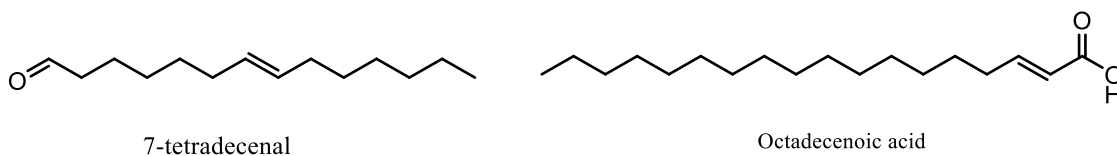


Figure 2.14: Chemical structure of 7-tetradecenal and Octadecenoic acid

Doughty and co-workers (2016) worked on synthesizing impurities in manufacturing Amphetamine Type Stimulants shown in **(Figure 2.15)**. The impurities formed during phenyl-2-propanone synthesis have been identified and selectively synthesized as potential route-specific markers for this sequence of synthetic steps [118].

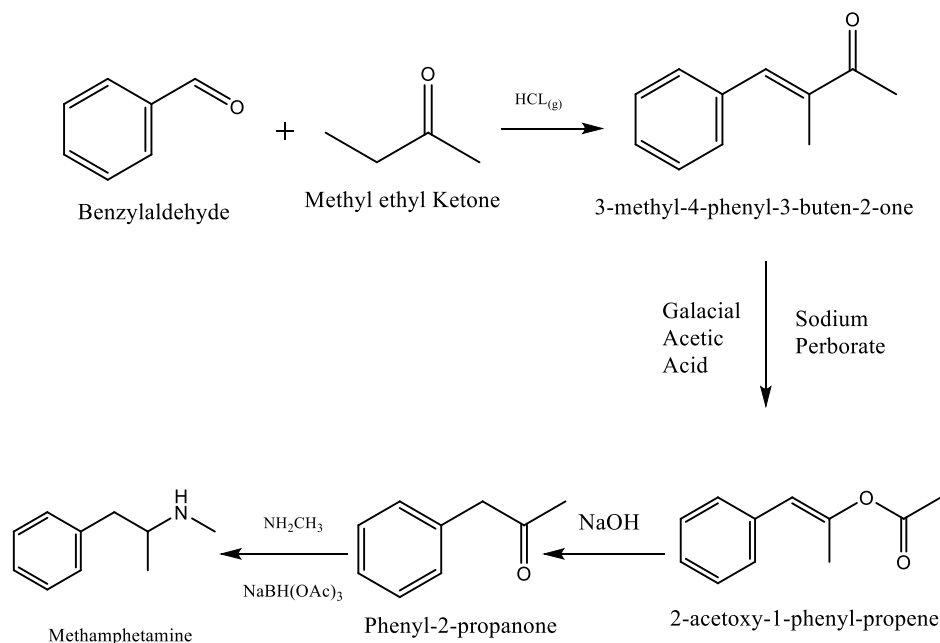


Figure 2.15: Impurities found in Amphetamine Type Stimulants

Douša and co-workers (2016) investigated a method for detecting and quantitatively determining GIs in the vortioxetine manufacturing method using photochemically induced fluorescence detection RP-HPLC. The technique was developed to control the nitro sulfide and H₄N₂S impurities in Vortioxetine shown in **(Figure 2.16)**, with a limit of 75 ppm for each impurity based on the maximum daily dose of APIs. It involved using a mobile phase containing aqueous solutions of 10 mM NH₄HCO₂ and ACN and a post-column photochemical reaction to achieve higher sensitivity and selectivity than UV detection. The selectivity and optimization of the process were confirmed through various experiments and analyses, demonstrating its effectiveness in pharmaceutical analysis [119].

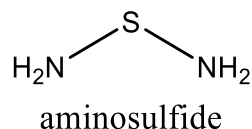


Figure 2.16: Impurities found in Vortioxetine

Wang and co-workers (2016) developed a highly accurate and sensitive method to measure small amounts of hydrazine shown in **(Figure 2.17)** in pharmaceutical substances. They used RP-LC and UV derivatization to enhance the separation of compounds and improve the technique's sensitivity and selectivity. The researchers employed derivatizing reagent (2-Hydroxy-1-Naphthalaldehyde), which yielded a detection limit of 0.25 ppm [120].

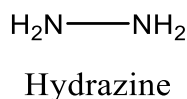


Figure 2.17: Chemical structure of API

Plummer and coworkers (2016) worked on the chemical synthesis of MDMA shown in **(Figure 2.18)** from piperonal extracted from black pepper. A catalytic RuO_4 oxidation of piperine was used to remove piperonal, and various oxidation conditions were experimented with. It was found that 6-Cl-MDMA was an impurity within the sample. The developed methodology makes it easy to synthesize a large quantity of precursor material using readily available reagents [121].

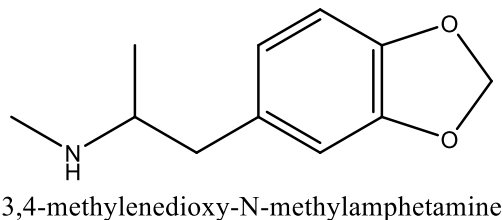
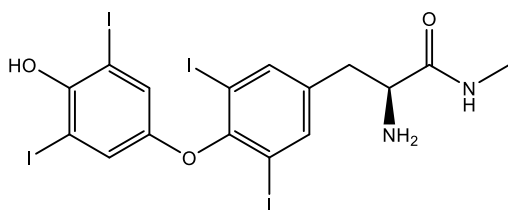
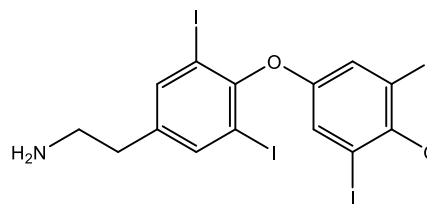


Figure 2.18: Chemical structure of MDMA

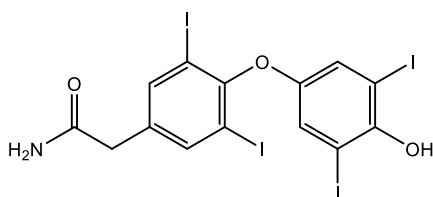
Panmanad and co-researchers (2016) synthesized and characterized five potential USP-grade levothyroxine impurities. Levothyroxine is a synthetic form of thyroxine used to treat thyroid hormone deficiency and goiter. The synthesis is done from the levothyroxine drug or readily available raw materials. These impurities were fully characterized using IR, ¹H NMR, and MS. The impurities shown in (**Figure 2.19**) were obtained from commercially available corresponding acids [122].



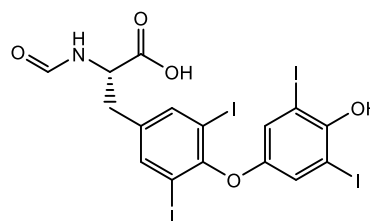
levothyroxine N-methyl amide



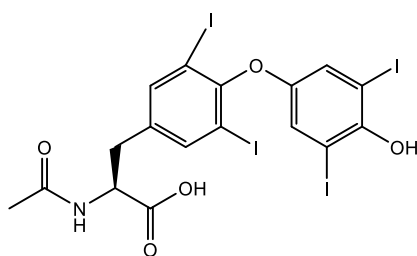
2-(4-(3,5-diiodo-4-methoxyphenoxy)-3,5-diiodophenyl)ethanamine



2-(4-(4-hydroxy-3,5-diiodophenoxy)-3,5-diiodophenyl)acetamide



(S)-2-formamido-3-(4-(4-hydroxy-3,5-diiodophenoxy)-3,5-diiodophenyl)propanoic acid



(S)-2-acetamido-3-(4-(4-hydroxy-3,5-diiodophenoxy)-3,5-diiodophenyl)propanoic acid

Figure 2.19: Chemical Structure of Levothyroxine Impurities

Nema and coworkers (2016) worked on developing and validating an HPLC method for identifying and assessing impurities of eletriptan shown in **(Figure 2.20)** formed during its synthesis. The impurities were characterized using FTIR, GC-MS, and NMR. Separation was done by HPLC and C18 analytical column. The technique was confirmed according to ICH guidelines [123].

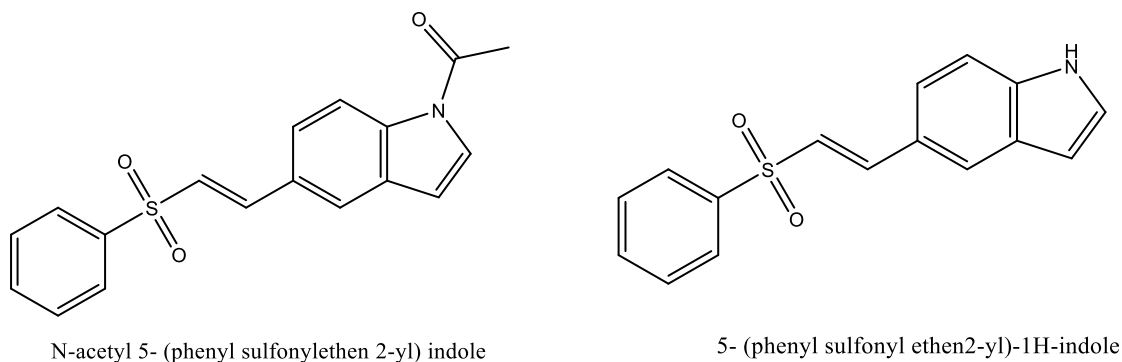
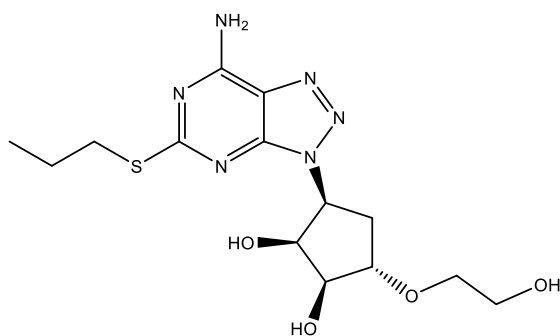
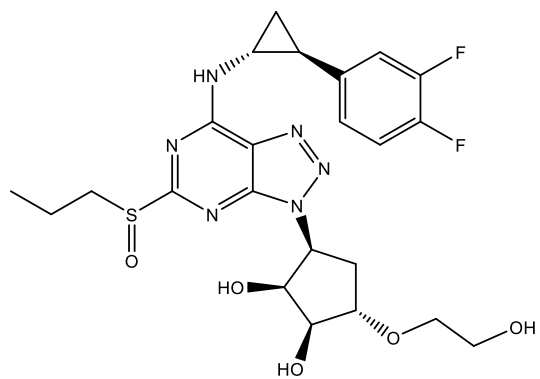


Figure 2.20: Impurities of Eletriptan

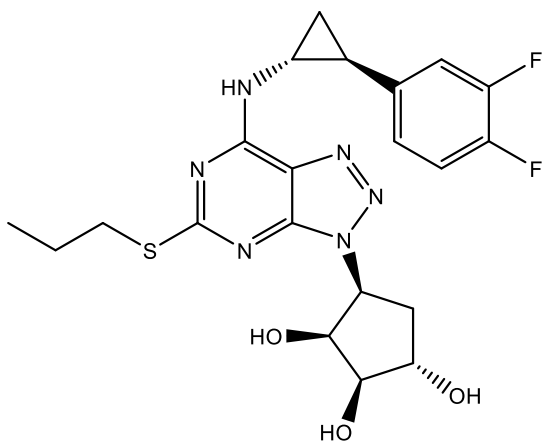
Kumar and co-researchers (2016) delved into the identification, isolation, structural characterization, and prospects for forming several analogs detected in TIC lab batches using LC-MS and HPLC methods. Five analogs were found, four unknown and named Imp-I to IV. The chemical structures of these new findings were identified using an LC-ESI/MS_n analysis. These analogs shown in **(Figure 2.21)** were isolated from augmented raw samples by column and preparative HPLC [124].



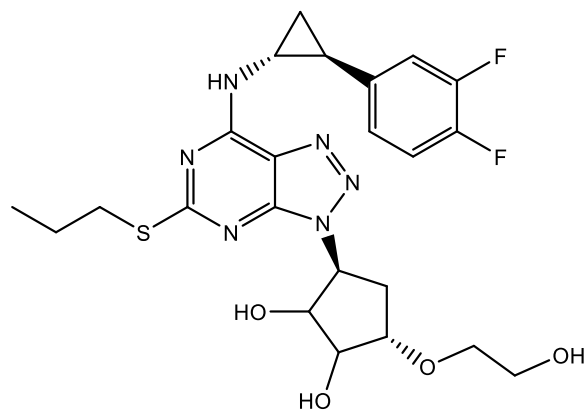
Ticaglor Imp I



Ticaglor Imp II



Ticaglor Imp III

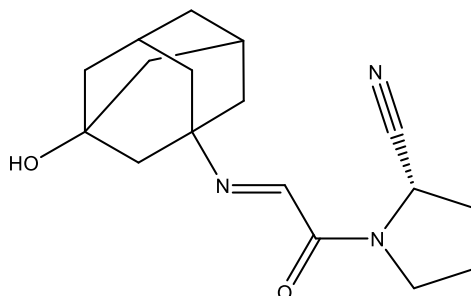


Ticaglor Imp IV

Figure 2.21: Impurities of Ticaglor

Kumar and coworkers (2016) conducted a study on an unknown impurity, Impurity-E, discovered during HPLC analysis of different batches of vildagliptin. The concentration of this impurity ranged from 0.01% to 0.06%. LC/ESI-MSn analysis determined that Impurity-E is unstable in H₂O: CH₃CN and degrades into another stable impurity, Impurity-F. Various techniques were used to identify Impurity-F, including FT-IR, MS, NMR, and 2D NMR. The study also examined the fragmentation mechanism, provided

structural elucidation, identified the impurity shown in (**Figure 2.22**), and discussed the abnormal behavior of Impurity-E [125].



(2S)-1-[2-[(3-hydroxyadamantan-1-yl)imino]acetyl]pyrrolidine-2-carbonitrile

Figure 2.22: Impurity of Vildagliptin

Ruggenthaler and co-authors (2017) discussed the USP monograph for L-thyroxine shown in (**Figure 2.23**), which uses two HPLC methods to identify organic impurities in the drug. The first method's impurity profile has been extensively studied, but the second method has a distinct impurity profile that still needs improvement in terms of structural elucidation; slightly adjusting the chromatographic parameters and using comprehensive structural elucidation techniques led to the discovery of 24 compounds that had yet to be previously reported in the literature, including two new classes of L-thyroxine analogs. They identified five of these novel compounds through the isolation/synthesis of reference substances, followed by NMR spectroscopic analysis [126].

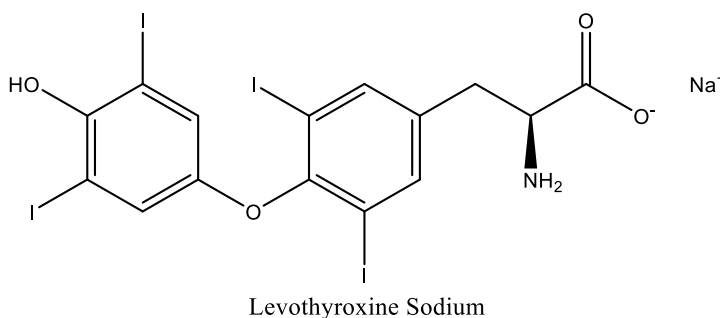


Figure 2.23: Chemical Structure of Levothyroxine

Zhao and co-authors (2017) detected eight impurities in anidulafungin bulk drug through HPLC. Preparative HPLC was used to isolate 4 impurities characterized through NMR and ESI-MS spectral data. Imp-I was identified as a known open-chain hydrolysis product formed during synthesis and degradation. II and III lacked a -OH group at the C-4 and C-8 positions. Additionally, VIII was discovered to contain an OH group at the C-23 position. These 3 new impurities were determined to be process-related substances [127].

Kumar and his colleagues (2017) analyzed batches of isoproterenol HCL and discovered an impurity called Imp-II. Through LC-MS, the proposed structure was confirmed using NMR and IR spectroscopy. The purity and retention time of the impurity was verified through HPLC, and a new chemical route was established to produce the impurity in the necessary quantity with the required purity level. This impurity shown in **(Figure 2.24)** serves as a reference standard [128].

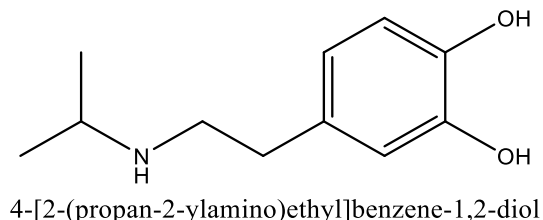
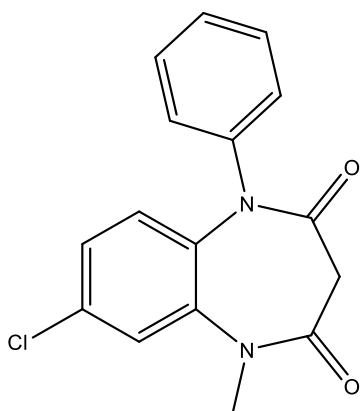
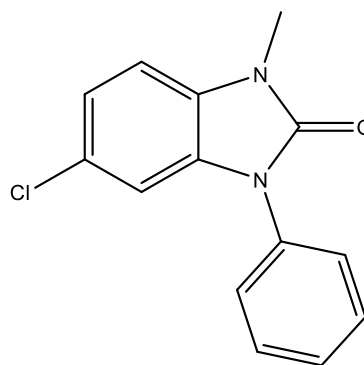


Figure 2.24: Impurities of isoproterenol hydrochloride

Kumar and co-researchers (2017) worked on the identification, synthesis, structural characterization, and prospects for optimizing the process for clobazam, an anxiolytic agent. Eight impurities were detected during the procedure, six enumerated by the European Pharmacopoeia. Two new impurities were discovered and identified through the LC-ESI/MSⁿ study Imp-G and H. The structures of these impurities shown in **(Figure 2.25)** were completed by synthesis and spectral analysis [129].



8-chloro-1-methyl-5-phenyl-1,5-dihydro-3H-1,5-benzodiazepine-2,4-dione



5-chloro-1-methyl-3-phenyl-1H-benzo[d]imidazol-2(3H)-one

Figure 2.25: Impurities of clobazam

Bondre and co-researchers (2017) delved into two impurities in the final compound during the commercial production process of Sertraline Hydrochloride (an antidepressant drug) that must be identified for regulatory compliance. The impurities shown in **(Figure 2.26)** were identified, synthesized, and characterized.

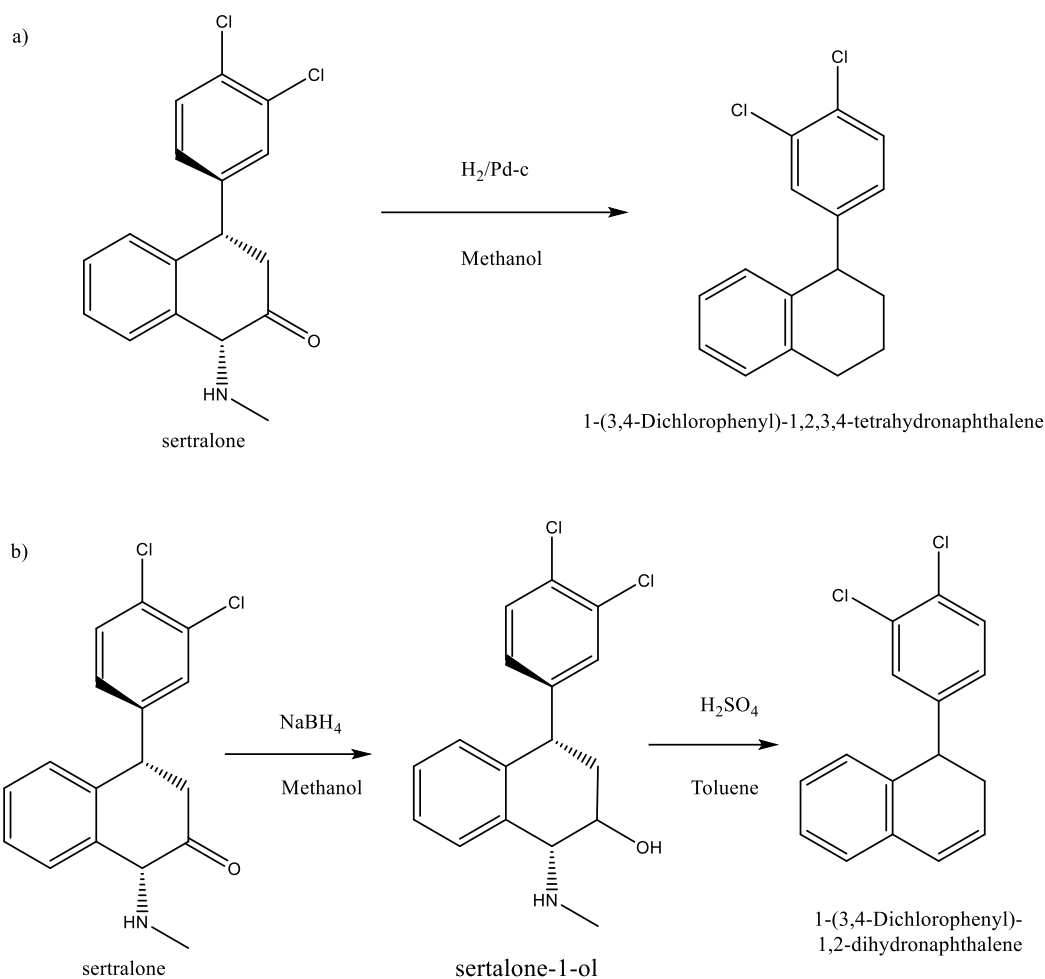


Figure 2.26: Impurities of Sertalone

Rahman and co-researchers (2017) discussed the potential GIs, DMS, and MMS shown in **Figure 2.27** that can be created by synthesizing some APIs. Novel and sensitive methods were developed and confirmed as per ICH rules to determine the presence of these impurities. LC-MS/MS was used to determine MMS, while liquid-liquid extraction was used to determine DMS. These methods offer reliable recovery, accuracy, and precision across various concentrations. They can also choose whether patients exceed the toxicological concern threshold [131].

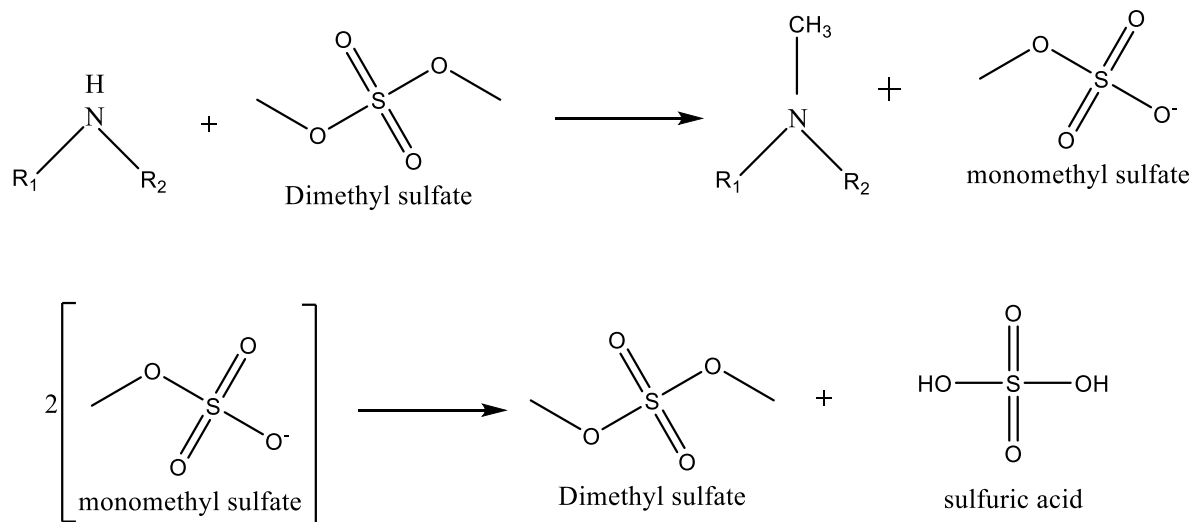


Figure 2.27: The conversion of MMS into DMS and sulfuric acid.

Kumar and coworkers (2017) investigated a new process-related impurity of the carisoprodol drug substance. They identified, synthesized, and characterized the impurity shown in **(Figure 2.28)**. It was consistently observed at a level of 0.14% and was not reported in the U.S. pharmacopeia. This study provides a reference standard for this impurity and is helpful to the pharmaceutical industry for similar drugs [132].

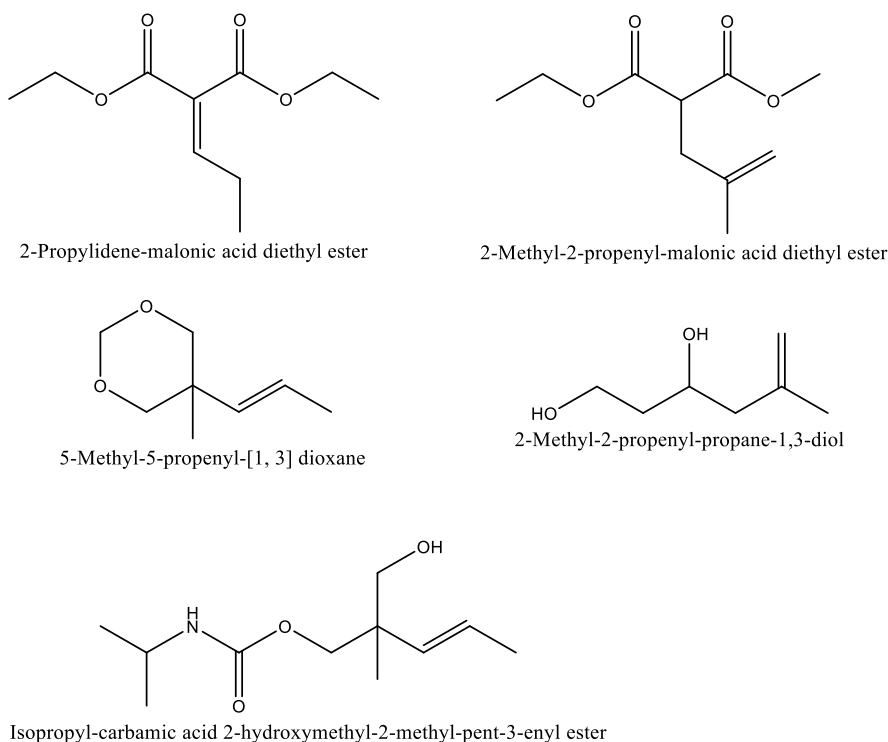
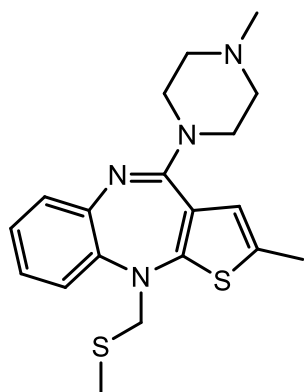
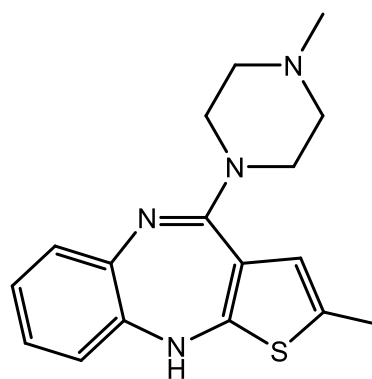


Figure 2.28: Impurities of Carisoprodol

Zhuang and colleagues (2018) conducted a study on synthesizing the olanzapine drug. This synthesis involved the reaction between thienobenzodiazepine HCL and N-methylpiperazine. During the manufacturing process of olanzapine, pilot batches were found to contain two unknown impurities, which were detected through HPLC analysis and ranged in concentration from 0.08-0.22%. Preparative HPLC was used on the reaction's mother liquor to isolate these impurities. The impurities shown in **(Figure 2.29)** were then characterized using many analytical methods, including LC-MS/TOF, UV, 1D-NMR, 2D-NMR, FT-IR, and single-crystal XRDA. Based on a thorough spectral analysis and knowledge of the synthetic route, the researchers successfully identified these two new impurities [133].



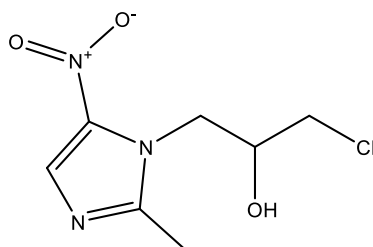
Olanzapine Impurity 1



Olanzapine Impurity 2

Figure 2.29: Chemical Structure of Olanzapine Impurities

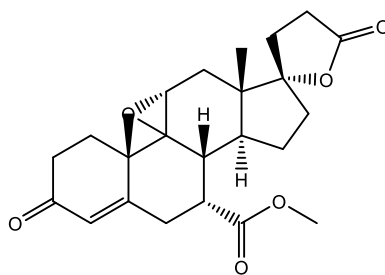
Leontiev and co-authors (2018) focused on synthesizing and characterizing impurities of ornidazole, which is crucial for confirming the safety and quality of drugs. Reference standards of related impurities are required for the reliable determination of impurities in medicinal items. Ornidazole-epoxide and -diol are known impurities formed in aqueous solutions and are commercially available for research. Efficient methods for synthesizing these impurities have been developed, and their profiles in ornidazole (**Figure 2.30**) substance and infusion solution have been studied [134].



[a-(chloromethyl)-2 methyl -5 nitroimidazole -1-ethanol]

Figure 2.30: Chemical Structure of Ornidazole

Filip and his co-researchers (2018) developed and validated two new HPLC methods. These methods were used to analyze the PRIs of the eplerenone drug (**Figure 2.31**) and its starting material. The Kromasil C18 column was utilized to monitor and control the process impurities. At the same time, the polysaccharide-based Kromasil 5-AmyCoat chiral stationary phase was employed to maintain the stereochemical purity of the starting material. Raman spectroscopy was utilized to confirm the identity of the PRIs. The most distinctive feature in identifying these impurities was the difference in wave numbers of the C-C and C-O stretching vibrations [135].



9,11a-epoxy-7a-methoxycarbonyl-3-oxo-
-17a-pregn-4-ene-21,17-carbolactone

Figure 2.31: Chemical Structure of Eplerenone

Mythili (2018) discussed the synthesis of various pyridine derivatives of Dalfampridine, particularly genotoxic impurities. These derivatives shown in (**Figure 2.32**) were synthesized using different waste applications of chemical reactions. The objective was to achieve high yield and purity, focusing on automated combi flash. The synthesized genotoxic impurities were analyzed using a hyphenated analytical technique, and their HPLC purity was documented. These impurities can serve as a reference in the medicinal industry for assessing the drug. In-vitro antibacterial activity against gram-positive and gram-negative bacteria was tested for the synthesized compounds. It was found that some of these compounds showed considerable antibacterial activity [136].

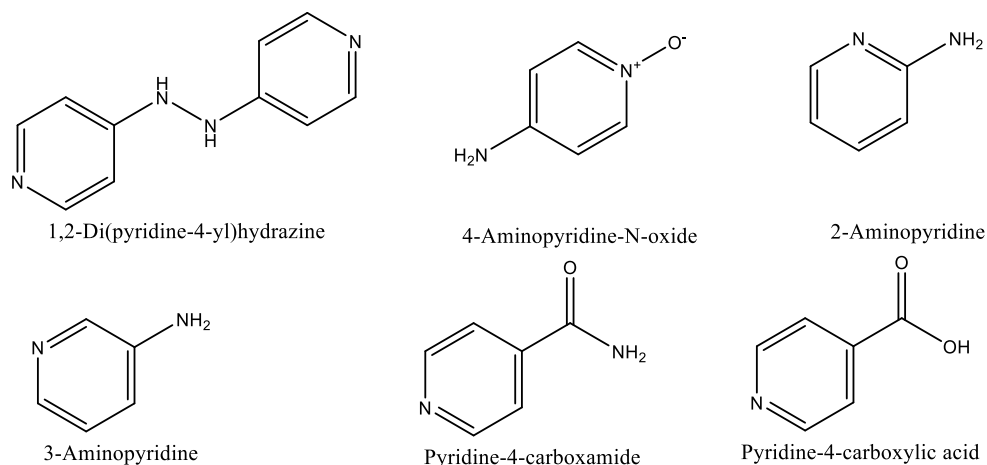
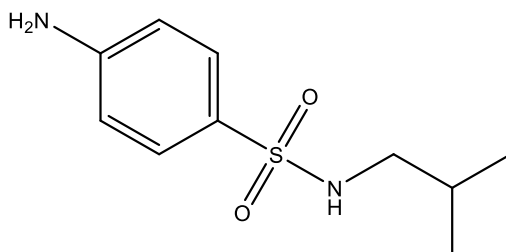


Figure 2.32: Impurities of Dalfampridine

Wagh and coworkers (2018) worked on synthesizing, characterizing, and quantifying process-related impurities in Ritonavir shown in **(Figure 2.33)**, a chemical compound used in medication. This synthesis included isobutyl amine, sulfanilic acid, and methanol as catalysts. The impurity was evaluated on a lab scale, and its conformation was determined using highly developed instruments like FT-IR, NMR, UV, and RP-HPLC. An RP-HPLC method was developed to identify and quantify the impurity of Ritonavir in both bulk samples and manufacturing samples. The impurity was present at 0.32% in the tablet and 0.84% in the bulk sample. [137].



4-amino-N-(2-methyl propyl) benzene sulphonamide

Figure 2.33: Impurities of Ritonavir Hydrochloride

Yadav discussed synthesizing and characterizing impurities and metabolites of Rabeprazole, an antiulcer drug. The work aimed to identify and minimize impurities to ensure the assurance of the final product. It also included synthesizing various compounds related to Rabeprazole, such as Rabeprazole Sulfone, Rabeprazole Chloro Impurity, and Methoxy Rabeprazole shown in **(Figure 2.34)** [138].

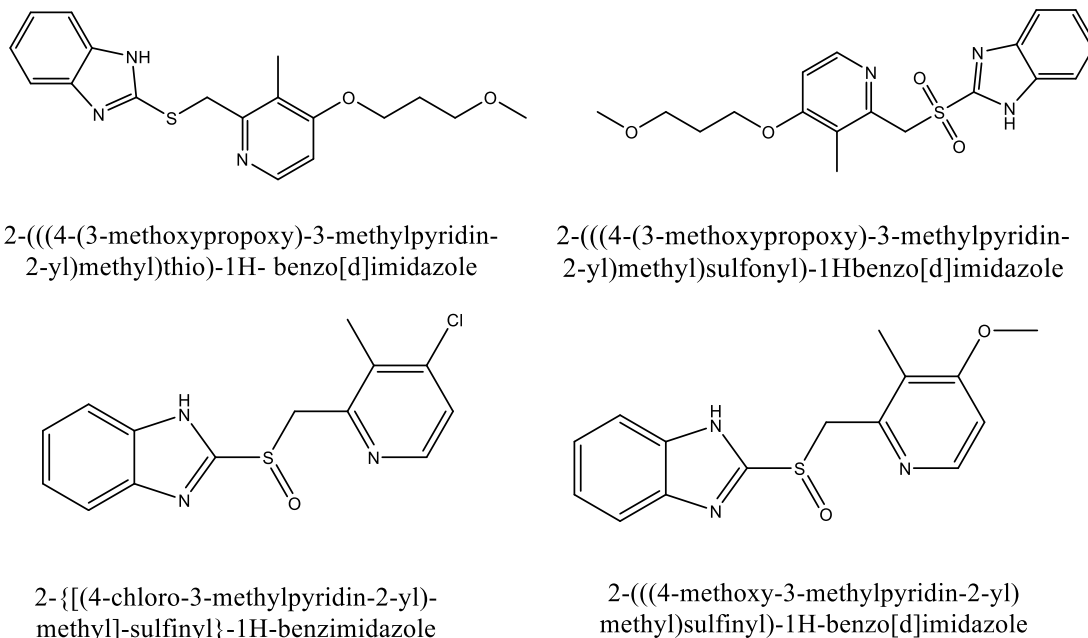


Figure 2.34: Impurities of Rabeprazole

Scherf-Clavel and coworkers (2019) focused on the limitations of targeted impurity profiling plans and introduced a generic untargeted approach for impurity profiling of sartan drug products shown in **(Figure 2.35)**. The untargeted plan can distinguish between batches, production sites, and variations resulting from changes in the production process. This plan employs MS and multivariate analysis to interpret the data. It has shown successful discrimination between samples contaminated with N-nitrosodimethylamine and free samples. Furthermore, this untargeted approach has uncovered two previously

unknown impurities, valeramide and N, N-dimethylvaleramide, in various sartan drug products [139].

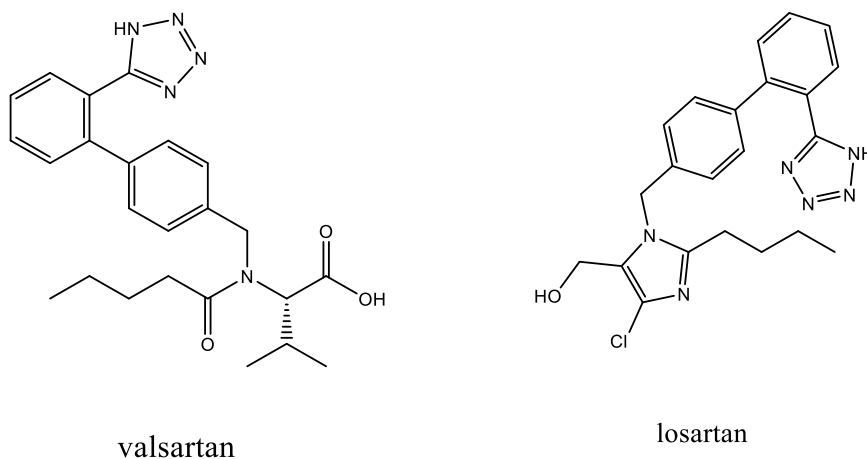


Figure 2.35: Chemical Structure of Sartan Drugs

Zhang and colleagues (2020) detected and isolated 7 impurities in the doramectin bulk drug using HPLC analysis. Two impurities have yet to be described previously. The structure of these impurities was determined through spectral analysis, and their formation mechanism and insecticidal activity were discussed. Imp-IV was identified as a product of furan ring-opening, whereas Imp-V did not contain the -OH group at C-14 in doramectin [140].

Reddy and colleagues (2020) worked on synthesizing and characterizing sildenafil sulfonyl esters associated with sildenafil. Given their governing importance, the synthesized compound has proven valuable for the medicinal industry—a simple and effective method to prepare sildenafil sulfonyl esters. They also investigated impurities in sildenafil shown in (**Figure 2.36**) and used different techniques to analyze them. Through spectroscopic methods, we identified and characterized the other sulfonyl esters present in sildenafil [141].

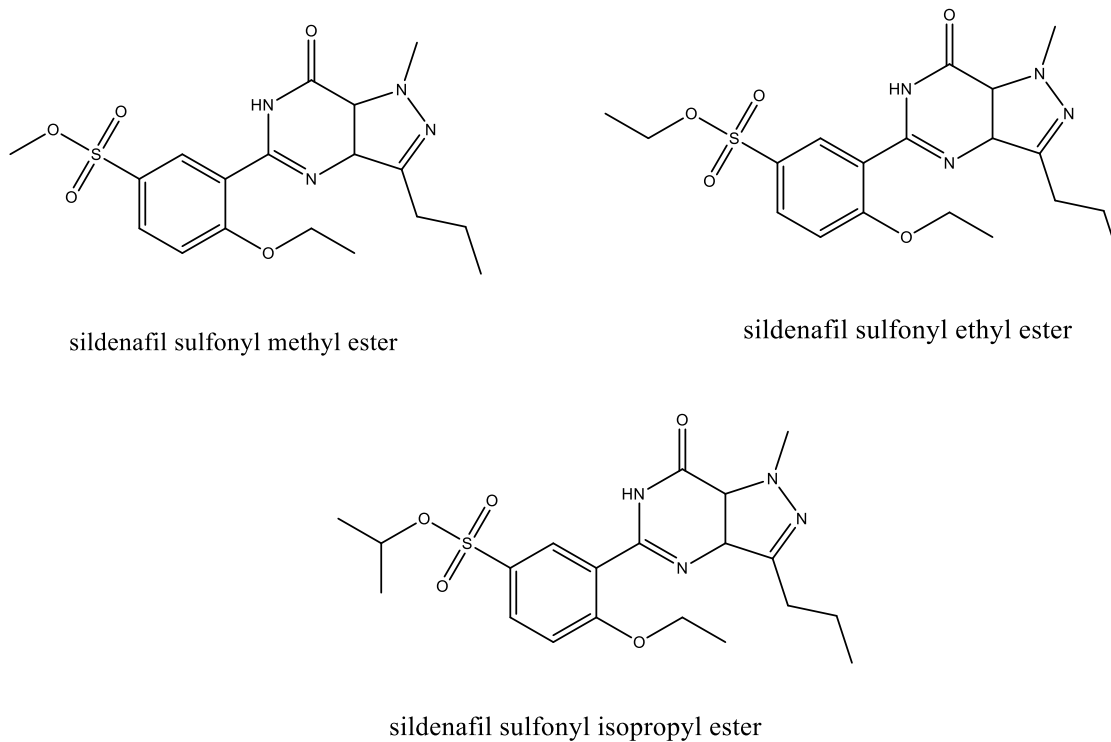


Figure 2.36: Impurities of Sildenafil Citrate

Crawford and co-researchers (2020) worked on Hydantoin-based APIs, such as nitrofurantoin and dantrolene shown in **(Figure 2.37)**, which were synthesized using twin-screw extrusion (TSE), with minimal or no solvent employed. No post-synthetic workup was necessary. The feasibility of continuously conducting solvent-free synthesis for pharmaceutical products is showcased in this study [142].

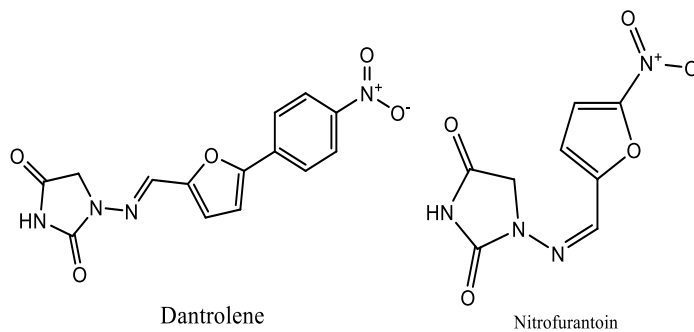


Figure 2.37: Chemical Structure of API

Zate and co-researchers (2021) developed an LC method for quantifying genotoxic impurities in Salbutamol Sulphate. Potential genotoxic impurities were identified, and an LC was designed and authorized, successfully quantifying the reported compound at the ppm level. The settled method is suitable for quantifying genotoxic impurities shown in **(Figure 2.38)** in Salbutamol Sulphate [143].

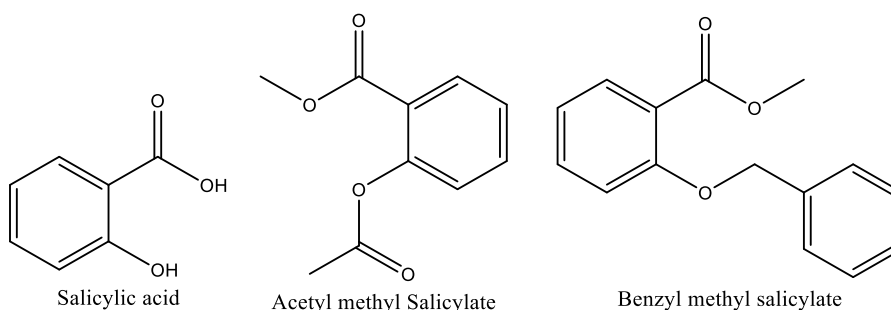


Figure 2.38: Impurities of Salbutamol Sulphate

Soyseven and co-researchers (2021) conducted a study on a novel analytical method and successfully confirmed the presence of a compound called GI, 5A2Cl shown in **(Figure 2.39)**, in a sample of TNX, a model API. The method employed an HPLC-UV detection system and a mobile phase of H₂O and MeOH. The results demonstrated that the method was highly reliable, quick, easy to use, and suitable for detecting the GIs with great sensitivity [144].

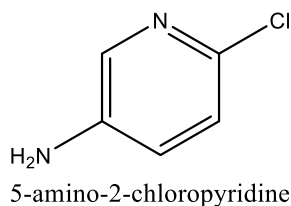


Figure 2.39: Chemical Structure of API

Jireš and co-workers (2021) developed a sensitive method to detect genotoxic impurities in drug products containing tetrazole-based sartans. Their method used HPLC-MS and accurately quantified impurities below 1/10th of the specification limit. The limit of quantification for GTI-azide-1 was 0.033 ppm, while for GTI-azide-2 shown in **(Figure 2.40)** it was 0.025 ppm. [145].

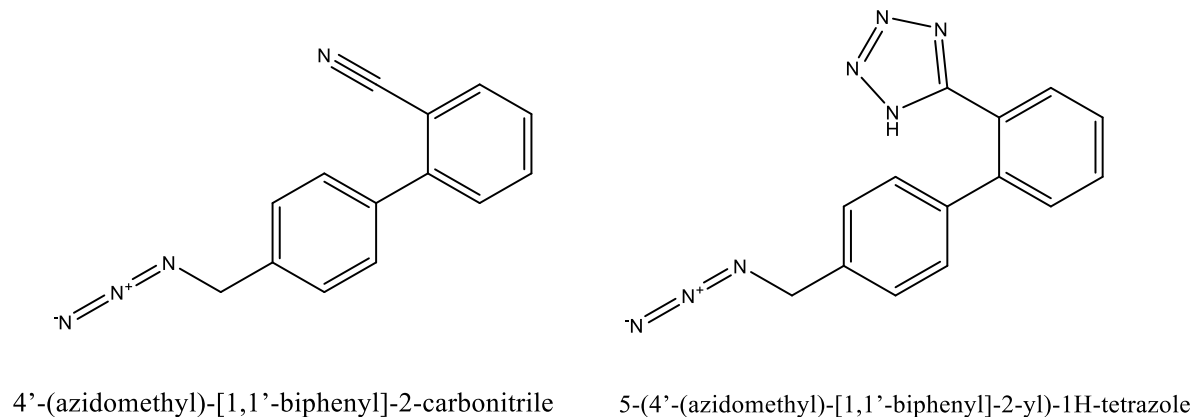


Figure 2.40: Chemical Structure of Impurities

Prculovska and co-researchers (2022) worked on various pharmaceutical products' nitrosamine impurities shown in **(Figure 2.41)** and mutagenic carcinogens. The main contamination routes are using contaminated starting materials and the synthesis process. The formation of the CH₂N₄ ring in sartans and ranitidine is identified as the root cause of nitrosamine contamination. Medicine governing authorities rules to identify and solve the problem. The presence of nitrosamines in therapeutic products must be limited due to their mutagenic and carcinogenic effects [146].

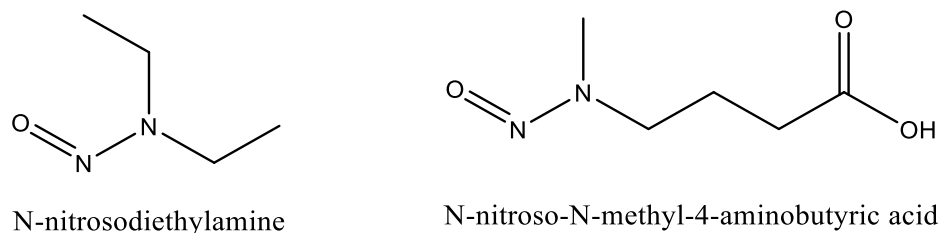


Figure 2.41: Chemical Structure of Nitrosamine

Bellur and coworkers (2022) developed a method for quantifying organic impurities in fingolimod hydrochloride using EP and USP. The manufacturing of fingolimod HCL shown in **(Figure 2.42)** is complex, requiring stringent controls of intermediates, precursors, and process steps. Eight process-related impurities and one previously unknown process-related impurity were recognized and characterized using various spectroscopical techniques. Two impurities were assessed for potential genotoxicity. An RP-UPLC method was developed and authorized to effectively control these impurities and maintain the assurance of the drug [147].

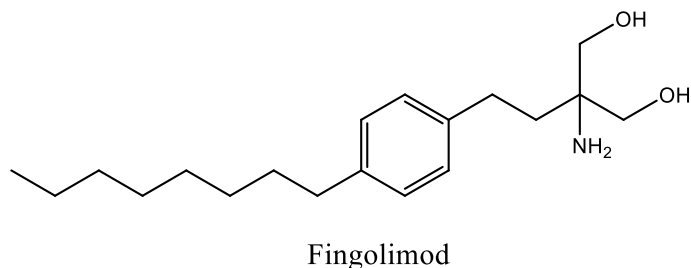


Figure 2.42: Chemical Structure of API

Vadlamani and co-researchers (2022) developed a new method to detect and quantify GTI-1 and GTI-2 in Telbivudine drugs shown in **(Figure 2.43)**. The technique uses RP-UPLC-MS and is specific, complex, reproducible, and suitable for quantifying GTIs in Telbivudine drug and formulation. The method was authorized per ICH rules and demonstrated stability for up to 24 hours at room temperature [148].

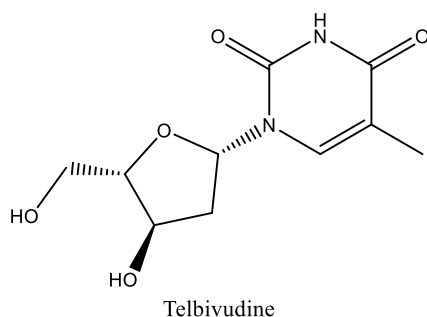


Figure 2.43: Chemical Structure of API

Gopa and coworkers (2022) discussed the importance of impurity profiling in synthesizing APIs. It highlights the importance of effective impurity control to ensure drug products' assurance, safety, and efficiency. The study synthesized and characterized five impurities of mirabegron shown in **(Figure 2.44)** and confirmed the established synthesis route's simplicity, convenience, and cost-effectiveness. The generated impurity standards were used in developing and validating analytical methods, facilitating the optimization of the process development stage, and minimizing or eliminating the formation of impurities in the production process of mirabegron. This contributes to creating pharmaceutical products with enhanced safety [149].

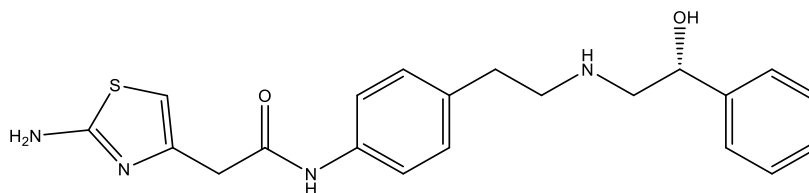


Figure 2.44: Chemical Structure of Mirabegron

Kalauz and co-authors (2022) focused on potential GTIs in the Crotamiton drug. A straightforward and reliable GC was formulated to detect these impurities within the Crotamiton drug substance shown in **(Figure 2.45)**. The key benefit of this method lies in its capability to quantitatively assess all potential GTIs that may be present throughout the synthesis process of the Crotamiton drug. During the method development phase, separation was achieved for toluidine isomers, N-methyl-toluidine isomers, and N-ethyl-

toluidine isomers. Thus, GC was authorized according to relevant guidelines, establishing its efficacy at a specification limit of not more than 40 ppm [150].

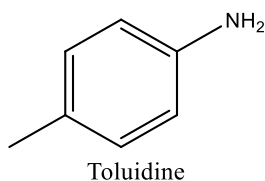


Figure 2.45: Chemical Structure of API

Lavayssiere and co-workers (2023) delved into the amidation process, essential in synthesizing various organic compounds, particularly APIs. However, its efficiency and sustainability still need to be improved. To address this challenge, a solventless approach was employed to synthesize an amide using a twin-screw extruder in the presence of a coupling agent. This innovative method demonstrated high yields and productivity. Through carefully assessing reaction conditions, this approach was successfully applied to prepare two APIs: teriflunomide and moclobemide shown in **(Figure 2.46)**. This advancement expands the capabilities of twin-screw extrusion as a synthetic tool for organic molecule preparation, with the potential for broader industrial applications [151].

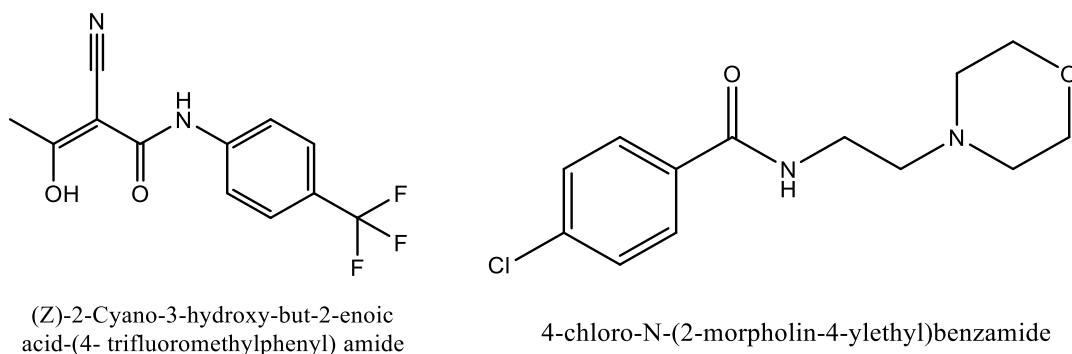


Figure 2.46: Chemical Structure of teriflunomide and moclobemide

Satheesh and his co-researchers (2023) discussed the synthesis, characterization, and origin of ezetimibe impurities shown in **(Figure 2.47)**, which are the drug's positional isomers. Ezetimibe is a drug substance that belongs to the azetidine analog and substituted β -lactam class. It functions as a hypolipidemic agent, helping to lower cholesterol levels in the body [152].

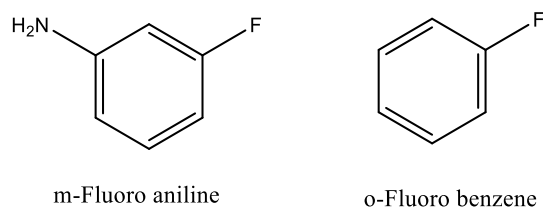


Figure 2.47: Impurities of Ezetomibe

Objectives

The synthesis and characterization of genotoxic and process impurities of APIs are essential in pharmaceutical development and manufacturing. This is because it guarantees safety, compliance with regulatory standards, and the overall quality of pharmaceutical products. Pharmaceutical companies can proactively ensure their products meet safety and efficacy standards by identifying and analyzing potential impurities. This is especially important given pharmaceuticals' critical role in maintaining public health. Therefore, pharmaceutical companies must prioritize thoroughly characterizing and monitoring API impurities. The main objectives of this research are:

1. Synthesis of APIs Impurities
 - a) Synthesis of Rufinamide Impurities
 - b) Synthesis of Lidocaine Impurities
2. Characterization of API Impurities (Rufinamide and Lidocaine)

CHAPTER 3: SYNTHESIS AND CHARACTERISATION OF ANTI-EPILEPTIC DRUG (RUFINAMIDE) IMPURITIES

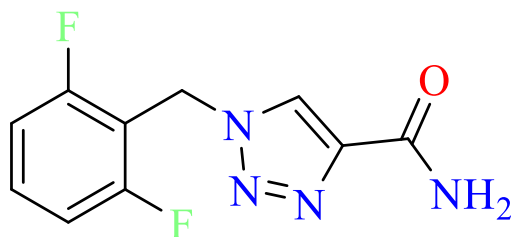
3.1 INTRODUCTION TO RUFINAMIDE

Rufinamide (Ruf) is a type of medication in the triazole derivative class. It is considered a third-generation anti-epileptic drug (AED) and is believed to work by reducing the inactive phase of voltage-gated sodium channels (VGSCs). This reduction in activity helps to decrease the hyperactivity of neurons. In 2008, the United States FDA approved rufinamide as an additional cure for seizures that accompany LGS in patients aged four and above. Then, in 2015, the FDA extended its approval to include children aged one year and older. LGS is a type of epilepsy that begins in childhood and is characterized by a range of seizures that can hinder intellectual growth in young children. Unfortunately, seizures associated with LGS are often challenging to treat [153].

Initially developed by Novartis using a click chemistry approach, Eisai currently produces Rufinamide under Inovelon. It is primarily prescribed for the treatment of LGS and is classified as an antiepileptic drug. Antiepileptic medications are categorized according to their mechanism of action, with some targeting specific channels or utilizing unknown mechanisms. VGSCs are membrane proteins vital in controlling cellular impulsiveness by regulating sodium ions. Malfunctioning VGSCs have been associated with epileptic seizures, and most antiepileptic drugs function as Na channel blockers by stabilizing the inactive state of the channels, preventing them from returning to an active state. The sales of Banzel, Inovelon, Rufinamide generics, and Banzel generics in the pharmaceutical markets of the United States and European Union collectively reached billions of dollars in 2012 [154].

3.1.1 Chemistry

Rufinamide is a crystalline substance known as 1-(2,6-difluorophenyl)methyl-1*H*-1,2,3-triazole-4-carboxamide, as illustrated in **Figure 3.1**. This substance is colorless, odorless, and has a slight bitterness. Rufinamide exhibits low solubility in H₂O, 0.1 N HCL (63 mg/L), and SIF (59 mg/L). It follows a structural formula of C₁₀H₈F₂N₄O, with a molecular weight of 238.20. Rufinamide is commercially available in tablet form, with dosages of 100, 200, and 400 mg tablets. It is important to note that rufinamide can absorb moisture even in environments with 100% relative humidity. It has a provisional shelf-life of three years and should be stored below 30 degrees Celsius [155–157].



Rufinamide

Figure 3.1: Chemical Structure of Rufinamide

3.1.2 Pharmacology

3.1.2.1 Activities in experimental models of epilepsy and seizures

Research on Rufinamide's efficacy in experimental models of epilepsy has been comprehensive. Conducted under initiatives like the NIH anticonvulsant development program of drugs and at Novartis, the studies have showcased promising results. The drug's effectiveness has been assessed using the MES test, a well-established method for evaluating antiepileptic medications' potential in managing general tonic-clonic seizures and, to some degree, focal seizures. Rufinamide established protective effects in mice and rats during this test, with an oral ED⁵⁰ range of 6–24 mg/kg, indicating its ability to reduce seizures induced by MES. Furthermore, Rufinamide effectively suppressed MES-induced

tonic-clonic seizures in mice, with ED⁵⁰ values of 23.9 mg/kg for oral administration and 15.5 mg/kg for intraperitoneal administration. The drug also effectively reduced pentylenetetrazole-induced clonic seizures in mice, with ED⁵⁰ values of 45.8 mg/kg (oral) and 54.0 mg/kg. Notably, no tolerance to Rufinamide's anticonvulsant effects was observed after five days of repeated dosing at 6 mg/kg orally. In the MES test, the drug's anticonvulsant impact lasted 4 hours in mice and extended to 8 hours in rats [158–160].

In the pentylenetetrazole (PTZ) test using mice, a model for clonic seizures and absence seizures demonstrated an ED⁵⁰ of 300 mg/kg, resulting in a protection rate of 60%. When the subcutaneous PTZ test was assessed in mice, oral administration yielded an ED⁵⁰ of 458 mg/kg. It effectively prevented clonic seizures from GABA antagonists bicuculline and picrotoxin in mice, with ED⁵⁰ values of 50.5 and 76.3 mg/kg orally. However, its efficacy was limited in glycine-inhibition seizures caused by strychnine. In a separate study, oral doses of 100 to 300 mg/kg of rufinamide effectively delayed kindling progression and suppressed after-discharges in amygdala-kindled cats experiencing general tonic-clonic convulsions [148,149,150,155,158,161]. Rufi has been proven to be a safe and effective anticonvulsant in various seizure scenarios. It reduces seizure frequency in monkeys and inhibits cat discharges. It is versatile in handling many types of seizures at non-toxic doses. Ruf is more effective in most animal models than other commonly used antiepileptic drugs. However, it faces challenges in countering strychnine-induced tonic seizures [162].

3.1.2.2 Mechanism of action

The specific mechanisms underlying the antiepileptic effects of rufinamide still need to be fully understood. However, in vitro studies have provided some insights into its primary mode of action. It appears that rufinamide primarily acts by modulating Na channels, specifically by protracting the inactive phase of the channel [148, 156]. Another possible mechanism involves inhibiting responses at mGluR5. This inhibition is more prominent at higher concentrations, resulting in approximately 60% inhibition of quisqualate-induced phosphoinositide turnover of 100 μmol/L [159]. The interactions of Ruf with a range of receptor ligands have been investigated. Notably, it does not affect receptor binding for

substances such as α 1-adrenergic, α 2-adrenergic), β -adrenergic), 5HT-1, 5HT-2, cholinergic muscarinic agonists, and antagonists. Furthermore, rufinamide does not interact with NMDA receptors, strychnine-induced glycine, glutamate receptors (R1, R2, R4, and R5), or kainate receptors [148-150]. Importantly, concentrations of rufinamide up to 100 μ mol/L do not influence benzodiazepine or GABA receptors. Mechanism of Rufinamide shown in **Figure 3.2**.

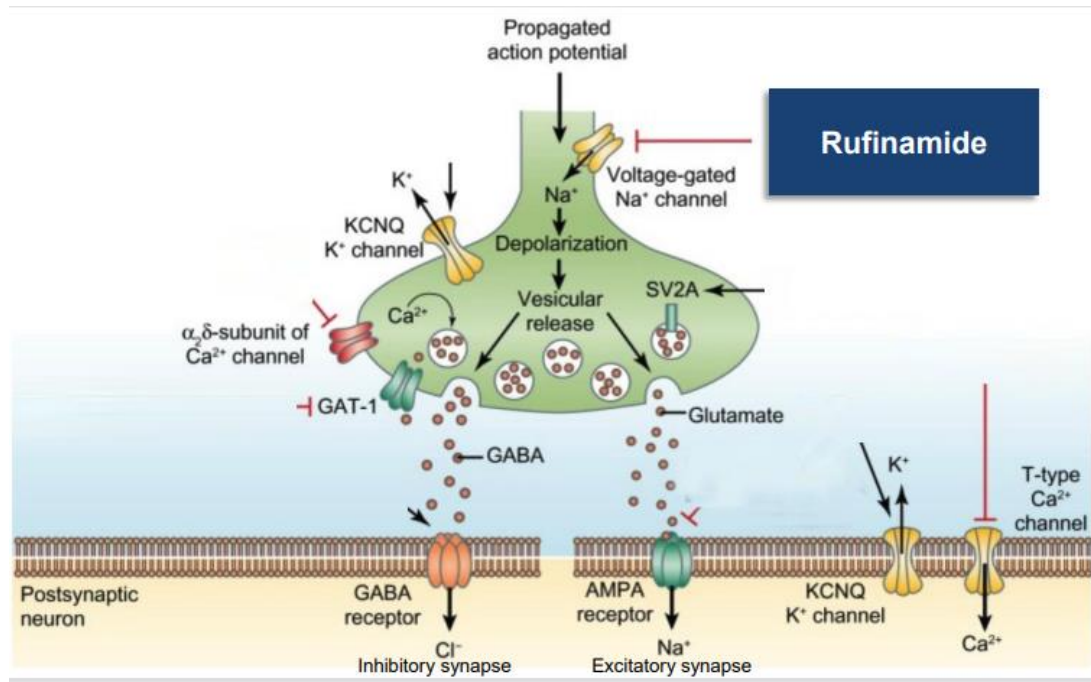


Figure 3.2: Mechanism of action of Rufinamide [172]

3.1.3 Pharmacokinetics

3.1.3.1 Bioavailability and Absorption

In initial studies, a preparation with 50% bioavailability was used, different from the current commercially available. The exact bioavailability of the commercial preparation is still unknown. However, a study was conducted with three healthy males to determine the absorption of rufinamide. Each volunteer received a single dose of 600 mg of radiolabeled gelatin capsules with food. The study showed that at least 85% of the drug was absorbed.

The absorption of rufinamide is limited by its slow dissolution in gastrointestinal contents, and its bioavailability depends on the dose. As the dose increases, the fraction of rufinamide absorbed decreases, resulting in a non-linear relationship between steady-state plasma concentration and dosage. Single-dose studies also revealed that taking rufinamide with oily meal increased the area under the concentration-time curve by approximately 30-40% compared to fasting. Although the impact of food on Ruf bioavailability during many doses has not been definitively established, it is recommended to take rufinamide with meals consistently. Rufinamide is moderately quickly absorbed in the gastrointestinal tract, reaching peak plasma levels between 4 and 6 hours after a single dose, with this timeframe varying from 1.5 to 10 hours. The absorption of rufinamide is not affected by the formulation or whether it is taken with or without food [163, 164].

3.1.3.2 Distribution

Rufinamide has a moderate plasma protein binding of approximately 26% to 34%. It is worth noting that at a dosage of 3200 mg/day, normalized to a bioavailability of 100% (V_d/F) is approximately 0.8 L/kg. However, it is important to remember that this value may be higher than actual due to the probable incomplete bioavailability at that dosage. As expected, those who receive higher dosages have larger V_d/F values due to the dose-dependent drop off in bioavailability [165]. Ruf is distributed evenly between red blood cells and plasma. A study conducted using radiolabeled (Eisai, data on file) in rats and rabbits examined the transfer of the drug to embryos. The findings suggest that after 24 hours, the levels in the embryo and amniotic fluid were approximately 50% of those present in the mother's bloodstream. The process of transfer was identified to be reversible. Radioactivity was further noted in the mammary glands of rats and rabbits, with levels comparable to those found in the blood and plasma, implying that it was probably discharged in breast milk [166].

3.1.3.3 Elimination and Metabolism

In healthy individuals, rufinamide has a plasma exclusion $\frac{1}{2}$ life of 8 to 12 hours, with an average of 10 hours. However, patients with epilepsy have been observed to have notably shorter half-lives of approximately 7 hours, possibly due to the initiation of rufinamide metabolism by other antiepileptic drugs. Despite its relatively short $\frac{1}{2}$ life, rufinamide's serum concentration experiences moderate fluctuations over a 12-hour dosing interval during a stable state as the continued absorption phase of the product. Body size also plays a significant role in determining rufinamide's apparent oral clearance, with females showing a slightly lower clearance rate than males. The study analyzed the concentrations of radioactive rufinamide and its metabolite in the plasma, urine, blood, and feces of three healthy adult male volunteers. These participants consumed 600 mg of ^{14}C -labeled microcrystalline gelatin capsules of rufinamide and their regular meals [167,168].

When administered at a lower dose, rufinamide, the primary compound detected in plasma, showed an absorption rate of at least 85%. The drug was mainly eliminated through the renal route, with nearly complete excretion within seven days. It underwent an extensive metabolic transformation, with only a tiny fraction excreted unaffected in urine and fecal matter. The most protruding metabolite identified was the inactive COOH derivative. In vitro studies using human liver microsomes revealed that the critical metabolic way involves hydrolysis, mediated by carboxylesterases, leading to the formation of COOH derivative [169].

3.1.4 Pharmacokinetics in Special Populations

Children: To better understand the impact of children on pharmacokinetics, further investigation is needed due to variations in dosages and co-medications across different age groups. To gain insights into the assurance of pharmacokinetics in children with epilepsy, a study was conducted on 16 children aged 2–17. In a study, rufinamide was administered twice daily, with 10 mg during the first week and 30 mg during the second week. Blood specimens were taken weekly to determine the pharmacokinetic profiles. The results showed that the increase in serum levels of rufinamide was not proportional when

the dosage was increased from 10–30 mg. Another study found that children under 12 had significantly lower levels, 19%; $P < 0.001$ compared to those above 18 years old getting the same mg/kg doses. This suggested a higher apparent oral clearance (CL/F) of rufinamide in children than in adults receiving similar mg doses. [170]

Older adults: To examine the age effect on pharmacokinetics by comparing 7 elderly healthy individuals (aged 66 to 77 years) to 7 younger healthy individuals (aged 18 to 40). The research involved single and multiple-dose conditions, with nine doses of 400 mg administered twice daily. The study utilized an open-label parallel-group design. The results showed that rufinamide's absorption and elimination $\frac{1}{2}$ life values in older adults were like those of younger individuals, and these values remained unchanged following multiple-dose treatments. Furthermore, the study found that time-independent kinetics were observed during multiple-dose administration in older and younger groups. These results proposed that the pharmacokinetics of rufinamide remain unchanged in older individuals compared to their non-elderly adult counterparts [170].

3.1.4.1 Impaired Renal Function

A study was conducted to assess the levels of rufinamide in patients with severe renal problems (creatinine clearance below 30 mL/min) compared to healthy participants who were given a single 400 mg dose. The findings revealed no notable variation in rufinamide levels between the 2 groups. However, an interesting observation was made when hemodialysis was initiated 3 hours after the dose: it reduced approximately 30%. This outcome indicated that hemodialysis could be a potential therapeutic approach for patients with toxic levels of the drug [171].

3.2 EXPERIMENTAL PART

3.2.1 Materials/Chemicals

All chemicals and solvents utilized in this research were of Analytical grade procured from Sigma, Aldrich, Mumbai, India. Freshly distilled moisture-sensitive reagents were dried under nitrogen/argon in positive-pressure oven-dried glassware. The completion and purity of compounds were checked using TLC (Merck 60 F254 precoated silica gel plates 0.2 mm thickness), while spot visualizations were performed under Ultraviolet light (254nm) and using various kinds of TLC stains like ninhydrin ceric ammonium molybdate, or KMnO_4 . The yield of the compounds was determined by calculating it using the following formula:

$$\text{Percent Yield} = (\text{Actual mass of product} / \text{Theoretical yield}) * 100\%$$

Table 3.1: List of Organic solvents used for the synthesis of Rufinamide process impurities

S. No	Name of the organic solvents	Purity (%)	Grade and Procured From
1.	Dichloromethane	>95%	AR, Sigma Aldrich
2	Ethanol	>95%	AR, Sigma Aldrich
3.	Methanol	>95%	AR, Sigma Aldrich
4	Acetone	>95%	AR, Sigma Aldrich
5	DMF	>95%	AR, Sigma Aldrich
6	Toluene	>95%	AR, Sigma Aldrich
7	Ethyl Acetate	>95%	AR, Sigma Aldrich
8	Distilled Water	>95%	AR, Sigma Aldrich

Note: Solvents used in the synthesis were distilled at their boiling points before use.

Table 3.2: List of chemicals used for the synthesis of Rufinamide process impurities

S. No	Name of the Chemicals/Reagents	Purity (%)	Grade and Procured From
1	Sodium Azide	>95%	AR, Sigma Aldrich
2	Potassium Iodide	>95%	AR, Sigma Aldrich
3	Tert-butyl Ammonium Bromide	>95%	AR, Sigma Aldrich
4	2-Chloroacrylonitrile	>95%	AR, Sigma Aldrich
5	Sodium Hydroxide	>95%	AR, Sigma Aldrich
6	Propargyl alcohol	>95%	AR, Sigma Aldrich
7	Thionyl Chloride	>95%	AR, Sigma Aldrich
8	Sulphuric Acid	>95%	AR, Sigma Aldrich
9	Sodium Bicarbonate	>95%	AR, Sigma Aldrich
10	Mono methyl amine	>95%	AR, Sigma Aldrich

3.2.2 Methods

i) Synthesis of benzyl azide (2a–2c)

In a four-neck round bottom flask, (5.0gm, 1.0 mol equivalent) of benzyl bromide (1a) or its derivatives (1b or 1c), sodium azide (1.2 mol equivalent), potassium iodide (0.49gm, 0.1 mol equivalent) and tert-butyl ammonium bromide (0.1 mol equivalent) in toluene (35ml, 7v/w) was heated to reflux with continuous stirring for 12 hours (**Figure 3.3**). The progress of the reaction was confirmed using TLC. After that, the RM was quenched using distilled water (20ml, 4v/w). The organic layer was separated and washed with a saturated NaHCO₃ solution. Again, it was separated and distilled to obtain benzyl azide (**2a**) or its derivatives (**2b** or **2c**).

ii) 1-(azidomethyl)-Benzene (2a)

It was obtained as a white solid (79%).

iii) 1-(azidomethyl)-2-fluorobenzene (2b)

It was accepted as a white solid (83%).

iv) 2-(azidomethyl)-1,3-difluorobenzene (2c)

It was got as a white solid (76%).

v) Synthesis of benzyl-1*H*-1,2,3-triazole-4- carbonitrile (3a–3c)

In a four-neck round bottom flask, derivatives of benzyl azide (**2a/2b/2c**) (5.0gm, 1.0eq.) and 2-chloroacrylonitrile (1.1eq.) were taken in distilled water (25 ml, 5v/w) and RM was heated from 75–80 °C for 24–36 hours (**Figure 3.3**). The progress of the reaction was confirmed using TLC. The RM was cooled to RT while stirring overnight to make the solid. Then, after approximately half an amount of solvent was distilled from the reaction flask, (10ml, 2v/w) of distilled water was added and stirred for 15 minutes. Then (25 ml, 5v/w) acetone, (25 ml, 5v/w) DM water, and 0.1 mol equivalent sodium hydroxide were added, and the RM was heated with stirring to 55–60 °C for 12 hours. The RM was cooled to RT and stirred for 2 hours. Then, the reaction mass was filtered out, isolated, and dried to obtain the solid **3a** or related derivatives **3b** or **3c** and characterized using ¹H NMR and mass spectroscopy.

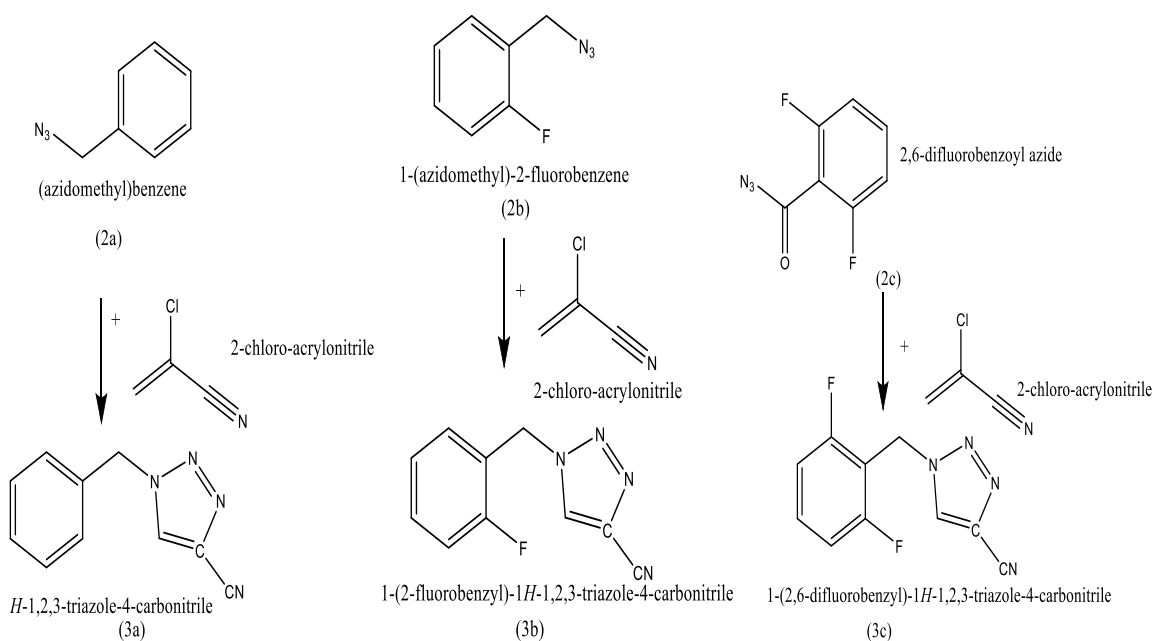


Figure 3.3: Synthesis of 3a–3c

vi) 1-benzyl-1*H*-1, 2, 3-triazole-4-carbonitrile (3a)

It was obtained as a white solid (77%).

vii) 1-(2-fluorobenzyl)-1*H*-1, 2, 3-triazole-4-carbonitrile (3b)

It was obtained as a white solid (70%).

viii) 1-(2, 6-difluorobenzyl)-1*H*-1, 2, 3-triazole-4-carbonitrile (3c)

It was obtained as a white solid (79%).

ix) Synthesis of (1-(2, 6-difluorobenzyl)-1*H*-1, 2, 3-triazol-4-yl)methanol (3d)

In a four-neck round bottom flask, 1 mol equivalent of already synthesized 2-6-difluorobenzyl azide (**2c**) and 2 mol equivalent of propargyl alcohol was taken in distilled water (4ml, 4v/w), and RM was heated to 90 °C for 12 hours (**Figure 3.4**). The progress of the reaction was confirmed using TLC. The stirring was continued for 2–3 hours after cooling RM at RT. Then, 5 ml distilled water was added, and RM was stirred for 10–20 min. The half solvent was purified from the reaction flask, and 3 ml of (3v/w) methanol was added and refluxed for one hour. Then RM was filtered, isolated, and dried as the white product (solid) 3d was characterized using ¹H NMR and MS.

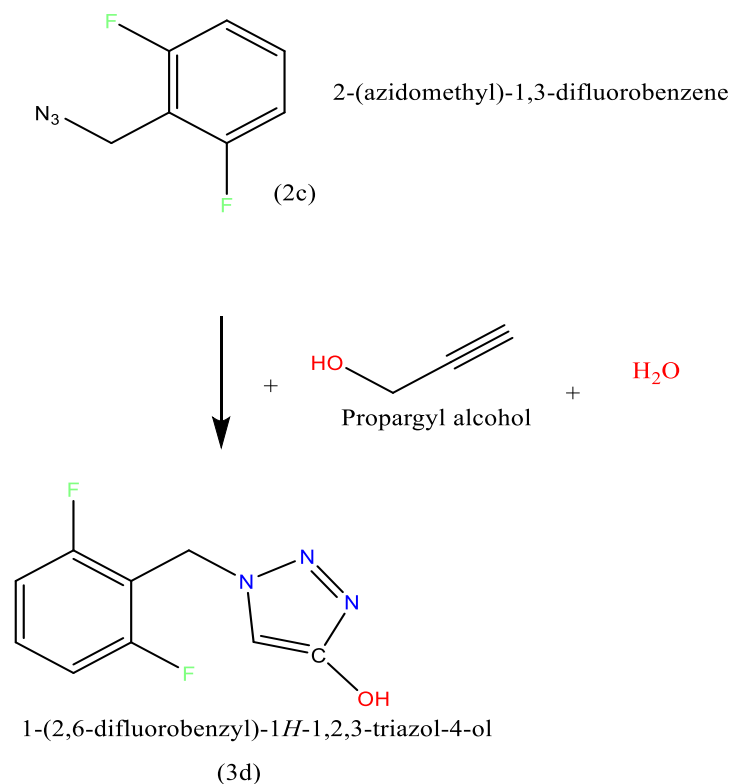


Figure 3.4: Synthesis of 3d

x) Synthesis of benzyl-1*H*-1,2,3-triazole-4-carboxamide and its derivatives (4a–4c)

In a four-neck round bottom flask, 1.0 mol equivalent of (3a/3b/3c) and sodium hydroxide (50mg, 10% w/w) (25ml, 5v/w) acetone and (25ml, 5v/w) distilled water were subjected to the constant reaction temperature of 55 °C for 8–10 hours (**Figure 3.5**). The reaction was confirmed using TLC, and RM was left overnight while stirring. The product was then isolated, dried as a white solid (4a/4b/4c), and characterized using ¹H NMR and mass spectroscopy.

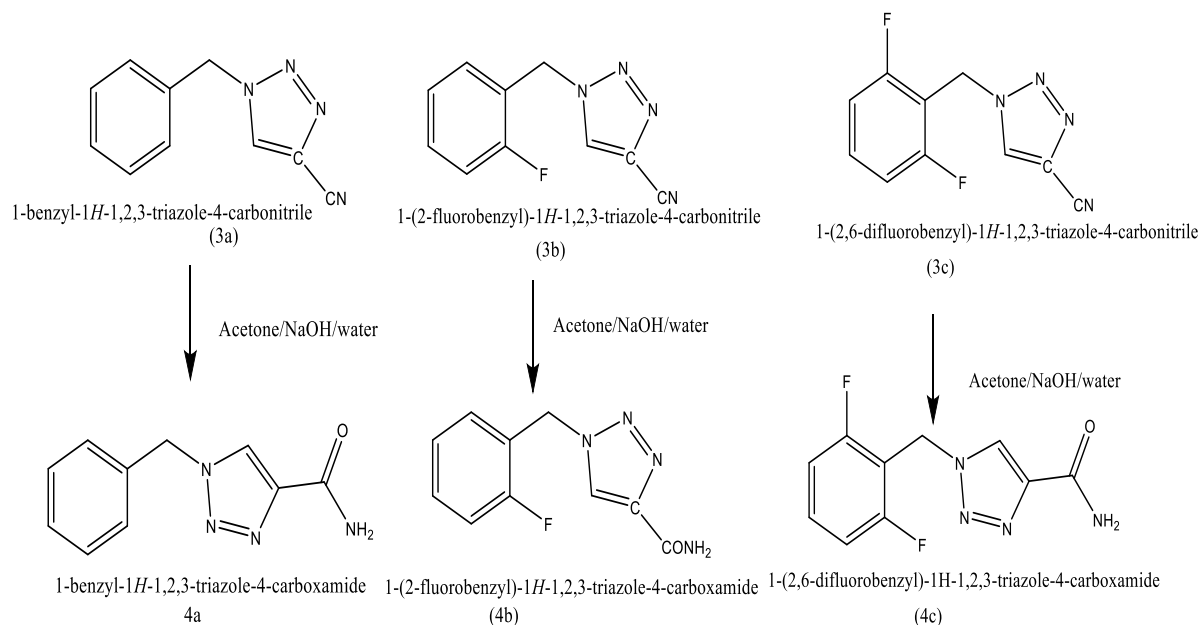


Figure 3.5: Synthesis of 4a–4c

xi) 1-benzyl-1*H*-1,2,3-triazole-4-carboxamide (4a)

It was obtained as a white solid (82%).

xii) 1-(2-fluorobenzyl)-1*H*-1,2,3-triazole-4-carboxamide (4b)

It was obtained as a white solid (80%).

xiii) 1-(2, 6-difluorobenzyl)-1*H*-1,2,3-triazole-4-carboxamide (4c)

It was obtained as a white solid (74%).

xiv) Synthesis of 1-(2,6-difluorobenzyl)-1*H*-1,2,3-triazole-4-carboxylic acid (4d)

In a four-neck round bottom flask, 1.0 mol equivalent of 1,2,3-triazole derivative 3c was heated to reflux with 5ml, and 75% of sulphuric acid was heated at a constant temperature of 60 °C overnight (**Figure 3.6**). Upon completion of the reaction (confirmed by TLC), ice

water was charged into the reaction to get the white solid, which was then filtered, isolated, and dried under vacuum to obtain the product (4d) as a white solid (0.4gm 75%).

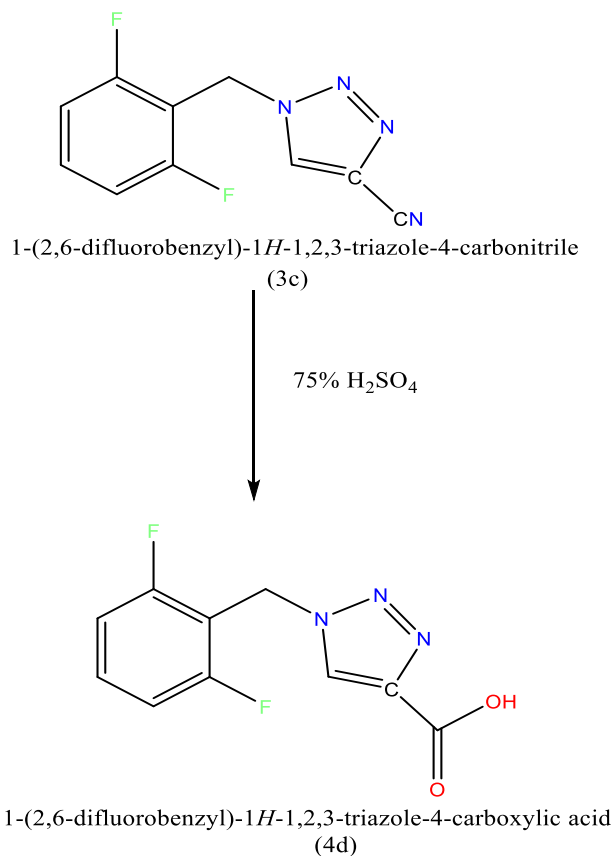


Figure 3.6: Synthesis of 4d

xv) Synthesis of alkyl-1-(2,6-difluorobenzyl)-1H-1, 2, 3-triazole-4-carboxylate (5a/5b)

In a four-neck round bottom flask, 1 mol equivalent of 4d was taken in alkyl alcohol (5ml, 10v/w) (methanol or ethanol) at 0–5 °C and 1.1mol equivalent of SOCl₂ was added dropwise. The temperature was raised to RT, and stirring was continued for 12 hours (**Figure 3.7**). TLC was used to confirm reaction completion. Excess alcohol was distilled,

and the remaining part was dissolved into DCM. The organic layer was washed with a saturated NaHCO_3 solution, followed by distilled water flowing into the organic layer. Then, the solvent was distilled to obtain an alkyl ester compound (**5a/5b**).

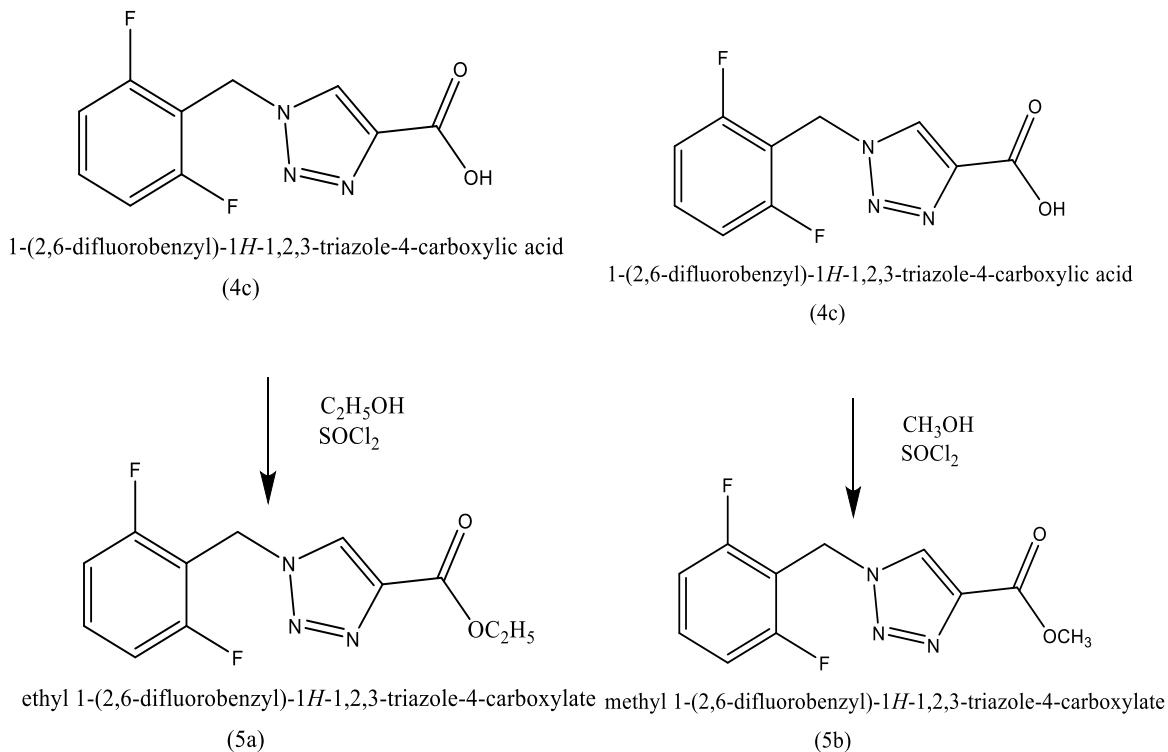


Figure 3.7: Synthesis of 5a and 5b

xvi) Ethyl-1-(2,6-difluorobenzyl)-1H-1,2,3-triazole-4-carboxylate (5a)

It was obtained as a white solid (80%).

xvii) Methyl 1-(2,6-difluorobenzyl)-1H-1,2,3-triazole-4-carboxylate (5b)

It was obtained as a white solid (77%).

xviii) 1-(2,6-difluorobenzyl)-N-methyl-1H-1,2,3-triazole-4-carboxamide (5c)

In a four-neck flask, 1 mol equivalent of 4d was mixed in 2.5 ml of DCM at 0–5 °C, and 1.2 mol equivalent of SOCl₂ was added dropwise. The RM was stirred to reflux between 45–50 °C for one hour. The solvent was distilled, and after that, the RM was cooled to RT, and mono methyl amine was added dropwise. The RM was stirred for 2 h, and the progress of the reaction was confirmed using TLC (**Figure 3.8**). DCM was charged into RM, and the organic layer was washed with DM water. Then, the solvent was distilled to obtain the desired amide derivative **5c** as a solid (0.38gm, 72%).

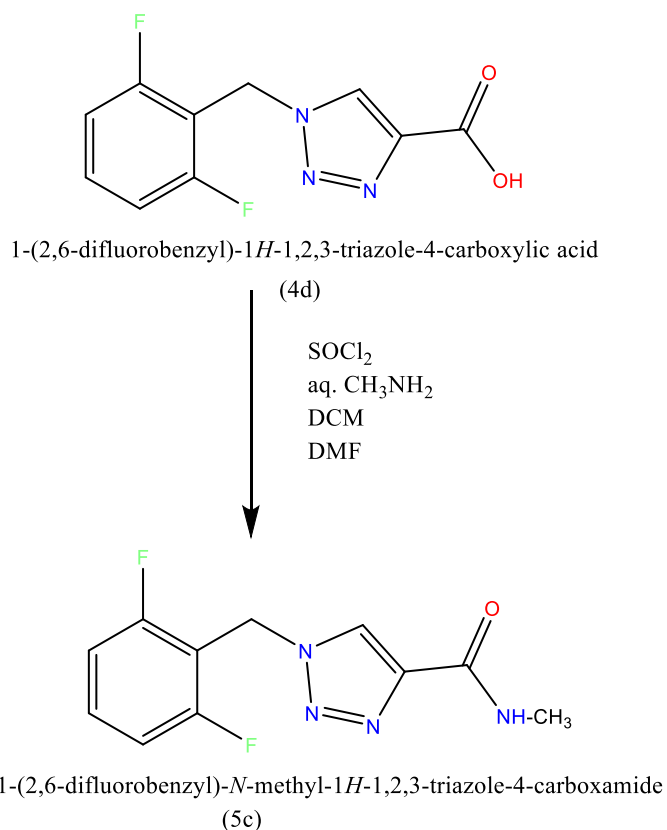


Figure 3.8: Synthesis of 5c

3.3 Result and Discussion

The practical and economical green methodology was successfully developed for synthesizing APIs, which has resulted in creating a cost-effective and environmentally friendly route for producing Rufinamide. Rufinamide is a crucial medication used for treating Lennox-Gastaut Syndrome, and our approach is based on a retrosynthetic method, as illustrated in **Figure 3.9**. Our innovative approach has significantly reduced Rufinamide synthesis's environmental impact and cost, making it a more accessible and sustainable treatment option.

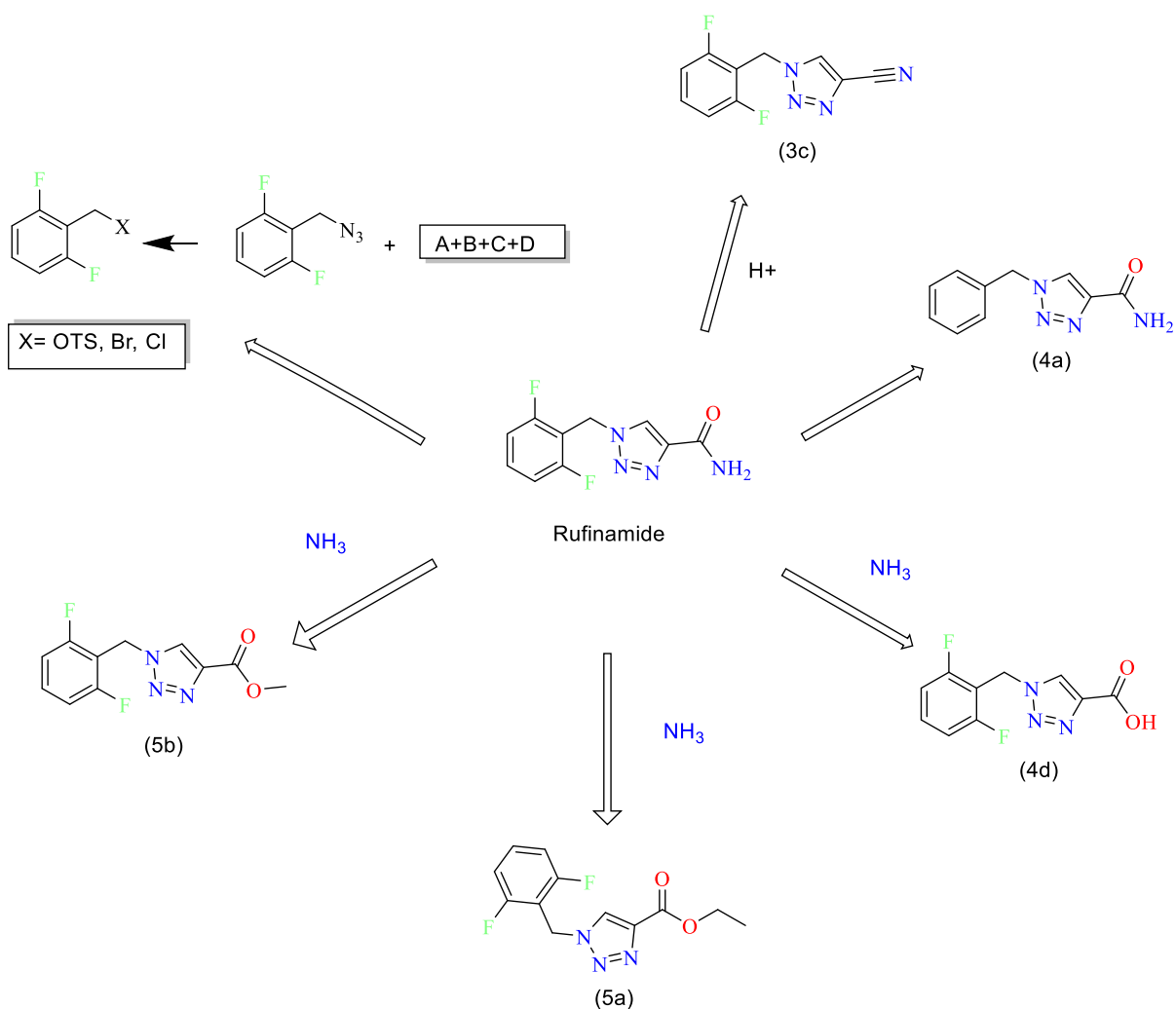


Figure 3.9: Retrosynthesis scheme of Rufinamide Impurities

In **Figure 3.9**, the nucleophilic azide derivative was prepared either from benzyl halogen derivatives or with the tosyl derivatives. However, the chloro reaction as a leaving group took seven days to complete in the presence of potassium iodide, and the iodide derivative is expensive. Therefore, a different response was tried with 1c. The reaction was performed with sodium azide in DMF and proceeded with 97% conversion. Although the atom economy is approximately 50% as compound 1c, it was still chosen as the key SM for the synthesis of rufinamide.

The reaction of 1c was carried out using different solvents like water, methanol, CHCl₃, DCM, DMSO, DMF, ACN, and toluene. The reaction results were analyzed and compared, and it was found that the highest conversion was obtained in DMSO, DMF, and H₂O, as depicted in **Table 3.3**. Therefore, these solvents were chosen for further experiments. It is imperative to note that the usage of DMSO, DMF, and H₂O increased the efficiency of the reaction and led to the formation of the desired product in a shorter time. These findings are significant for developing more efficient synthetic methods for rufinamide.

Table 3.3: Reaction Conversion in Different Solvents

S. No	Solvents	Mol equivalent of NaN ₃	% Reaction Conversion*	Time (h)
1.	CHCl ₃	1	7%	48
2.	DCM	1	5%	48
3.	DMSO	1	93%	16
4	DMF	1	94%	18
5	H ₂ O	1	95%	18
6	ACN	1	92%	20
7	H ₂ O	1.2	98%	10
8	DMF	1.2	94%	12
9	ACN	1.2	92%	20
10	DMSO	1.2	93%	16

*Based on qualitative Thin Layer Chromatography

A further study on sodium azide's impact in different solvents found that excess sodium azide does not affect the reaction rate. Hence, H₂O and 1.2 mol equivalent of azide were chosen for further optimization based on the results recorded in **Table 3.3**. It is worth observing that water is a solvent and treating aqueous effluent is an essential area of focus for developed countries. Therefore, the study's findings hold significant implications for the field of aqueous effluent treatment, which is crucial for the sustainable development of modern society. The volume of water was optimized for further reaction, as shown in **Table 3.4**.

Table 3.4: Optimization of Volume of water

S. No.	The volume of water (v/w)	Temperature	% Reaction Conversion	Remarks
1	2	60-65° C	55 %	The reaction mass is very thick and non-stirrable
	2	90- 100° C	92 %	
2	5	60-65° C	65 %	The reaction mass is very thick and non-stirrable
	5	90- 100° C	97%	
3	7	60-65° C	70 %	Stirrable
	7	90- 100° C	98 %	
4	10	60-65° C	70 %	Stirrable
	10	90- 100° C	98 %	

The volume of H₂O used in the reaction does not change the reaction rate and product quality. Using a lower volume of water leads to a thick and difficult-to-stir reaction mass. Therefore, a volume of 7 is used. The maximum conversion was achieved at reflux temperature. At a temperature below 70 °C, only 70% of the product was obtained. For the reaction, sodium azide (1.2 mol equivalent) was used with 2,6-benzyl bromide in water at reflux temperature.

The study of the thermal cycloaddition of 1,3-dipolarophiles, azides with alkynes/alkenes, found that 2-chloro acrylonitrile is the most effective and economical dienophile for thermal cycloaddition on a commercial scale. The different solvents were tested, and it was found that high-boiling polar solvents such as N-methyl pyrrolidine, DMSO, DMF, and H₂O favor thermal cycloaddition. The other solvents, such as chloroform, DCM, hydrocarbon, and mixed xylene, were also studied, but only 10–15% conversion was obtained in a chlorinated hydrocarbon solvent. The different mol equivalents of 2-chloro acrylonitrile were used for the reaction conversion, and it was found that a minimum of 1.1

mol equivalent is needed to obtain maximum conversion. Beyond the 1.1 mol equivalent, no impact was observed on product yield and quality.

It found that water and other polar solvents showed promising results in the reaction conversion, so water was chosen as the solvent. The formation of 1,2,3 triazoles was also observed due to thermal cycloaddition, which was also observed during our studies at different temperatures, as shown in **Table 3.5**.

Table 3.5: Reaction Conversion at different temperatures

S. No.	Temperature	Reaction Conversion	Isolated Yield**
1	40–45° C	15%	8%
2	45–70 °C	72–74%	65%
3	70–95° C	85–90%	83%

** Isolation done via column chromatography

Maximum product conversion was achieved using 1.1 mol equivalents of 2-chloro acrylonitrile in 5:1 H₂O at 75–80°C.

Converting a cycloadduct product to rufinamide was thoroughly investigated under basic and acidic conditions. Previous studies have suggested that the nitrile present in the product can be hydrolyzed to an amide form in the presence of certain compounds like H₂SO₄, NaOH, KOH, and others. Sulphuric acid is used as the catalyst to investigate the conversion process of the reaction conducted with varying quantities of the catalyst, ranging from one-mole to ten-mole equivalents. Through our experimentation, it was found that hydrolysis using acid leads to the form of an acid derivative. This was confirmed through the synthesis process depicted in **Figure 3.9**.

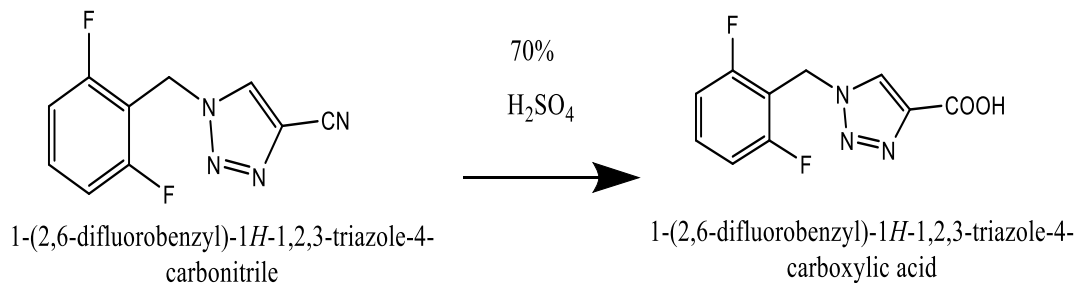


Figure 3.10: Impurity of Rufinamide Acid derivatives

The hydrolysis process involved using sodium hydroxide, and we found that only a catalytic amount of sodium hydroxide was required to complete the hydrolysis of cyano to an amide. The experiments were shown to regulate the optimum conditions for the reaction, and an astounding result was discovered. The reaction was completed under specific conditions, only in acetone, using a 10% mol equivalent of sodium hydroxide.

It was found that the sodium hydroxide reacts with acetone to form mesityl oxide, which acts as a base to help hydrolyze cyano to an amide. This reaction highly depends on the solvent used and the concentration of sodium hydroxide. Using a higher concentration of sodium hydroxide or a different solvent may lead to incomplete hydrolysis or the development of unwanted by-products.

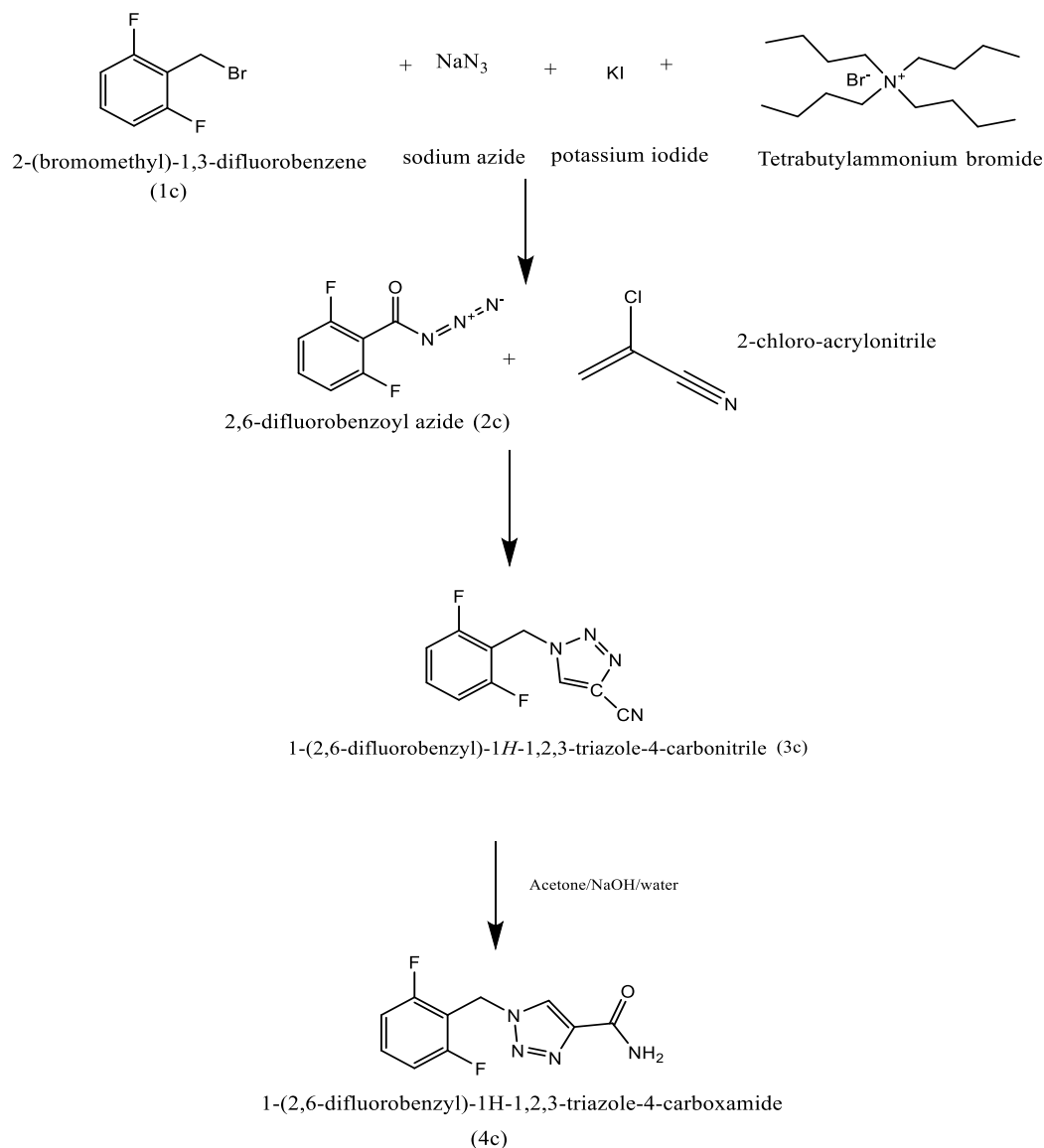


Figure 3.11: Synthesis of 4c

The optimization process allowed us to synthesize rufinamide without isolating it as a single intermediate, significantly reducing the overall cycle time by 35–40%. This was achieved by streamlining the process and eliminating the need for intermediate isolation. To ensure the efficacy of the process and demonstrate the absence of impurities in the API. This step allowed us to evaluate the final product's quality and confirm the streamlined process's effectiveness. Implementing this optimized synthesis method has significantly saved time and cost while maintaining high product quality.

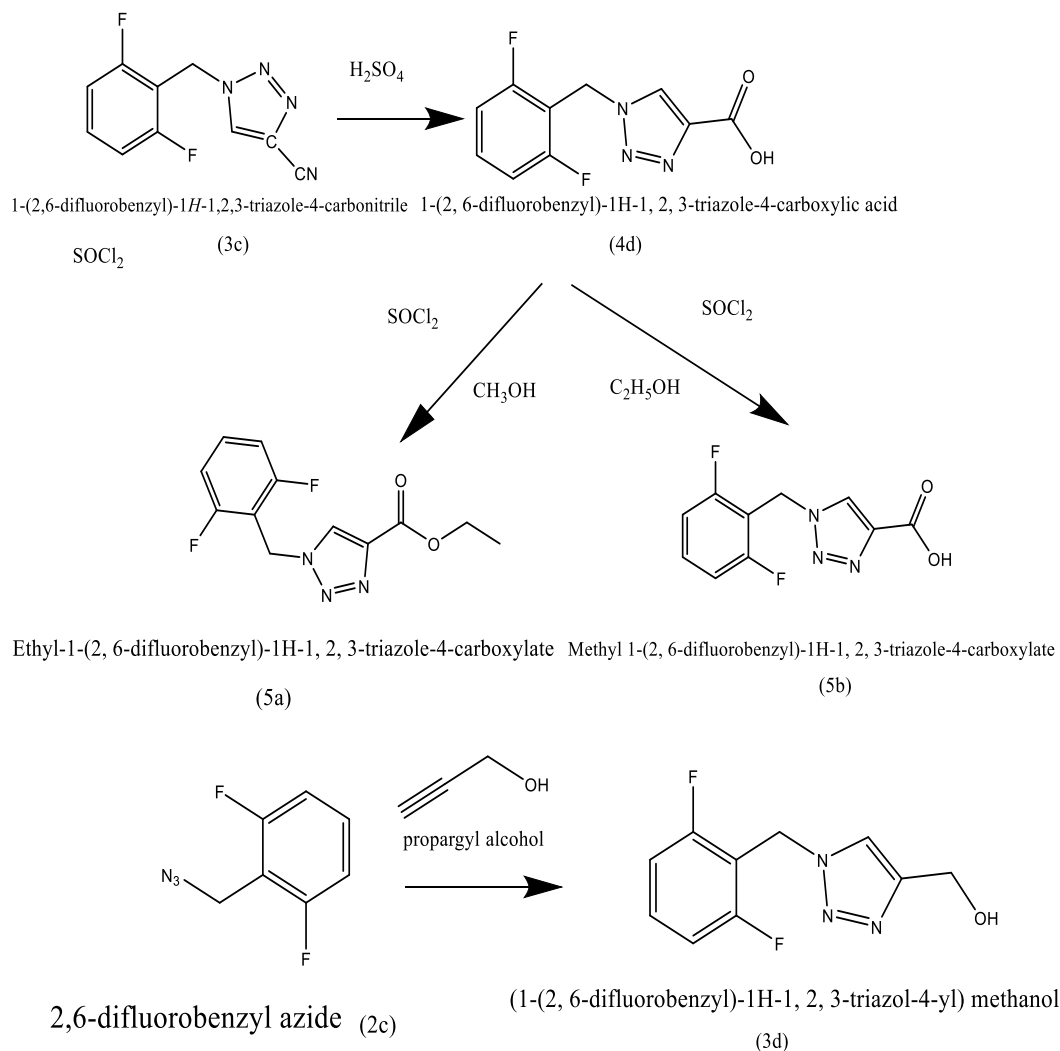


Figure 3.12: Synthesis of Rufinamide Impurities

The research found that rufinamide, an essential anticonvulsant drug, can be prepared using the developed, optimized process. It is worth noting that the rufinamide produced in this process is free of all impurities except for acid impurities, which can be effectively removed during the purification process in acetone. This means the rufinamide obtained has a purity level of over 99.5%, which is well above the regulatory guidelines for quality and safety.

Further optimizing and developing the production process for various APIs, including rufinamide, ensure that the final products meet the highest quality, safety, and efficacy standards. It believes these efforts will advance pharmaceutical science and benefit patients worldwide who rely on these life-saving medications.

3.4. Characterisation of Impurities

Impurities are identified and analyzed using advanced techniques, including Mass Spectrometry and Nuclear Magnetic Resonance, which are defined below:

a) Mass Spectrometry

The analysis was conducted on an Agilent ORBITRAP MS using MeOH as the solvent and the ESI-positive method TOF. The technique used was low-resolution mass spectral analysis (LRMS).

b) Nuclear Magnetic Resonance

The NMR experiment to test the 1H impurity was conducted at a frequency of 400 MHz and a temperature of 25 °C. The research utilized a Varian NMR instrument from Palo Alto, California. In ¹H NMR spectra, the chemical shifts are denoted as δ in ppm relative to the signal of chloroform-d (δ 7.28, singlet) and deuterated DMSO-d₆, δ = 2.50 for 1H. The multiplicity of the signals is indicated using the following abbreviations: s (singlet), brs (broad singlet), d (doublet), t (triplet), q (quartet), dd (doublets of doublet), dt (doublets of triplet), or m (multiplet). The letter n represents the number of protons contributing to a specific resonance. Coupling constants are reported as J values in hertz.

3.5. Spectral Analysis of Impurities

Table 3.6: Spectral data of impurities

S. No.	Name	¹ H-NMR	Mass	Yield
1.	1-(2,6-difluorobenzyl)-1 <i>H</i> -1,2,3-triazole-4-carbonitrile (3c)	The ¹ H-NMR spectrum of the product showed the presence of the characteristic's peaks at δ 8.17 (s, 1H), 7.41 (m, 1H), 7.00 (m, 2H), 5.70 (s, 2H).	The mass spectrum of the product showed a peak at m/z 221.06, which corresponded to the product's molecular weight (221.05).	79%
2.	(1-(2,6-difluorobenzyl)-1 <i>H</i> -1,2,3-triazol-4-yl) methanol (3d)	The ¹ H-NMR spectrum of the product showed the presence of the characteristic's peaks at δ 7.58 (s, 1H), 7.36 (m, 1H), 6.97 (m, 2H), 5.62 (s, 2H), 4.76 (d, <i>J</i> = 5.6 Hz, 2H), 2.62 (t, <i>J</i> = 5.6 Hz, 1H).	The mass spectrum of the product showed a peak at m/z 227.11, which corresponded to the product's molecular weight (226.07).	80%
3.	1-benzyl-1 <i>H</i> -1,2,3-triazole-4-carboxamide (4a)	The ¹ H-NMR spectrum of the product showed the presence of the characteristic's peaks at δ 8.61 (s, 1H), 7.88 (b, 1N-H), 7.49 (b, 1N-H), 7.39 (m, 5H), 5.65 (s, 2H).	The mass spectrum of the product showed a peak at m/z 203.11, which corresponded to the product's molecular weight (203.09).	82%

4	1-(2-fluorobenzyl)-1 <i>H</i> -1,2,3-triazole-4-carboxamide (4b)	The ¹ H-NMR spectrum of the product showed the presence of the characteristic's peaks at δ 8.57 (s, 1H), 7.88 (b, 1N-H), 7.49 (b, 1N-H), 7.45 (m, 1H), 7.39 (m, 1H), 7.25 (m, 2H), 5.72 (s, 2H).	The mass spectrum of the product showed a peak at m/z 221.16, which corresponded to the product's molecular weight (221.08).	80%
5.	1-(2,6-difluorobenzyl)-1 <i>H</i> -1,2,3-triazole-4-carboxamide (4c)	The ¹ H-NMR spectrum of the product showed the presence of the characteristic's peaks at δ 8.11 (s, 1H), 7.40 (m, 1H), 6.99 (m, 2H), 5.68 (s, 2H).	The mass spectrum of the product showed a peak at m/z 239.009, which corresponded to the product's molecular weight (239.10).	74%
6.	1-(2,6-difluorobenzyl)-1 <i>H</i> -1,2,3-triazole-4-carboxylic acid (4d)	The ¹ H-NMR spectrum of the product showed the presence of the characteristic's peaks at δ 8.18 (s, 1H), 7.42 (m, 1H), 7.01 (m, 2H), 5.71 (s, 2H).	The mass spectrum of the product showed a peak at m/z 240.00, which corresponded to the product's molecular weight (240.05).	75%

7	Ethyl-1-(2,6-difluorobenzyl)-1 <i>H</i> -1,2,3-triazole-4-carboxylate (5a)	The ¹ H-NMR spectrum of the product showed the presence of the characteristic's peaks at δ 8.09 (s, 1H), 7.41 (m, 1H), 6.99 (m, 2H), 5.68 (s, 2H), 4.41 (q, J = 7.2 Hz, 2H), 1.39 (t, J = 6.8 Hz, 3H).	The mass spectrum of the product showed a peak at m/z 268.10, which corresponded to the product's molecular weight (268.08).	80%
8.	Methyl-1-(2,6-difluorobenzyl)-1 <i>H</i> -1,2,3-triazole-4-carboxylate (5b)	The ¹ H-NMR spectrum of the product showed the presence of the characteristic's peaks at δ 8.11 (s, 1H), 7.41 (m, 1H), 7.00 (m, 2H), 5.69 (s, 2H), 3.94 (s, 3H).	The mass spectrum of the product showed a peak at m/z 254.07, which corresponded to the product's molecular weight (254.07).	77%
9.	1-(2,6-difluorobenzyl)- <i>N</i> -methyl-1 <i>H</i> -1,2,3-triazole-4-carboxamide (5c)	The ¹ H-NMR spectrum of the product showed the presence of the characteristic's peaks at δ 8.07 (s, 1H), 7.40 (m, 1H), 7.13 (b, 1N-H), 6.99 (m, 2H), 5.66 (s, 2H), 2.99 (d, J = 4.8 Hz, 3H).	The mass spectrum of the product showed a peak at m/z 253.10, which corresponded to the product's	72%

i)

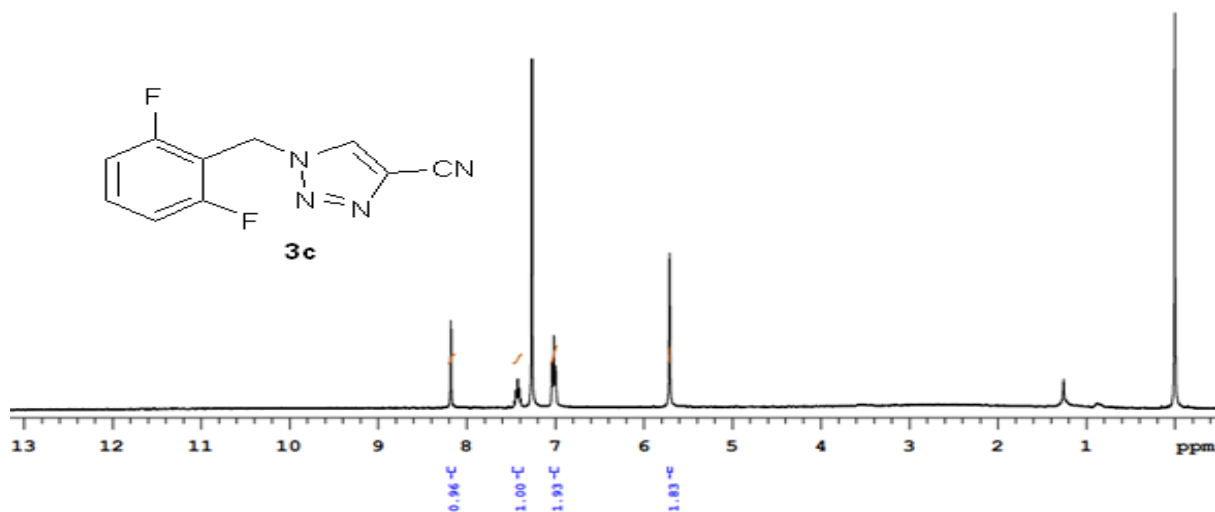


Figure 3.13: NMR Spectra (3c)

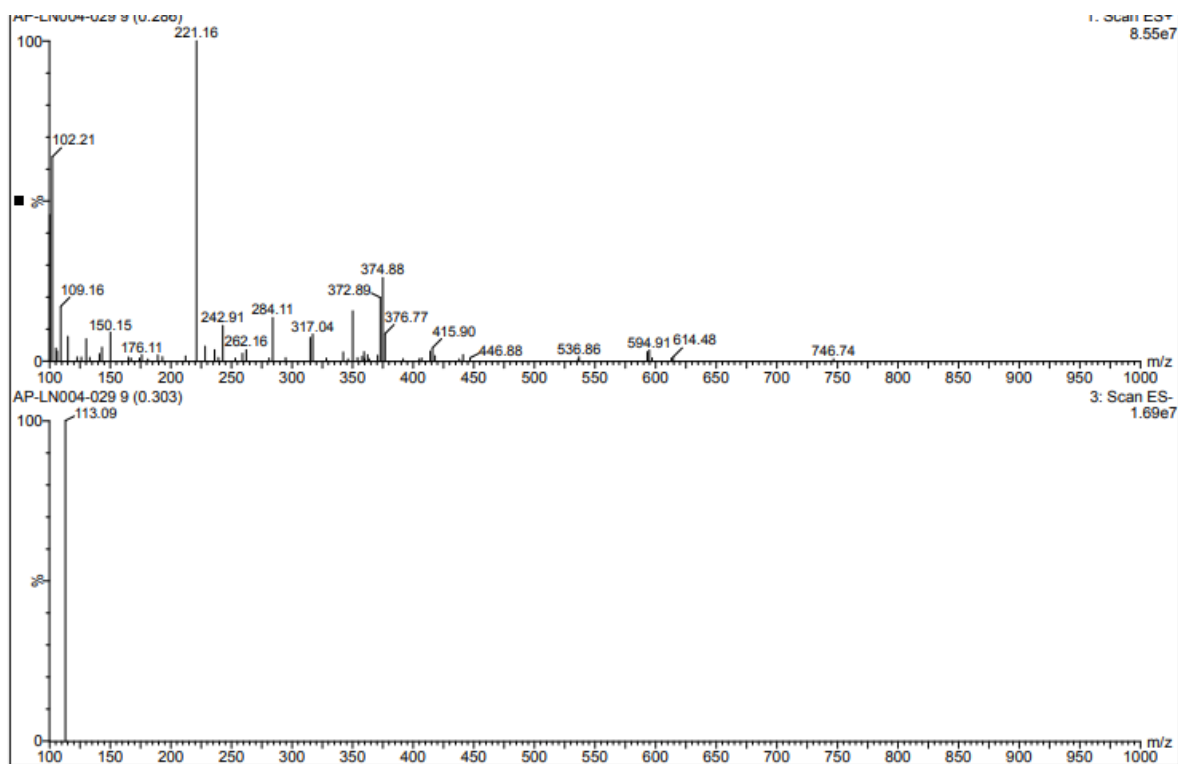


Figure 3.14: Mass Report (3c)

ii)

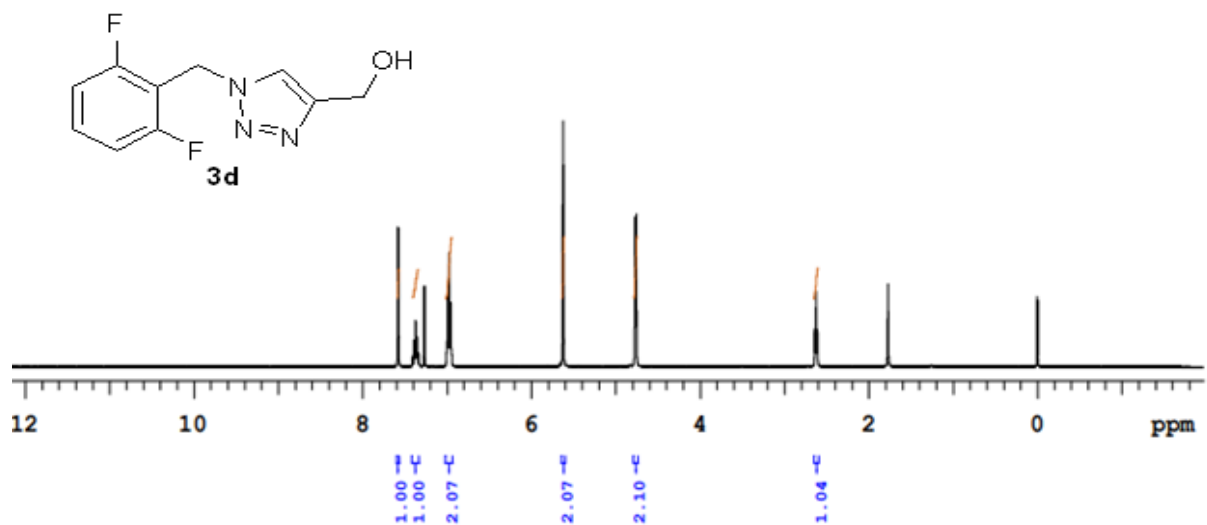


Figure 3.15: NMR Spectra (3d)

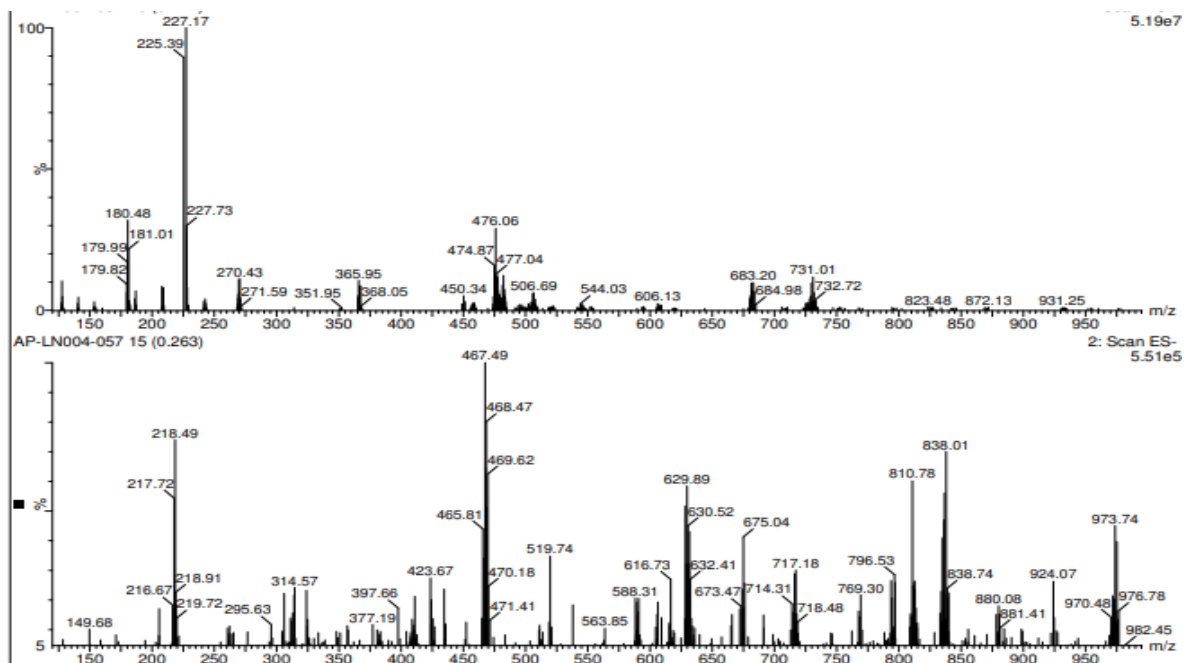


Figure 3.16: Mass Report (3d)

iii)

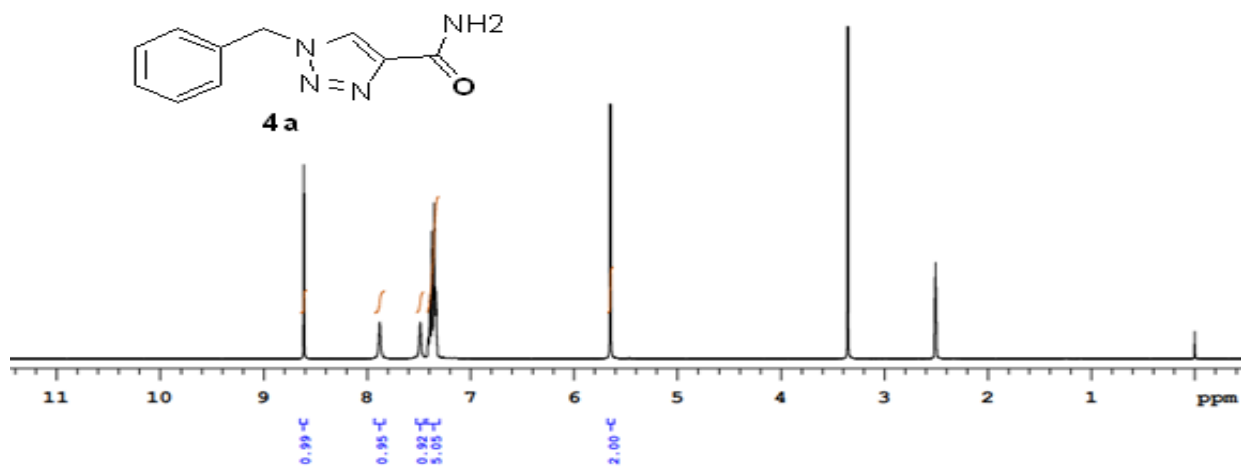


Figure 3.17: NMR Spectrum (4a)

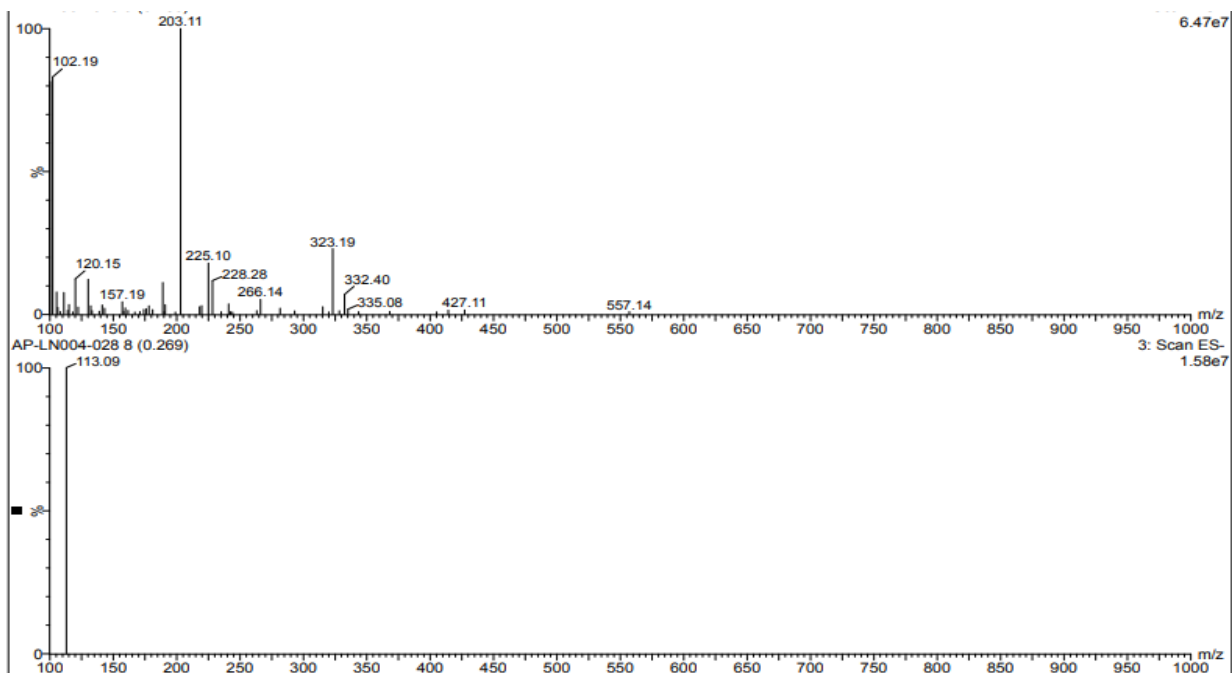


Figure 3.18: Mass Report (4a)

iv)

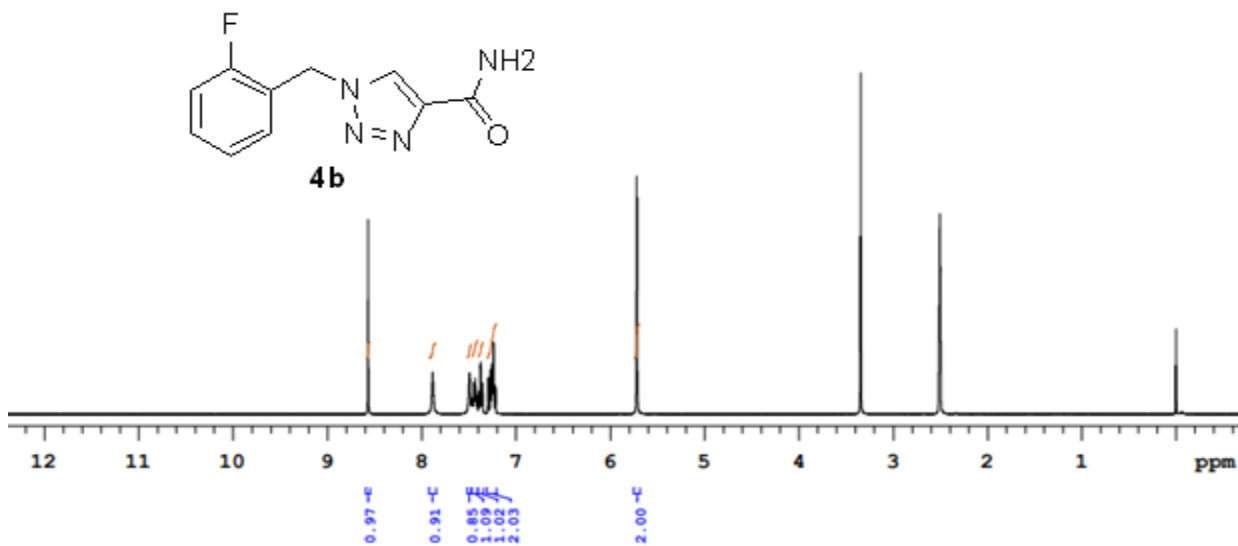


Figure 3.19: NMR Spectrum (4b)

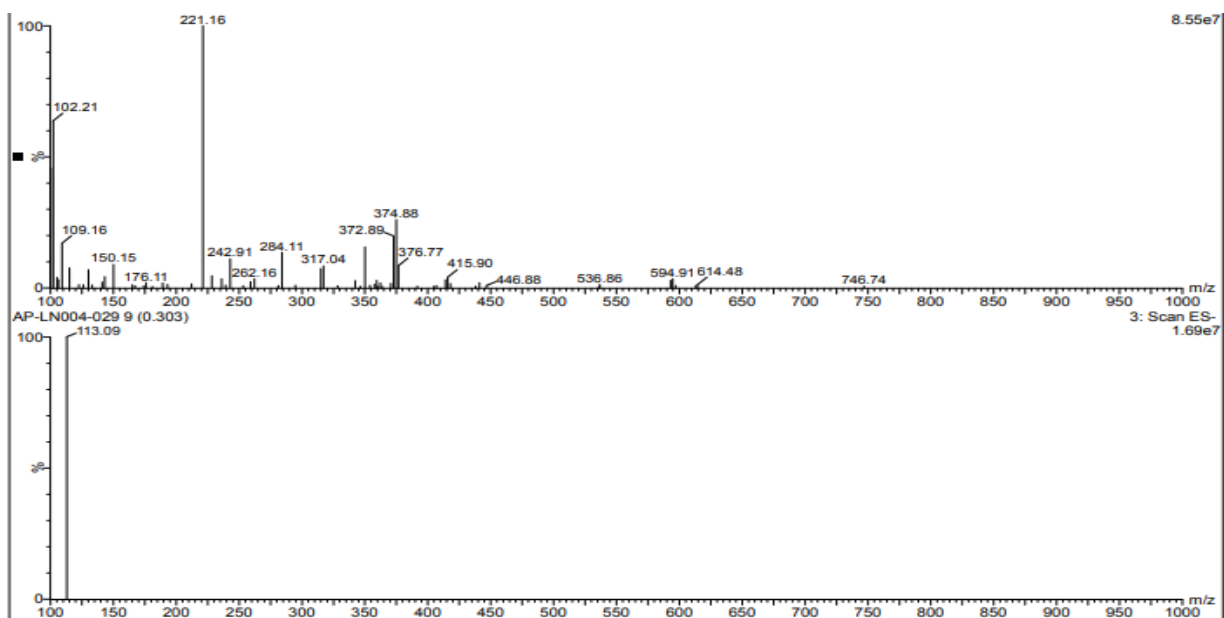


Figure 3.20: Mass Report (4b)

v)

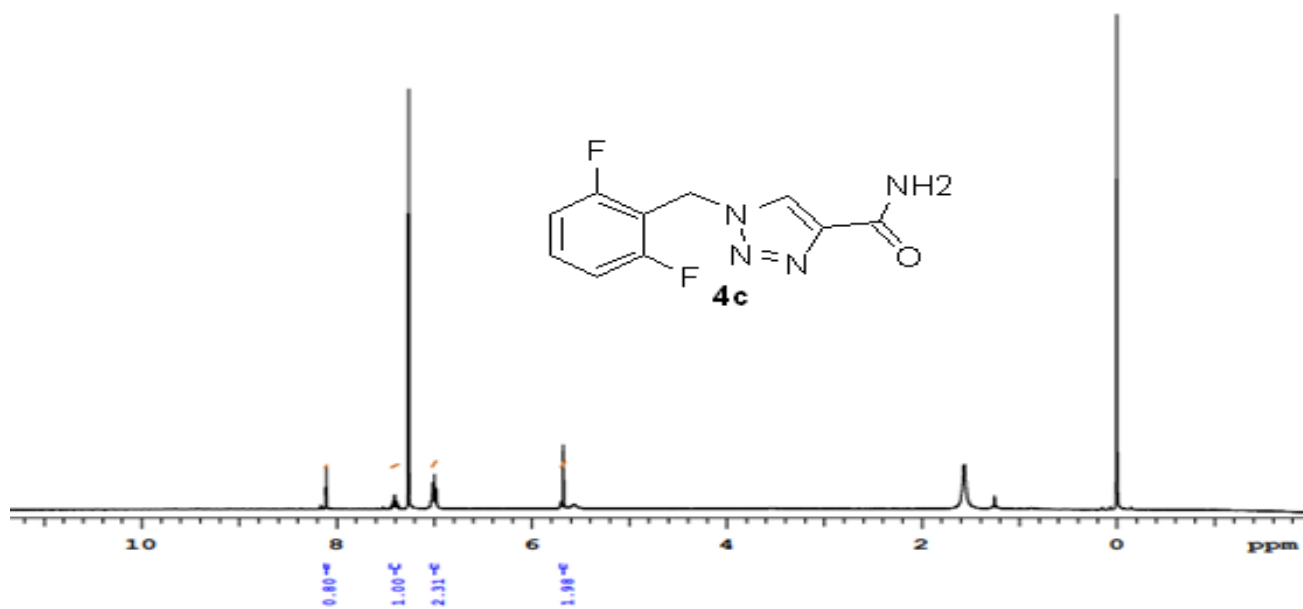


Figure 3.21: NMR Spectrum (4c)

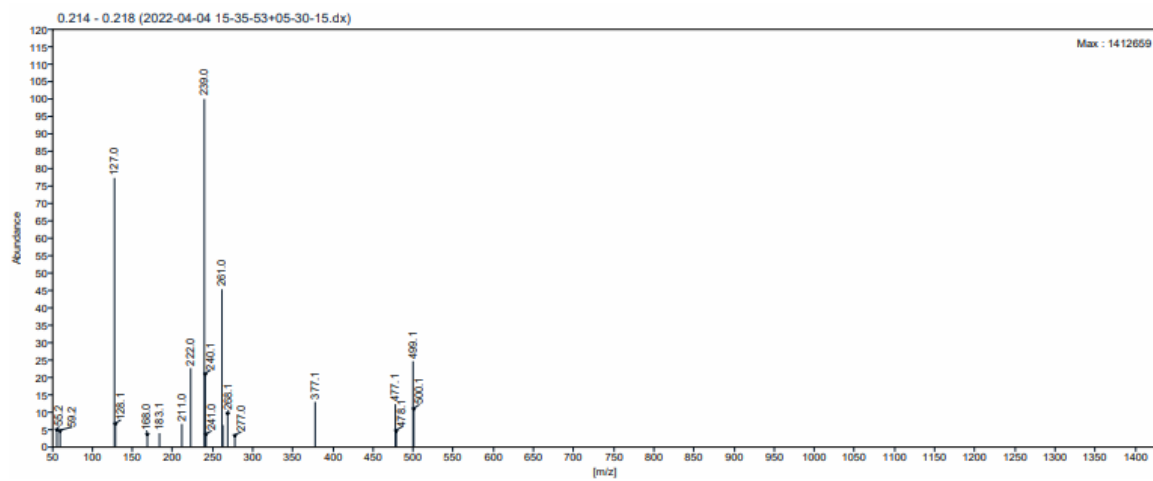


Figure 3.22: Mass Report (4c)

vi)

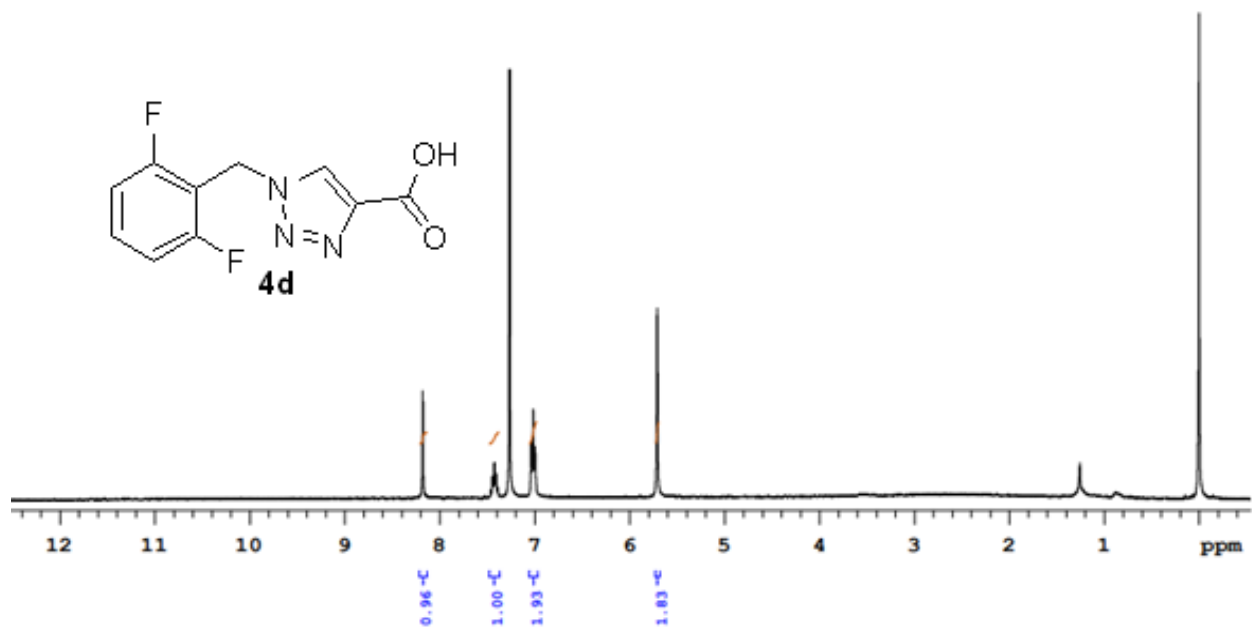


Figure 3.23: NMR Spectrum (4d)

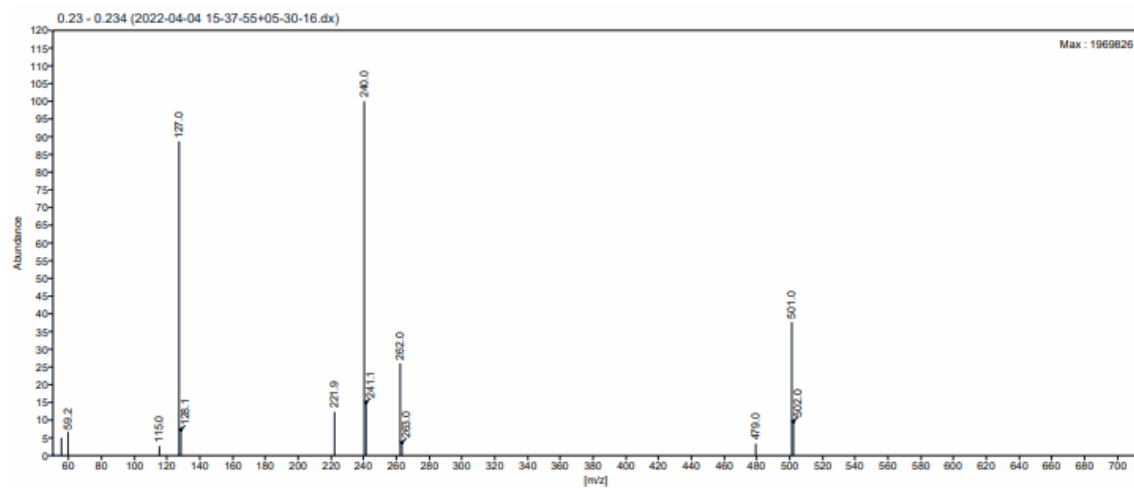


Figure 3.24: Mass Report (4d)

vii)

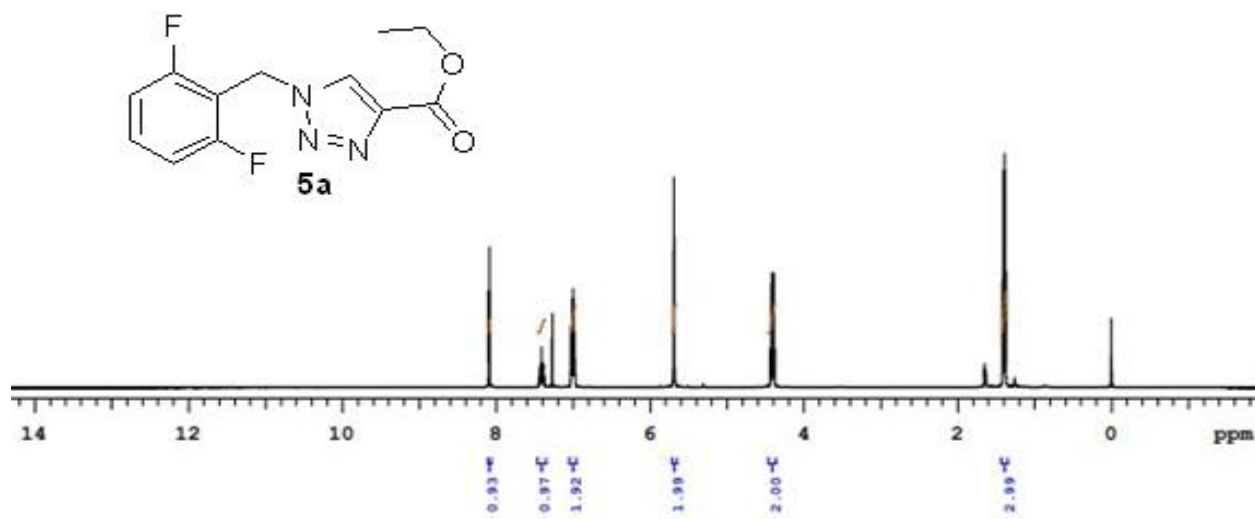


Figure 3.25: NMR Spectrum (5a)

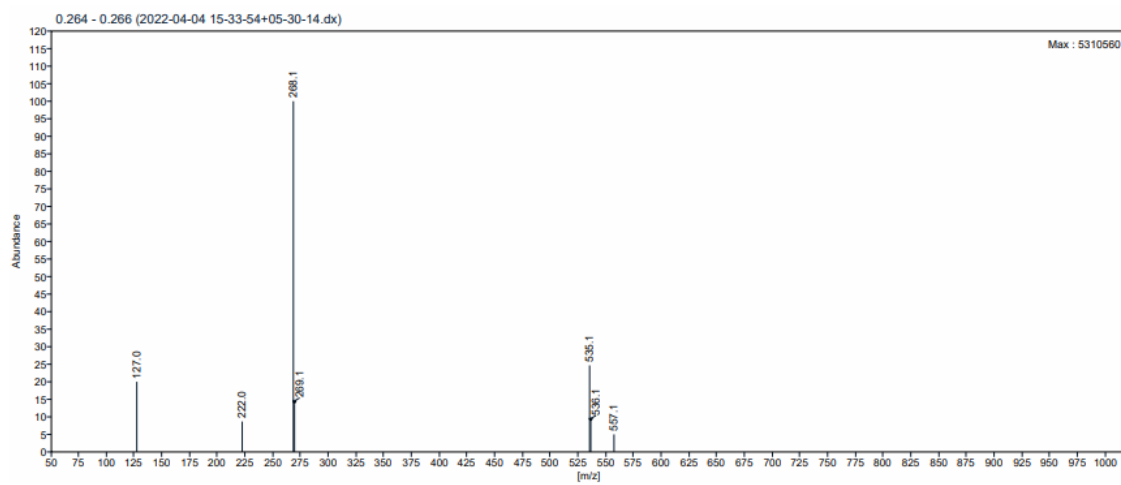


Figure 3.26: Mass Report (5a)

viii)

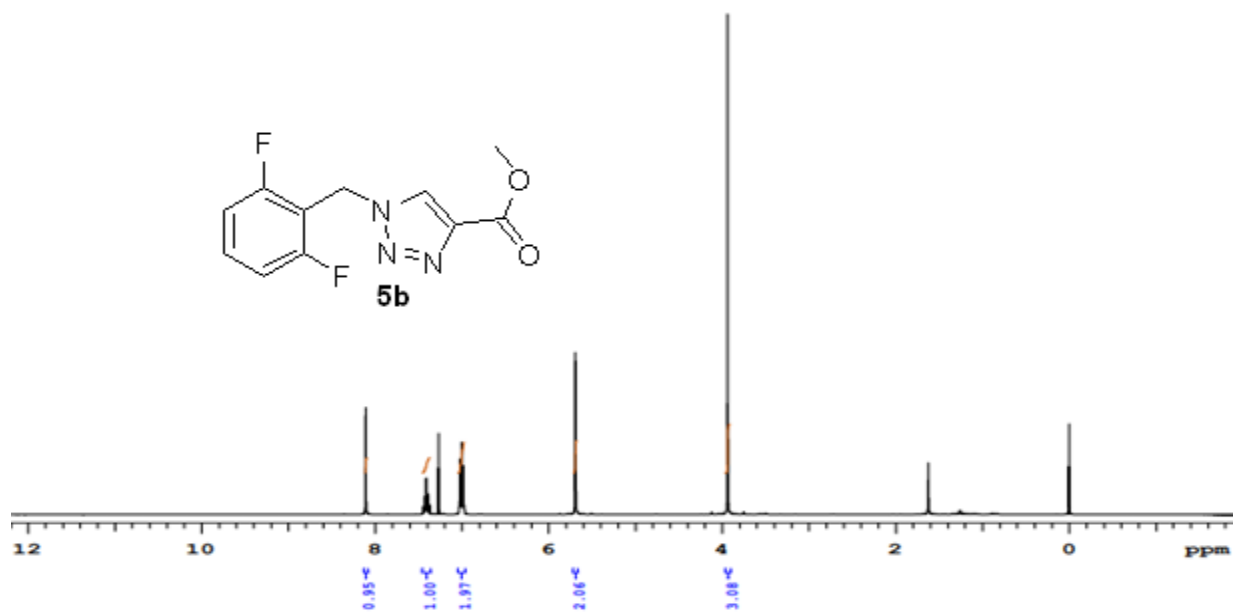


Figure 3.27: NMR Spectrum (5b)

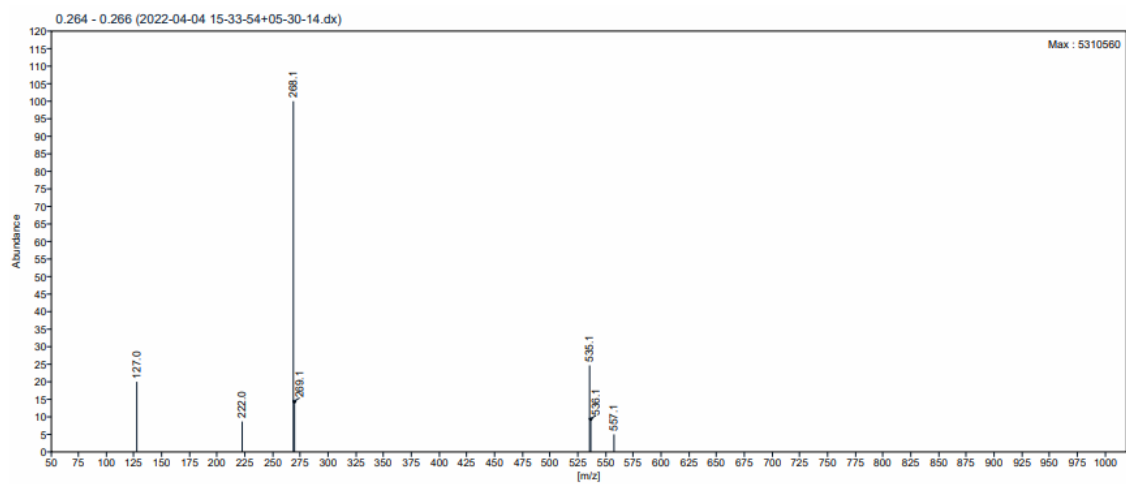


Figure 3.28: NMR Spectrum (5b)

ix)

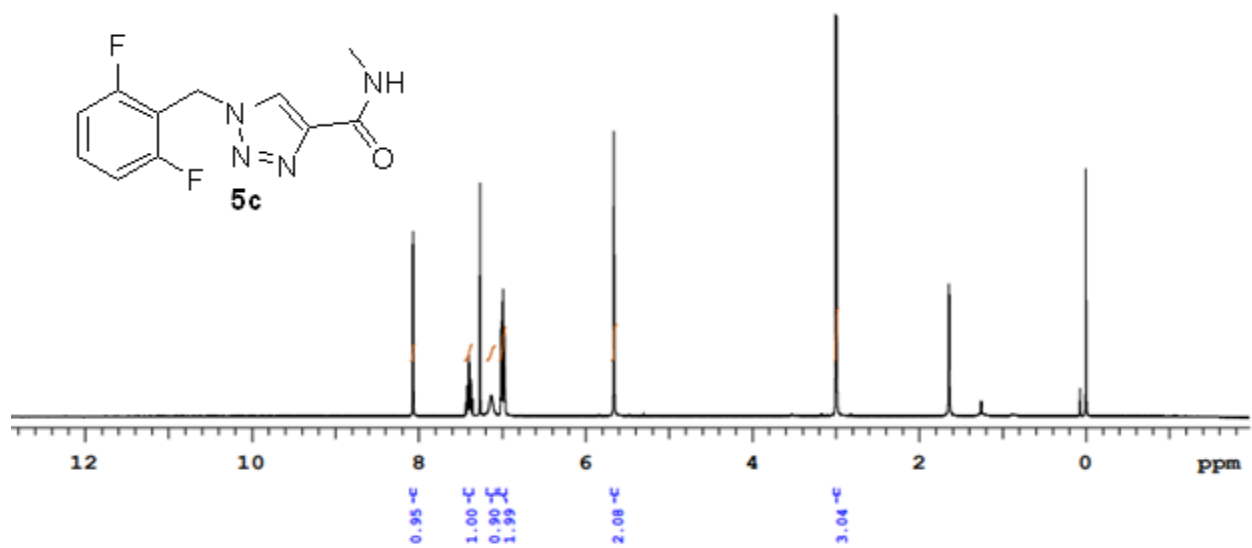


Figure 3.29: NMR Spectrum (5c)

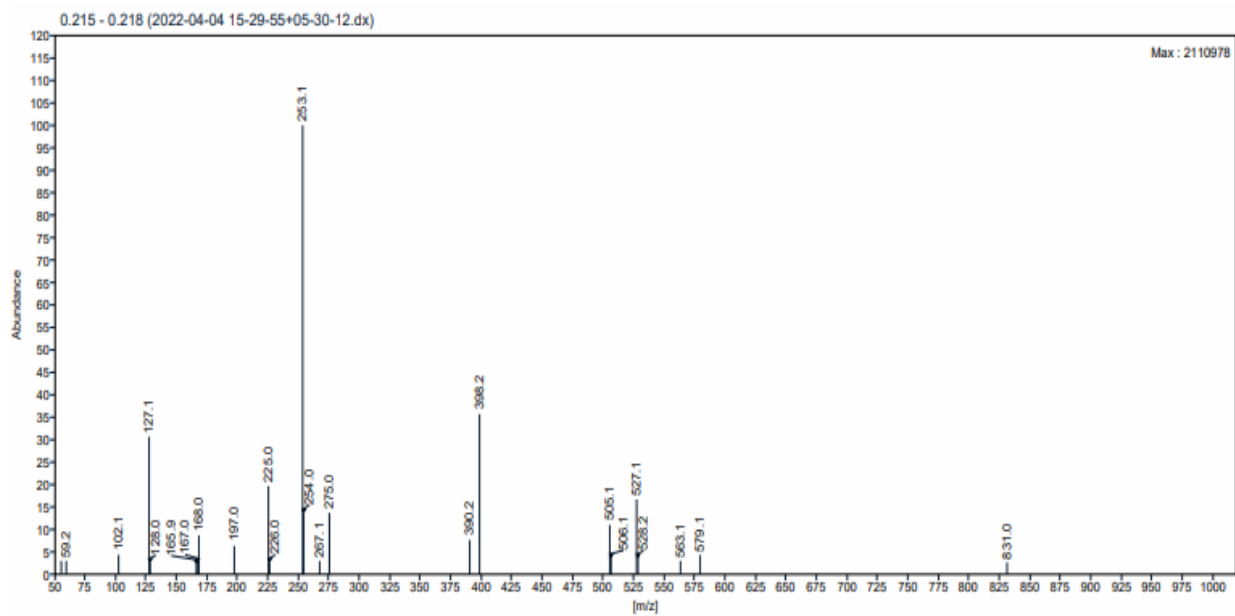
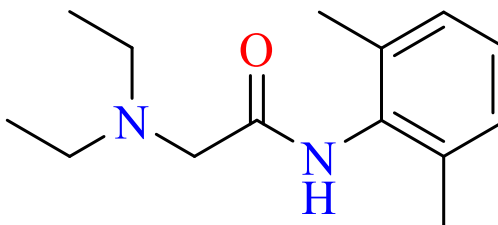


Figure 3.30: Mass Report (5c)

CHAPTER 4: SYNTHESIS AND CHARACTERIZATION OF ANAESTHETIC DRUG (LIDOCAINE) IMPURITIES

4.1 INTRODUCTION TO LIDOCAINE

Lidocaine [173] (**Figure 4.1**) is a commonly used class of pharmaceutical compounds known as local anesthetics. It is available under various trade names, including Novocaine, Xylocaine, and Anestacon. The systematic chemical name of this compound is 2-(diethylamino)-N-(2',6'-dimethylphenyl)acetamide. Another notable compound in this category is procaine [174], which is also known as Isocaine. Isocaine is not only used as a topical anesthetic but is also commonly added to "sunscreens" to protect the skin from sunburn by absorbing ultraviolet rays. Lidocaine acts as a local anesthetic and has antiarrhythmic and analgesic properties. It can also be used for tracheal intubation. According to the Vaughan-Williams classification, it falls under the class Ib antiarrhythmic agents as a tertiary amine [175].



Lidocaine

Figure 4.1: Chemical structure of Lidocaine

4.1.1 Indications

Lidocaine, or lignocaine, is a local analgesic from the amide group. Synthesized by Nils Löfgren and Bengt Lundquist between 1943 and 1946 using xyloidine, lidocaine is a tertiary amine. This anesthetic rose to prominence for its enhanced assurance profile compared to earlier options. It is commonly used with epinephrine to act as a vasopressor and enhance

its effects by counteracting its vasodilatory properties at the application site. In advanced airway management, lidocaine is administered intravenously to facilitate tracheal intubation and reduce the hypertensive response during laryngoscopy. It may also reduce the risk of myalgia and hyperkalemia when succinylcholine is administered. According to the Vaughan-Williams classification, lidocaine is categorized as a class Ib antiarrhythmic agent, demonstrating efficacy in the treatment of acute ventricular tachydysrhythmias. It also serves as a supplementary painkilling for acute and chronic pain conditions [176].

4.1.2 Mechanism of Action

Like other local anesthetics, lidocaine targets sodium ion channels in nerve cell membranes. When uncharged, it enters the axoplasm and combines with hydrogen ions to undergo ionization. The resulting cation temporarily binds to sodium channels and prevents nerve depolarization. It is characterized as a weak base with a pKa of 7.7. At a physiological pH of 7.4, approximately 25% of lidocaine molecules remain un-ionized. This property enables lidocaine to act swiftly, leading to its quick action in comparison to other analgesics with higher pKa values [177]. It is important to note that the effectiveness of lidocaine may be compromised in the presence of soreness, a condition influenced by factors such as acidosis [178] shown in **Figure 4.2**.

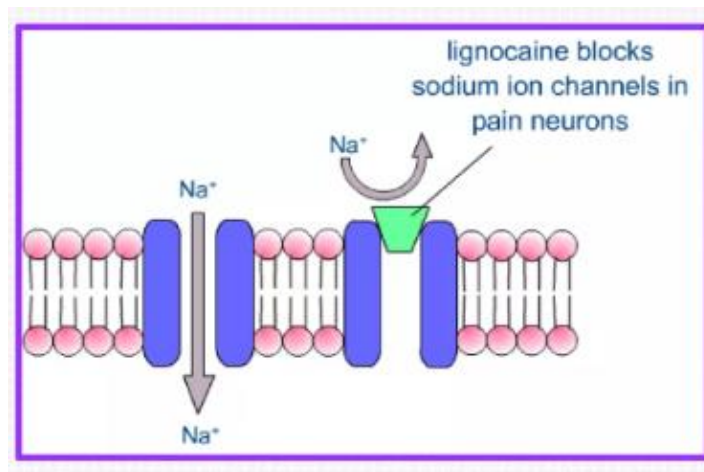


Figure 4.2: Mechanism of action of lidocaine [179]

4.1.3 Administration

Lidocaine is a versatile substance that is used for various purposes, depending on how it is administered. The concentration of lidocaine varies depending on its intended use. For tumescent local anesthesia, 0.05-0.1% diluted concentrations are used. Intravenous regional anesthesia requires dilute solutions of 0.25-0.5%, while regional nerve blocks or epidural anesthesia commonly use 1-2% solutions. Lidocaine is also used topically and as a lubricant before specific procedures, like Foley catheterization, using aqueous gels containing 1-2%. In the airway field, a 4% solution is used for mucous membrane topical anesthesia, and a 10% solution administered with a metered-dose atomizer is often used for airway anesthesia. For skin or rectal surfaces, a 5% ointment with hydrocortisone is applied topically, and aqueous preparations range from 0.5-2%, with or without preservatives, and may include epinephrine for dental applications. There are various products available to manage chronic postherpetic neuralgia, such as medicated plasters containing lidocaine. For minor skin areas, a popular choice is a 5% cream with premixed lidocaine and prilocaine, which can be used for anesthesia before medical procedures. The regional anesthesia dosage depends on the specific block being performed, and the recommended dose generally ranges from 1-2 mg/kg. The initial dose for managing cardiac dysrhythmias is usually 1-1.5 mg/kg delivered Endovenous, following an infusion regimen. Through adjunctive vein therapy for acute pain, it is recommended to administer an initial dose of more than 1.5 mg/kg over 10 minutes, following an infusion not exceeding 1.5 mg/kg/h for up to 24 hours. Close and vigilant monitoring of the clinical response and any signs of toxicity is essential during this period [180].

4.1.4 Side Effects

As the blood concentration of the drug reaches toxic levels, side effects may manifest. The drug is most quickly absorbed when directed in the intercostal space, accompanied by the epidural, caudal, subcutaneous region, femoral, and brachial plexus. Generally, the utmost safe dosage based on body weight is around 3 mg/kg, but this may increase to 7 mg/kg when using formulations with epinephrine. It is essential to be aware that even small doses

of the drug can cause toxicity and unintended side effects if mistakenly injected into the bloodstream. Lidocaine has a higher risk of neurotoxicity compared to other analgesics, mainly when used in high concentrations and directly applied to neural tissue. The utilization of highly concentrated 2.5-5% for spinal anesthesia has been related to an elevated occurrence of temporary radicular irritation syndrome, leading to temporary pain in the calves, thighs, and buttocks [181].

4.1.5 Contraindications

Lidocaine should not be given to patients who have had severe adverse reactions to the drug. While anaphylactic reactions to lidocaine are sporadic, they can occur. Methemoglobinemia is a condition where an abnormal form of hemoglobin decreases the blood's ability to carry oxygen. This can happen when lidocaine is metabolically converted to O-toluidine. Increased doses of lidocaine are associated with a higher probability of producing this metabolite. However, even lower doses can lead to its formation in patients who are concurrently using medications known to cause methemoglobinemia or who have underlying conditions like hemoglobinopathies or anemia. Caution should be exercised when using lidocaine as an antiarrhythmic if the arrhythmia may be caused by toxicity from local anesthesia. Lidocaine formulations that contain epinephrine can have cardiovascular effects, even at low doses. Therefore, it is recommended to closely monitor the patient's hemodynamics before and during using solutions containing vasopressors. This is especially important if there are worries about the patient's cardiovascular health [182].

4.1.6 Monitoring

To ensure safe administration, diligent monitoring of plasma levels of lidocaine is necessary, especially for patients with impaired liver function who are receiving prolonged infusions. Dosing calculations should be based on the patient's ideal weight rather than their actual weight. This method effectively prevents dangerously high plasma concentrations, with a maximum limit of 120 mg/h for lidocaine infusions [183].

4.1.7 Toxicity

The onset of mild toxicity from lidocaine occurs when plasma levels exceed 5 mcg/mL. This is typically characterized by slurred speech, tinnitus, tingling around the mouth, and lightheadedness. When plasma levels surpass 10 mcg/mL, the risk of loss of consciousness increases. Concentrations of 15 mcg/mL or higher can further depress the central nervous system and myocardium, leading to cardiac arrhythmias, cardiac arrest, and even respiratory failure at levels exceeding 20 mcg/mL. Animal research has shown that the amount of lidocaine needed to cause cardiac collapse is significantly higher (7.1 +/- 1.1 times) than the dose required to affect the CNS. This ratio, known as "CC/CNS," sets lidocaine apart from other local anesthetics. In cases of toxic dosing in conscious patients, lidocaine may take longer to progress from neurological to cardiovascular effects compared to other drugs. However, if neurological symptoms are masked by sedation, arrhythmias may be the first signs of toxicity. If toxicity is suspected during drug administration, it is crucial to stop it immediately. In the event of breathing assistance, cardiorespiratory collapse, and airway support should be provided to thwart respiratory acidosis, which can worsen toxicity and increase the adverse effects of lidocaine on the heart's rhythm and pumping ability. Essential vital function support should be initiated, including administering oxygen, IV fluids, and inotropes. In cases of unresponsive cardiovascular collapse, intravenous lipid emulsion can be considered as a rescue therapy [184].

4.2 Enhancing Healthcare Team Outcomes

It is crucial for healthcare professionals in the interprofessional team, including doctors, practitioners, physician assistants, nurses, and pharmacists, to understand lidocaine's potential toxicity and effective management strategies comprehensively. It is important to note that when lidocaine is administered, it can initially cause significant discomfort upon injection as it stimulates nociceptors before its action on sodium channels becomes apparent. To minimize this discomfort, practitioners can use techniques such as buffering the lidocaine with small amounts of NaHCO₃ immediately to reduce its acidity. Additionally, warming the solution to body temperature, injecting it at a controlled pace,

using narrow cannulas, and employing a 90-degree injection angle can help alleviate pain [185].

Administering lidocaine through intravenous infusions should be approached with great care and recognized as a high-risk scenario. According to a 2020 consensus statement, patients receiving IV lidocaine infusions outside of controlled environments, such as operating rooms or post-anesthesia care units, should ideally be monitored in high-dependency settings. To ensure safety, a distinct and dedicated cannula should be used with a tamper-proof pump for the infusion. This method promotes vigilance and helps prevent complications associated with IV lidocaine administration [186].

4.3 EXPERIMENTAL PART

4.3.1 Materials/ Chemicals

All the chemicals and solvents utilized in this research were of Analytical grade procured from Sigma, Aldrich, Mumbai, India. Freshly distilled moisture-sensitive reagents were dried under nitrogen/argon in positive-pressure oven-dried glassware. The completion and purity of compounds were checked using TLC (Merck 60 F254 precoated silica gel plates 0.2 mm thickness), while spot visualizations were performed under Ultraviolet light (254nm) and using various kinds of TLC stains like ninhydrin ceric ammonium molybdate, or KMnO_4 . The yield of the compounds was determined by calculating it using the following formula:

$$\text{Percent Yield} = (\text{Actual mass of product} / \text{Theoretical yield}) * 100\%$$

Table 4.1: List of Organic solvents used for the synthesis of Lidocaine process impurities

S. No	Name of the organic solvents	Purity (%)	Grade and Procured From
1.	Dichloromethane	>95%	AR, Sigma Aldrich
2	Ethanol	>95%	AR, Sigma Aldrich
3.	Methanol	>95%	AR, Sigma Aldrich
4	Acetone	>95%	AR, Sigma Aldrich
5	DMF	>95%	AR, Sigma Aldrich
6	Toluene	>95%	AR, Sigma Aldrich
7	Ethyl Acetate	>95%	AR, Sigma Aldrich
8	Distilled Water	>95%	AR, Sigma Aldrich
9	Hexane	>95%	AR, Sigma Aldrich
10	Acetonitrile	>95%	AR, Sigma Aldrich

Table 4.2: List of chemicals used for the synthesis of Lidocaine process impurities

S. No	Name of the Chemicals/Reagents	Purity (%)	Grade and Procured From
1	N-phenylethylamine	>95%	AR, Sigma Aldrich
2	Potassium Iodide	>95%	AR, Sigma Aldrich
3	Piperazine	>95%	AR, Sigma Aldrich
4	Diethylamine	>95%	AR, Sigma Aldrich
5	Sodium Hydroxide	>95%	AR, Sigma Aldrich
6	Potassium carbonate	>95%	AR, Sigma Aldrich
7	Benzylamine	>95%	AR, Sigma Aldrich
8	Sulphuric Acid	>95%	AR, Sigma Aldrich
9	Sodium Bicarbonate	>95%	AR, Sigma Aldrich
10	2,6-dimethyl aniline	>95%	AR, Sigma Aldrich
11	Isopropyl phenylamine	>95%	AR, Sigma Aldrich

Synthesized Lidocaine impurities are shown in **Figure 4.3**.

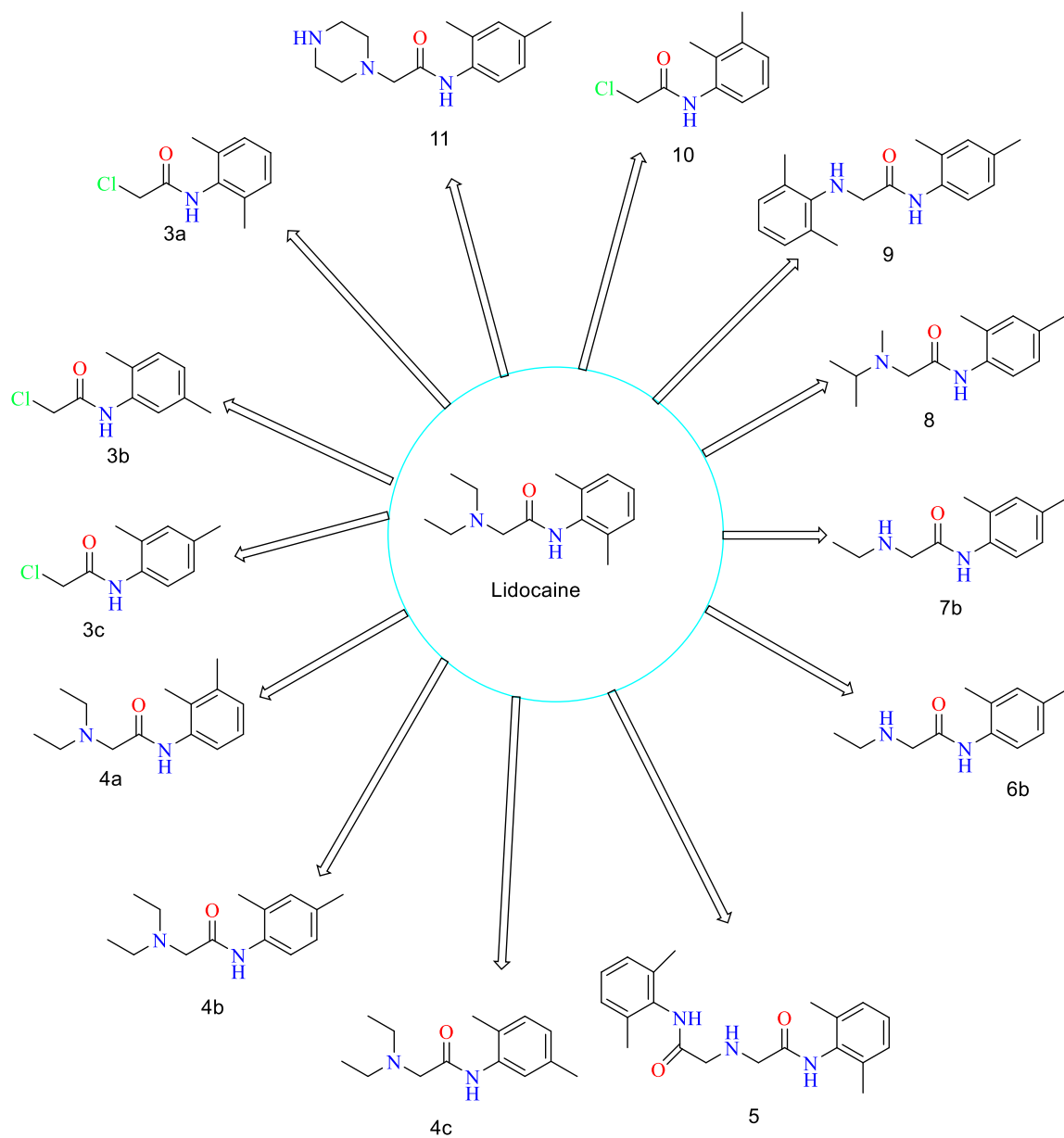
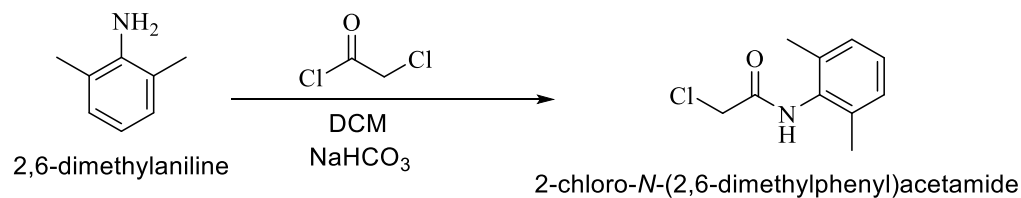


Figure 4.3: Synthesized Lidocaine impurities

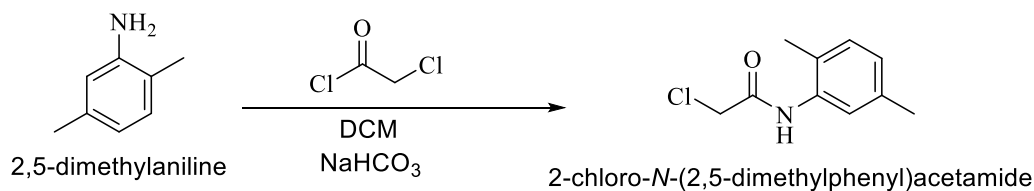
4.3.2 Methods

i) Synthesis of 2-Chloro-*N*-(2,6-Dimethyl Phenyl)Acetamide (3a–3c)

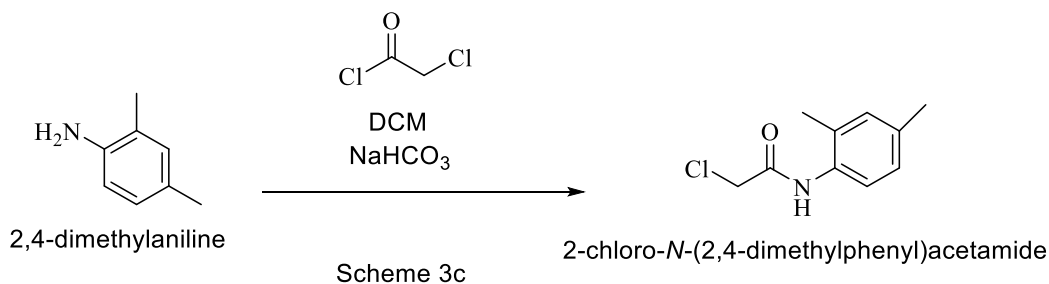
In a four-neck round bottom flask, 10 g (0.0825 m mol) of 2,6-dimethyl aniline (1a–1c) was taken, 50 ml of dichloromethane (DCM), and 6.9 g (0.0825 m mol) NaHCO₃ was added at RT. After that, the suspension was cooled at 5–10 °C, and 9.3 g (0.0825 m mol) of chloroacetyl chloride dropwise was added. The RM was stirred for 60 minutes, maintaining the temperature at 5–10 °C. The progress of the reaction was observed via TLC (20% ethyl acetate in hexane). Following the reaction, 250 ml of H₂O and 200 ml of DCM were introduced to RM. The organic layer was separated, and the final product, 3a, was obtained by vacuum distillation at 55 °C. The solid was then washed with hexane to eliminate excess chloroacetyl chloride. The product was analyzed using ¹H-NMR and MS. **Figures 4.3, 3b, and 3c** show the lidocaine impurities synthesized using the above procedure. The yield of the products is given in **Table 4.3**.



Scheme 3a



Scheme 3b



Scheme 3c

Figure 4.4: Synthesis of Chloro-substituted Lidocaine Impurities

ii) Synthesis of 2-(diethylamino)-*N*-(2,3-dimethyl Phenyl)acetamide (4a–4c)

In a four-neck round bottom flask, 10 g (0.0505 m mol) of 3a–3c was taken to it, 100 ml of acetone, 3.7 g (0.0505 m mol) of diethylamine, and 6.9 g (0.0505 m mol) of K_2CO_3 and added a pinch of KI. The RM was refluxed for 8 hours with continuous stirring. The progress of the reaction was observed via TLC (5% MeOH in DCM). After that, acetone was filtered out from RM, and the spent liquor was distilled in the vacuum. In the obtained purple mass, 250 ml of H_2O and 200 ml of DCM were added, and the organic layer was separated and distilled at 55 °C under a vacuum. After distillation, 1,4 dioxane HCl and acetone were added to the vessel, and a pH of 2–3 was maintained (if no solid was formed, the pH was changed to 7 by adding NaHCO_3). The final product was obtained as a solid

mass of 4a, 4b, and 4c, respectively, given in **Figure 4.5**, and the product was analyzed using $^1\text{H-NMR}$ and MS,

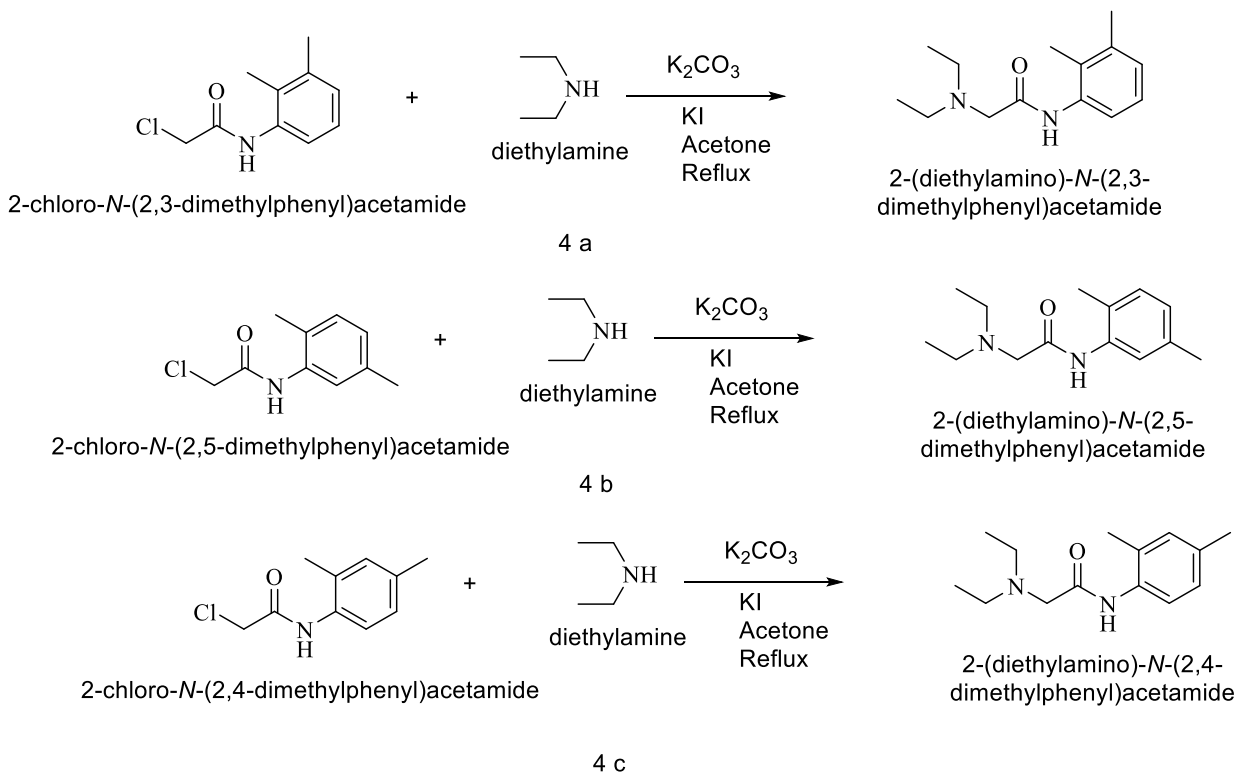


Figure 4.5: Synthesis of Diethylamino-substituted lidocaine impurities

iii) Synthesis of 2,2'-azanediylbis (*N*-(2,6-dimethylphenyl)acetamide) (5)

In a four-neck round bottom flask, 10 g (0.0505 m mol) of 3a was taken to it, 100 ml acetone, 5.4 g (0.0505 m mol) of benzylamine, 6.9 g (0.0505 m mol) of K_2CO_3 , and a pinch of KI were added. The RM was stirred at RT for 15 minutes, then stirred and refluxed for 12 hours. The progress of the reaction was observed via TLC (30% ethyl acetate in hexane). After that, acetone was distilled out via downward distillation. To cool the RM, 100 ml of H_2O and 150 ml of DCM were added. The organic layer was then separated and washed twice with 250 ml of distilled water at a neutral pH. Finally, distillation was performed under a vacuum. (**Figure 4.5**). The product was characterized using $^1\text{H-NMR}$ and MS.

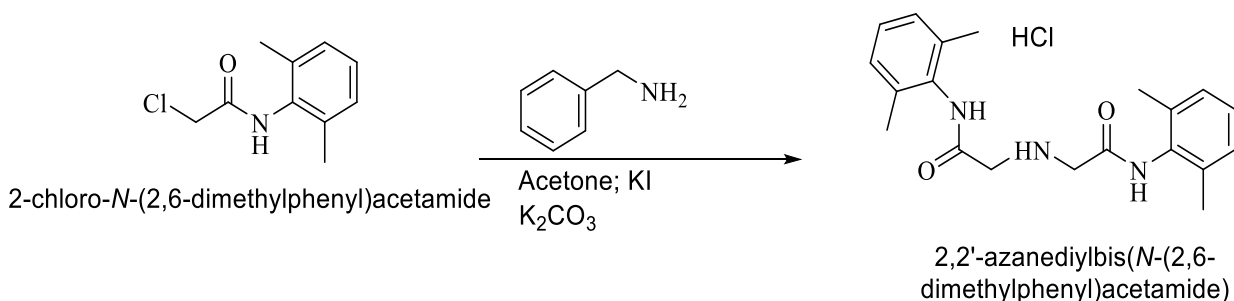


Figure 4.6: Synthesis of Dimethylphenyl-substituted lidocaine impurities

iv) Synthesis of *N*-(2,6-dimethylphenyl)-2-(ethylamino)acetamide (6b)

6b is synthesized in a two-step. The intermediate 6a was formed in the first step and as a precursor to synthesize 6b.

Synthesis of intermediate [*N*-(2,6-dimethylphenyl)-2-(phenethylamino)acetamide (6a)]

In a four-neck round bottom flask, 10 g (0.0505 m mol) of 3a was taken, and to it, 100 ml of acetone and 6.1 g (0.0505 m mol) of *N*-phenylethylamine, 50 ml acetonitrile, 6.9 g (0.0505 m mol) of K₂CO₃, and a pinch of KI were added. The RM was stirred for 12 hours. The progress of the reaction was observed via TLC (5% MeOH in DCM). The RM was subjected to vacuum distillation to remove excess acetonitrile, and the product of this reaction was transferred into another round bottom flask. Next, 40 ml of DMF was added to RM and refluxed at 60–65 °C for two hours. The RM was left overnight at RT and quenched by adding ice, which resulted in a solid that could be filtered and dried to obtain the final product 6a.

Synthesis of *N*-(2,6-dimethylphenyl)-2-(ethylamino)acetamide (6b)

10 g (0.0484 m mol) of 6a and 110 ml of methanol were hydrogenated over 1.1 g of Pd/C at 6 mmHg hydrogen pressure. The progress of the reaction was observed via TLC (5% methanol in DCM), and RM was filtered through a high-flow celite bed (**Figure 4.6**). The mother liquor was distilled under a vacuum. After distillation, the product was separated using ethyl acetate. The product was characterized using ¹H-NMR and MS.

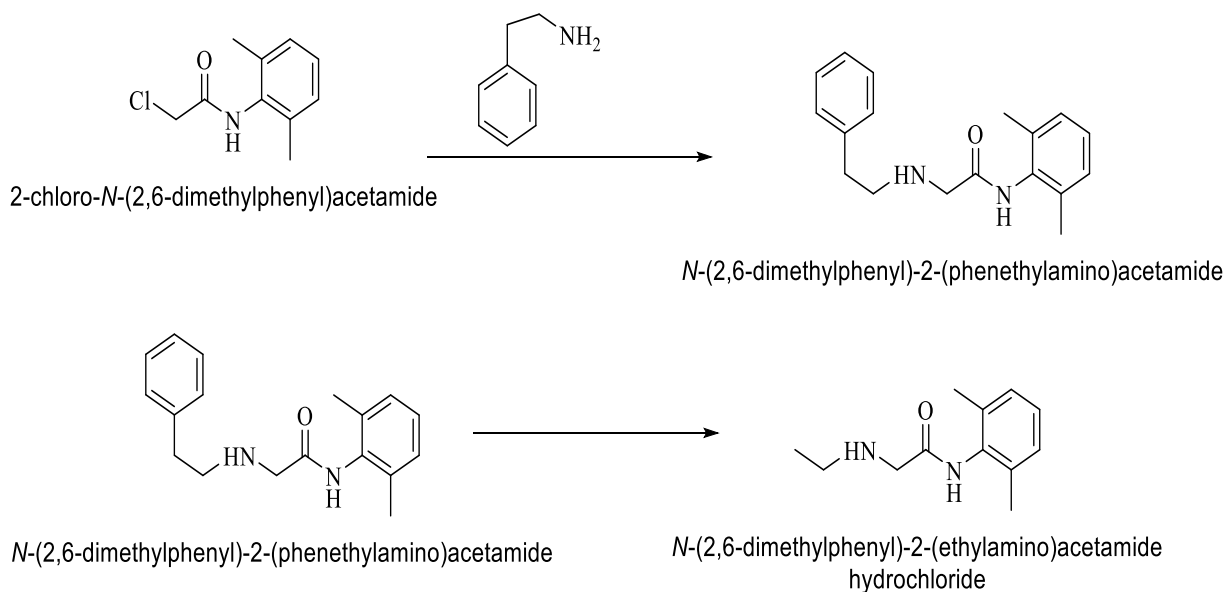


Figure 4.7: Synthesis of Ethylamino-substituted lidocaine impurities

v) Synthesis of *N*-(2,6-dimethylphenyl)-2-(isopropylamino)acetamide (7b)

7b is synthesized in a two-step. The intermediate 7a was formed in the first step, which was used as a precursor to synthesize 7b.

Synthesis of Intermediate (7a)

In a four-neck round bottom flask, 10 g (0.0505 m mol) of 3a was taken, and to it, 10 ml of acetone and 7.5 g (0.0505 m mol) of isopropyl phenylamine, 6.1 g (0.0505 m mol) of K_2CO_3 , and a pinch of KI were added. The RM was refluxed for 10 hours. The progress of the reaction was observed via TLC (20% ethyl acetate in hexane) (**Figure 4.8**). After that, the acetone was removed using a vacuum distillation process. 100 ml of H_2O and 150 ml of DCM were added to RM, and the organic layer was separated and distilled. A solid white product was obtained, recrystallized in hexane, and filtered out. The pure white solid product was confirmed using TLC as a reference.

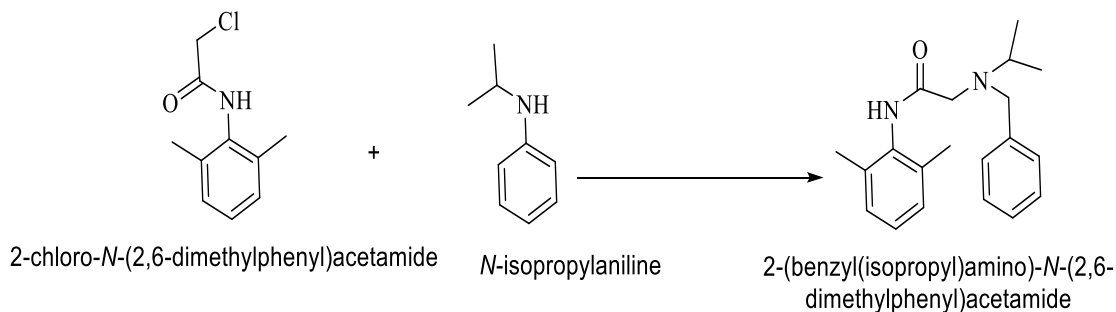


Figure 4.8: Synthesis of intermediate 7a

Synthesis of *N*-(2,6-Dimethylphenyl)-2-(Isopropylamino)Acetamide (7b)

11 g of 7a and 110 ml of methanol were hydrogenated over 1.1 gm of Pd/C at 8 mmHg hydrogen pressure (**Figure 4.9**). The progress of the reaction was checked after 4 hours via TLC (5% methanol in DCM), and the RM was filtered through a high-flow celite bed. The mother liquor was distilled under a vacuum. After distillation, the product was chased using hexane and methyl tert-butyl ether. The product was characterized using ¹H-NMR and MS.

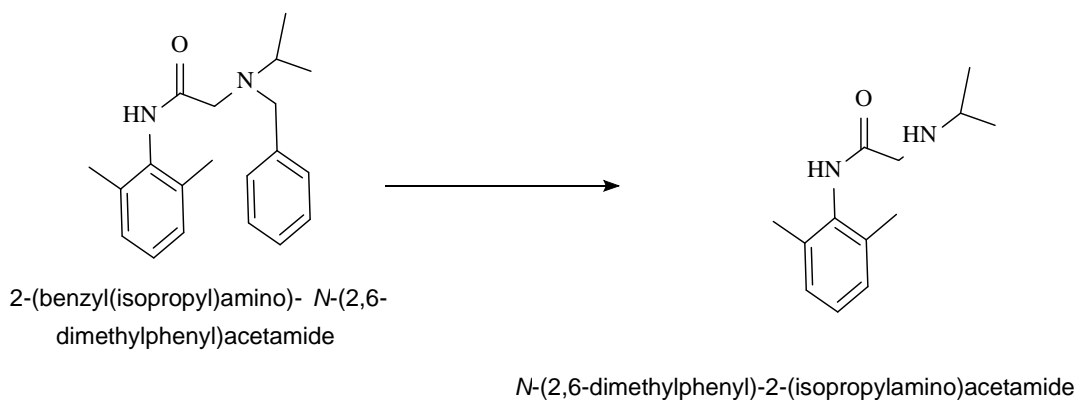


Figure 4.9: Synthesis of isopropyl-substituted lidocaine impurities

vi) Synthesis of *N*-(2,6-dimethylphenyl)-2-(ethyl(methyl)amino)acetamide (8)

In a four-neck round bottom flask, 10 g (0.0266 m mol) of 3a was taken, and to it, 100 ml acetone, 1.5 g (0.0266 m mol) of *N*-ethyl(methyl)amine, 3.6 g (0.0266 m mol) of K_2CO_3 , and a pinch of KI were added. The round bottom flask was closed airtightly with teflon, leaving the RM overnight with constant stirring. The RM was stirred and refluxed for 12 hours. The progress of the reaction was observed via TLC (5% MeOH in DCM). After that, RM was filtered out, and the spent liquor was removed using a vacuum distillation process. RM was cooled, adding 50 ml H₂O and 30 ml DCM. The organic layer was separated and washed twice using 250 ml of distilled water at neutral pH, followed by distillation. The product was purified using a column to get the pure solid mass (**Figure 4.10**). The product was characterized using ¹H-NMR and MS.

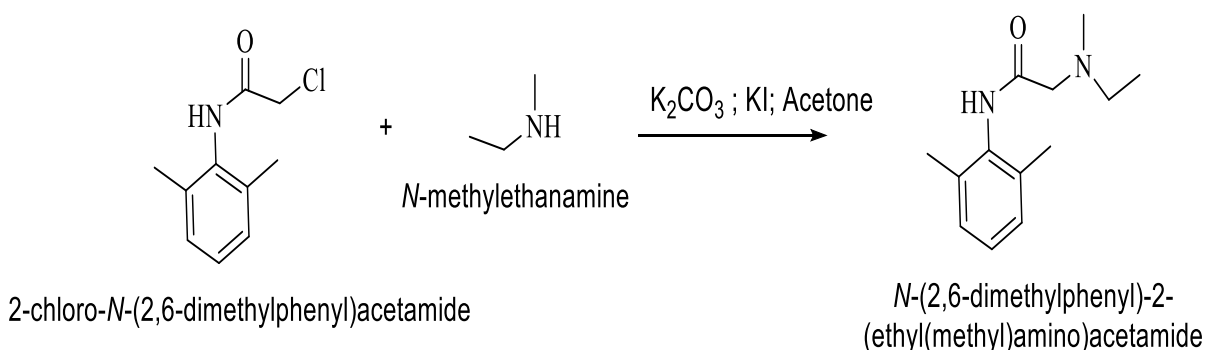


Figure 4.10: Synthesis of Ethyl methylamino-substituted lidocaine impurities

vii) Synthesis of *N*-(2,6-dimethylphenyl)-2-((2,6-dimethylphenyl)amino)acetamide (9)

In a four-neck round bottom flask, 10 g (0.0505 m mol) of 3a was taken; to it, 100 ml acetone, 6.1 g (0.0505 m mol) of 2,6 dimethyl aniline, 6.9 g (0.0505 m mol) of K_2CO_3 and a pinch of KI were added, and RM was refluxed whole night. The progress of the reaction was observed via TLC (20% ethyl acetate in hexane). After that, RM was filtered out, and the spent liquor was removed using vacuum distillation. The RM was cooled, adding 50

ml of H₂O and 30 ml of DCM. The organic layer was separated and washed twice using 250 ml of distilled water at neutral pH, followed by distillation under vacuum and recrystallized in a minimum amount of ethyl acetate with hexane to get the pure yellow solid mass (**Figure 4.11**). The product was characterized using ¹H-NMR and MS.

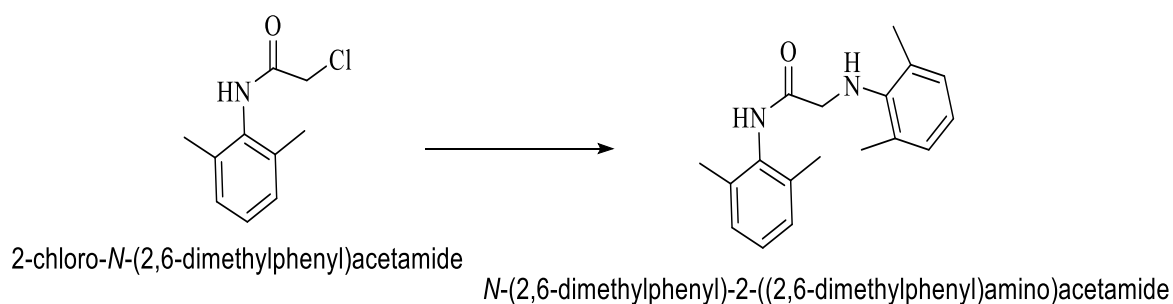


Figure 4.11: Synthesis of Dimethyl phenylamino-substituted lidocaine impurities

viii) Synthesis of 2-chloro-*N*-(2,3-dimethylphenyl)acetamide (10)

In a four-neck round bottom flask, 10 g (0.0825 m mol) of 2,3 dimethyl aniline was taken, 150 ml DCM and 6.9 g (0.0825 m mol) of NaHCO₃ were added, and RM was cooled down at 5–10 °C. 9.3 g (0.0825 m mol) of chloroacetyl chloride was added dropwise and stirred for 1 hour at 10–15 °C. The progress of the reaction was observed via TLC (20% ethyl acetate in hexane). The RM was cooled by adding 100 ml H₂O and 30 ml DCM. The organic layer was separated and washed twice using 250 ml of distilled water, followed by distillation under a vacuum. The product was recrystallized to a solid purple mass (**Figure 4.12**). The product was characterized using ¹H-NMR and MS.

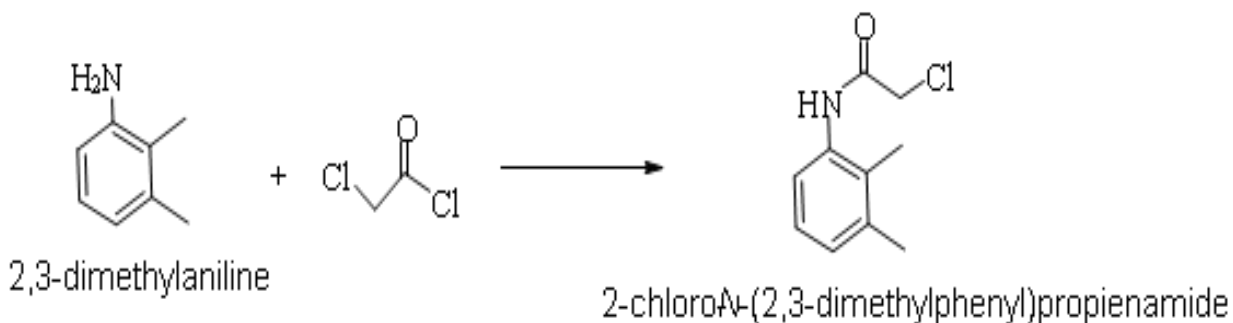


Figure 4.12: Synthesis of Propienamide-substituted lidocaine impurities

ix) Synthesis of *N*-(2,6-dimethylphenyl)piperazine Amide (11)

In a four-neck round bottom flask, 10 g (0.0505 m mol) of 3a was taken, 50 ml of acetonitrile, 3.5 g (0.0505 m mol) of K_2CO_3 , and 4.3 g (0.0505 m mol) of piperazine were added, and RM was stirred at RT for 12 hours (**Figure 4.13**). The progress of the reaction was observed via TLC (5% MeOH in DCM). After that, RM was distilled to remove acetonitrile. Next, DCM and water were used to remove excessive piperazine. Finally, the organic layer was removed and distilled to get the final product. TLC was done to confirm the product's purity, which was further characterized using 1H -NMR and mass spectroscopy.

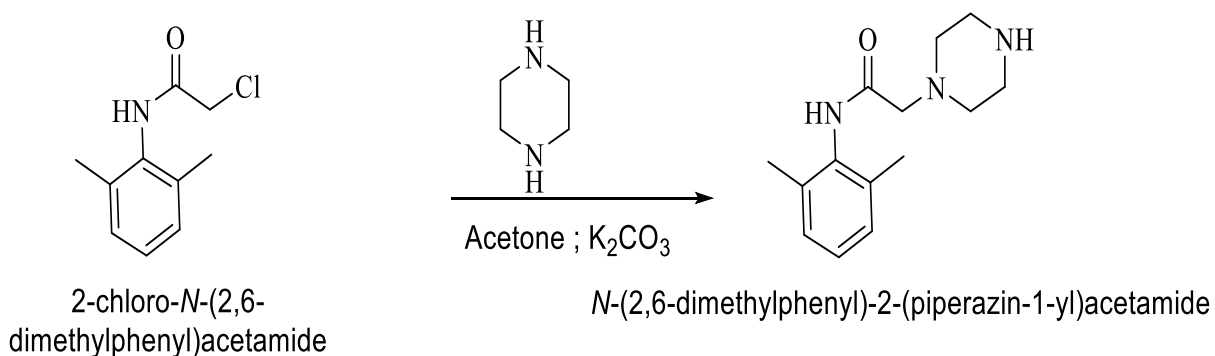


Figure 4.13: Synthesis of piperazine-substituted lidocaine impurities

4.3.3 Characterization of Impurities

Impurities are identified and analyzed using advanced techniques, including Mass Spectrometry and Nuclear Magnetic Resonance, which are defined below:

a) Mass Spectrometry

The analysis was conducted on an Agilent ORBITRAP MS using MeOH as the solvent and the ESI-positive method TOF. The technique used was low-resolution mass spectral analysis (LRMS).

b) Nuclear Magnetic Resonance

The NMR experiment to test the ^1H impurity was conducted at a frequency of 400 MHz and a temperature of 25 °C. The research utilized a Varian NMR instrument from Palo Alto, California. In ^1H NMR spectra, the chemical shifts are denoted as δ in ppm relative to the signal of chloroform-d (δ 7.28, singlet) and deuterated DMSO-d₆, δ = 2.50 for 1H. The multiplicity of the signals is indicated using the following abbreviations: s (singlet), brs (broad singlet), d (doublet), t (triplet), q (quartet), dd (doublets of doublet), dt (doublets of triplet), or m (multiplet). The letter n represents the number of protons contributing to a specific resonance. Coupling constants are reported as J values in hertz.

4.4 Results and Discussion

The continuous strive to develop a cost-effective and commercially viable green methodology for synthesizing APIs has led to the successful discovery of a green method for synthesizing 13 lidocaine impurities commonly used as local anesthetics.

i. Synthesis of 2-Chloro-*N*-(2,6-dimethylphenyl)acetamide (3a–3c)

In the synthesis of 3a-3c, the reaction mechanism involves the nucleophilic attack of the nitrogen atom of 2,6-dimethyl aniline on the chloroacetyl chloride, eliminating the chloride ion and forming an iminium ion intermediate. The intermediate then undergoes hydrolysis in the presence of NaHCO₃ to get the final product. The maximum yield of products in all three cases, 3a–3c, was obtained at a 1:1 molar ratio and stirred for 1 hour at RT. This confirms that 1:1 is the optimum molar ratio to synthesize 3a–3c. A further change in the molar ratio either increases or leads to no change in the yield. Similarly, further increases in the reaction duration from 60–70 minutes do not show any change in the amount of product formed. The reaction was achieved at the optimum temperature of 25–30 °C. The progress of the reaction was observed via TLC. This confirms the formation of the maximum amount of products as per the stoichiometry of reactions. The intended product's formation and purity were verified by characterizing it through ¹H-NMR and MS.

❖ Characterization of Products:

3a: The Melting Point of obtained products was 150–151 °C. The ¹H-NMR spectrum exhibited the presence of the characteristic's peaks at δ 7.9 (brs, 1H(-NH)), 7.05-7.55 (m, 3H), 4.24 (s, 2H), 2.32 (s, 3H), 2.19 (s,3H) as depicted in (Figure 4.14).

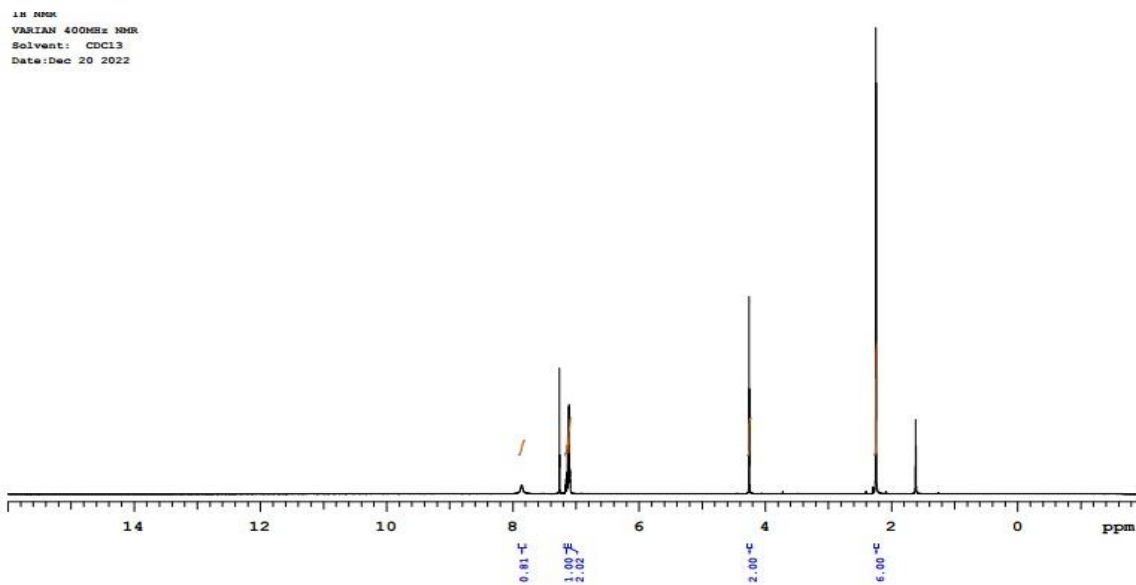


Figure 4.14: NMR Spectra (3a)

The mass spectrogram unveiled a zenith at m/z 198.1, corresponding to the product's molecular weight (196.66), as depicted in (**Figure 4.15**).

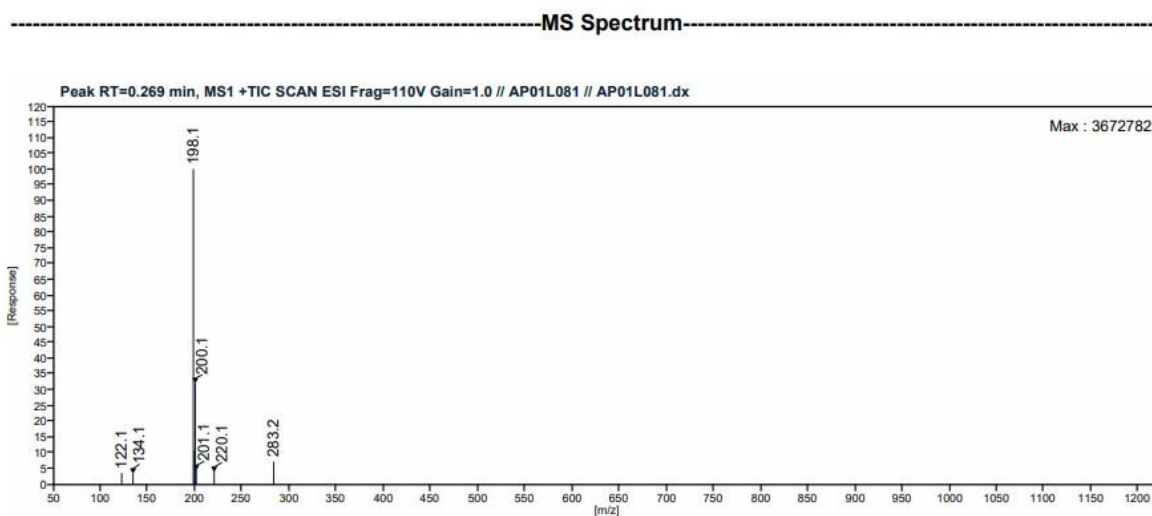


Figure 4.15: Mass Report (3a)

3b: The Melting Point of obtained products was 150–151 °C. The $^1\text{H-NMR}$ spectrum exhibited the presence of the characteristic's peaks at δ 8.18 (brs, 1H), 7.70 (m, 1H), 7.09(d, $J=7.6\text{Hz}$), 6.94 (d, $J=7.6\text{ Hz}$, 1H), 4.23 (s, 2H), 2.33 (s, 3H), 2.26 (s,3H) as depicted in (Figure 4.16).

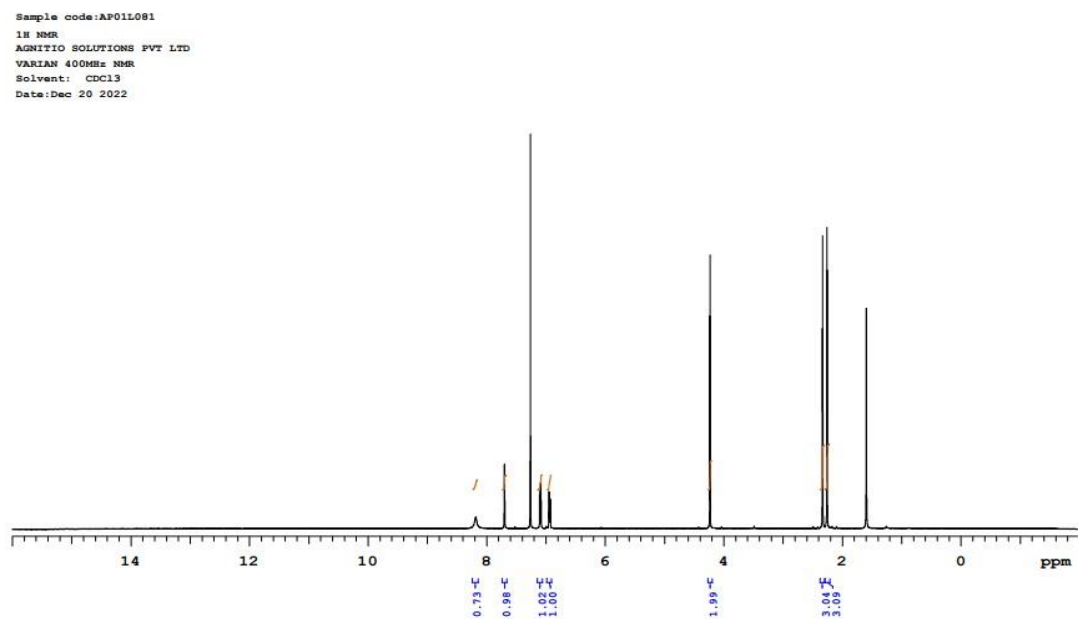


Figure 4.16: NMR Spectra (3b)

The mass unveiled a zenith at m/z 198.1, corresponding to the product's molecular weight (196.66), as depicted in (**Figure 4.17**).

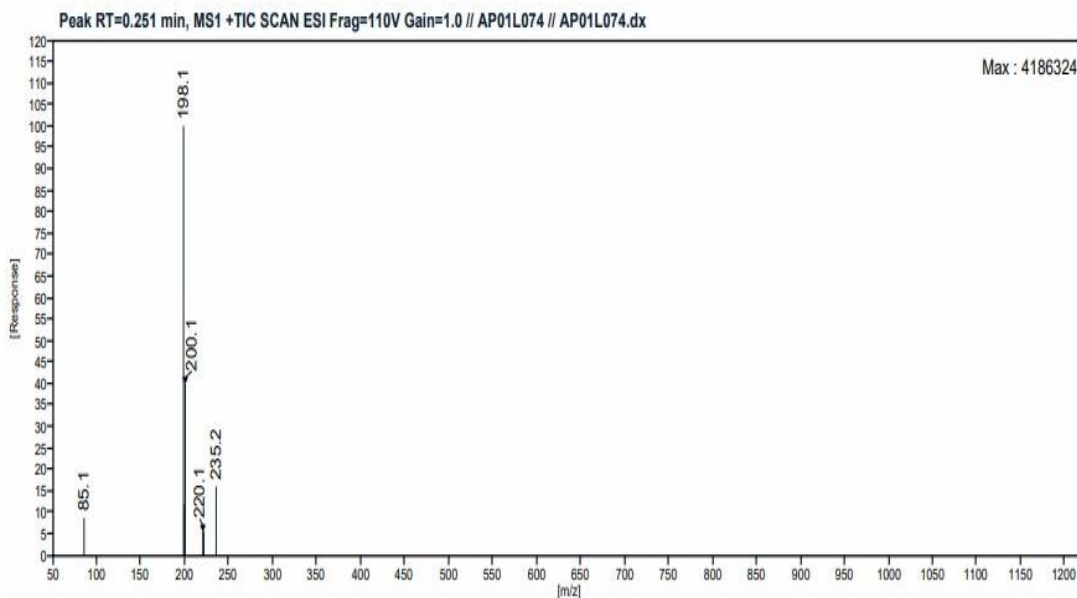


Figure 4.17: Mass Report (3b)

3c: The Melting Point of obtained products was 150–151 °C. The $^1\text{H-NMR}$ spectrum exhibited the presence of the characteristic's peaks at δ 8.15 (brs, 1H), 7.67 (m, 1H), 7.03 (m, 2H), 4.22 (s, 2H), 2.30 (s, 3H), 2.26 (s, 3H) as depicted in (**Figure 4.18**).

Sample code: AP01L080
AGNITIO SOLUTIONS PVT LTD
1H NMR
VARIAN 400MHz NMR
Solvent: CDCl3
Date: Dec 20 2022

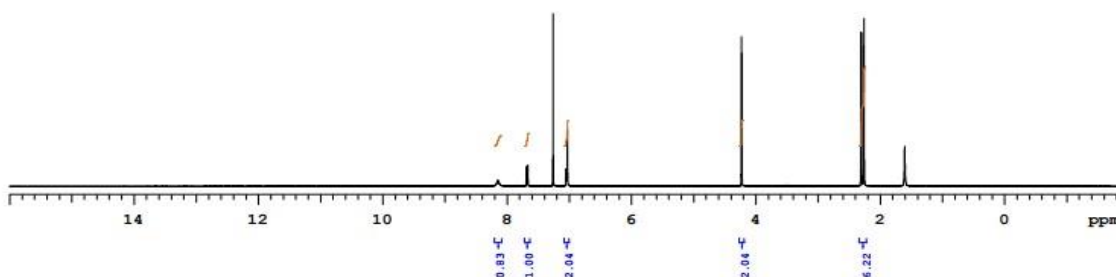


Figure 4.18: NMR Spectra (3c)

The mass unveiled a zenith at m/z 198.1, which corresponded to the product's molecular weight (196.66), as depicted in (Figure 4.19)

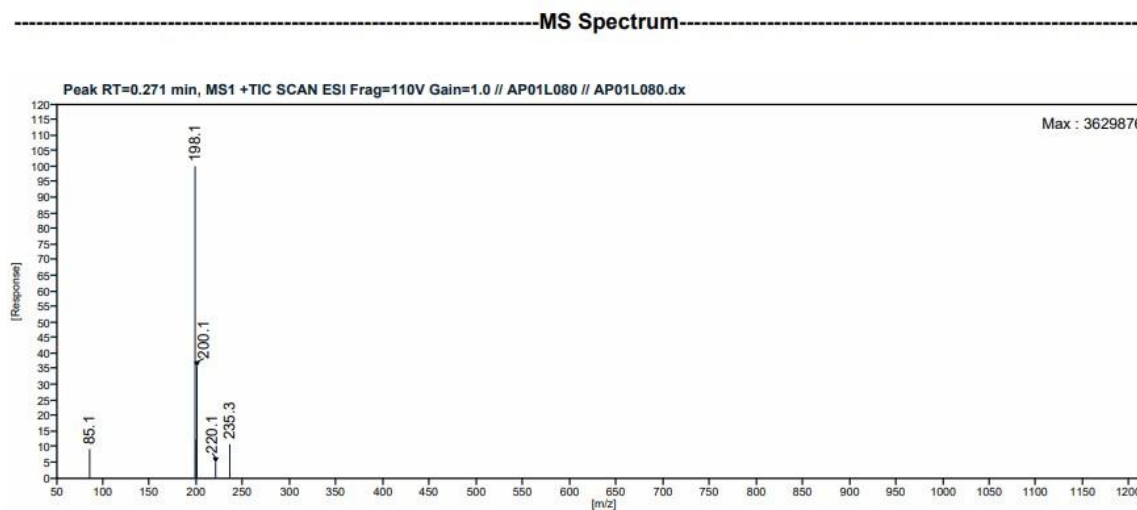


Figure 4.19: Mass Report (3c)

ii) **Synthesis of 2-(Diethylamino)-N-(2,3-dimethylphenylacetamide (4a-4c)**

In the synthesis of 4a-4c, the reaction using diethylamine as a nucleophile and potassium carbonate as a base allowed for the formation of the amide bond, while acetone as a solvent and potassium iodide as a catalyst facilitated the reaction to yield the product. The maximum yield of products in all three cases, 4a–4c, was obtained at a 1:1 molar ratio and stirred for 6 hours of reaction duration at room temperature. This confirms that 1:1 is the optimum molar ratio to synthesize 4a–4c. A further change in the molar ratio either increases or leads to no change in the yield. Similarly, further increases in the reaction duration from 6–8 hours do not show any change in the amount of product formed. The reaction was achieved at reflux. The progress of the reaction was observed via TLC. This confirms the formation of the maximum amount of products as per the stoichiometry of reactions. The intended product's formation and purity were verified by characterizing it through ¹H-NMR and MS.

❖ **Characterisation of Products:**

4a: The melting point of obtained products was 110–112 ° C. The ¹H-NMR spectrum exhibited the presence of the characteristic's peaks at δ 11.05 (brs, 1H), 10.31 (s, 1H), 7.22(m, 2H), 7.02 (m, 2H), 4.38 (s, 2H), 3.52 (m, 2H), 3.37 (m, 2H), 2.24 (s, 3H) 2.29 (s, 3H), 1.47 (t, J=7.2H, 6H) as depicted in (**Figure 4.20**).

Sample code:AP01L072
AGNITIO SOLUTIONS PVT LTD
1H NMR
VARIAN 400MHz NMR
Solvent: CDCl3
Date:Dec 20 2022

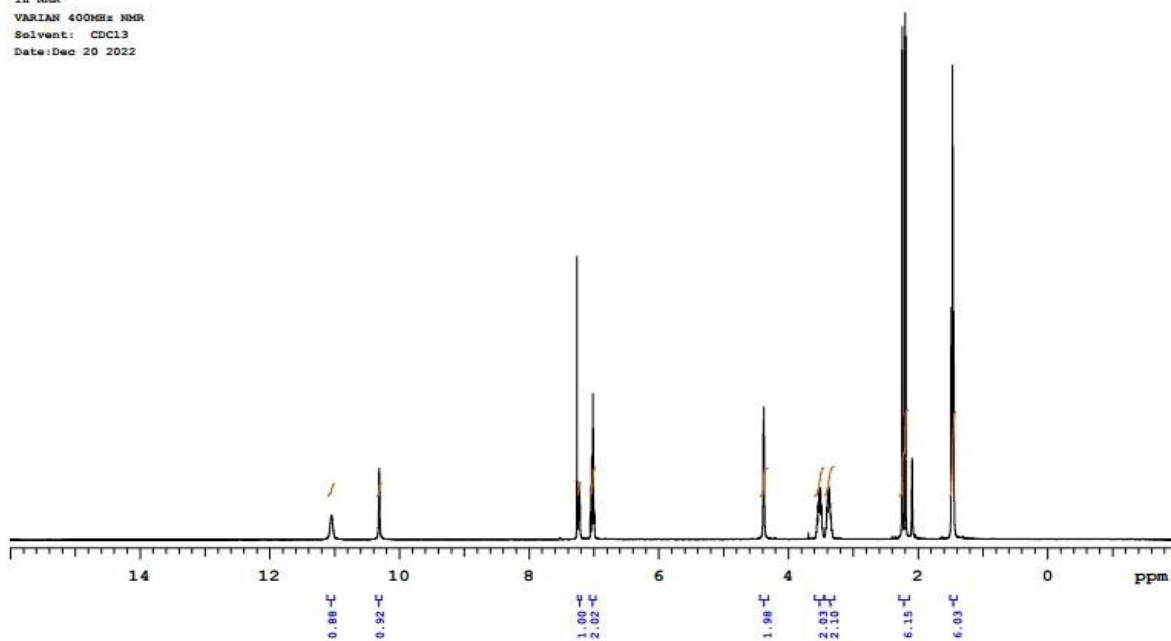


Figure 4.20: NMR Spectra (4a)

The mass unveiled a zenith at m/z 235.2, corresponding to the product's molecular weight (234.17), as depicted in **(Figure 4.21)**.

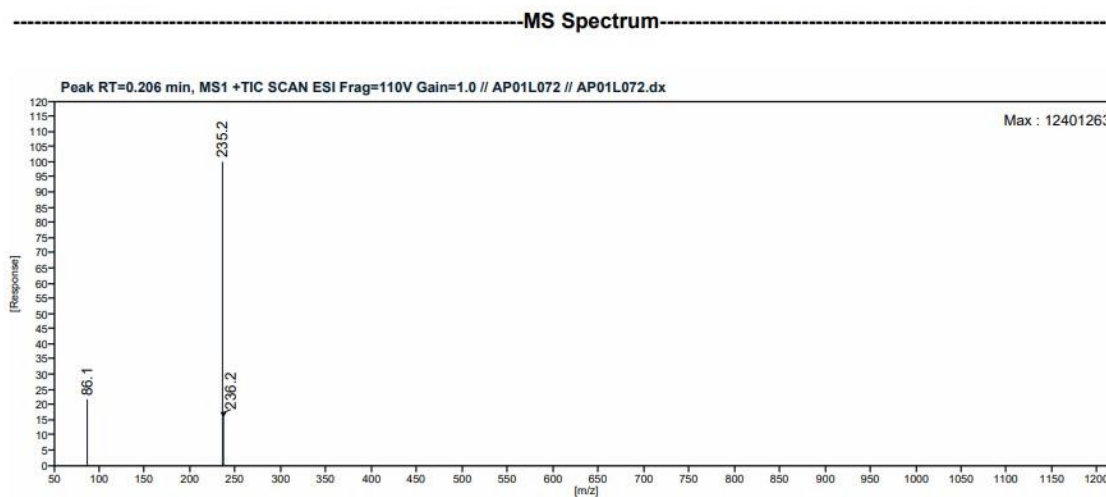


Figure 4.21: Mass Report (4a)

4b: The melting point of obtained products was 110–112 ° C. The $^1\text{H-NMR}$ spectrum exhibited the presence of the characteristic's peaks at δ 11.16 (brs, 1H), 10.15 (s, 1H), 7.28 (s, 1H), 7.05 (d, $J=7.6$ Hz, 1H), 6.92 (d, $J=7.6$ Hz, 1H), 4.38 (s, 2H), 3.54 (m, 2H), 3.39 (m, 2H) 2.28 (d, $J=6.8$ Hz, 6H) 1.48 (t, $J=7.2$ H, 6H) as depicted in (**Figure 4.22**)

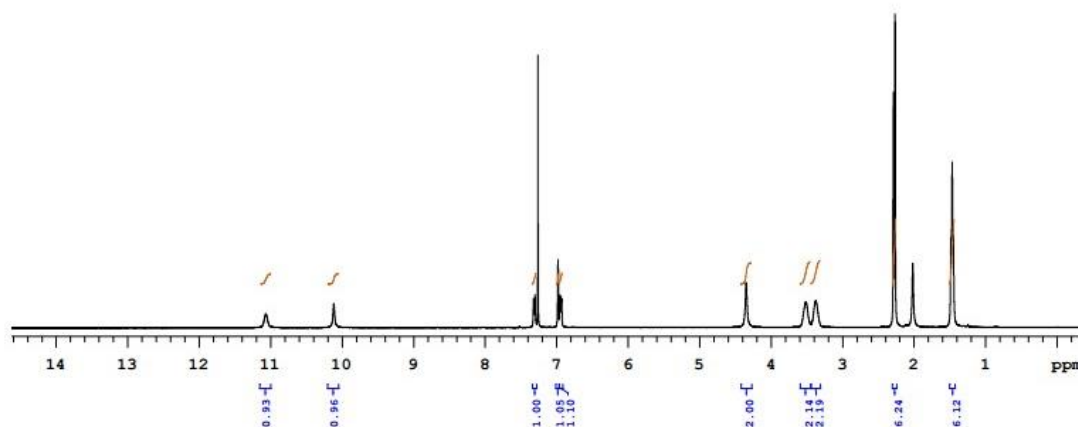


Figure 4.22: NMR Spectra (4b)

The mass unveiled a zenith at m/z 235.2, corresponding to the product's molecular weight (234.17), as depicted in (Figure 4.23).

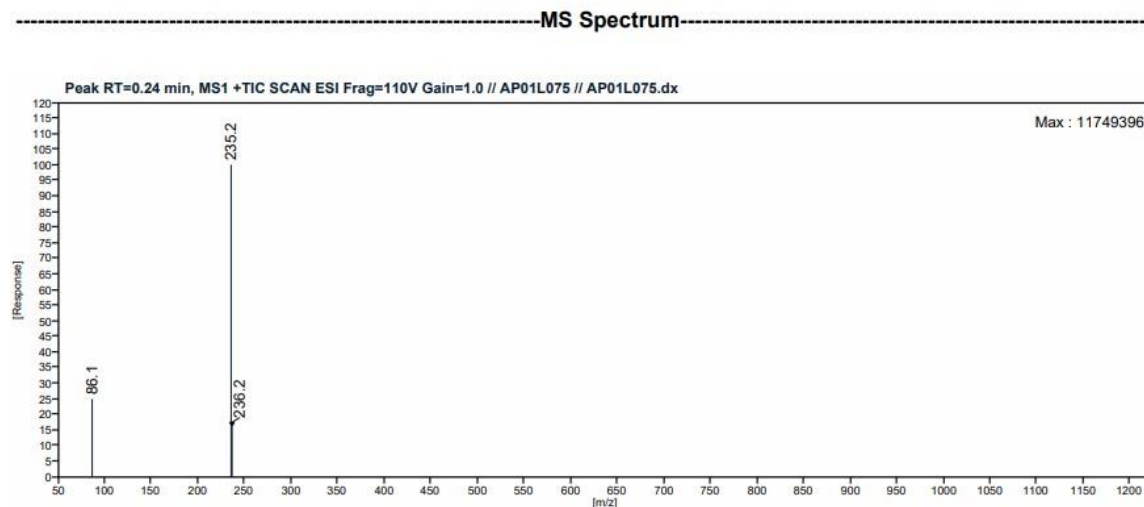


Figure 4.23: Mass Report (4b)

4c: The melting point of obtained products was 110–112 ° C. The $^1\text{H-NMR}$ spectrum exhibited the presence of the characteristic's peaks at δ 11.06 (brs, 1H), 10.12 (s, 1H), 7.31 (m, 1H), 6.95 (m, 2H), 4.35 (s, 2H), 3.52 (b, 2H), 3.37 (b, 2H), 2.24 (s, 3H) 2.28 (s, 3H), 2.26 (s, 3H), 1.47 (t, $J=7.2\text{Hz}$, 6H) as depicted in (Figure 4.24).

Sample code:AP01L076
AGNITIO SOLUTIONS PVT LTD
1H NMR
VARIAN 400MHz NMR
Solvent: CDCl3
Date:Dec 20 2022

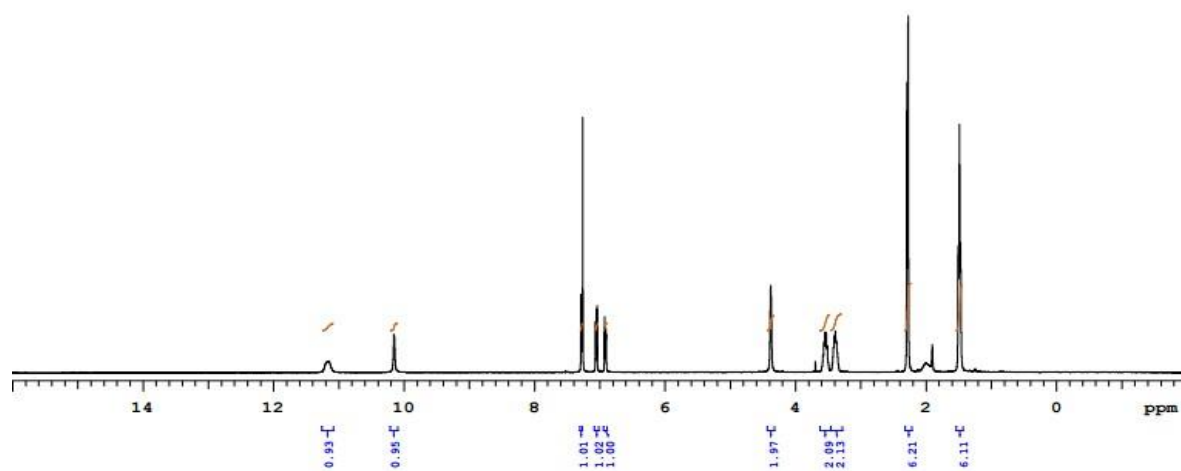


Figure 4.24: NMR Spectra (4c)

The mass unveiled a zenith at m/z 235.2, corresponding to the product's molecular weight (234.17), as shown in (Figure 4.25).

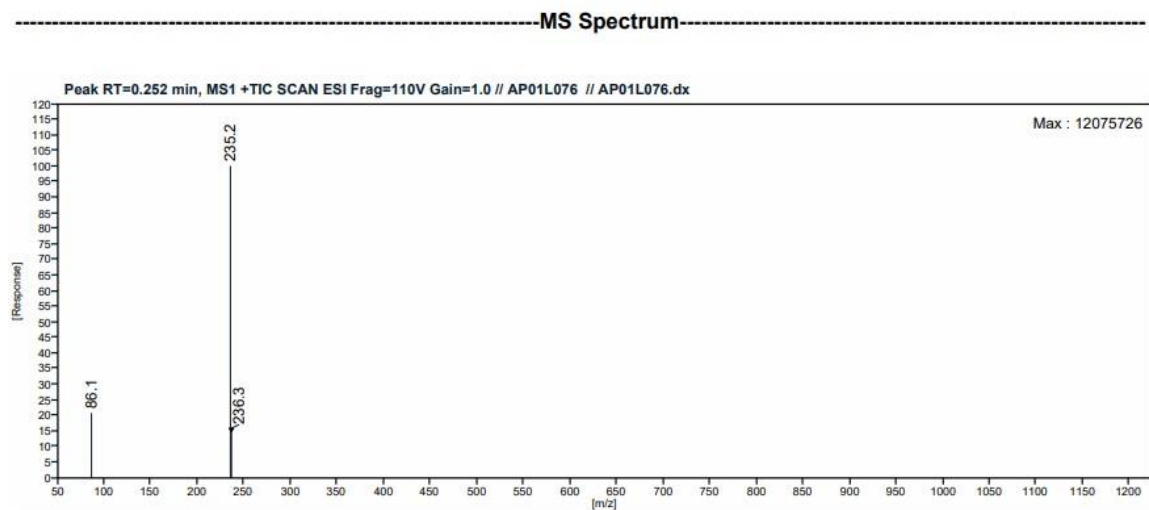


Figure 4.25: Mass Report (4c)

iii) Synthesis of 2,2'-azanediyllbis(*N*-(2,6-dimethylphenyl)acetamide) (5)

In the synthesis of 5, benzylamine is used as a nucleophile, and K_2CO_3 is used as a base in the reaction mixture, which promotes the formation of the desired product. The reaction also involved using KI, which acted as an additive to enhance the reaction rate by promoting the formation of a more favorable product yield. The maximum yield of products in reaction 5 was obtained at a 1:1 molar ratio and stirred for 12 hours of reaction duration at room temperature. This confirms that 1:1 is the optimum molar ratio to synthesize 5. A further change in the molar ratio either increases or leads to no change in the yield. Similarly, further increases in the reaction duration from 12–14 hours do not show any change in the amount of product formed. The reaction was achieved at reflux. The progress of the reaction was observed via TLC. This confirms the formation of the maximum amount of products as per the stoichiometry of reactions. The intended product's formation and purity were verified by characterizing it through 1H -NMR and MS. The 1H -NMR spectrum of 5 exhibited the presence of the characteristic's peaks at δ 9.47 (s, 2H), 7.07 (m, 6H), 3.41(s, 4H), 3.35 (b, 1H), 2.15(s, 12H). The mass of 5 unveiled a zenith at m/z 340.3, corresponding to the product's molecular weight (339.44), as depicted in **(Figures 4.26 and 4.27)**.

Sample code:AP01L071
1H NMR
AGNITIO SOLUTIONS PVT LTD
VARIAN 400MHz NMR
Solvent: dmsd
Date:Dec 29 2022

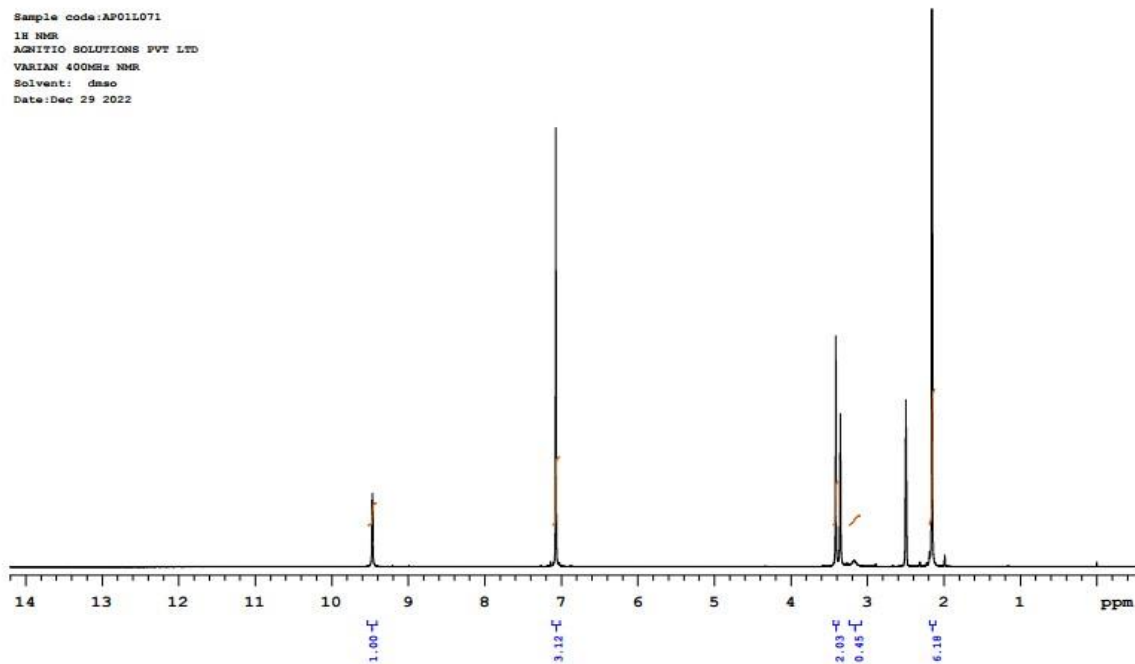


Figure 4.26: NMR Spectra (5)

-----MS Spectrum-----

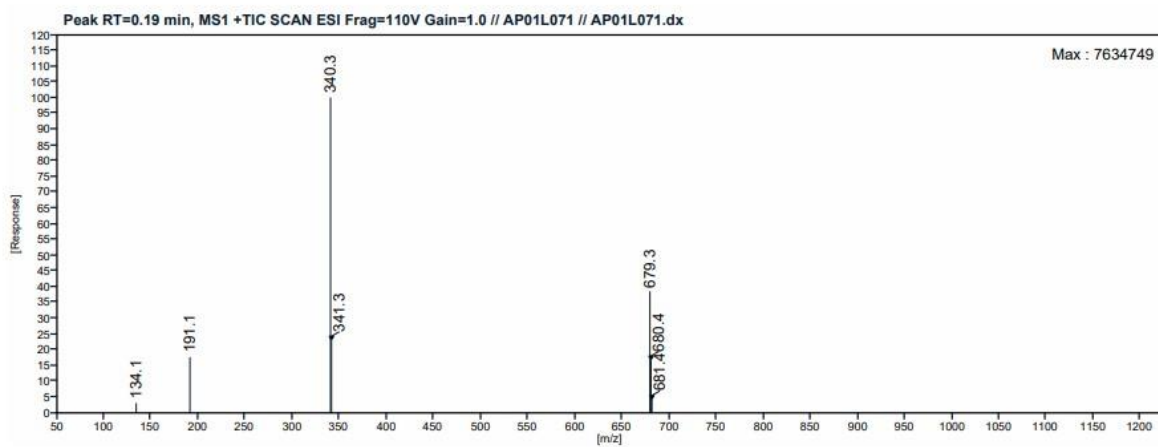


Figure 4.27: Mass Report (5)

iv) Synthesis of *N*-(2,6-dimethylphenyl)-2-(ethylamino)acetamide (6b)

6b in two steps. In the first step, intermediate 6a was formed from 3a and *N*-phenylethylamine using K_2CO_3 as a base and DMF as a solvent. After the reaction, excess acetonitrile was removed from RM using vacuum distillation. Then, the product was transferred to another round bottom flask and refluxed with DMF for two hours. The RM was left the whole night at RT with constant stirring to ensure complete conversion of the SM to the desired product. The reaction was confirmed using TLC. In the second step, 6b was synthesized using hydrogenation of 6a as the precursor and methanol over Pd/C at 6 mmHg hydrogen pressure. The maximum yield of products in reaction 6b was obtained at a 1:1 molar ratio and stirred for 1 hour of reaction duration at RT. This confirms that 1:1 is the optimum molar ratio for synthesizing 6b. A further change in the molar ratio either increases or leads to no change in the yield. Similarly, a further increase in the reaction duration from 4–5 hours shows no change in the amount of product formed. The reaction was achieved at the optimum temperature of 25–30 °C. The progress of the reaction was observed via TLC. This confirms the formation of the maximum amount of products as per the stoichiometry of reactions. The intended product's formation and purity were verified by characterizing it through 1H -NMR and MS. The 1H -NMR spectrum showed the presence of the characteristic's peaks at δ 10.08 (s, 1H), 9.12 (b, 2H), 7.096 (m, 3H), 4.00 (s, 2H), 3.01(d, 2H), 3.01 (d, J=7.2 Hz, 2H), 2.17 (s, 6H), 1.23(t, J=7.2 Hz, 3H). The mass unveiled a zenith at m/z 207.1, corresponding to the product's molecular weight (206.14), as depicted in (Figures 4.28 and 4.29).

1H NMR
AGNITIO SOLUTIONS PVT LTD
VARIAN 400MHz NMR
Solvent: dmsc
Date: Dec 29 2022

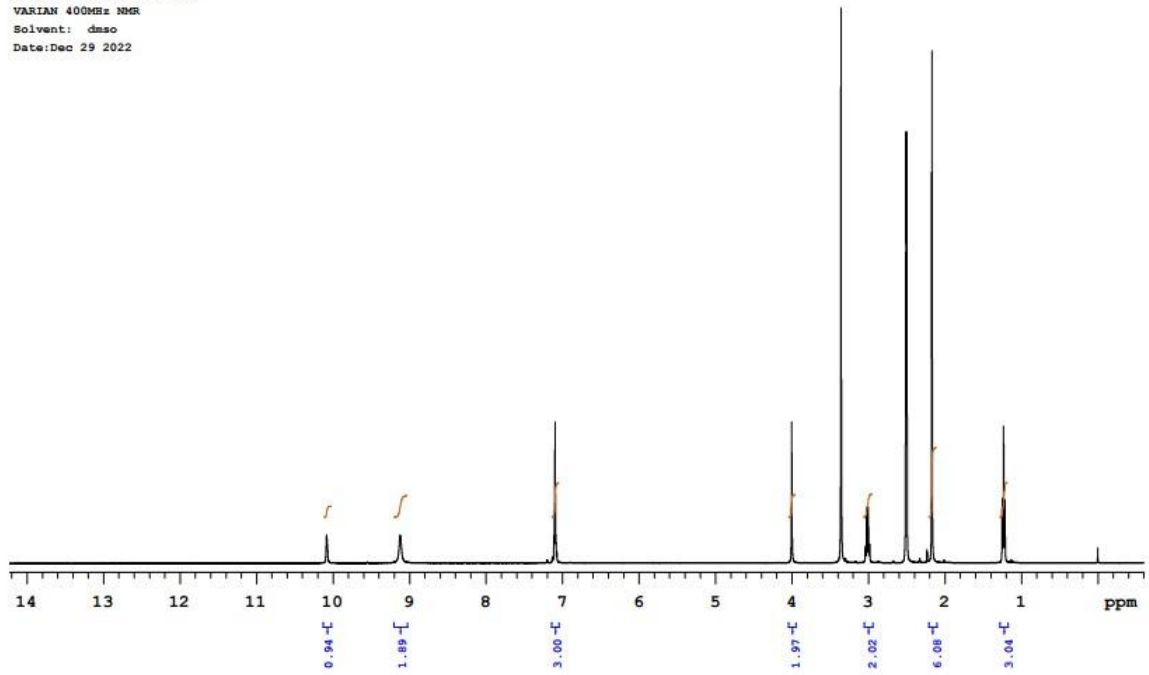


Figure 4.28: NMR Spectra (6b)

-----MS Spectrum-----

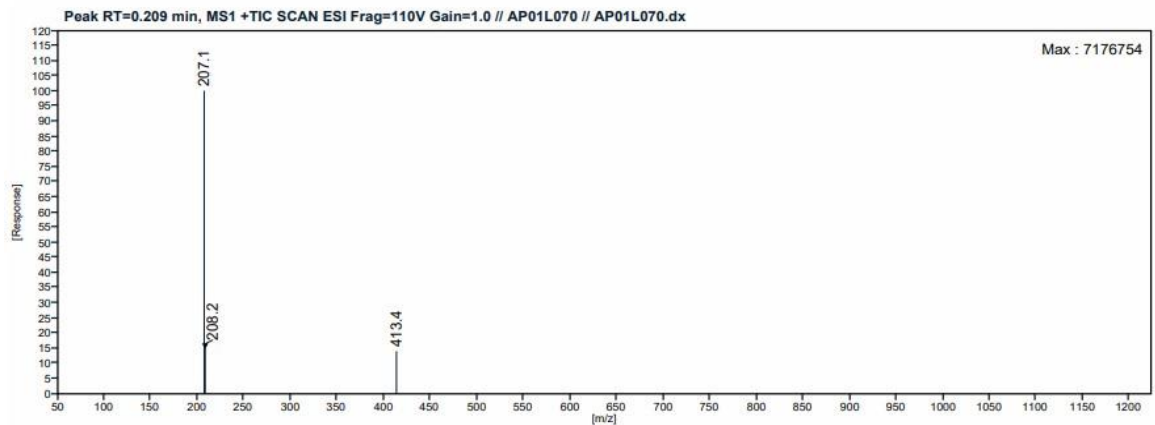


Figure 4.29: Mass Report (6b)

v) **Synthesis of *N*-(2,6-dimethylphenyl)-2-(isopropylamino)acetamide (7b)**

The synthesis of 7b was successfully achieved in two steps. In the first step, intermediate 7a was formed from 3a in the presence of K_2CO_3 and KI as catalysts, and isopropyl phenylamine was used as a nucleophile. Acetone was used as a solvent to facilitate the reaction, and the RM was refluxed for 10 hours. The progress of the reaction was observed via TLC. In the second step, 7b was synthesized using hydrogenation of 7a as the precursor and methanol over Pd/C at 6 mmHg hydrogen pressure. The maximum yield of products in reaction 7b was obtained at a 1:1 molar ratio and stirred for 4 hours at RT. This confirms that 1:1 is the optimum molar ratio to synthesize 7b. A further change in the molar ratio either increases or leads to no change in the yield. Similarly, a further increase in the reaction duration from 4–5 hours shows no change in the amount of product formed. The progress of the reaction was observed via TLC. This confirms the formation of the maximum amount of products as per the stoichiometry of reactions. The intended product's formation and purity were verified by characterizing it through 1H -NMR and MS. The 1H -NMR spectrum showed the presence of the characteristic's peaks at δ 8.93 (brs, 1H), 9.12 (b, 2H), 7.65 (m, 3H), 3.44 (s, 2H), 2.91 (m, 1H), 2.23 (s, 6H), 1.14 (t, $J=6.44$ Hz, 6H). The mass unveiled a zenith at m/z 221.1, corresponding to the product's molecular weight (220,32), as depicted in **(Figures 4.30 and 4.31)**.

VARIAN 400MHz NMR
Solvent: CDCl3
Date: Dec 20 2022

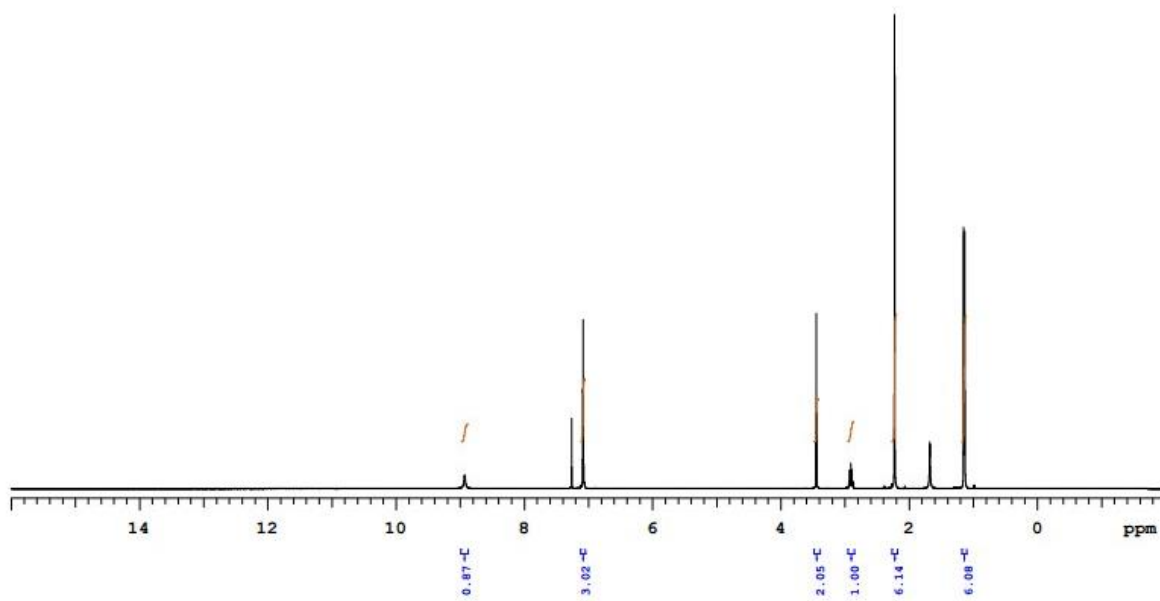


Figure 4.30: NMR Spectra (7b)

-----MS Spectrum-----

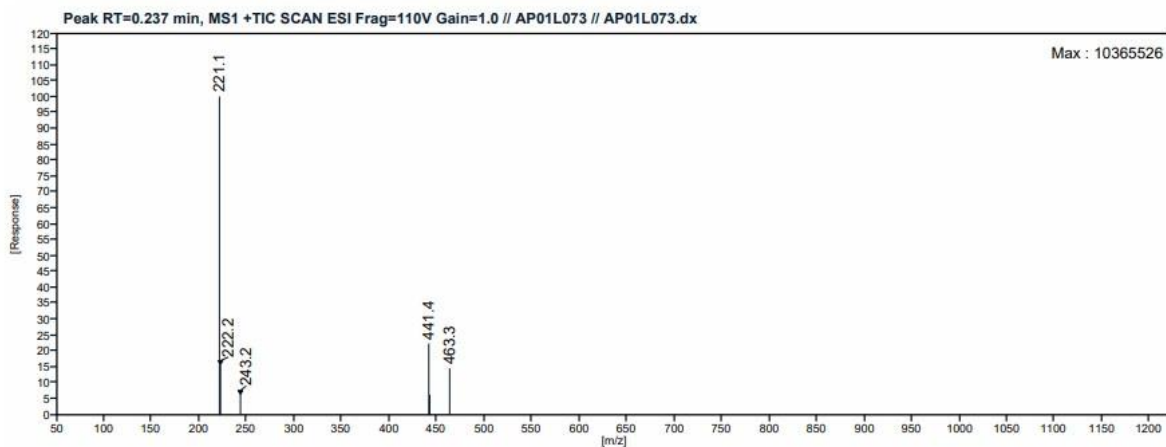


Figure 4.31: Mass Report (7b)

vi) Synthesis of *N*-(2,6-dimethylphenyl)-2-(ethyl (methyl)amino)acetamide (8)

In the synthesis of 8 the reaction, acetone was used as the solvent, *N*-ethyl(methyl)amine was used as the amine, K₂CO₃ was used as the base, and KI was used as a catalyst. The reaction mixture was stirred for 12 hours and refluxed for another night. The maximum yield of products in the reaction (8) was obtained at a 1:1 molar ratio. This confirms that 1:1 is the optimum molar ratio to synthesize 8. A further change in the molar ratio either increases or leads to no change in the yield. Similarly, a further increase in the reaction duration from 12–14 hours shows no change in the amount of product formed. The reaction was achieved at reflux. The progress of the reaction was observed via TLC. The product obtained was purified using column chromatography, which resulted in a solid mass of the pure product. The melting point of obtained product is 166–168 °C. This confirms the formation of the maximum amount of products as per the stoichiometry of reactions. The intended product's formation and purity were verified by characterizing it through ¹H-NMR and MS. The ¹H-NMR spectrum showed the presence of the characteristic's peaks at δ 10.07 (brs, 1H), 7.05 (m, 1H), 7.01 (m, 2H), 4.32 (s, 2H), 3.54 (b, 2H), 2.93 (s, 3H), 2.21 (s, 6H), 1.39 (t, J=7.2 Hz, 3H). The mass unveiled a zenith at m/z 221.1, corresponding to the product's molecular weight (220,32), as shown in (Figures 4.32 and 4.33).

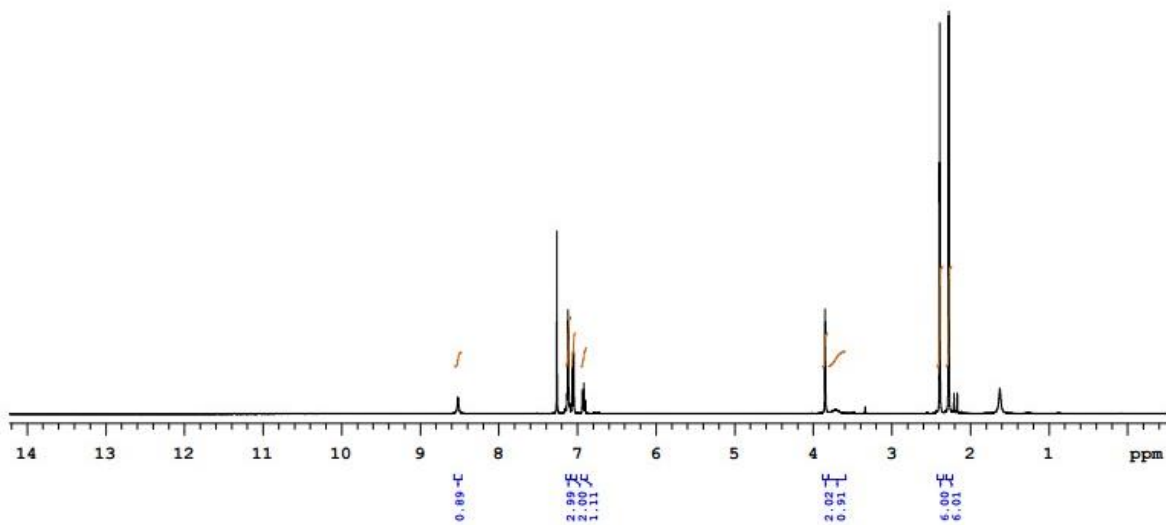


Figure 4.32: NMR Spectra (8)

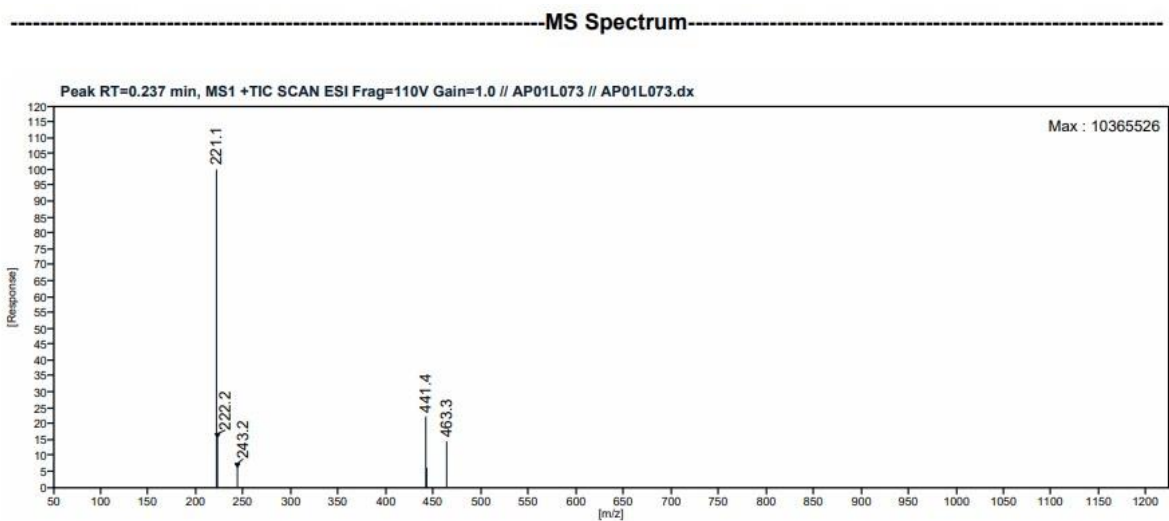


Figure 4.33: Mass Report (8)

vii) **Synthesis of *N*-(2,6-dimethylphenyl)-2-((2,6-dimethylphenyl)amino)acetamide (9)**

In the reaction of 9, K₂CO₃ and KI were used as catalysts to ensure a high product yield. The maximum yield of products in reaction 9 was obtained at a 1:1 molar ratio and stirred for 12 hours of reaction duration at reflux. This confirms that 1:1 is the optimum molar ratio to synthesize 9. A further change in the molar ratio either increases or leads to no change in the yield. Similarly, an additional increase in the duration from 12–14 hours shows no change in the amount of product formed. The reaction was achieved at reflux. The progress of the reaction was observed via TLC. The product was obtained as a yellow solid mass, and its purity was confirmed by recrystallization in a minimum amount of ethyl acetate with hexane. This confirms the formation of the maximum amount of products as per the stoichiometry of reactions. The intended product's formation and purity were verified by characterizing it through ¹H-NMR and MS. The ¹H-NMR spectrum showed the presence of characteristic peaks at δ 8.52 (brs, 1H), 7.13 (m, 3H), 7.08 (m, 2H), 6.92 (m, 1H), 3.85 (b, 1H), 2.93 (s, 3H), 2.39 (s, 6H), 2.28 (s, 6H). The mass unveiled a zenith at *m/z* 283.3, corresponding to the product's molecular weight (282.39), as depicted in **(Figures 4.34 and 4.35)**.

Sample code: AP01L077
1H NMR
AGNITIO SOLUTIONS PVT LTD
VARIAN 400MHz NMR
Solvent: CDCl3
Date: Dec 20 2022

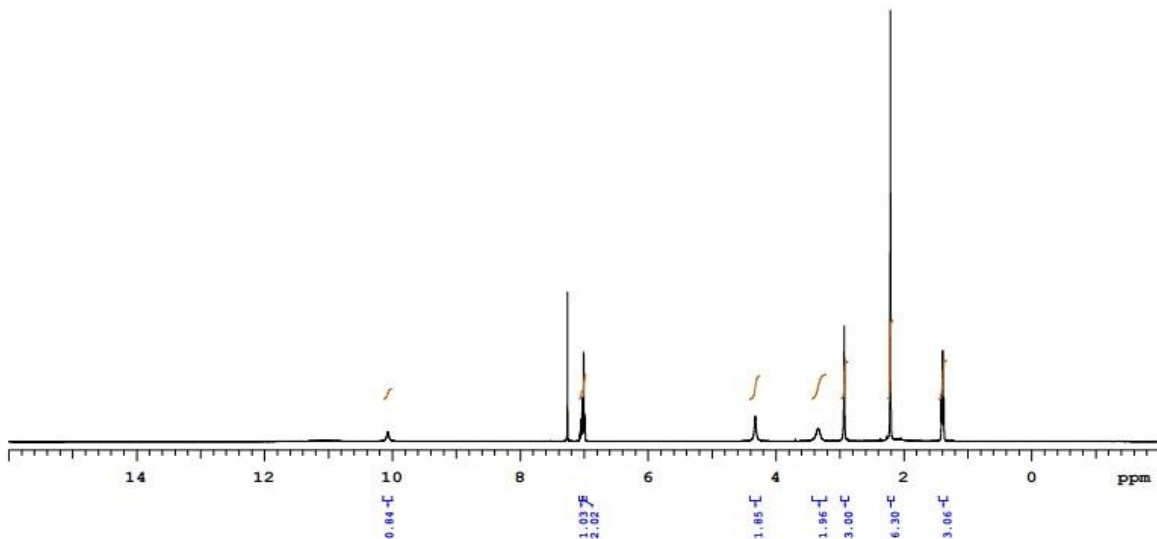


Figure 4.34: NMR Spectra (9)

-----MS Spectrum-----

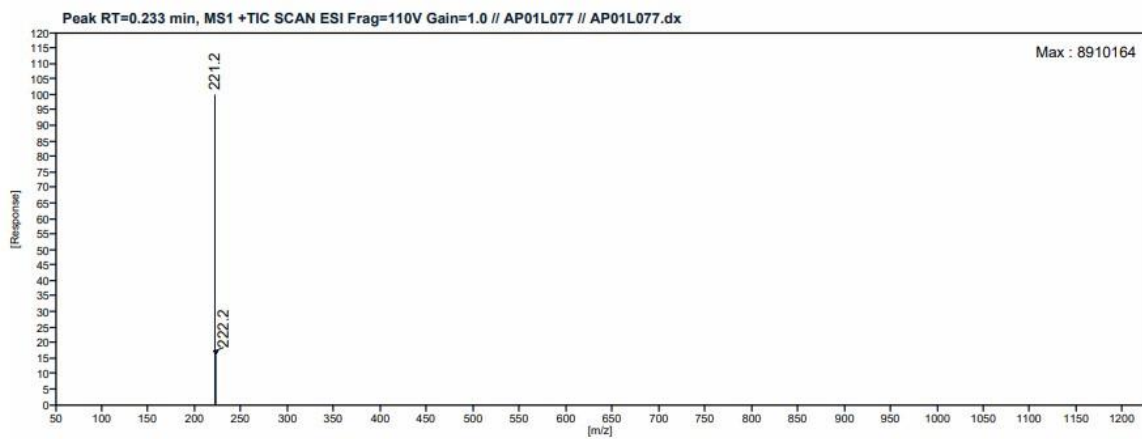


Figure 4.35: Mass Report (9)

viii) Synthesis of *N*-(2,3-dimethylphenyl)propienamide (10)

In the reaction of 10, NaHCO₃ was used as a base, which helped neutralize any excess chloroacetyl chloride and minimize the formation of unwanted byproducts. The maximum yield of products in 10 was obtained at a 1:1 molar ratio and stirred for 1 hour of reaction duration at 10-15 °C. This confirms that 1:1 is the optimum molar ratio to synthesize 10. A further change in the molar ratio either increases or leads to no change in the yield. Similarly, a further increase in the reaction duration from 60–70 minutes shows no change in the amount of product formed. The reaction was achieved at the optimum temperature of 10–15 °C. The progress of the reaction was observed via TLC. The organic layer was then separated and washed twice with distilled water to remove impurities. This confirms the formation of the maximum amount of products as per the stoichiometry of reactions. The intended product's formation and purity were verified by characterizing it through ¹H-NMR and MS. The ¹H-NMR spectrum showed the presence of characteristic peaks at δ 8.21 (brs, 1H), 7.55 (m, 1H), 7.14(m, 1H), 7.05 (m, 1H), 4.24 (s, 2H), 2.32 (s, 3H), 2.19 (s, 3H). The mass unveiled a zenith at m/z 198.1, which corresponded to the product's molecular weight (197.66), as shown in (**Figures 4.36 and 4.37**).

Sample code:AP01L079
1H NMR
AGNITIO SOLUTIONS PVT LTD
VARIAN 400MHz NMR
Solvent: CDCl3
Date:Dec 20 2022

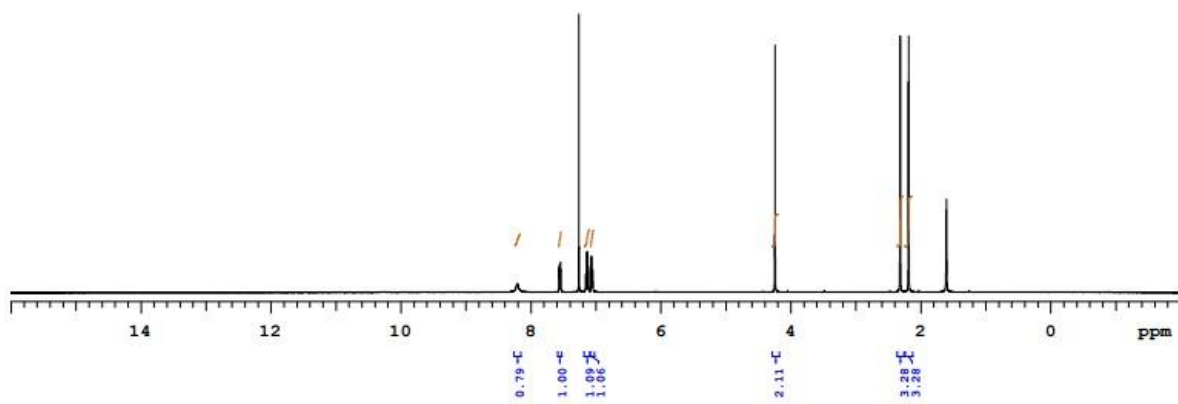


Figure 4.36: NMR Spectra (10)

-----MS Spectrum-----

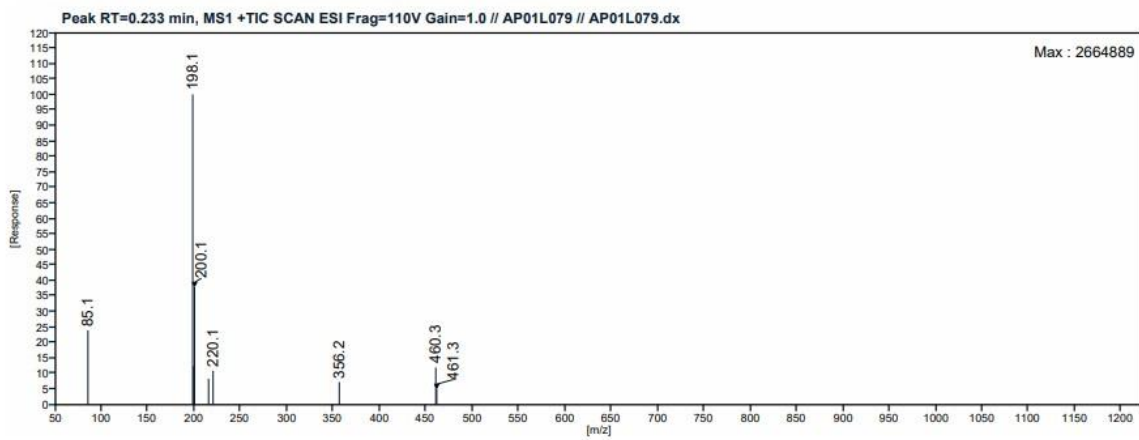


Figure 4.37: Mass Report (10)

ix) Synthesis of *N*-(2,6-dimethylphenyl)-2-(piperazine-1-yl)acetamide (11)

In the reaction of 11, acetonitrile is used as the solvent, and K_2CO_3 is used as the base. Piperazine was used as the nucleophile to react with the substrate in the presence of K_2CO_3 . The reaction was carried out at RT for 12 hours, sufficient for the reaction to complete. The maximum yield of products in reaction 11 was obtained at a 1:1 molar ratio. This confirms that 1:1 is the optimum molar ratio to synthesize 11. A further change in the molar ratio either increases or leads to no change in the yield. Similarly, a further increase in the duration from 12–14 hours shows no change in the amount of product formed. The progress of the reaction was observed via TLC. This confirms the formation of the maximum amount of products as per the stoichiometry of reactions. The intended product's formation and purity were verified by characterizing it through 1H -NMR and MS. The 1H -NMR spectrum showed the presence of characteristic peaks at δ 8.67 (brs, 1H), 7.09 (m, 3H), 3.21 (s, 2H), 2.68 (b, 4H), 2.98 (m, 4H), 2.23(s, 6H). The mass unveiled a zenith at m/z 248, which corresponded to the product's molecular weight (247.17), as depicted in **(Figures 4.38 and 4.39)**.

Sample code:AP01L082
1H NMR
AGNITIO SOLUTIONS PVT LTD
VARIAN 400MHz NMR
Solvent: CDCl3
Date:Dec 20 2022

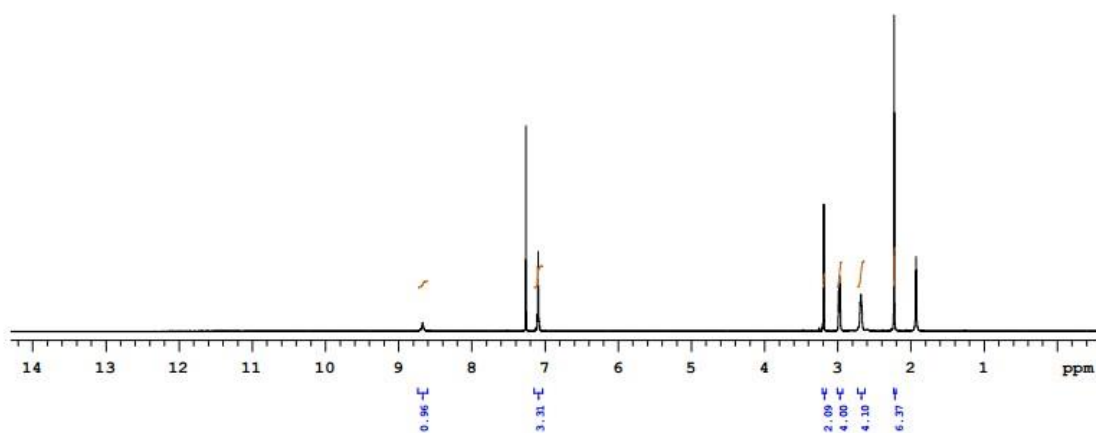


Figure 4.38: NMR spectra (11)

-----MS Spectrum-----

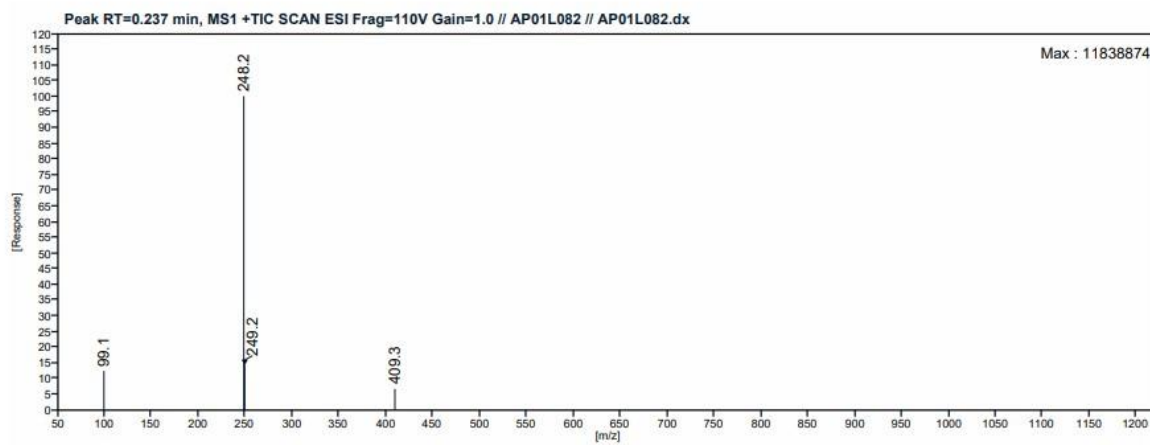
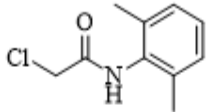
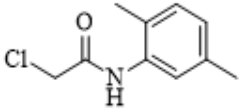
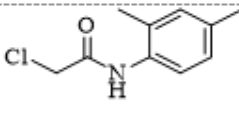
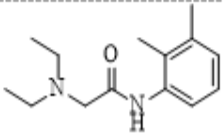
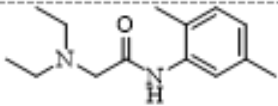
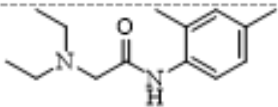
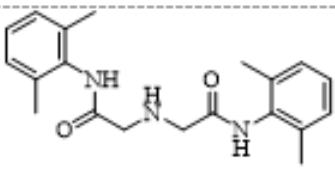
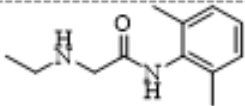
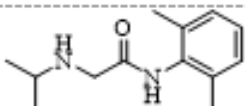
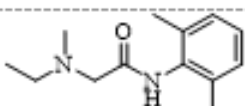
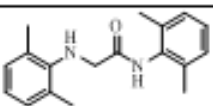
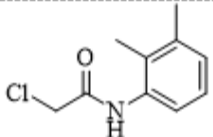
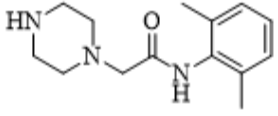


Figure 4.39: Mass Report (11)

Table 4.3: Maximum yield of lidocaine impurities

S. No.	Name of Impurities	Structure	Yield (%)
1.	2-chloro- <i>N</i> -(2,6-dimethylphenyl)acetamide		92%
2.	2-chloro- <i>N</i> -(2,5-dimethylphenyl)acetamide		94%
3.	2-chloro- <i>N</i> -(2,4-dimethylphenyl)acetamide		91%
4.	2-(diethylamino)- <i>N</i> -(2,3-dimethylphenyl)acetamide		80%

5.	2-(diethylamino)- <i>N</i> -(2,5-dimethyl phenyl)acetamide		82.5%
6.	2-(diethylamino)- <i>N</i> -(2,4-dimethyl phenyl)acetamide		85.9%
7.	2,2'-(benzyl azanediyl) bis (<i>N</i> -(2,6-dimethyl phenyl) acetamide)		90.5%
8.	<i>N</i> -(2,6-dimethylphenyl)-2-(ethyl amino)acetamide		95%
9.	<i>N</i> -(2,6-dimethylphenyl)-2-(isopropyl amino)acetamide		92%
10.	<i>N</i> -(2,6-dimethylphenyl)-2-(ethyl (methyl)amino)acetamide		90.4%
11.	<i>N</i> -(2,6-dimethylphenyl)-2-((2,6-dimethylphenyl)amino)acetamide		94.4%

12.	<i>N</i> -(2,3-dimethylphenyl)propionamide		91%
13.	<i>N</i> -(2,6-dimethylphenyl)-2-(piperazine-1-yl)acetamide		95%

CONCLUSION

The synthesis of pharmaceuticals and associated compounds is essential in the fields of chemistry and drug discovery. One example is the synthesis of rufinamide, an AED, and its impurities using a 1,3-dipolar cycloaddition approach. Rufinamide is an established antiepileptic drug that effectively treats different seizure disorders. This synthetic route utilizes benzyl bromide derivatives as starting materials and has been proven to be both convenient and productive in experimental settings. However, the isolation of certain impurities during the synthesis of rufinamide has presented challenges. As a result, researchers have explored a retrosynthetic route to access these impurities, which hold academic and industrial significance across various disciplines. While its synthesis has been previously described, isolating contaminants from the mother liquor has been problematic. A systematic approach for separately synthesizing these impurities based on retrosynthetic analysis has been developed to address this issue. This approach serves as the standard method for evaluating the purity of pharmaceutical products. By isolating and characterizing these impurities, researchers can better understand potential byproducts that may occur during the synthesis of rufinamide. This contributes to enhancing the clarity and flow of the overall reaction mechanism while also aiding in optimizing the synthesis process. The impurities produced during the synthesis while synthesizing groups and multipleazole derivatives have value beyond their role as contaminants. These compounds have applications in various scientific disciplines.

Azole derivatives with tri- and tetra-moieties have attracted attention in organic synthesis due to their unique structural features, making them valuable building blocks for complex molecular structures. These structures have shown promise in drug discovery efforts across different therapeutic areas, including antibacterial, anticancer, antiviral, and antiretroviral agents. Theazole motifs in these compounds provide biological activity, facilitating the development of novel pharmaceuticals. The significance of these impurities extends beyond their presence in pharmaceuticals, as they have implications for polymer chemistry, chemical biology, and materials science. Incorporatingazole-containing structures into

polymers allows the creation of materials with specific properties, like electrical conductivity, improved mechanical strength, and thermal stability. These compounds also have versatile applications in chemical biology, serving as probes for studying biomolecular interactions and cellular processes. Additionally, their fluorescent properties make them suitable for bioimaging and bioconjugation. Some impurities containing azole derivatives have potential uses in explosive and propellant applications. Heterocyclic compounds with fluoro-derivatives and tetra-azole moieties exhibit energetic properties, making them viable candidates for explosives and rocket propellants. This dual application showcases these compounds' versatility and multifaceted nature, demonstrating how a single synthetic pathway can yield materials with different functionalities.

Developing an efficient synthetic protocol for rufinamide and its impurities through a 1,3-dipolar cycloaddition approach exemplifies the intricate relationship between chemical synthesis, pharmaceuticals, and diverse scientific domains. Though isolating these impurities presents challenges, the resulting compounds have proven invaluable in academia and industries. Their roles span from foundational organic synthesis and drug discovery to polymer chemistry, chemical biology, materials science, and even explosive applications. This underscores the interconnectedness of chemical research and its far-reaching impact on various aspects of our technological and scientific landscape.

The second is developing an efficient and cost-effective protocol for synthesizing lidocaine impurities, a significant milestone in the pharmaceutical industry. Lidocaine is a local anesthetic with the amide group with broad applications, and the synthetic approach paves the way for innovation and drug discovery. By adopting a retro-synthesis route as the standard for determining purity levels, pharmaceutical manufacturing emphasizes its commitment to quality and safety. This approach ensures that lidocaine impurities produced using this method meet rigorous standards, guaranteeing their efficacy and reliability in medical applications. The discovery of lidocaine impurities containing chloro, amino, and piperazine derivatives has excellent potential for addressing medical conditions. Chloro derivatives can enhance the analgesic properties of these drugs, making

them valuable for pain management and anesthesia. Amino derivatives offer opportunities for tailoring the pharmacological profiles of these compounds, potentially leading to more targeted treatments. Piperazine derivatives provide a platform for developing drugs that target neurological and psychiatric disorders. The synthesis protocol for these impurities is cost-effective, benefiting both the pharmaceutical industry and patients. Lower production costs can make medications more affordable, increasing access to essential treatments worldwide. This affordability also drives further research into lidocaine impurities, enabling the development of even more effective and accessible pharmaceuticals. The successful development of a robust synthesis protocol for lidocaine impurities represents a leap forward in drug discovery and production. The applications of these impurities in the pharmaceutical industry are vast, promising improved medical treatments and enhancing patients' overall well-being. As research advances, we can anticipate the emergence of novel lidocaine impurities that will revolutionize how we address medical conditions, ultimately improving healthcare quality globally. API impurities are crucial in forensic investigations involving pharmaceutical products. They can provide valuable information about the product's source, manufacturer, and specific batches or production runs. This information is essential for determining whether a product has been illegally diverted, counterfeited, or tampered with. Additionally, identifying and analyzing impurities can provide crucial insights into the nature and extent of the criminal activity involved. Therefore, thoroughly characterizing and monitoring API impurities is essential to ensuring pharmaceutical products' safety, effectiveness, and integrity in forensic contexts.

REFERENCES

1. Kumar, V., Bansal, V., Madhavan, A., Kumar, M., Sindhu, R., Awasthi, M. K., ... & Saran, S. (2022). Active pharmaceutical ingredient (API) chemicals: a critical review of current biotechnological approaches. *Bioengineered*, 13(2), 4309-4327.
2. Bharate, S. S., Bharate, S. B., & Bajaj, A. N. (2016). Interactions and incompatibilities of pharmaceutical excipients with active pharmaceutical ingredients: a comprehensive review. *Journal of Excipients and Food Chemicals*, 1(3).
3. Dey, A. (2023). Handbook on Active Pharmaceutical Ingredients (API), Drugs & Pharmaceutical Products. Handbook on Active Pharmaceutical Ingredients (API), Drugs & Pharmaceutical Products.
4. Am Ende, M. T. (Ed.). (2019). Chemical engineering in the pharmaceutical industry: Active pharmaceutical ingredients. John Wiley & Sons.
5. Burke, A. J., Marques, C. S., Turner, N. J., & Hermann, G. J. (2018). Active pharmaceutical ingredients in synthesis: catalytic processes in research and development. John Wiley & Sons.
6. Darji, M. A., Lalge, R. M., Marathe, S. P., Mulay, T. D., Fatima, T., Alshammari, A., ... & Narasimha Murthy, S. (2018). Excipient stability in oral solid dosage forms: a review. *Aaps Pharmscitech*, 19, 12-26.
7. Chaudhari, S. P., & Patil, P. S. (2012). Pharmaceutical excipients: a review. *Int J Adv Pharm Biol Chem*, 1(1), 21-34.
8. Elder, D. P., Kuentz, M., & Holm, R. (2016). Pharmaceutical excipients—quality, regulatory, and biopharmaceutical considerations. *European journal of pharmaceutical sciences*, 87, 88-99.
9. Shah, H., Jain, A., Laghate, G., & Prabhudesai, D. (2021). Pharmaceutical excipients. In Remington (pp. 633-643). Academic Press.
10. Koo, O. M. (Ed.). (2016). Pharmaceutical excipients: properties, functionality, and applications in research and industry. John Wiley & Sons.

11. Nema, S., & Brendel, R. J. (2011). Excipients and their role in approved injectable products: current usage and future directions. *PDA Journal of Pharmaceutical Science and Technology*, 65(3), 287-332.
12. Narang, A. S., & Boddu, S. H. (2015). Excipient applications in formulation design and drug delivery (pp. 1-10). Springer International Publishing.
13. Gadamasetti, K. (Ed.). (1999). *Process Chemistry in the Pharmaceutical Industry* (1st ed.). CRC Press. <https://doi.org/10.1201/9781482276091>
14. P. Ramiya; (2019) in *Peptide Therapeutics: Strategy and Tactics for Chemistry, Manufacturing and Controls*, ed. V. Srivastava, The Royal Society of Chemistry, ch. 4, pp. 97-110.
15. Taylor, K. M., & Aulton, M. E. (Eds.). (2021). *Aulton's pharmaceuticals E-Book: The design and manufacture of medicines*. Elsevier Health Sciences.
16. <https://cdn.technologynetworks.com/ep/pdfs/active-pharmaceutical-ingredient-analysis.pdf>
17. Silverstein, I. (2019). 16 Pharmaceutical Excipient Good Manufacturing Practices. *Good manufacturing practices for pharmaceuticals*, 227.
18. World Health Organization. (2016). *WHO expert committee on specifications for pharmaceutical preparations: fiftieth report (Vol. 996)*. World Health Organization.
19. Tiwari, P., & Chowdhury, S. R. (2014). Sustainable Production of Highly Active Pharmaceutical Ingredients (HAPIs). *International Journal of Scientific and Research Publications*, 4(3), 1-5.
20. Dunny, E., O'Connor, I., & Bones, J. (2017). Containment challenges in HPAPI manufacture for ADC generation. *Drug Discovery Today*, 22(6), 947-951.
21. Faber, M. J., Galati, G. I. U. S. E. P. P. E., & Dinyer, J. S. (2014). Handling of Highly Potent Pharmaceutical Compounds. *Chimica Oggi—Chemistry Today*, 32(3), 34-38.
22. Chi, Y. T., Chu, P. C., Chao, H. Y., Shieh, W. C., & Chen, C. C. (2014). Design of CGMP production of 18 F-and 68 Ga-radiopharmaceuticals. *BioMed Research International*, 2014.

23. Kleynhans, J., Grobler, A. F., Ebenhan, T., Sathekge, M. M., & Zeevaart, J. R. (2018). Radiopharmaceutical enhancement by drug delivery systems: A review. *Journal of Controlled Release*, 287, 177-193.
24. Hickey, A. J., & Ganderton, D. (Eds.). (2016). *Pharmaceutical process engineering*. CRC Press.
25. Jagschies, G., Lindskog, E., Lacki, K., & Galliher, P. M. (Eds.). (2018). *Biopharmaceutical processing: development, design, and implementation of manufacturing processes*. Elsevier.
26. Chadha, R., & Bhandari, S. (2014). Drug–excipient compatibility screening—role of thermoanalytical and spectroscopic techniques. *Journal of pharmaceutical and biomedical analysis*, 87, 82-97.
27. Buddhadev, S. S., & Garala, K. C. (2021). Pharmaceutical cocrystals—a review. *Multidisciplinary Digital Publishing Institute Proceedings*, 62(1), 14.
28. Nazir, A., Masih, M., & Iqbal, M. (2021). Formulation, optimization, qualitative and quantitative analysis of new dosage form of corticosteroid. *Future Journal of Pharmaceutical Sciences*, 7, 1-11.
29. Nusim, S. (Ed.). (2016). *Active pharmaceutical ingredients: development, manufacturing, and regulation*. CRC Press. Arnold, C. (2013). The new danger of synthetic drugs. *The Lancet*, 382(9886), 15-16.
30. Laird, T. (2012). Innovation in generic API synthesis and manufacture. *Organic Process Research & Development*, 16(3), 365-365.
31. Lugovoi, I., Andritsos, D. A., & Senot, C. (2022). Manufacturing process innovation in the pharmaceutical industry. *Manufacturing & Service Operations Management*, 24(3), 1760-1778.
32. Lugovoi, I., Andritsos, D., & Senot, C. (2018). Process innovation in the pharmaceutical industry. HEC Paris Research Paper No. MOSI-2018-1314.
33. Chatterjee, P., & Alvi, M. M. (2014). Excipients and active pharmaceutical ingredients. In *Pediatric Formulations: A Roadmap* (pp. 347-361). New York, NY: Springer, New York.

34. Mullin, R. (2014). Tufts study finds big rise in cost of drug development. *Chem. Eng. News*, 92(47), 6.
35. Görög, S. (2008). Drug safety, drug quality, drug analysis. *Journal of pharmaceutical and biomedical analysis*, 48(2), 247-253.
36. Hepler, C. D. (2004). Clinical pharmacy, pharmaceutical care, and the quality of drug therapy. *Pharmacotherapy: The Journal of Human Pharmacology and Drug Therapy*, 24(11), 1491-1498.
37. Ahuja, S. S. (2007). Assuring quality of drugs by monitoring impurities. *Advanced drug delivery reviews*, 59(1), 3-11.
38. Nagpal, S., Upadhyay, A., R Bhardwaj, T., & Thakkar, A. (2011). A review on need and importance of impurity profiling. *Current Pharmaceutical Analysis*, 7(1), 62-70.
39. Venkatesan, P., & Valliappan, K. (2014). Impurity profiling: theory and practice. *Journal of pharmaceutical sciences and research*, 6(7), 254.
40. Bhagwat Ashlesha, B., & Khedkar, K. M. (2022). Impurity Profiling: A Review. *Asian J. Pharm. Res. Develop*, 10, 135-143.
41. Guideline, I. H. T. (2006). Impurities in new drug products. Q3B (R2), current step, 4, 1-5.
42. Guideline, I. H. T. (2006, October). Impurities in new drug substances Q3A (R2). In *Proceedings of the International Conference on Harmonization of Technical Requirements for Registration of Pharmaceuticals for Human Use, Geneva, Switzerland (Vol. 25)*.
43. Berridge, J. C. (1995). Impurities in drug substances and drug products: new approaches to quantification and qualification. *Journal of pharmaceutical and biomedical analysis*, 14(1-2), 7-12.
44. Rao, N. R., Kiran, S. S., & Prasanthi, N. L. (2010). Pharmaceutical impurities: an overview. *indian journal of pharmaceutical education and research*, 44(3), 301-310.
45. Singh, A., Afreen, S., Singh, D. P., & Kumar, R. (2017). A review on pharmaceutical impurities and their importance. *World J Pharm Pharmaceut Sci*, 6(10), 1337-1354.

46. Parajulim, R. R., Pokharel, P., & Shrestha, M. B. D. B. (2018). Impurity profiling: An emerging approach for pharmaceuticals. *World journal of pharmacy and pharmaceutical sciences*, 7(4).
47. Solanki, R. (2012). Impurity profiling of active pharmaceutical ingredients and finished drug products. *International Journal of Research and Technology*, 2(3), 231-238.
48. Venkatesan, P., & Valliappan, K. (2014). Impurity profiling: theory and practice. *Journal of pharmaceutical sciences and research*, 6(7), 254.
49. Federal Register, International Conferences on Harmonization. Impurities in New Drug Substances U.S. Department of Health and Human Services Food and Drug Administration Centre for Drug Evaluation and Research (CDER) Centre for Biologics Evaluation and Research (CBER), Q3A, 2008:1-14
50. Jadhav, G. P., Kasture, V. S., Pawar, S. S., Vadgaonkar, A. R., Lodha, A. P., Tuse, S. K., ... & Borbane, S. A. (2014). Drug impurity profiling: A scientific approach. *Journal of Pharmacy Research*, 8(6), 696-706.
51. Patel, S., & Apte, M. (2016). A Review on Significances of Impurity Profiling. *Research Journal of Pharmaceutical Dosage Forms and Technology*, 8(1), 31-36.
52. Misra, B., Thakur, A., & Mahata, P. P. (2015). Pharmaceutical impurities: a review. *International Journal of Pharmaceutical Chemistry*, 5(7), 232-239.
53. Saibaba, S. V., Kumar, M. S., & Ramu, B. (2016). Pharmaceutical impurities and their characterization: A review. *European Journal of Pharmaceutical and Medical Research*, 3(5), 190-196.
54. Liu, K. T., & Chen, C. H. (2019). Determination of impurities in pharmaceuticals: why and how?. In *Quality management and quality control-new trends and developments* (pp. 1-17). London, UK: IntechOpen.
55. Pilaniya, K., Chandrawanshi, H. K., Pilaniya, U., Manchandani, P., Jain, P., & Singh, N. (2010). Recent trends in the impurity profile of pharmaceuticals. *Journal of Advanced Pharmaceutical Technology & Research*, 1(3), 302-310.
56. Goel, N. (2008). Impurities in pharmaceutical substances.

57. Patel, A. B., Bundheliya, A. R., Vyas, A. J., Patel, N. K., Patel, A. I., & Lumbhani, A. N. (2021). A Review on Metal Impurities in Pharmaceuticals. *Asian Journal of Pharmaceutical Analysis*, 11(3), 212-222.
58. Wadekar, K. R., Bhalme, M., Rao, S. S., Reddy, K. V., Kumar, L. S., & Balasubrahmanyam, E. (2012). Evaluating impurities in drugs (Part I of III). *Pharmaceutical Technology*, 36(2), 46-51.
59. Cok, I., & Emerce, E. (2012). Overview of impurities in pharmaceuticals: Toxicological aspects. *Asian Chemistry Letters*, 16(1), 87-97.
60. Alothman, Z. A., Rahman, N., & Siddiqui, M. R. (2013). Review on pharmaceutical impurities, stability studies and degradation products: an analytical approach. *Reviews in Advanced Sciences and Engineering*, 2(2), 155-166.
61. Lee, H. (Ed.). (2014). *Pharmaceutical industry practices on genotoxic impurities*. CRC Press.
62. Szekely, G., Amores de Sousa, M. C., Gil, M., Castelo Ferreira, F., & Heggie, W. (2015). Genotoxic impurities in pharmaceutical manufacturing: sources, regulations, and mitigation. *Chemical reviews*, 115(16), 8182-8229.
63. Madhuresh, K. S., Rusha, G., Rohit, S., Sanjay, M., Purbita, C., & Anil, T. (2016). Genotoxic impurities evaluation in active pharmaceutical ingredients (API)/drug substance. *Pharm Lett*, 8(12), 234-243.
64. Reddy, A. V. B., Jaafar, J., Umar, K., Majid, Z. A., Aris, A. B., Talib, J., & Madhavi, G. (2015). Identification, control strategies, and analytical approaches for the determination of potential genotoxic impurities in pharmaceuticals: A comprehensive review. *Journal of Separation Science*, 38(5), 764-779.
65. Regulska, K., Michalak, M., Murias, M., & Stanisz, B. (2021). Genotoxic impurities in pharmaceutical products—regulatory, toxicological and pharmaceutical considerations. *Journal of Medical Science*, 90(1), e502-e502.
66. EFSA Scientific Committee, More, S., Bampidis, V., Benford, D., Boesten, J., Bragard, C., ... & Schlatter, J. (2019). Genotoxicity assessment of chemical mixtures. *Efsa Journal*, 17(1), e05519.

67. Swartz, M. E., & Krull, I. S. (Eds.). (2018). Analytical method development and validation. CRC press.
68. Ravisankar, P., Gowthami, S., & Rao, G. D. (2014). A review on analytical method development. *Indian journal of research in pharmacy and biotechnology*, 2(3), 1183.
69. Breaux, J., Jones, K., & Boulas, P. (2003). Analytical methods development and validation. *Pharm. Technol*, 1, 6-13.
70. Snodin, D. J., & McCrossen, S. D. (2012). Guidelines and pharmacopoeial standards for pharmaceutical impurities: overview and critical assessment. *Regulatory Toxicology and Pharmacology*, 63(2), 298-312.
71. Bliesner, D. M. (2006). *Validating chromatographic methods: a practical guide*. John Wiley & Sons.
72. Peris-Vicente, J., Esteve-Romero, J., & Carda-Broch, S. (2015). Validation of analytical methods based on chromatographic techniques: An overview. *Analytical separation science*, 1757-1808.
73. Sharma, S., Singh, N., Ankalgi, A. D., Rana, A., & Ashawat, M. S. (2021). Modern trends in analytical techniques for method development and validation of pharmaceuticals: A review. *Journal of Drug Delivery and Therapeutics*, 11(1-s), 121-130.
74. Sanap, G. S., Zarekar, N. S., & Pawar, S. S. (2017). Review on method development and validation. *International journal of pharmaceutics and drug analysis*, 177-184.
75. Kamboj, S., Kamboj, N., K Rawal, R., Thakkar, A., & R Bhardwaj, T. (2014). A compendium of techniques for the analysis of pharmaceutical impurities. *Current Pharmaceutical Analysis*, 10(2), 145-160.
76. ALSaeedy, M., Al-Adhrai, A., Öncü-Kaya, E. M., & Şener, E. (2023). An overview of advances in the chromatography of drugs impurity profiling. *Critical Reviews in Analytical Chemistry*, 53(7), 1455-1471.
77. Ayre, A., Varpe, D., Nayak, R., & Vasa, N. (2011). Impurity profiling of pharmaceuticals. *Adv Res Pharm Biol*, 1(2), 76-90.

78. D Tzanavaras, P. (2010). Recent advances in analysing organic impurities of active pharmaceutical ingredients and formulations: a review. *Current Organic Chemistry*, 14(19), 2348-2364.
79. Shah, S. R., Patel, M. A., Naik, M. V., Pradhan, P. K., & Upadhyay, U. M. (2012). RECENT APPROCHES OF" IMPURITY PROFILING" IN PHARMACEUTICAL ANALYSIS: A REVIEW. *International Journal of pharmaceutical sciences and research*, 3(10), 3603.
80. Wells, M., & Zibas, S. (2019). Validation of chromatographic methods. In *Ewing's Analytical Instrumentation Handbook, Fourth Edition* (pp. 943-962). CRC Press.
81. Ahuja, S., & Alsante, K. M. (Eds.). (2003). *Handbook of isolation and characterization of impurities in pharmaceuticals* (Vol. 5). Academic Press.
82. Liu, G., Luan, B., Liang, G., Xing, L., Huang, L., Wang, C., & Xu, Y. (2018). Isolation and identification of four major impurities in capreomycin sulfate. *Journal of Chromatography A*, 1571, 155-164.
83. Zhao, L., Wang, Q., Bie, Y., & Lu, X. (2017). Isolation, identification and characterization of potential impurities of anidulafungin. *Journal of Pharmaceutical and Biomedical Analysis*, 141, 192-199.
84. Alsante, K. M., Hatajik, T. D., Lohr, L. L., & Sharp, T. R. (2001). Isolation and identification of process-related impurities and degradation products from pharmaceutical drug candidates, Part I. *American Pharmaceutical Review*, 4, 70-78.
85. Kumar, N., Devineni, S. R., Gajjala, P. R., Dubey, S. K., & Kumar, P. (2017). Synthesis, isolation, identification and characterization of new process-related impurity in isoproterenol hydrochloride by HPLC, LC/ESI-MS and NMR. *Journal of pharmaceutical analysis*, 7(6), 394-400.
86. Terfloth, G. (2007). Preparative isolation of impurities. *Analysis of Drug Impurities*, 215-234.
87. Chen, H., Wang, Y. F., Yang, Z. D., & Li, Y. C. (2006). Isolation and identification of novel impurities in spironolactone. *Journal of pharmaceutical and biomedical analysis*, 40(5), 1263-1267.

88. Holm, R., & Elder, D. P. (2016). Analytical advances in pharmaceutical impurity profiling. *European Journal of Pharmaceutical Sciences*, 87, 118-135.
89. Pilaniya, K., Chandrawanshi, H. K., Pilaniya, U., Manchandani, P., Jain, P., & Singh, N. (2010). Recent trends in the impurity profile of pharmaceuticals. *Journal of Advanced Pharmaceutical Technology & Research*, 1(3), 302-310.
90. Qiu, F., & Norwood, D. L. (2007). Identification of pharmaceutical impurities. *Journal of liquid chromatography & related technologies*, 30(5-7), 877-935.
91. Chandrul Kaushal, K., & Srivastava, B. (2010). A process of method development: A chromatographic approach. *J. Chem. Pharm. Res*, 2(2), 519-545.
92. Ramachandra, B. (2017). Development of impurity profiling methods using modern analytical techniques. *Critical reviews in analytical chemistry*, 47(1), 24-36.
93. Maggio, R. M., Calvo, N. L., Vignaduzzo, S. E., & Kaufman, T. S. (2014). Pharmaceutical impurities and degradation products: Uses and applications of NMR techniques. *Journal of pharmaceutical and biomedical analysis*, 101, 102-122.
94. Baghel, U. S., Singh, A., Singh, D., & Sinha, M. (2017). Application of mass spectroscopy in pharmaceutical and biomedical analysis. *Spectroscopic Analyses- Developments and Applications*, 105-121.
95. Gillespie, T. A., & Winger, B. E. (2011). Mass spectrometry for small molecule pharmaceutical product development: a review. *Mass spectrometry reviews*, 30(3), 479-490.
96. Parasuraman, S., Anish, R., Balamurugan, S., Muralidharan, S., Kumar, K. J., & Vijayan, V. (2014). An overview of liquid chromatography-mass spectroscopy instrumentation. *Pharmaceutical methods*, 5(2), 47-55.
97. Orr, J. D., Krull, I. S., & Swartz, M. E. (2003). Validation of impurity methods, Part II. *LC GC NORTH AMERICA*, 21(12), 1146-1181.
98. Yamamoto, E., Nijjima, J., & Asakawa, N. (2013). Selective determination of potential impurities in an active pharmaceutical ingredient using HPLC-SPE-HPLC. *Journal of pharmaceutical and biomedical analysis*, 84, 41-47.

99. Lee, H., Shen, S., & Grinberg, N. (2008). Identification and control of impurities for drug substance development using LC/MS and GC/MS. *Journal of Liquid Chromatography & Related Technologies®*, 31(15), 2235-2252.
100. Hommerson, P., Khan, A. M., Bristow, T., Harrison, M. W., de Jong, G. J., & Somsen, G. W. (2009). Drug impurity profiling by capillary electrophoresis/mass spectrometry using various ionization techniques. *Rapid Communications in Mass Spectrometry: An International Journal Devoted to the Rapid Dissemination of Up-to-the-Minute Research in Mass Spectrometry*, 23(18), 2878-2884.
101. Phadke, R., Mali, R., Mundhe, A., & Gosar, A. (2019). Drug impurity profiling an emerging task to pharmaceutical industries now days-a review. *Am J Pharm Tech Res*, 9(2), 94-111.
102. Sherikar, O. D., Mehta, P. J., & Khatri, D. M. (2011). Various approaches for impurity profiling of pharmaceuticals-An overview. *J. Pharm. Res*, 4(6), 1937-42.
103. Friscia, O., Pulci, R., Fassio, F., & Comelli, R. (1994). Chemical reagents as potential impurities of pharmaceutical products: investigations on their genotoxic activity. *Journal of Environmental Pathology, Toxicology and Oncology: Official Organ of the International Society for Environmental Toxicology and Cancer*, 13(2), 89-110.
104. Sahasrabuddhey, B., Nautiyal, R., Acharya, H., Khyade, S., Luthra, P. K., & Deshpande, P. B. (2007). Isolation and characterization of some potential impurities in ropinirole hydrochloride. *Journal of pharmaceutical and biomedical analysis*, 43(4), 1587-1593.
105. Thatipalli, P., Kumar, R., Bulusu, C., Chakka, R., Padi, P. R., Yerra, A., & Bollikonda, S. (2008). Synthesis and characterization of impurities of an anti-psychotic drug substance, Olanzapine. *Arkivoc*, 11, 195-201.
106. BUCHI REDDY, R., VENKATESHWAR GOUD, T., Nagamani, N., PAVAN KUMAR, N., Alagudurai, A., Murugan, R., ... & Balaji, P. (2012). Identification and characterization of potential impurities in raloxifene hydrochloride. *Scientia Pharmaceutica*, 80(3), 605-618.

107. Wang, X., Zhou, H., Zheng, J., Huang, C., Liu, W., Yu, L., & Zeng, S. (2012). Identification and characterization of four process-related impurities in retigabine. *Journal of pharmaceutical and biomedical analysis*, *71*, 148-151.
108. Schulz, K., Oberdieck, U., & Weitschies, W. (2013). Degradation products of proguanil—4-chloroaniline and related components with regard to genotoxicity. *Chemical Papers*, *67*, 657-666.
109. Zhang, D., Song, X., & Su, J. (2014). Isolation, identification and characterization of novel process-related impurities in flupirtine maleate. *Journal of Pharmaceutical and Biomedical Analysis*, *90*, 27-34.
110. Turhan, K., Ozturkcan, S. A., Turgut, Z., Karadayi, M., Aslan, A., & Gulluce, M. (2014). Genotoxic and antigenotoxic assessment of four newly synthesized dihydropyridine derivatives. *Toxicology and Industrial Health*, *30*(3), 275-283.
111. Vadgaonkar, A. R., Kasture, V. S., Gosavi, S. A., Pawar, S. S., & Jadhav, G. P. (2014). Synthesis, isolation, characterisation, and quantification of process related impurity of zidovudine. *Rasayan Journal Chemistry*, *7*(2), 181-189.
112. Rudovica, V., Viksna, A., & Actins, A. (2014). Application of LA-ICP-MS as a rapid tool for analysis of elemental impurities in active pharmaceutical ingredients. *Journal of pharmaceutical and biomedical analysis*, *91*, 119-122.
113. Mahender, M., Saravanan, M., Sridhar, C., Chandrashekar, E. R. R., Kumar, L. J., Jayashree, A., & Bandichhor, R. (2014). Identification and characterization of potential impurities of dronedarone hydrochloride. *Organic Process Research & Development*, *18*(1), 157-162.
114. Harigaya, K., Yamada, H., Yaku, K., Nishi, H., & Haginaka, J. (2014). Novel sensitive determination method for a genotoxic alkylating agent, 4-chloro-1-butanol, in active pharmaceutical ingredients by LC-ICP-MS employing iodo derivatisation. *Analytical Sciences*, *30*(3), 377-382.
115. Halim, Nadiah and Nadzri, Noor Izzati and Sanghiran Lee, Vannajan, (2014). Active Pharmaceutical Ingredients co-crystals via solvent-free reactions. *Acta Crystallographica Section A* (C1786).

116. Evrykleia G. Karagiannidou, E. Panagiotidis, Theodoros Tsatsas, Efstratios, Neokosmidis, Pharmathen (2014) CHARACTERIZATION OF DULOXETINE HCL API AND ITS PROCESS RELATED IMPURITIES
117. Gowdhami, T., Rajalakshmi, A. K., & Sugumar, N. (2015). Phytochemical characterisation using various solvent extracts and GC analysis of ethanolic extract of *Jasminum sambac* Linn. *International Journal of Current Research*, 7(9), 19950-19955.
118. Doughty, D., Painter, B., Pigou, P. E., & Johnston, M. R. (2016). The synthesis and investigation of impurities found in Clandestine Laboratories: Baeyer–Villiger Route Part I; Synthesis of P2P from benzaldehyde and methyl ethyl ketone. *Forensic science international*, 263, 55-66.
119. Douša, M., Doubský, J., & Srbek, J. (2016). Using photochemically induced fluorescence detection for HPLC determination of genotoxic impurities in the vortioxetine manufacturing process. *Journal of chromatographic science*, 54(9), 1625-1630.
120. Wang, J., Yang, S., & Zhang, K. (2016). A simple and sensitive method to analyse genotoxic impurity hydrazine in pharmaceutical materials. *Journal of pharmaceutical and biomedical analysis*, 126, 141-147.
121. Plummer, C. M., Breadon, T. W., Pearson, J. R., & Jones, O. A. (2016). The synthesis and characterisation of MDMA derived from a catalytic oxidation of material isolated from black pepper reveals potential route specific impurities. *Science & Justice*, 56(3), 223-230.
122. Panmanad, D. E. E. P. A. K., Joshi, M. A. N. D. A. R., Patil, R. A. H. U. L., Joshi, P. R. I. Y. A. N. K. A., & Jadhav, V. I. D. Y. A. D. H. A. R. (2016). Synthesis and Characterization of Potential Impurities in Levothyroxine. *Chemical Science*, 5(4), 1082-1089.
123. Nema, M., Gawali, A., Wagh, S. B., & Sharma, H. K. (2016). Synthesis and Characterization of Impurities of Eletriptan and its HPLC Method Development and Validation. *Current Research in Pharmaceutical Sciences*, 74-81.

124. Kumar, N., Devineni, S. R., Gajjala, P. R., Gupta, D. K., Bhat, S., Kumar, R., ... & Kumar, P. (2016). Four process-related potential new impurities in ticagrelor: Identification, isolation, characterization using HPLC, LC/ESI-MSn, NMR and their synthesis. *Journal of pharmaceutical and biomedical analysis*, 120, 248-260.
125. Kumar, N., Devineni, S. R., Singh, G., Kadirappa, A., Dubey, S. K., & Kumar, P. (2016). Identification, isolation and characterization of potential process-related impurity and its degradation product in vildagliptin. *Journal of pharmaceutical and biomedical analysis*, 119, 114-121.
126. Ruggenthaler, M., Grass, J., Schuh, W., Huber, C. G., & Reischl, R. J. (2017). Levothyroxine sodium revisited: A wholistic structural elucidation approach of new impurities via HPLC-HRMS/MS, on-line H/D exchange, NMR spectroscopy and chemical synthesis. *Journal of pharmaceutical and biomedical analysis*, 135, 140-152.
127. Zhao, L., Wang, Q., Bie, Y., & Lu, X. (2017). Isolation, identification and characterization of potential impurities of anidulafungin. *Journal of Pharmaceutical and Biomedical Analysis*, 141, 192-199.
128. Kumar, N., Devineni, S. R., Gajjala, P. R., Dubey, S. K., & Kumar, P. (2017). Synthesis, isolation, identification and characterization of new process-related impurity in isoproterenol hydrochloride by HPLC, LC/ESI-MS and NMR. *Journal of pharmaceutical analysis*, 7(6), 394-400.
129. Kumar, N., Devineni, S. R., Dubey, S. K., & Kumar, P. (2017). Potential impurities of anxiolytic drug, clobazam: Identification, synthesis and characterization using HPLC, LC-ESI/MSn and NMR. *Journal of Pharmaceutical and Biomedical Analysis*, 137, 268-278.
130. Bondre, N., Pradhan, N., Telange, V., Dashpute, V., Pol, S., & Aher, S. (2017). Synthesis, characterization and identification of sertraline hydrochloride related impurities. *World Journal of Pharmaceutical Sciences*, 54-57.
131. Rahman, M. H. A., Gullick, D. R., Hoerner, J., & Bartlett, M. G. (2017). Determination of genotoxic impurities monomethyl sulfate and dimethyl sulfate in active pharmaceutical ingredients. *Analytical Methods*, 9(7), 1112-1118.

132. Kumar, K. A., Lakshmipathi, V. S., Meenakshi, S., & Balakrishnan, M. H. (2017). Synthesis and characterization of potential impurity of muscle relaxant drug carisoprodol. *J. Chem. Sci*, 7(4), 352-360.
133. Zhuang, T., Zhang, W., Cao, L., He, K., Wang, Y., Li, J., ... & Zhang, G. (2018). Isolation, identification and characterization of two novel process-related impurities in olanzapine. *Journal of pharmaceutical and biomedical analysis*, 152, 188-196.
134. Leontiev, D., Bevz, O., Volovyk, N., Gella, I., & Georgiyants, V. (2018). The synthesis and study of profiles of the ornidazole impurities. *ScienceRise: Pharmaceutical Science*, (1 (11)), 4-11.
135. Filip, K., Łaszcz, M., Leś, A., & Chmiel, J. (2018). Process-related impurities of eplerenone: determination and characterisation by HPLC methods and Raman spectroscopy. *Journal of Pharmaceutical and Biomedical Analysis*, 159, 466-476.
136. Mythili, A. (2018). Synthesis, Characterisation and Biological Evaluation of Dalfampridine Genotoxic Impurities (Doctoral dissertation, JKK Nattraja College of Pharmacy, Komarapalayam).
137. Wagh, V. H., Singh, S., Buchade, R. S., Shariff, A., Tandale, S. D., & Chaure, P. P. (2019). Synthesis, Characterization and Development of Validated Analytical Methods for Process Related Impurity in Ritonavir Hydrochloride Bulk and Formulation. *Journal of Pharmaceutical Sciences and Research*, 11(8), 2878-2885.
138. Yadav, C. H., & Medarametla, V. Synthesis of degradants and impurities of rabeprazole.
139. Scherf-Clavel, O., Kinzig, M., Besa, A., Schreiber, A., Bidmon, C., Abdel-Tawab, M., ... & Holzgrabe, U. (2019). The contamination of valsartan and other sartans, Part 2: Untargeted screening reveals contamination with amides additionally to known nitrosamine impurities. *Journal of Pharmaceutical and Biomedical Analysis*, 172, 278-284.
140. Zhang, Q., Cheng, Y., Yang, J., Zheng, C., & Lu, X. (2020). Isolation, identification, and characterization of potential impurities of doramectin and evaluation of their insecticidal activity. *Journal of Pharmaceutical and Biomedical Analysis*, 191, 113600.

141. Rajesh Reddy, P., Musunuri, S., Rama Sekhara Reddy, D., Chittala, V. S., Murthy P, V. N. S., & Krishnamohan, K. (2020). Identification, synthesis, and characterisation of potential genotoxic impurities of sildenafil citrate drug substance. *Future Journal of Pharmaceutical Sciences*, 6, 1-10.
142. Crawford, D. E., Porcheddu, A., McCalmont, A. S., Delogu, F., James, S. L., & Colacino, E. (2020). Solvent-free, continuous synthesis of hydrazone-based active pharmaceutical ingredients by twin-screw extrusion. *ACS Sustainable Chemistry & Engineering*, 8(32), 12230-12238.
143. Prashant B. Zate, S. K. (2021). DETERMINATION OF PROCESS RELATED GENOTOXIC IMPURITIES OF SALBUTAMOL SULPHATE BY LC METHOD. *INDIAN JOURNAL F RESEARCH*.
144. Soyseven, M., Keçili, R., Aboul-Enein, H. Y., & Arli, G. (2021). Determination of Potential Genotoxic Impurity, 5-Amino-2-Chloropyridine, in Active Pharmaceutical Ingredient Using the HPLC-UV System. *Journal of Chromatographic Science*, 59(3), 241-245.
145. Jireš, J., Gibala, P., Kalášek, S., Douša, M., & Doubský, J. (2021). Determining two analogues of 4-(azidomethyl)-1, 1'-biphenyl as potential genotoxic impurities in the active pharmaceutical ingredient of several sartans containing a tetrazole group. *Journal of Pharmaceutical and Biomedical Analysis*, 205, 114300.
146. Prculovska, M., Acevska, J., Panovska, A. P., Nakov, N., Dimitirovska, A., & Brezovska, K. (2022). Root causes for the presence of nitrosamine impurities in active pharmaceutical substances and finished pharmaceutical products. *Macedonian Pharmaceutical Bulletin*
147. Bellur Atici, E., Yazar, Y., & Rıdvanoğlu, N. (2022). Synthesis, characterisation, and control of eight process-related and two genotoxic fingolimod impurities by a validated RP-UPLC method. *Biomedical Chromatography*, 36(4), e5316.
148. Annapoorna Vadlamani, K. Ravindhranath, B. S. Rao 2022 Detection and Quantification of Two Potential Genotoxic Impurities in Telbivudine Active Pharmaceutical Ingredient by Targeted Ultra Performance LC-MS/MS Analysis *Asian Journal of Chemistry*

149. Sudheer Kumar Reddy Gopa, P. K. (2022). Synthesis and Structural Characterization of Process Related Impurities of Mirabegron: A Beta-3 Adrenergic Agonist Drug. *Asian Journal of Chemistry*.
150. Kalauz, A., & Kapui, I. (2022). Determination of potentially genotoxic impurities in crotamiton active pharmaceutical ingredient by gas chromatography. *Journal of Pharmaceutical and Biomedical Analysis*, 210, 114544.
151. Lavayssiere, M., & Lamaty, F. (2023). Amidation by reactive extrusion for synthesising active pharmaceutical ingredients teriflunomide and moclobemide. *Chemical Communications*, 59(23), 3439-3442.
152. Satheesh, D., Devi, D. R., Basavaiah, K., Sreenivasulu, B., Reddy, B. S., Aegurla, B., ... & Chavakula, R. (2023). Synthesis and characterization of potential impurities of ezetimibe. *Journal of Heterocyclic Chemistry*, 60(2), 318-326.
153. Biton, V. (2015). Rufinamide. The treatment of epilepsy, 617-627.
154. Oesch, G., & Bozarth, X. L. (2020). Rufinamide efficacy and association with phenotype and genotype in children with intractable epilepsy: a retrospective single center study. *Epilepsy research*, 168, 106211.
155. Mastrangelo, M. (2017). Lennox–Gastaut syndrome: a state of the art review. *Neuropediatrics*, 48(03), 143-151.
156. Dhriavastava, A. K., Shrivastav, A., Shrivastav, M., Gupta, A., Prakash, S., Fatima, A., & Srivastav, A. (2019). Epilepsy: the next generation drugs (a review). *Journal of Drug Delivery and Therapeutics*, 9(1), 286-292.
157. Kaur, H., Kumar, B., & Medhi, B. (2016). Antiepileptic drugs in development pipeline: a recent update. *Eneurologicalsci*, 4, 42-51.
158. C. Walker, M., & Surges, R. (2015). Mechanisms of antiepileptic drug action. The treatment of epilepsy, 1-91.
159. Gáll, Z., Vancea, S., Szilágyi, T., Gáll, O., & Kolcsár, M. (2015). Dose-dependent pharmacokinetics and brain penetration of rufinamide following intravenous and oral administration to rats. *European Journal of Pharmaceutical Sciences*, 68, 106-113.
160. Al-Banji, M. H., Zahr, D. K., & Jan, M. M. (2015). Lennox-Gastaut syndrome: management update. *Neurosciences Journal*, 20(3), 207-212.

161. Holmes, M. D. (2012). Rufinamide: A broad-spectrum anti-seizure medication. *Journal of Pediatric Epilepsy*, 1(02), 075-076.
162. La Marca, G., Rosati, A., Falchi, M., Malvagia, S., Della Bona, M. L., Pellacani, S., & Guerrini, R. (2013). A pharmacokinetic study and correlation with clinical response of rufinamide in infants with epileptic encephalopathies. *Pharmacology*, 91(5-6), 275-280.
163. Moshé, S. L., Perucca, E., Ryvlin, P., & Tomson, T. (2015). Epilepsy: new advances. *The Lancet*, 385(9971), 884-898.
164. Zaccara, G., & Perucca, E. (2014). Interactions between antiepileptic drugs, and between antiepileptic drugs and other drugs. *Epileptic Disorders*, 16(4), 409-431.
165. Iapadre, G., Balagura, G., Zagaroli, L., Striano, P., & Verrotti, A. (2018). Pharmacokinetics and drug interaction of antiepileptic drugs in children and adolescents. *Pediatric Drugs*, 20, 429-453.
166. Ming-Chi, L., & Chin-Wei, H. (2022). Rufinamide, a Triazole-Derived Antiepileptic Drug, Stimulates Ca²⁺-Activated K⁺ Currents While Inhibiting Voltage-Gated Na⁺ Currents. *International Journal of Molecular Sciences*, 23(22), 13677.
167. Patsalos, P. N. (2013). Drug interactions with the newer antiepileptic drugs (AEDs)—part 1: pharmacokinetic and pharmacodynamic interactions between AEDs. *Clinical pharmacokinetics*, 52, 927-966.
168. Vala, D. P., Vala, R. M., & Patel, H. M. (2022). Versatile Synthetic Platform for 1, 2, 3-Triazole Chemistry. *Acs Omega*, 7(42), 36945-36987.
169. Italiano, D., & Perucca, E. (2013). Clinical pharmacokinetics of new-generation antiepileptic drugs at the extremes of age: an update. *Clinical pharmacokinetics*, 52, 627-645.
170. Łukawski, K., Gryta, P., Łuszczki, J., & Czuczwar, S. J. (2016). Exploring the latest avenues for antiepileptic drug discovery and development. *Expert Opinion on Drug Discovery*, 11(4), 369-382.
171. Patsalos, P. N., Spencer, E. P., & Berry, D. J. (2018). Therapeutic drug monitoring of antiepileptic drugs in epilepsy: a 2018 update. *Therapeutic drug monitoring*, 40(5), 526-548.

172. Hassan, A. (2017). Fourth Wave Digital Journalism Research: Theoretical Perspectives in Journalism Studies. , 18(5), 579-597.
173. Panebianco, M., Prabhakar, H., & Marson, A. G. (2018). Rufinamide add-on therapy for refractory epilepsy. *Cochrane Database of Systematic Reviews*, (4).
174. Anderson, L. L., Thompson, C. H., Hawkins, N. A., Nath, R. D., Petersohn, A. A., Rajamani, S., ... & George Jr, A. L. (2014). Antiepileptic activity of preferential inhibitors of persistent sodium current. *Epilepsia*, 55(8), 1274-1283.
175. Chan, P. S., Zhang, C., Zuo, Z., Kwan, P., & Baum, L. (2014). In vitro transport assays of rufinamide, pregabalin, and zonisamide by human P-glycoprotein. *Epilepsy research*, 108(3), 359-366.
176. Jacob, S., & Nair, A. B. (2016). An updated overview on therapeutic drug monitoring of recent antiepileptic drugs. *Drugs in R&D*, 16, 303-316.
177. Wright, H. M., Chen, A. V., Martinez, S. E., & Davies, N. M. (2012). Pharmacokinetics of oral rufinamide in dogs. *Journal of veterinary pharmacology and therapeutics*, 35(6), 529-533.
178. Bahar, E., & Yoon, H. (2021). Lidocaine: a local anesthetic, its adverse effects and management. *Medicina*, 57(8), 782.
179. <https://www.slideshare.net/vandita002/lidocain-ppt>
180. Beecham, G. B., Nessel, T. A., & Goyal, A. (2019). Lidocaine.
181. Decloux, D., & Ouanounou, A. (2021). Local anaesthesia in dentistry: a review. *International dental journal*, 71(2), 87-95.
182. Foo, I., Macfarlane, A. J. R., Srivastava, D., Bhaskar, A., Barker, H., Knaggs, R., ... & Smith, A. F. (2021). The use of intravenous lidocaine for postoperative pain and recovery: international consensus statement on efficacy and safety. *Anaesthesia*, 76(2), 238-250.
183. Forget, P., Borovac, J. A., Thackeray, E. M., & Pace, N. L. (2019). Transient neurological symptoms (TNS) following spinal anaesthesia with lidocaine versus other local anaesthetics in adult surgical patients: a network meta-analysis. *Cochrane Database of Systematic Reviews*, (12).

184. Barash, M., Reich, K. A., & Rademaker, D. (2015). Lidocaine-induced methemoglobinemia: a clinical reminder. *Journal of Osteopathic Medicine*, 115(2), 94-98.
185. Becker, D. E., & Reed, K. L. (2012). Local anesthetics: review of pharmacological considerations. *Anesthesia progress*, 59(2), 90-102.
186. Gabbe, S. G., Niebyl, J. R., Simpson, J. L., Landon, M. B., Galan, H. L., Jauniaux, E. R., ... & Grobman, W. A. (2016). *Obstetrics: normal and problem pregnancies e-book*. Elsevier Health Sciences.
187. Torp, K. D., Metheny, E., & Simon, L. V. (2018). Lidocaine toxicity.
188. Shah, J., Votta-Velis, E. G., & Borgeat, A. (2018). New local anesthetics. *Best Practice & Research Clinical Anaesthesiology*, 32(2), 179-185.
189. Sekimoto, K., Tobe, M., & Saito, S. (2017). Local anesthetic toxicity: acute and chronic management. *Acute medicine & surgery*, 4(2), 152-160.
190. Skarsvåg, T. I., Wågø, K. J., Tangen, L. F., Lundbom, J. S., Hjelseng, T., Ballo, S., & Finsen, V. (2015). Does adjusting the pH of lidocaine reduce pain during injection?. *Journal of Plastic Surgery and Hand Surgery*, 49(5), 265-267.
191. Finsen V. Reduced pain when injecting lidocaine. *Tidsskr Nor Laegeforen*. 2017 May;137(9):629-630.